

ICON Project Data Management Plan

ICON Principal Investigator – Thomas Immel

Date

10/31/22

ICON Project Scientist – Scott England

Date

MIGHTI Instrument Lead – Christoph Englert

Date

IVM Instrument Lead – Rod Heelis

Date

FUV Instrument Lead – Stephen Mende

Date

EUV Instrument Lead – Eric Korpela

Date

Archive Project Scientist – Robert Candey

Date

HQ Program Scientist – Susanna Finn

Date

By signing this document, signatories are certifying that the content herein is acceptable direction for managing the project's data and that they will ensure its implementation by those over whom they have authority.

Copy to: HQ Program Executive

Change History Log

Revision	Effective Date	Description of Changes
Baseline	10/31/22	Mission-specific document rewritten to match Senior Review format

1. Introduction

1.1 Purpose and Scope

This section provides a brief description/listing of the specific aspects of data management covered by this plan.

The ICON Project Data Management Plan (PDMP) is the interface document between NASA, the ICON mission systems, and the instrument teams. This document describes the science and ancillary data associated with the ICON mission and how the data will be managed. This document describes how the mission will meet the Level-1 requirements (found within the Program Level Requirements (PLRA)) that address the preparation and distribution of processed science data for the general community.

1.2 Plan Development, Maintenance, and Management Responsibility

This section identifies who within the project/mission is responsible for maintaining the PDMP along with who should be providing assistance in doing so. Ideally, the instrument teams provide assistance for updating information on their respective instruments within the PDMP.

The ICON Project Scientist is responsible for maintaining the ICON PDMP. Assistance in maintaining this document is provided by the instrument leads for MIGHTI, IVM, FUV and EUV, the Science Data Center Lead and the Mission Operations Center Lead. Specifically, updates relating to any one instrument are made in coordination with the instrument lead; updates relating to the ground system, and data acquisition are made in coordination with the Mission Operations Center Lead; and updates relating to the data storage and processing are made in coordination with the Science Data Center Lead.

1.3 Change Control

This section identifies any change control or configuration management plans and processes that apply to this document.

This document provides an interface between the ground system, data center, instrument teams and NASA. Once this document is placed under change control, all changes will be subject to approval by all parties.

It also identifies any key milestones or reviews that draft and/or final versions of the document are tied to.

As ICON is beyond its prime mission, no key milestones or planned reviews have been identified at this time, but this document will be revisited as and when any significant updates to the data products or their handling is made.

1.4 About this Document

This section provides a brief overview of what each section of the document covers.

Section 1 covers the scope of this document, and how it relates to the project team and other documents.

Section 2 summarizes the mission, the ICON spacecraft and its four instruments, to provide its role and importance with the context of the SMD portfolio.

Section 3 summarizes each of the four instruments, their measurement requirements and capabilities, and data acquisition modes.

Section 4 describes the data products for the ICON mission. It describes the data levels, instruments, a full list of the data products and their contents.

Section 5 describes the ground system, and each element through which the data from ICON is routed.

Section 6 describes the end-to-end flow of the data from the spacecraft to the science data center, its handling and timeline for delivery from each element to the other.

Section 7 describes the process for archiving the ICON data and how those archives may be accessed. It provides the data volume by product. Software provided by the ICON team to read and visualize the data are described. The documentation of the data products are included, along with a description of the metadata.

Appendix A provides a list of acronyms.

Throughout, the layout matches that prescribed in the template provided for the Senior Review, 2022. Instructions from that have been copied here as headings/introduction statements to aid in finding the appropriate information. *These are highlighted in blue text.*

1.5 Relevant Documents

This section identifies (in tabular format) any other project/mission documentation with higher-level guiding requirements or that provide more detail or context. The Program Level Requirements Appendix (PLRA) version(s) and date(s) that this documentation captures data products for shall be listed.

Title	Document Number	Publication Date
CMAD	ICON_CMAD_V1	10/31/2022
PLRA	ICN_PM_007_PLRA	12/01/2013

Table 1.5.1 List of other project documentation that provide context for this plan.

2 Mission Overview

This section briefly summarizes the mission, spacecraft, and/or instruments to provide its role and importance within the context of the SMD portfolio.

ICON explores the boundary between Earth and space to understand the physical connection between our atmosphere and our space environment. Recent NASA missions have shown how dramatically variable the region of space near Earth is, where ionized plasma and neutral gas collide and interact. This region, the ionosphere, has long been known to respond to space weather drivers from the sun, but in this century the energy and momentum of our own atmosphere have newly emerged as regularly having effects of equal or greater magnitude. ICON weighs the impacts of these two drivers as they exert change on our space environment.

Though the solar inputs are now well quantified, the drivers of ionospheric variability originating from lower atmosphere regions are not. ICON is a single spacecraft mission that measures and analyzes these drivers. ICON presents a revolutionary concept of combining remote optical imaging and *in situ* measurements of the plasma at points where these are tied together by Earth's magnetic field. With these measurements, ICON simultaneously retrieves all of the properties of the system that both influence and result from the dynamical and chemical coupling of the atmosphere and ionosphere. With this approach, ICON is unique in its capability to quantify each driver and pinpoint the real cause of the variability. ICON gives us the ability to explain how energy and momentum from the lower atmosphere propagate into the space environment, and how these drivers interact with solar and magnetospheric effects during the extreme conditions of solar-driven magnetic storms.

The ICON payload consists of four instruments. The first is a pair of imaging interferometers (MIGHTI), which measure the Doppler shift of two emission lines from atomic oxygen (5577 and 6300 Å) in order to determine neutral wind speeds over a range of altitudes. In addition MIGHTI also measures the brightness of 3 components of the O₂ emission band around 7620 Å in order to determine neutral temperatures over a range of altitudes. The second is a spectrographic imager in the Far UV range (FUV) that measures the brightness of the emission from atomic oxygen at 1356 Å and from molecular nitrogen in the LBH band (near 1550 Å), from which both the daytime thermospheric composition and nighttime ionospheric O⁺ density can be determined over a range of altitudes. The third is an imaging spectrometer in the Extreme UV range (EUV) that measures the brightness of two emission lines from atomic oxygen at 834 and 617 Å in order to determine the daytime O⁺ density over a range of altitudes. Finally, a pair of ion velocity meters (IVM-A/B) measure the 3-dimensional vector motion of O⁺ ions *in situ* (these are pointed in opposite directions and only one operates at a time). The instrument suite is designed to work together so that the remote sensing instruments (EUV, FUV, MIGHTI) are viewing a volume that is magnetically connected to the spacecraft when the spacecraft is at the geomagnetic equator, allowing ICON to compare their measurements with the local ion drift measurements of IVM, after suitable mapping of IVM measurements along the magnetic field line.

2.1 Mission Objectives

This section describes the science objective(s) of the mission.

ICON's science objectives are to understand: 1) the sources of strong ionospheric variability; 2) the transfer of energy and momentum from our atmosphere into space; and 3) how solar wind and magnetospheric effects modify the internally driven atmosphere-space system. These are described in terms of three science questions: Science Question 1: What causes the highly-structured variability in the daytime low-latitude ionosphere?; Science Question 2: How do large-scale atmospheric waves control the ionosphere at low latitudes?; and Science Question 3: How do ion-neutral coupling processes respond to increases in solar forcing and geomagnetic activity?

It shall also identify other mission stakeholders, partner agencies, and their science contributions.

The mission stakeholder is NASA. There are no partner agencies.

2.2 Launch, Orbit and Operations

This section notes the launch date for the mission.

ICON launched October 10, 2019, from Cape Canaveral Air Force Station on a Pegasus XL launch vehicle dropped by the Northrop Grumman Stargazer L-1011 carrier aircraft at 21:59 Eastern Daylight Time, and after on-orbit checkout entered its 2-year period of prime mission science operations on December 15, 2019.

The observatory was launched into the desired low-Earth orbit, characterized by the following parameters: inclination 26.99 degrees; perigee height 576 km; apogee height 601 km; eccentricity 0.0018295.

It summarizes key operational activities such as orbital maneuvers, checkout, and commissioning in order to provide checkpoints for potentially flagging initial flaws in the data as well as to provide a timeline of when primary project data collection occurs within the mission life cycle.

The observatory has no fuel and performs no maneuvers. During regular science operations, it flies in a local-vertical, local-horizontal orientation (LVLH) to afford the remote sensing instruments a view of the Earth's limb. The observatory performs several operations during which it changes attitude as part of either early commissioning activities or regular science calibration operations. These are detailed in Tables 1 and 2 below.

Table 2.2.1 – Summary of key operational activities performed only once (e.g. during commissioning).

Operation name	Instrument Involved	Description
MIGHTI stellar inertial	MIGHTI A, B	Inertial point of one MIGHTI unit at a time to a known star field, while ensuring both star trackers had view of stars. This confirms the MIGHTI to star tracker rotation matrices, identify any possibly shift during launch. Inertial hold, keeping star field in both FOVs. Repeat for both MIGHTI instruments. This is performed during local nighttime.
MIGHTI limb track	MIGHTI A, B	Roll of S/C to point MIGHTI FOV lower & higher than the science target, while otherwise flying in LVLH (bottom of FOV set to 90 km altitude during science). This helped confirm the LVLH pointing was working as intended by imaging both the airglow layers beyond the full FOV of the instrument, and the Rayleigh scattered light at lower altitude. This is performed for one or more full orbits.
EUV Lunar inertial	EUV	Inertial point of the EUV instrument towards the full moon. Moon then slowly drifted through the FOV perpendicular to the imaging direction. Used to determine the EUV pointing and ensure the rotation matrices used in the science algorithms were correct. This is performed during local nighttime.
FUV stellar inertial	FUV	Inertial point of the FUV instrument to a known star field with bright Far-UV stars, while ensuring both star trackers had view of stars. This confirms the FUV to star tracker rotation matrices, identify any possibly shift during launch. Inertial hold, keeping star field in both FOVs. Repeated at different FUV turret angles. This is performed during local nighttime.

Table 2.2.2 – Summary of regularly scheduled operational activities to support ongoing calibration of science instruments.

Operation name	Instrument Involved	Description
MIGHTI Zero wind	MIGHTI	The spacecraft slews to point one MIGHTI into ram, and then wake to measure the same volume of air a few minutes apart. This is used as part of the MIGHTI wind calibration. This is performed for both MIGHTI units on separate orbits. This is performed approximately once per month.

FUV nadir	FUV	The spacecraft rolls to point the center of the FUV FOV toward nadir. This is performed close to local noon, and provides the full FOV with near uniform illumination. This is used as part of the FUV flatfield calibration. This is performed approximately once per month.
EUV nadir	EUV	The spacecraft rolls to point the center of the EUV FOV toward nadir. This is performed close to local noon, and provides the full FOV with near uniform illumination. This is used as part of the EUV flatfield calibration. This is performed approximately once per month.
EUV lunar	EUV	The spacecraft moves to point EUV at the moon. The spacecraft slews to move the moon across the EUV FOV, perpendicular to the imaging direction at several points along its imaging axis. This is used as part of the EUV radiometric calibration. This is performed during local nighttime, and within +/- 1 day of the full moon. It is performed once per lunar month.
FUV stellar	FUV	Inertial point of the FUV instrument to a known star field with bright Far-UV stars, while ensuring both star trackers had view of stars. This is used as part of the FUV radiometric calibration. This is performed during local nighttime. This is performed approximately once per month.

This section also describes how the mission will operationally fulfil its science goals.

The primary project data is collected in a near continuous manner, beginning after commissioning finished. ICON completed commissioning and began regular science in December 15, 2019. Regular science data is predominantly collected by the in situ IVM as it faces ram, and the remote instruments point generally towards the north as the spacecraft flies in LVLH. This ensures the remote sensing instrumentation has the correct view of the Earth's limb. Beyond this, regular science data is collected in two other ways. The first is by rotating the spacecraft such that IVM-B points to ram, and the remote sensing instruments look generally towards the south. This is referred to as reverse LVLH. Other than generally looking southwards, and collecting in situ data with IVM-B, operations are identical to regular LVLH. The final way in which regular science data is collected is by performing a spacecraft reorientation called a conjugate operation. ICON's Conjugate Operation is used to gather the observations for the complete, instantaneous comparison of the magnetically connected winds and ion drifts. The Conjugate Operation involves a sequence of 4 yaw maneuvers shown in Figure 2.2.1. Through this sequence of maneuvers, ICON is able to observe the horizontal neutral winds along both the northern and southern dynamo regions connected to the *in situ* drifts, allowing for a complete determination of the dynamo drivers at the optimal location on the planet. The optimal locations for conjugate operations are regions where the remotely measured winds are closest to the magnetic field line that extends down into the E-region from the point where

ICON crosses the dip equator. Regions of optimal geometry for these observations are identified in Figure 2.2.2. Locations on the ICON orbit from which point the remotely observed winds at 120 km are within 500 km of the field line that the observatory crosses, on either side of the equator, are identified in blue. This sequence will be performed as ICON is crossing the geomagnetic equator during daylight, usually between 9 and 15 LT. The Conjugate Operations maneuver can occur up to twice per day.

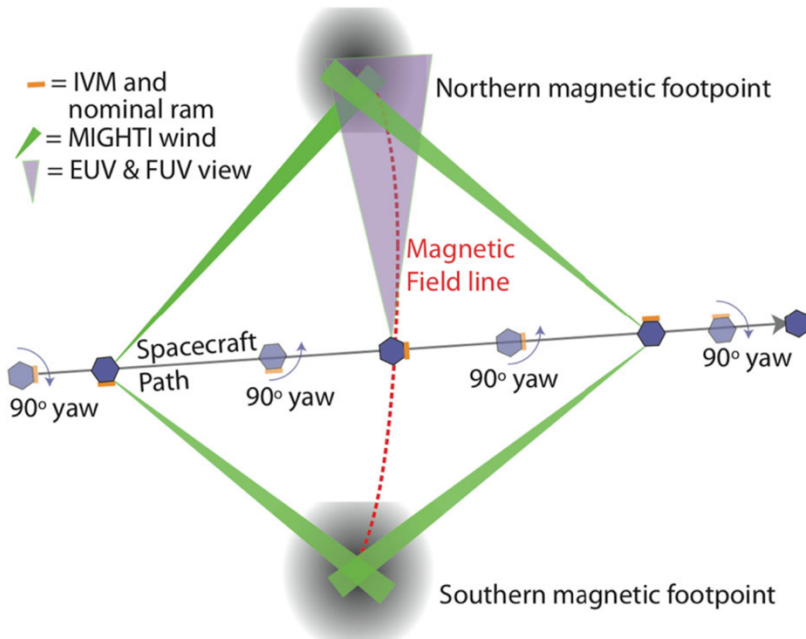


Figure 2.2.1 – Diagram of the ICON conjugate operation. At pre-scheduled times when the geometry is correct, ICON initiates four timed yaw maneuvers (approximately -90° , $+90^\circ$, $+90^\circ$ and -90° , exact angle depends on declination and initial orientation of the observatory) to make wind observations at two magnetically conjugate points

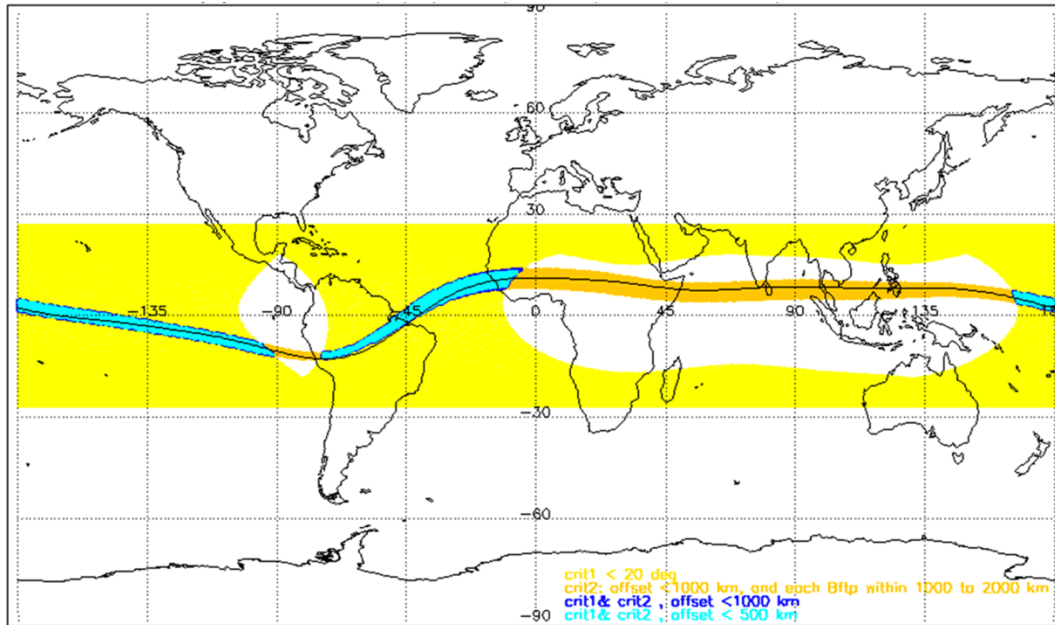


Figure 2.2.2 - Map of regions of potential Conjugate Operations. Regions in *light blue* show where Conjugate Operations may be centered in order to match northern and southern footpoint observations that are also magnetically conjugate. The combined offset of the wind measurements from the conjugate points is never 0 km but often less than 500 km, the width of two MIGHTI wind samples on the limb. Locations over the Pacific show regions where operations are possible in the descending node of the orbit. Locations over the Atlantic offer opportunities in the ascending node

Individual instruments provide data over portion of each orbit. In brief, MIGHTI collects data during both day and night, with very brief interruptions as the instrument switches from day to night mode. When the spacecraft is within the SAA, the MIGHTI data are collected, but flagged as compromised. IVM collects data continuously both day and night in the same mode. FUV collects data during both day and night. EUV collects regular science data only during daylight. Further details of all the instrument operating modes are given in Section 3. ICON performs regular calibrations described in Table 2.2.2, which briefly interrupt regular data collection. Finally, there have been four anomalies to-date related to the star tracker, during which science data collection was interrupted as the observatory went into safe mode. These are listed in Table 2.2.3.

Table 2.2.3 Observatory Safe Mode dates.

Start Time	End Time
February 19 2020 16:00 UT	February 25 2020 00:00 UT
April 29 2021 4:09 UT	May 5 2021 00:25 UT
June 13 2021 UT	June 16 2021 03:48 UT

September 2 2021 20:19 UT	September 8 2021 18:30 UT
---------------------------	---------------------------

Using the combination of data collection described above, ICON meets all of the relevant Baseline Level 1 Requirements in the PLRA. These are listed below, followed by a description of how these are met.

SR-6 Orbit

ICON shall make all measurements from a near-circular low-earth orbit:

- a) with an inclination between 24-30; and
- b) from altitudes between 450 and 670 km.

Description – These orbital parameters have been achieved, as described at the start of this section.

SR-7 Scientific Survey Observations

ICON shall make scientific measurements:

- a) With an observing geometry such that at the magnetic dip equator, the magnetic field line that intersects the orbit track also intersects each one of the remotely measured volumes on the limb within 15 minutes of a magnetic dip equator crossing;
- b) for at least 60 days out of each 91 day season;
- c) over a period of at least four 91 day seasons;
- d) with an average observing efficiency of at least 80% per day; and
- e) within a two year mission.

To meet this Baseline L1 requirement, ICON needs to make observations that meet the geometry, date ranges and observing efficiency outlined above. Regarding the geometry, this is achieved through a combination of the orbit (affording appropriate tangent altitudes etc.) and the instrument orientation on the spacecraft. This is shown schematically in Figure 2.2.3. The payload alignment both on ground and in orbit (via calibrations noted in the table above) have demonstrated that this is met.

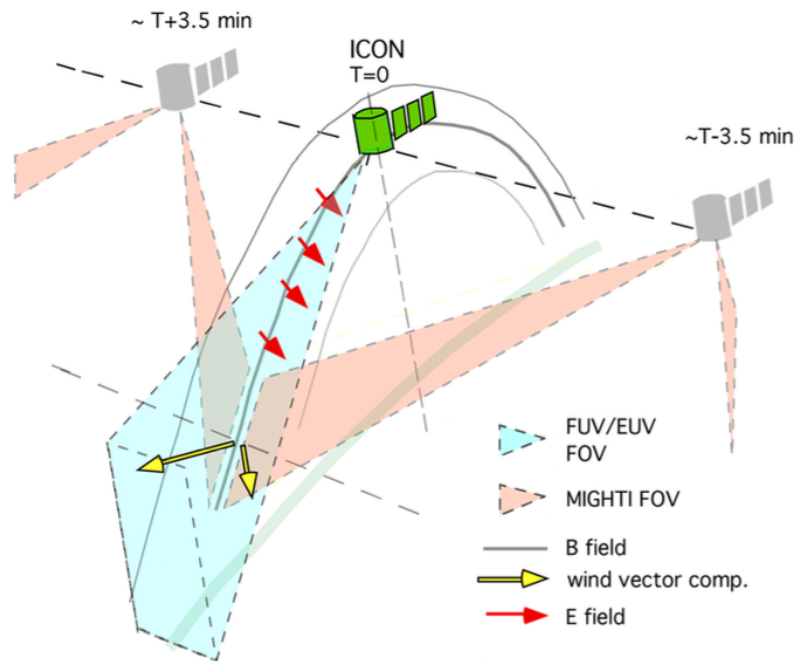


Figure 2.2.3 – Geometry of the ICON observations required for Requirement SR-7. ICON is shown near the magnetic equator. At position $T = 0$, FUV and EUV instruments view the limb thermosphere/ionosphere (fields of views shown in *light blue*) while the IVM measures the in situ ion drift, representative of the electric field present on the field line (*red arrows*). MIGHTI (fields of view shown in *light red*) measure the relevant wind vector components (*yellow*) at positions $T - 3.5$ min and $T + 3.5$ min. The tangent point locations where MIGHTI samples the wind field vary with altitude following closely the Earth's dipole magnetic field line that is intersecting the spacecraft at the $T = 0$ position.

Regarding the date ranges, ICON needed to provide observations from all 4 of its instruments for 4 seasons. Seasons are defined as periods of 91 days, from which data in 60 days would provide the sampling of that season. All instruments were fully checked out and in science mode by December 6th, 2019, with official start of science phase on December 15, 2019. The brief outages in science data collection associate with the anomalies related to the start-tracker were all short and did not impact the Level 1 requirements (accommodated well-within the 31 days of margin in each 91 day season). Thus, the four seasons used for the prime mission were as follows: Season 1 – 12/15/2019 – 3/14/2020; Season 2 3/15/2020 – 6/14/2020; Season 3 6/15/2020 – 9/14/2020; Season 4 9/15/2020 – 12/14/2020. Thus, by the middle of December 2020, ICON had obtained all the data to meet its Baseline Level 1 requirements within the 2 years of its prime mission, with the exception of IVM data near dawn which is discussed below. The data collected during the remainder of the Prime Mission has significantly enhanced the scientific return of the mission, adding to the parameter space of conditions observed.

Regarding the observational efficiency, ICON must make the appropriate scientific observations over each of the 60 of 91 days in each of the four seasons at least 80% of the time. For example, EUV makes observations of the dayside ionosphere, so for the case of this instrument, for one of the days to count as part of the 60 needed for that season, at least 80% of the time when the spacecraft is in daytime, EUV must make observations. This is met in two ways – the first is to ensure that the design of the instruments and operational plan allows for this, and by analysis of the data collected to track how ICON performs relative to this. The sections below first deal with the design, then the analysis.

Design: This places constraints on time spent performing other activities, including the observatory in safe mode (Table 2.2.3), performing calibrations that point the observatory away from the Earth’s limb (Tables 2.2.1 and 2.2.2), or some other effect that compromises the data (e.g., moon in FOV for MIGHTI). The safe holds are all short and made no impact within the 60 days each season. For the other events, these either depend on geometry (e.g., moon to FOV angles) and are thus predictable, or involve planned activities (e.g., stellar calibration). The 80% observational efficiency is ensured through the implementation of flight rules that govern the planning of spacecraft operations. These flight rules ensure that, on any given day, a limited amount of time is spent on any calibration or similar activity that would reduce the observational efficiency. Further, analysis tools are used by the science operations team to examine the timeline of spacecraft activities on any given day. An example of this is shown in Figure 2.2.4. In this example, the long segment in orbits 1256-1267 shows when the MIGHTI cal. lamps are on, but as uncompromised science data is taken at this time, this does not count against the observational efficiency. The outages shown for this example include the zero wind maneuver (calibration for MIGHTI), and the passages through the SAA. Accounting for all of these, ICON’s design-to observation efficiency budget is shown in Table 2.2.4.

Source	% Impact
South Atlantic Anomaly	8
Instrument Calibrations (both off-point and time in engineering mode)	4
MIGHTI dark images	0.5
Mode switching (day-night transitions, shutter moving etc.)	0.9
Total Impacted*	12.9
Total Efficiency	86.6

Table 2.2.4 – ICON Planned Observational Efficiency Budget

* - worst-case estimate – i.e., assumes mode switching never overlaps with SAA etc.

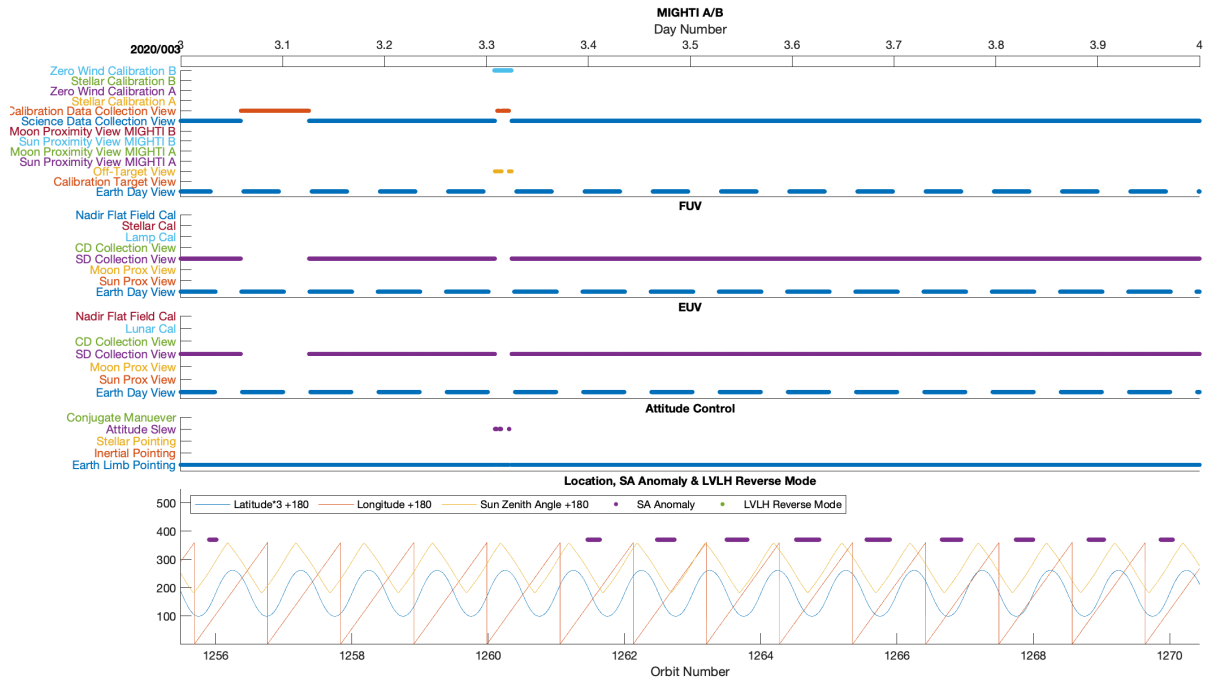


Figure 2.2.4 – Example of daily operations for ICON science instruments, shown for January 3, 2020. Along with the other tools described, this ensures ICON maintains is 80% observational efficiency.

Analysis: With ICON observations available, we also perform retrospective analysis of the observational efficiency. By its nature, this requires at least 91 days of data to begin the analysis. The figures below show the analysis that covers the prime mission for each of the scientific products listed in the L1 requirements. The overall observational efficiencies are noted, all of which exceed the L1 requirements with the exception of ion drifts early in the mission. At low solar F10.7 values, such as those present at solar minimum, the ambient plasma densities at the spacecraft were low. This, combined with the photoelectron current produced around sunrise as sunlight falls on the ICON spacecraft resulted in low quality cross-track ion drift measurements (further details are provided by Heelis *et al.*, 2022). The impact on observational efficiency is shown in Figure 2.2.7, where an outage in the high quality data is seen from around sunrise to pre-noon local times. This is shown in detail in Figure 2.2.8 (left), for a day when the solar F10.7 flux was 69 SFU. As the solar EUV flux levels have increased, this effect has diminished substantially. An example of this is shown in detail in Figure 2.2.8 (right), which corresponds to a moderate F10.7 = 108 SFU (representative of much of late 2021 and 2022). Here the impacts of the photoelectron current are evident only from ~5-6 hours LT, corresponding to an ~5% impact to the observation efficiency which is well within the requirements. As solar EUV flux is expected to increase towards solar maximum, Figure 2.2.8 represents the expected performance of IVM going forwards.

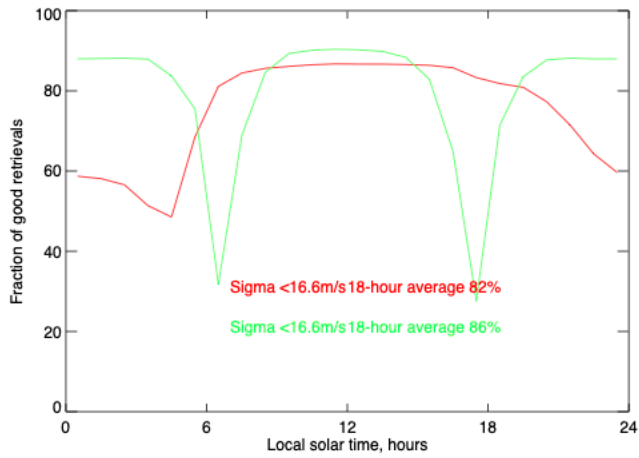


Figure 2.2.5 – Observational efficiency for neutral winds during the Prime mission. Notable dips near dawn and dusk are expected in the greenline, as the gradient in volume emission rate is particularly strong in these regions. In the redline, a dip in the late evening/pre-dawn is expected as the volume emission rates at mid latitudes can be very low at these local times.

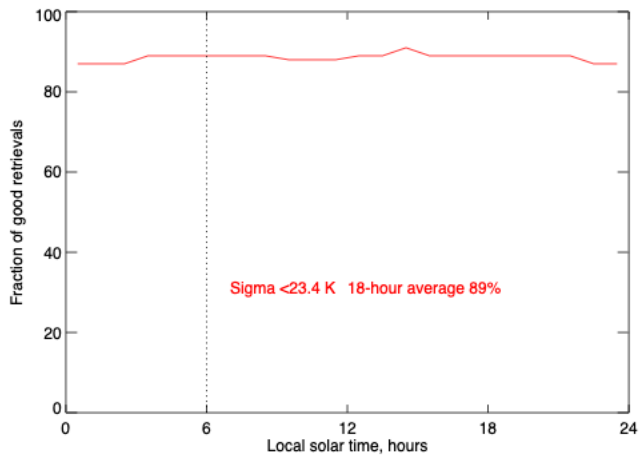


Figure 2.2.6 – Observational efficiency for neutral temperatures during the Prime mission.

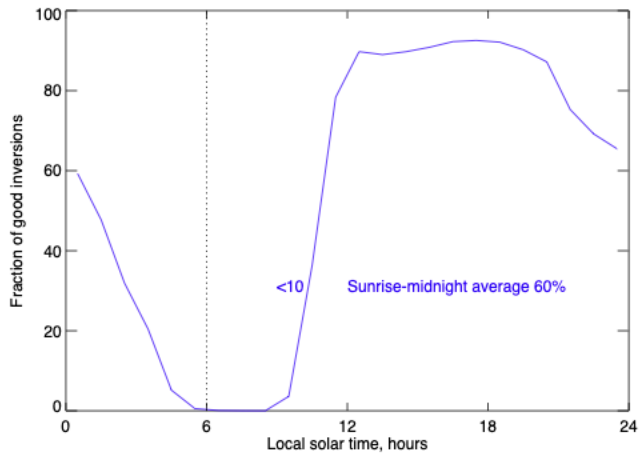


Figure 2.2.7 – Observational efficiency for ion drifts during the Prime mission. The low values near dawn correspond to the increased photoelectron current at this time.

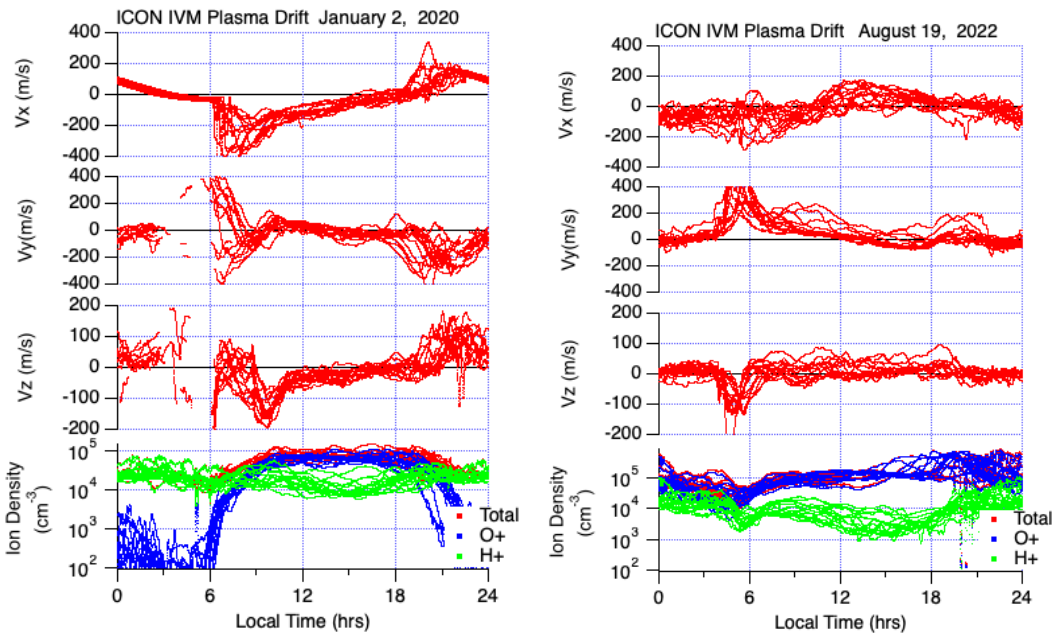


Figure 2.2.8 – Observational efficiency for ion drifts during (left) 2020 and (right) 2022 – examples from January 2 2020 and August 19 2021 are shown. F10.7 for these days were 69 and 108 SFU respectively. At low solar flux levels, the photoelectron current impacts were evident from $\sim 4 - 11$ hours LT. At higher solar flux levels, the photoelectron current impact is evident in the drifts from approximately 5 – 6 hours LT, corresponding to a $\sim 5\%$ impact to the observational efficiency.

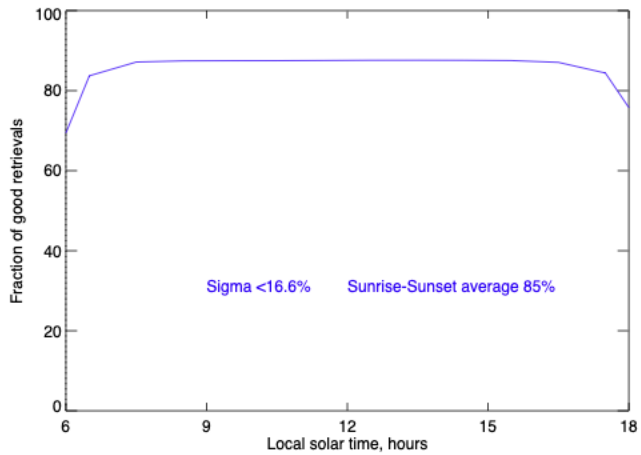


Figure 2.2.9 – Observational efficiency for neutral composition during the Prime mission.

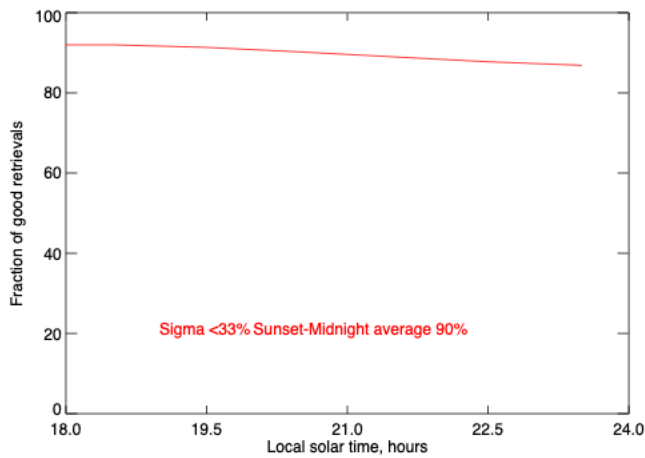


Figure 2.2.10 – Observational efficiency for nighttime O⁺ during the Prime mission.

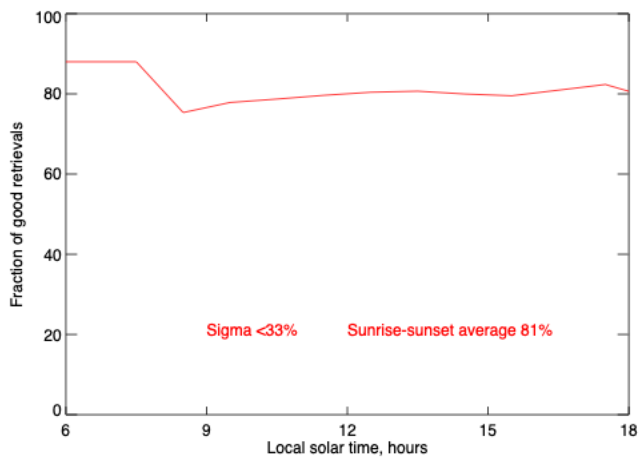


Figure 2.2.11 – Observational efficiency for daytime O⁺ during the Prime mission.

The final set of L1s in the PLRA related to the observations concern the conjugate observations that are used for Science Objective 1.

SR-8 Scientific Conjugate Observations

ICON shall make targeted scientific measurements:

- a) With observing campaigns to measure horizontal wind vectors both north and south of the orbit track within 10 minutes of a magnetic dip equator crossing in the daytime;
- b) with a frequency of up to once per day;
- c) over a period of at least 91 days;
- d) with a total number of conjugate observations of at least 40.

Item a is met with the operation shown in Figure 2.2.1. These are scheduled using the same science operations planning software as described above for the observational efficiency. This software is used to look both for the optimal times to perform these conjugate observations, while ensuring other constraints are met (observational efficiency, calibration of instruments etc.). During its prime mission, ICON performed a total of 180 conjugate observations, fulfilling this L1 requirement.

It identifies the entities involved with the handling of the mission's science data.

The ICON science data is handled by a number of entities. These fall into several categories – those that handle the RF signals from the spacecraft and deliver the telemetry to the Mission Operations Center, the Mission Operations Center, the Science Data Center, the instrument teams, and NASA's SPDF Data Archive. Table 2.2.5 lists the entities that handle the RF signals and telemetry. The Mission Operations Center and Science Data Center are co-located at the University of California, Berkeley. The Mission Operations Center receives the telemetry, sorts it by APID, and puts packets into a repository for the Science Data Center to receive. The Science Data Center handles the production of the Data Products described in Section 4. As part of this production process, the instrument teams access these data to both produce calibrations for the data, and approve the files that are produced (to ensure they processed correctly). Data are then provided to the public via an FTP site hosted at the Science Data Center, and delivered to SPDF, which also provides them to the public.

Entity Number	SN
1	TDRSS
2	White Sands
	NEN
3	White Sands, NM, SW 1
4	Wallops Island, VA, WGS

5	Santiago, Chile, AGO3
6	Santiago, Chile, AGO4
	Other Networks
7	UC Berkeley, CA, BGS
8	USN / South Point, HI, USHI01
9	USN / South Point, HI, USHI02
10	KSAT / Singapore, SING
11	SSC South Africa

Table 2.2.5 – List of Entities that handle ICON’s RF signals and raw telemetry.

3. Science Instrumentation

This section summarizes each instrument or investigation that this PDMP applies to (one 3.x subsection per instrument). Include a summary table that includes all of the mission's instruments and key details as shown in the example below.

This section summarizes each instrument that this PDMP applies to. Table 3.1 lists the ICON instruments and their key details. Further information on MIGHTI is provided in Section 3.1, IVM in Section 3.2, FUV in Section 3.3 and EUV in Section 3.4.

Inst. Name	In situ or Remote Sensing?	Mass (kg)	Power (W)	Data Rate (bps)	PI	PI Organization	Inst. Status
MIGHTI	Remote sensing	46	43.5	56,300	Christoph Englert	Naval Research Laboratory	Green
IVM	In situ	8.5	3.3	2,150	Rod Heelis	University of Texas at Dallas	Green
FUV	Remote sensing	33	11.3	2,150	Stephen Mende	University of California Berkeley	Green
EUV	Remote sensing	10	4.6	3,380	Eric Korpela	University of California Berkeley	Green, operating at reduced cadence – see Section 3.4.2

Table 3.1, List of the ICON instrument and their key properties. Power estimates are based on the sum of all components – including the detectors, control electronics, operational heaters (not survival heaters) and thermoelectric coolers. In general, the actual power draw is less than this number.

If the instrument has multiple operational/observation modes, those shall be described here.

MIGHTI has two science observation modes, corresponding to daytime and nighttime observations. During nighttime, the aperture of the instrument opens to around seven times that used in the day, and the exposure time increases from 30s (day) to 60s (night). MIGHTI also has calibration modes, including observing star fields with longer exposure and no on-board binning, and finally dark exposures where the aperture is closed. Further details on MIGHTI are in Section 3.1. IVM has only its primary science operating mode. Further details on IVM are in Section 3.2. For FUV, operating modes include regular daytime science in which 2D images consisting of 6 horizontal and 256 vertical bins are taken with the shortwave and longwave

channels every 12s. During nighttime, the shortwave channel continues this operation. In addition, at nighttime, a time-delay-integration is used for the shortwave images to build up a motion-compensated image of the limb and sublimb every 12s. Further details on FUV are in Section 3.3. Finally, FUV has an engineering mode in which images of stars are taken with no on-board binning. EUV has a science mode in which 2D spectra are collected every 12s. It also has an engineering mode in which individual the cross-delay line pulses are recorded, to provide information on the operation of the sensor. Further details on EUV are in Section 3.4.

3.1 Michelson Interferometer for Global High-resolution Thermospheric Imaging (MIGHTI)

3.1.1 Instrument Measurement Requirements

This subsection summarizes the required measurement parameters of the instrument.

Table 3.1.1.1 describes the key observable quantities that MIGHTI must observe, the ranges and times over which these observations must be made. These provide the remote sensing observations needed to meet the L1 observation requirements described in Section 3.1.3.

Measurement Parameter	Value
Greenline	
Parameter Measured	Altitude-resolved Doppler shift of O 557.7 nm airglow with two orthogonally mounted units (FOV at near 90 degrees through remote sensed location).
Tangent Altitude Range	Daytime 95 – 180 km Nighttime 95 – 105 km
Tangent Altitude Resolution	5 km, from 95 - 150 km during daytime 5 km from 95 – 105 km during nighttime 30 km from 150-180 km, daytime only
In-track sampling	500 km
Temporal Cadence Required	1 minute
Temporal Coverage	18 total hours of solar local time including all times between local sunrise and sunset
Redline	
Parameter Measured	Altitude-resolved Doppler shift of O 630.0 nm airglow with two orthogonally mounted units (FOV at near 90 degrees through remote sensed location).
Tangent Altitude Range	Daytime 180 – 280 km Nighttime 220 – 280 km
Tangent Altitude Resolution	30 km
In-track sampling	500 km
Temporal Cadence Required	1 minute
Temporal Coverage	18 total hours of solar local time including all times between local sunrise and sunset

O ₂ A-Band	
Parameter Measured	Altitude-resolved shape of the O ₂ Atmospheric Band around 762 nm, and background light (Rayleigh scattered light in the vicinity of the A-band). Shape to be determined with 3 band-passes FWHM 2nm, the ratio of any two of which is sufficient to provide the band shape.
Tangent Altitude Range	95 – 105 km
Tangent Altitude Resolution	5 km
In-track sampling	500 km
Temporal Cadence Required	1 minute
Temporal Coverage	18 total hours of solar local time including all times between local sunrise and sunset

Table 3.1.1.1 – Summary of the MIGHTI Instrument Measurement Requirements

3.1.2 Instrument Description

This subsection describes the primary scientific objectives of the instrument, its hardware, physical configuration, etc.

The Michelson Interferometer for Global High-resolution Thermospheric Imaging (MIGHTI) instrument was designed to provide thermospheric wind and temperature measurements for the Ionospheric Connection (ICON) Explorer mission. The wind velocity observation is based on the Doppler shift measurement of the forbidden atomic oxygen red and green lines at the wavelengths of 630.0 nm ($O(^1D \rightarrow ^3P)$) and 557.7 nm ($O(^1S \rightarrow ^1D)$) respectively, imaging the limb of the Earth between 90 and 300 kilometers tangent point altitude during day and night. Wind directions are determined by combining observations of two fields of view that are directed nominally at an azimuth angle of 45 degrees and 135 degrees from the spacecraft ram direction, each providing line of sight wind components. To measure the Doppler shift, MIGHTI uses the Doppler Asymmetric Spatial Heterodyne (DASH) technique (Englert et al. 2007), which is a modified version of Spatial Heterodyne Spectroscopy (SHS) (Harlander et al. 1992).

The temperature observation is based on the radiometric measurement of three narrow band regions within the temperature dependent molecular oxygen Atmospheric band (A-band, $O_2(b^1\Sigma \rightarrow x^3\Sigma(0,0))$) around the wavelength of 762 nm. Two additional passbands on either side of the band are used to observe the background contribution while avoiding signal from the (1,1) vibrational band. The A-band observations are performed utilizing the same optics and detector as the wind observations and cover an altitude region of about 90–140 km.

In the following we provide an overview of the instrument, details of the sensor design that was chosen based on the mission science requirements and available resources. The MIGHTI instrument design was driven by the ICON science requirements and the available spacecraft

accommodations. The ICON science requirements generally flow down to measurement requirements for each instrument. One fundamental measurement requirement for MIGHTI is to measure the horizontal wind speed and direction. Since a Doppler shift measurement is sensitive only to the wind velocity component parallel to the viewing direction (line of sight), MIGHTI uses two perpendicular fields of view nominally pointing 45° and 135° in azimuth from the spacecraft velocity (MIGHTI A and MIGHTI B). This way, the two MIGHTI fields of view measure virtually the same atmospheric volume about 8 minutes apart, given the targeted ICON orbit altitude of 575 km (Immel et al. 2017). The combination of colocated measurements at the observation tangent point then allows for the determination of the horizontal wind speed and direction (Harding et al. 2017). This technique has been used successfully by previous satellite-based wind sensors (e.g. Shepherd et al. 1993). MIGHTI measurement requirements are given in Section 3.1.1.

As mentioned above, MIGHTI requires two perpendicular fields of view to measure horizontal wind vector components. Thus, the MIGHTI instrument consists of two identical optical sensors, MIGHTI A (Ahead) and MIGHTI B (Behind), which view the Earth's limb with perpendicular FOVs as shown in Figure 3.1.2.1 shows the optical sensors and the calibration lamp assembly prior to the integration onto the payload interface plate. In addition to the optical sensors, MIGHTI consists of an external camera electronics assembly and an external calibration lamp assembly. The following sections provide details on the design of the main MIGHTI instrument components.

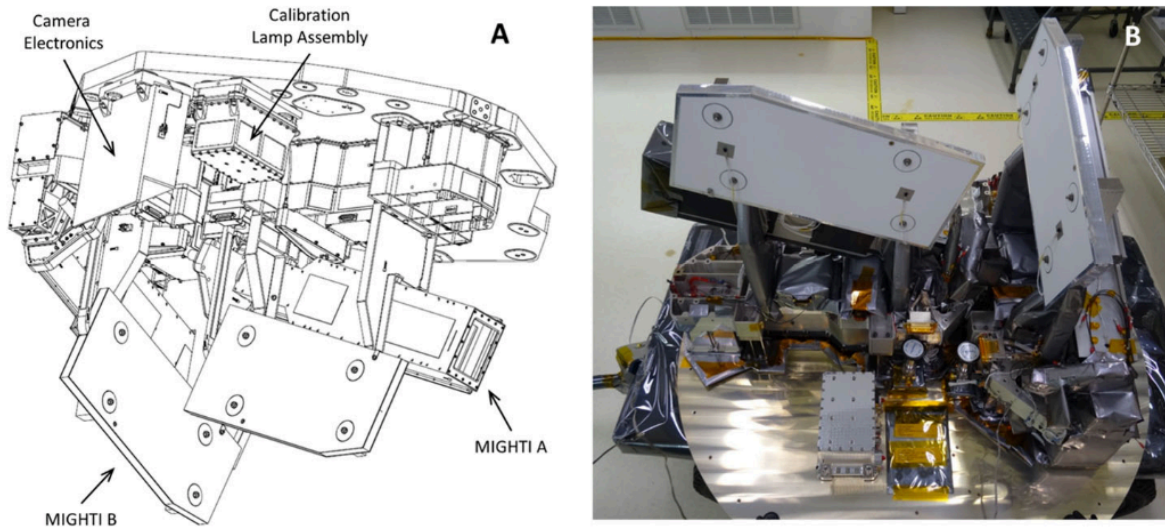


Figure 3.1.2.1 shows the optical sensors and the calibration lamp assembly prior to the integration onto the payload interface plate

This subsection lists the major elements of the instrument and provides a schematic of the conceptual design.

The key elements of MIGHTI are shown in Figure 3.1.2.2. The key optical elements are shown in Figure 3.1.2.3. These elements include:

Baffle - Each MIGHTI sensor is equipped with a blackened baffle tube (Figure 3.1.2.2) that extends forward of the entrance pupil located at A1. The primary purpose of the MIGHTI baffle is the suppression of signal that originates from angles outside the field of view. This is of vital importance, since the illuminated Earth's disk and the sun represent light sources that are many orders of magnitude brighter than the targeted airglow emissions, and during the day, the bright Earth is always close to the MIGHTI fields of view. Due to the ICON orbit and MIGHTI limb pointing geometry, the sun can also get close to or even enter the MIGHTI fields of view during the mission. A secondary purpose of the baffle is to reduce contamination from particles that could reach the first optical element and create a scattering source.

Entrance Optics - The MIGHTI entrance optics are shown in Figure 3.1.2.3 and include all optical elements between the first fold mirror (M1) and the interference filter (F1), located immediately in front of the interferometer. The purpose of the entrance optics is to (1) direct the beam from the baffle aperture (A1) onto the MIGHTI optical bench, (2) define the field of view for day and night aperture positions (note that the FOV is not defined by any baffle vanes), (3) superimpose signal from the calibration lamps onto the atmospheric signal, (4) eliminate signal from unwanted spectral regions between about 200–525 nm and 900–1100 nm, and (5) form an image of the limb at the fringe localization plane close to the gratings within the interferometer.

As shown in Figure 3.1.2.3, two flat mirrors (M1 and M2) are used to direct the beam onto the optical bench. The following lens, L1, simultaneously forms an image of the limb on the field stop and collimates light from the entrance pupil (A1). In front of the field stop is a cubic beam sampler which transmits 95% of the atmospheric signal and reflects into the beam 5% of the signal from the on-board calibration sources. Lens L2 collimates light from the field stop and images A1 onto the Lyot stop. The Lyot stop is slightly undersized with respect to the image of A1, so that the edges of A1 are blocked and the field of view is determined solely by the field stop and the Lyot stop. Immediately in front of the Lyot stop is a second adjustable aperture (A2). This aperture is equivalent to the adjustable aperture A1. In day mode, it also blocks about 85% of the rectangular Lyot stop by rotating a blackened vane into the beam. The vane is aligned so it blocks light originating from the edge of the daytime A1 aperture. Lens L3 collimates light from the Lyot stop and forms an image of the limb onto the fringe localization plane in the interferometer. The beam entering the interferometer is telecentric. The beam enters the interferometer enclosure after reflecting off a fold mirror (M3) and passing through a broad-band interference filter with a 525–900 nm passband. This filter reduces light going into the interferometer that is within the sensitivity range of the MIGHTI CCD detector, but outside any wavelengths of interest.

The optical bench and M1 enclosure are thermally stabilized using three separate zones comprised of strip heaters, temperature sensors and PID (Proportional-Integral-Derivative)

controllers. The bench is thermally controlled to maintain a temperature of about 20°C on orbit.

Interferometer - The DASH interferometer can be considered a combination of a stepped Michelson interferometer and a spatial heterodyne spectrometer. It consists of a beamsplitter and two interferometer arms of different lengths that are terminated with fixed, tilted diffraction gratings. Every individual groove of the grating is fundamentally equivalent to the return mirror in a stepped Michelson interferometer, and the imaging of the tilted grating allows the simultaneous measurement of many different optical path differences, corresponding to the positions of the grooves with respect to the beamsplitter. In addition, the MIGHTI interferometer is field widened with two fixed prisms positioned between the beamsplitter and the grating in each interferometer arm. Simultaneously sampling an optical path difference interval, the DASH interferometer superimposes low frequency spatial fringes oriented perpendicular to the horizon onto the limb image of the oxygen red and green line signals. The fringe frequencies are wavelength dependent, and are used to detect the Doppler shift of the emission lines. However, a wind velocity of $v = 3$ m/s results in a relative frequency change of only 10^{-8} , or one part in one hundred million. Instead of measuring the fringe frequency directly, the fringe pattern is measured around an optical path difference where the modulated signal is most sensitive to wind speed, which is similar to the stepped Michelson technique used by WINDII. The MIGHTI optical path difference center is about 5 cm or about 8.5×10^4 times the wavelengths of the targeted emission lines, so that the fringe phase change caused by a wind velocity of $v = 3$ m/s is about $10^{-8} \times 8.5 \times 10^4 \times 2\pi \approx 5$ mrad or about 1/1000 of a fringe.

The MIGHTI interferometers were designed to simultaneously work for the oxygen red and green lines. In addition, the interferometer efficiently transmits the wavelengths around 762 nm, so that the wind and temperature measurements are made using the same optics and detector. To accommodate all three wavelengths, a field-widened DASH design was implemented using low order échelle diffraction gratings. The gratings were designed to work in 8th order for the green line, in 7th order for the red line and in 6th order for the oxygen A-band. Note that the A-band measurement does not rely on measuring interference fringes, since the band shape measurement is based on a radiometric, narrow band filter approach (Stevens et al. 2018; 2022). Details on the interferometer design and performance are discussed by Harlander et al. (2017).

Exit Optics

The exit optics are all the optical elements between the interferometer and the CCD detector, which is located immediately behind a mosaic filter, as shown in Figure 3.1.2.3. The purpose of the exit optics is to spatially separate the signal of the green line from the red and infrared components to form two separate images of the fringe localization plane on the CCD focal plane array. Lens L4 collimates the light from the fringe localization plane within the interferometer and forms an image of the Lyot stop on the dichroic mirror. The dichroic mirror

is a wedge shaped element that introduces an angular separation between the red/IR and green beams. Its first surface reflects the red beam components (red line and A-band) and transmits the green line signal. Its second surface, which is slightly tilted with respect to the first, reflects the green line signal. The first surface is plane and acts as a simple mirror. The second surface has a weak cylindrical shape to correct for the astigmatism introduced into the green beam by the thickness of the dichroic wedge. Mirror M4 redirects the beams toward the CCD. Lens L5 forms two images of the limb/fringe scene, one green and one red, on the focal plane array. The imaging is accomplished by collimating the signal from the dichroic wedge, which is an image of the entrance pupil and the Lyot stop. Thus, the beam onto the CCD is telecentric. Telecentricity makes the recorded fringe phase less sensitive to temperature drifts of the optical bench, since the first order effect of a camera misalignment in the direction of the beam does not change the fringe spacing (i.e., focus shift is not coupled to image magnification).

A mosaic filter containing seven narrow band interference filters, is located immediately in front of the CCD. Two filter elements provide narrow spectral filtering for the green and red line images, and the other five elements are for the determination of the A-band shape and the broad band near infrared (NIR) background signal. Three of the NIR channels are located within the spectral region of the A-band while two channels are at slightly shorter and slightly longer wavelengths.

Calibration Lamps - As with every interferometer, thermal effects are a potential concern. For MIGHTI, there are two different effects that need to be considered and mitigated. The first one is that thermal distortions of the structural hardware, such as the optical bench or the interferometer holder, could result in a shift of the image on the CCD detector. A lateral shift of the fringe image on the CCD is equivalent to a fringe phase shift and would therefore be interpreted as a Doppler shift. To detect and quantify lateral image shifts, a periodic notch pattern that is inscribed on one of the interferometer gratings is used (Harlander et al. 2017). Using this notch pattern, sub-pixel scale movements can be detected and corrected as demonstrated by Englert et al. (2010b).

The second effect is a phase change due to a change in the optical path difference in the interferometer which could be caused by a thermal change in index of refraction of the interferometer field widening prisms, the thermal expansion of the diffraction gratings, and/or stresses induced in the interferometer due to the differences in the coefficient of thermal expansion of the interferometer elements. A proven approach to quantify interferometer thermal drifts is to measure the fringe drift of calibration lamp lines that are spectrally close to the atmospheric red and green line emissions (Thuillier et al. 1998; Englert et al. 2010b). The measured calibration line phase drifts directly track the equivalent phase drifts of the atmospheric signal. Note that the thermal phase drift due to the drift in image location on the CCD is a function of the spatial frequency of the recorded fringe pattern, which can be significantly different for the atmospheric and calibration lines, whereas the phase drifts originating from the interferometer are a function of the wavelength of the emission lines, which is chosen to be virtually identical for the atmospheric and calibration lines. Therefore,

both the grating notches and calibration lamp signals are needed to unambiguously quantify and correct for all thermal drifts in the data analysis.

The on-board calibration lamps at 630.48 nm (neon) and 557.03 nm (krypton) provide two spectrally narrow emission lines that are close in wavelength to the oxygen red and green lines respectively and are used on-orbit to track and quantify thermal drifts of the interferometer. Both of these lines have been used successfully in previous instruments such as WINDII and REDDI (Shepherd et al. 1993; Englert et al. 2012).

CCD Camera - MIGHTI uses two actively cooled CCD cameras based on the e2v CCD42-80 back illuminated detector chip (e2v technologies 2006). The CCD features a multiband antireflection coating to maximize quantum efficiency and is cooled to -40°C or below to minimize dark current. The 2048×4096 pixel format sensor has a pixel pitch of $13.5 \mu\text{m}$ and is used in frame transfer mode to avoid a mechanical shutter. Each MIGHTI sensor uses an identical camera head. The CCD is oriented so that the frame transfer direction is parallel to the limb, which minimizes the transfer of pixels with low signal, e.g., at the top of the airglow layer, through areas of high signal, e.g., the maximum of the path integrated airglow layer. CCD cooling is achieved using a thermoelectric cooler (TEC). The excess heat from the hot side of the TEC is conducted to a double-sided radiator via an ammonia filled heat pipe. The camera heads are fitted with vacuum windows so they can be evacuated in the laboratory and cooled to -40°C . This feature allows flight like test conditions on the ground without placing the entire instrument into a vacuum chamber. In addition, the polarity of the TEC can be reversed to heat the CCD to remove condensed contaminants on its surface on-orbit, if necessary.

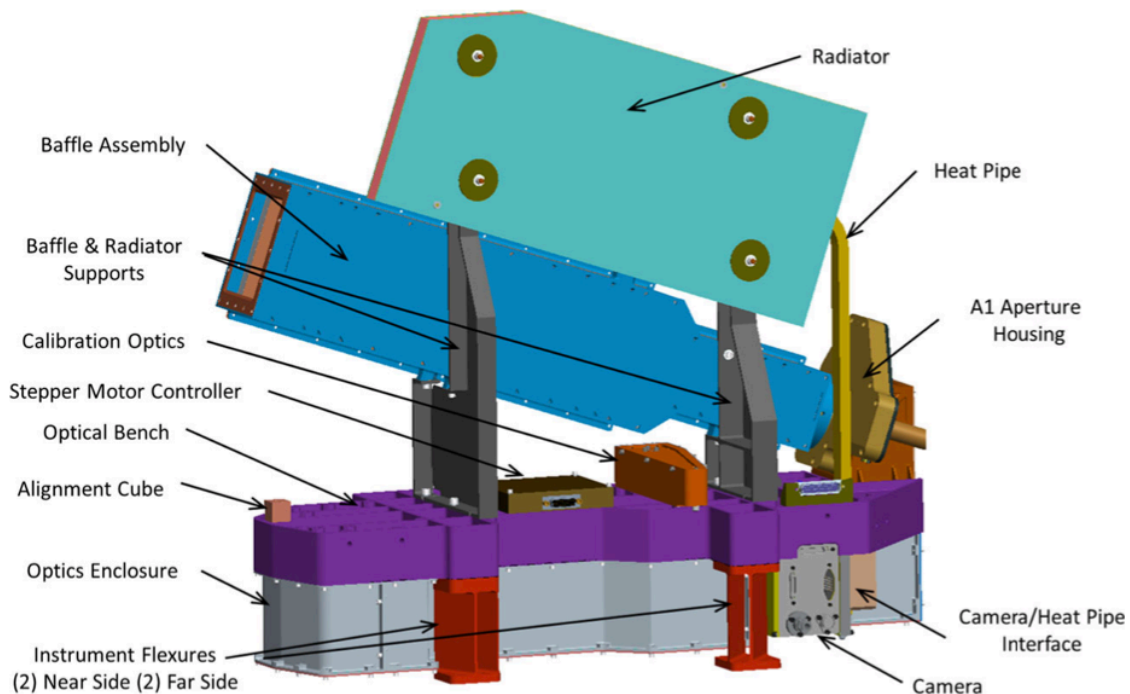


Figure 3.1.2.2 Schematic of a single MIGHTI sensor unit

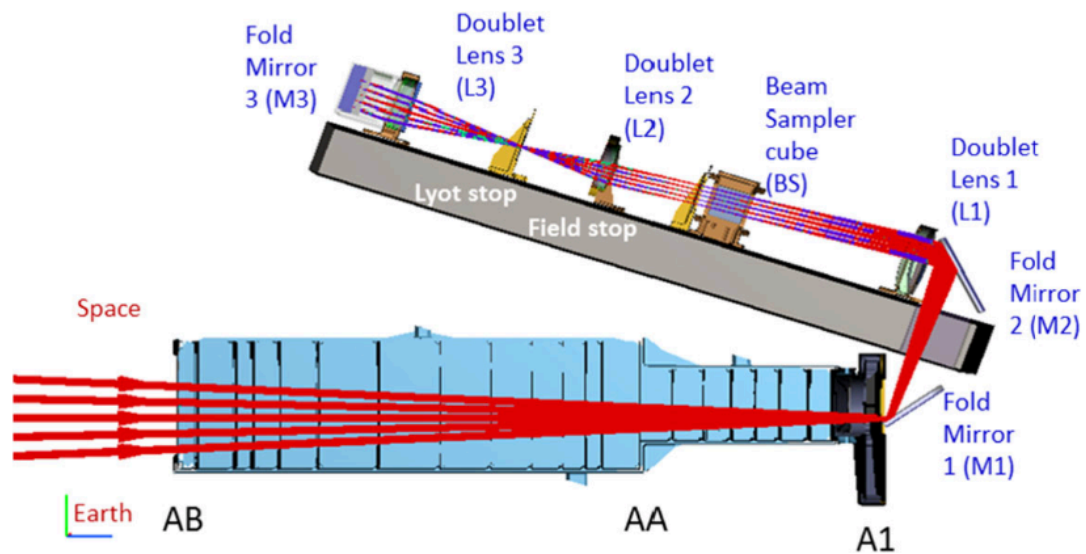
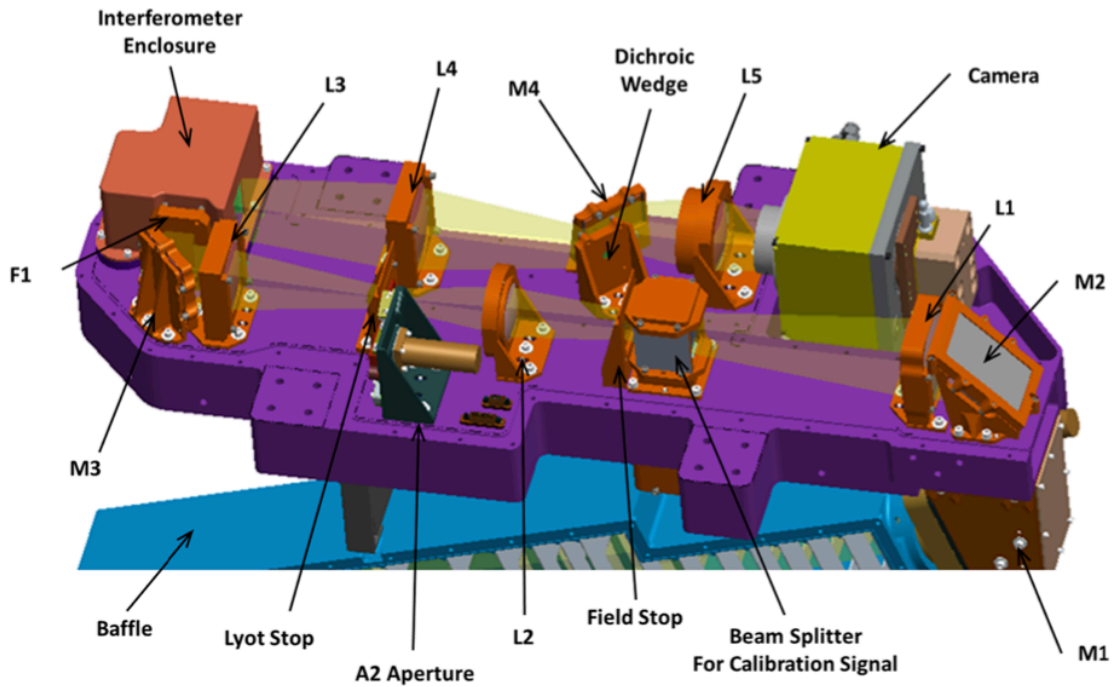


Figure 3.1.2.3 Key elements on the optical path through MIGHTI. MIGHTI optical bench (purple) populated with all optical elements. L denotes lenses, M denotes mirrors, F denotes interference filters. Geometry of MIGHTI baffle stray light model. Rays shown are for the A1 15% position.

Known issues due to external factors that could impact any long-term comparison or analysis (e.g., optical distortion due to gradual radiation degradation) should be captured.

MIGHTI does not use any consumables, other than electric power, so that consumable consumption is not a factor for instrument life expectancy, except the long term effect of S/C power generation, which is discussed elsewhere.

Most MIGHTI calibrations are continuously updated using on-orbit data, such as the thermal phase drift, the dark current and warm/hot pixel removal and correction, and the zero wind calibration [Englert et al., 2022].

The three main long term effects that are currently being monitored, and potentially mitigated, during an extended mission are (1) the imaging detector row-to-row flat field cross calibration, (2) the radiation-induced increase in dark current, and (3) a growing systematic phase shift at low signal levels.

The imaging detector row-to-row flat field cross calibration is critical for the Abel-type inversion of the MIGHTI wind and temperature data [Englert et al., 2017; Harding et al., 2017; Stevens et al., 2018; Stevens et al., 2022]. For the wind retrieval, the MIGHTI data analysis uses pre-flight laboratory flat field measurements and the temperature retrieval uses flat field data that is based on both pre-flight and on-orbit data. A long-term change in the flat field data could occur as a result of radiation induced, inhomogeneous darkening of MIGHTI optical elements. For the wind measurements, this effect can be assessed using the on-board calibration lamps and, up to this point in time, no significant change in the row-to-row cross-calibration has been observed. Given that the MIGHTI optical elements are fabricated using largely radiation-hard glasses, this is as-expected. A further mitigating factor is the fact that most MIGHTI optical elements are out-of-focus at the imaging detector, so that any non-homogeneous darkening of optical elements would result in an overall decrease in responsivity, which only results in a signal-to-noise impact on the retrieved Level 2 data, rather than systematic retrieval uncertainties.

The radiation-induced increase in dark current is a well-known and expected effect that is exhibited by Charge Coupled Devices (CCDs) in low earth orbit [Englert et al., 2017]. The on-orbit radiation environment generally causes all CCD pixels to produce more dark current versus time, due to the damage done to the detectors crystal-lattice structure. In addition, severe damage to the pixel can cause it to produce an excessive amount of dark current, which then leads to the creation of warm and hot pixels. Figure 3.1.2.3 shows the increase in observed dark counts versus time for MIGHTI-A 60s dark exposures. The curves show the counts in analog-digital-converter units (ADU) at the 50% (median), 75%, and 95% percentiles, for the typical MIGHTI binning of 2 x 16 pixels. For comparison, the full dynamic range of a binned MIGHTI pixel is 16-bit or approximately 65,500 counts. MIGHTI-B shows similar behavior.

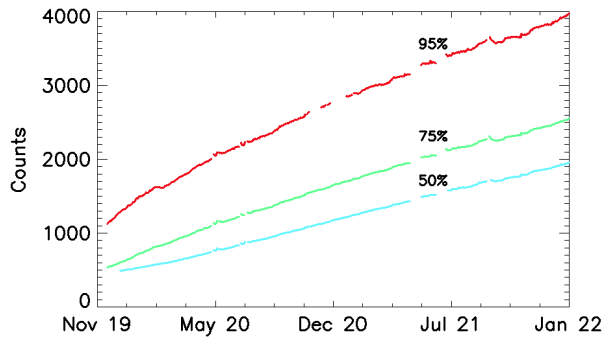


Figure 3.1.2.3: Evolution of MIGHTI-A CCD dark current. (see text for details)

The dark field is continuously measured on-orbit using every-day, routine dark measurements (closed aperture). These “current” data are used for the dark current correction of the data. The main effects of increased dark current are increased shot noise, yielding an increase in uncertainty in the level 2 data, and the increased uncertainty in the notch-fitting, which is part of the thermal phase drift correction [Englert et al., 2022]. At the time of writing this document, the increased dark current has not yet increased the uncertainty of the on-orbit data enough to violate mission requirements.

An effective way to mitigate the increase in dark current is annealing the CCD on orbit. Annealing the CCD involves the temporary increase of the CCD temperature, which results in the “repair” of lattice defects and thus the decrease in dark current. MIGHTI was designed with the option to reverse the polarity of the thermoelectric CCD cooler, so that the Peltier element heats the CCD to a controlled temperature value. The ICON team will consider annealing the MIGHTI CCDs, once the dark current increase is expected to impact the data quality beyond the mission requirements. Similar on-orbit annealing processes have been performed previously for imaging detectors, e.g. on the NASA Hubble Space Telescope and the NRL EIS instrument on the NASA/JAXA Hinode mission.

The last long-term effect is the so-called “low-signal phase shift.” As limb observations were obtained over a range of limb brightnesses it became apparent that there was a systematic shift in fringe phase with signal on the detector that was determined to be characteristic of the instrument rather than geophysical. Once this effect was noticed in 2021, special observations of the on-board calibrations lamps have been made with eight different exposure times to produce different signal levels. Figure 3.1.2.4 is a plot of the MIGHTI-A neon fringes from these calibration lamp-only measurements obtained on January 2, 2022. The different colors correspond to the exposure time of the observation bracketed by the red curve at 240 seconds and blue curve at 2 seconds. The vertical axis is in ADU per second which normalizes each of the curves to exposure time. Each of the curves has approximately the same mean value near 70 ADU/sec indicating the expected brightness scaling with exposure time. Since the wavelength of the calibration lamp does not change, one would expect each of these fringes to have the same phase. However, as the exposures become shorter (less signal) there is clearly a progressively larger phase shift and a decrease in fringe amplitude. Since these measurements

were obtained with the calibration lamps the phase shift and amplitude reduction is purely an instrumental effect. The cause is under investigation but these results indicate the shift is consistent with a linear smearing of the fringes, perhaps in the readout process, that affects the faint, short exposures (blue curve) more than the bright, longer exposures (red).

Although the root cause is still under investigation we have implemented a correction for this effect based on both the limb and calibration lamp measurements. The correction is slightly different for MIGHTI-A, MIGHTI-B, day and night but in all cases is determined from measured phase shifts with signal level. The correction curves asymptotically approach zero at the brightest signal levels, indicating that the brightest signals (e.g., those in the prime science region for tidal retrievals from 95-105 km) are unaffected. To account for the time dependence, the correction increases linearly in time from the start of the mission. The uncertainty associated with the correction is estimated to be 40% of the correction and is reported in the data files. We will continue to monitor this effect going forward using limb observations and periodic characterization using special calibration lamp observations and adjust the correction as needed. If CCD annealing is performed, the impact on the low-signal phase shift will be specifically evaluated using the calibration routine described above.

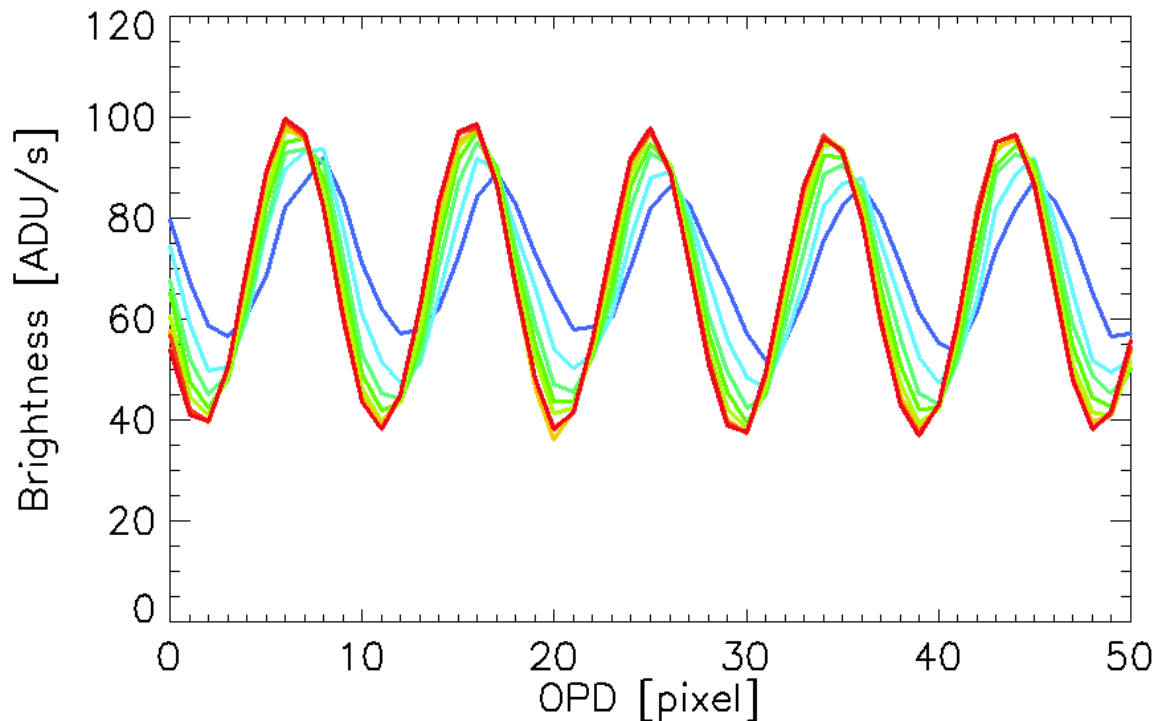


Figure 3.1.2.4: The phase shift seen in the calibration lamp fringes as the signal level changes. The measurements were made on January 2, 2022. The colors represent different exposure times (brightnesses) bracketed by red at 240 seconds and blue at 2 seconds. For clarity, only about one eighth of the row is plotted, and measured fringes are scaled by the exposure time.

3.1.3 Instrument Observation Requirements

This subsection summarizes the required observation parameters of the instrument. Not applicable for in situ measurements.

Table 3.1.3.1 describes the Observation Requirements that MIGHTI must meet, the ranges and times over which these must be met in order to meet the L1 requirements in the PLRA.

Attribute	Value
Winds	
Geophysical Quantity	Horizontal component of the neutral wind as a function of altitude, in cardinal directions (North, East).
Tangent Altitude Range	Daytime 95 – 280 km Nighttime 95 – 105 km and 220 – 280 km
Tangent Altitude Resolution	5 km below 150 km 30 km above 150 km
In-track sampling	500 km
Temporal Cadence Required	1 minute
Temporal Coverage	18 total hours of solar local time including all times between local sunrise and sunset
Precision	16.6 m/s
Dynamic Range	±250 m/s
Temperature	
Geophysical Quantity	Neutral temperatures as a function of altitude
Tangent Altitude Range	95 – 105 km
Tangent Altitude Resolution	5 km
In-track sampling	500 km
Temporal Cadence Required	1 minute
Temporal Coverage	18 total hours of solar local time including all times between local sunrise and sunset
Precision	23.4 K

Table 3.1.3.1 – Summary of the L1 MIGHTI Observation Requirements

3.1.4 Instrument Observation Capabilities

This subsection summarizes specific instrument parameters, such as number of detectors, field of view, wavelengths measured, time resolution, data rate, etc. Specify measurement capabilities for in situ instruments.

Table 3.1.4.1 describes key characteristics of the MIGHTI instrument and the observations it provides. Additional details can be found in Engler *et al.*, 2017 (doi:10.1007/s11214-017-0358-4).

Observation Parameter	Value
Observables	1 Doppler shift of 577.7 nm (green) airglow 2 Doppler shift of 630.0 nm (red) airglow 3 Shape of 762 nm (A-band) airglow band
Number of units	2 orthogonally mounted units (A&B), providing measurements at 45 and 135 degrees to ram
Number and Type of Detectors	1 CCD detector per unit, 2k x 2k active pixels with nominal 16 x 2 (vertical, horizontal) pixel binning on orbit
Field of View	5.36° vertical x 3.22° horizontal
Total Etendu AΩ	0.0495 cm ² sr (Night) 0.0074 cm ² sr (Day)
Interferometer optical path ± difference interval	Red 5.41 +/- 0.49 cm (A & B) Green 5.58 +/- 0.50 cm (A & B)
Monochromatic Interferometer Fringe Contrast	Red Day 78% (A); 78% (B) Red Night 73% (A); 72% (B) Green Day 78% (A); 85% (B) Green Night 75% (A); 83% (B)
A-Band pass-bands	3 channels in-band, 2 out of band, each with a full width half maximum of 2 nm
Pointing Stability	142 arcsec
Pointing Knowledge	86 arcsec
Exposure time	30s (Day) 60s (Night)

Table 3.1.4.1 MIGHTI Instrument Characteristics

Table 3.1.4.2 describes the measurement characteristics for MIGHTI, in terms of the geophysical quantities it is used to derive (winds and temperatures). For further details on the in-flight observations of the winds, see Englert *et al.*, [2022]. For further details on the in-flight observations of the temperatures see Stevens *et al.*, [2022] (Stevens, M.H. et al., Temperatures in the Upper Mesosphere and Lower Thermosphere from O2 Atmospheric Band Emission Observed by ICON/MIGHTI, submitted to Space Science Reviews, 2022.).

Attribute	In-flight Performance (Prime Mission)
Winds	
Geophysical Quantity	Horizontal component of the neutral wind as a function of altitude, in cardinal directions (North, East).
Tangent Altitude Range	Daytime: Exceeding 95 – 280 km Nighttime: Exceeding 95 – 105 km and 220 - 280 km
Tangent Altitude Resolution	Daytime: 2.9 km between 95 – 170 km; 30 km between 170 – 300 km

	Nighttime: 2.9 km between 95 – 110 km; 30 km between 170 – 300 km
In-track sampling	240 km daytime 480 km nighttime
Temporal Cadence	30s daytime 60s nighttime
Temporal Coverage	> 18 total hours of solar local time including all times between local sunrise and sunset, only limited by mode changes, calibrations, SAA and low airglow brightness, predominantly at the terminator
Precision	<16.6 see Figure 2.2.5 and CMAD for details, including variations with altitude
Dynamic Range	±250 m/s
Temperature	
Geophysical Quantity	Neutral temperatures as a function of altitude
Tangent Altitude Range	Day 90 – 127 km Night 90 – 108 km
Tangent Altitude Resolution	3.5 km Full width half max
In-track sampling	480 km
Temporal Cadence	30s daytime 60s nighttime
Temporal Coverage	24 total hours of solar local time including all times between local sunrise and sunset
Precision	Day <1K over 95 – 105 km (required altitude range) Night <1K over 95 – 105 km (required altitude range)

Table 3.1.4.2 Geophysical quantities derived from MIGHTI observations.

3.1.5 Data Acquisition

This subsection describes what data is obtained by the instrument, how it's obtained, any variation in data acquisition modes, etc.

MIGHTI data acquisition includes science data and periodic calibration data. The science data consists of 30s exposures during the day with a partially closed aperture to maximize stray light rejection and to limit the signal on the CCD, and 60s exposures during the night, with a fully opened aperture. Calibration measurements consist of periodic dark exposures with a closed aperture, calibration-lamp-only exposures, and calibration orbits, for which the CCDs are illuminated by both the calibration lamp and the atmospheric signal [Englert et al., 2017].

Figure 3.1.5.1 shows four typical, raw MIGHTI exposures of the Earth's limb in false color. The vertical dimension of the images is equivalent to tangent height in the atmosphere, ranging from approximately 90 km on the bottom to 300 km on the top. The horizontal dimension is equivalent to the optical path difference in the interferometer, which produces the fringe

modulation. The observed limb scene is imaged onto the CCD in both dimensions, so that features within the scene, such as stars, are in focus at the CCD. Panel A shows a daytime image with an integration time of 30 seconds, containing only airglow signal. On the left and top right of panel A, are the signals from the atomic oxygen green and red airglow lines, respectively. On the bottom right are the five separate filter areas for the multi-spectral measurement of the molecular oxygen A-band and the associated background [Stevens et al.; 2022] to retrieve temperature profiles. Panel B shows a typical nighttime exposure, with the narrow, lower nighttime thermospheric green line layer and a bright star within the field of view. The star's signal creates a line, due to the change in MIGHTI attitude with respect to the inertial frame during the 60s integration time. Panel C shows an exposure for which aperture A1 blocks all light from the atmosphere, and the calibration lamps are turned on. The illumination of the detector areas for the green and red calibration lines is nearly homogeneous, revealing the grating registration marks, or notches, on the top edge of the images. Panel D shows a daytime exposure containing both airglow and calibration signals. Especially for the red signal, one can easily see the beat-pattern of the two fringe patterns with different spatial frequencies. The dynamic range of the color scales in each image is not the same, but adjusted to avoid saturation. The speckles seen in all four images of Figure 3.1.5.1 and that are confined to one or a few binned pixels are due to hot pixels of the CCD, or signal generated by cosmic rays that pass through the FPA during the exposure.

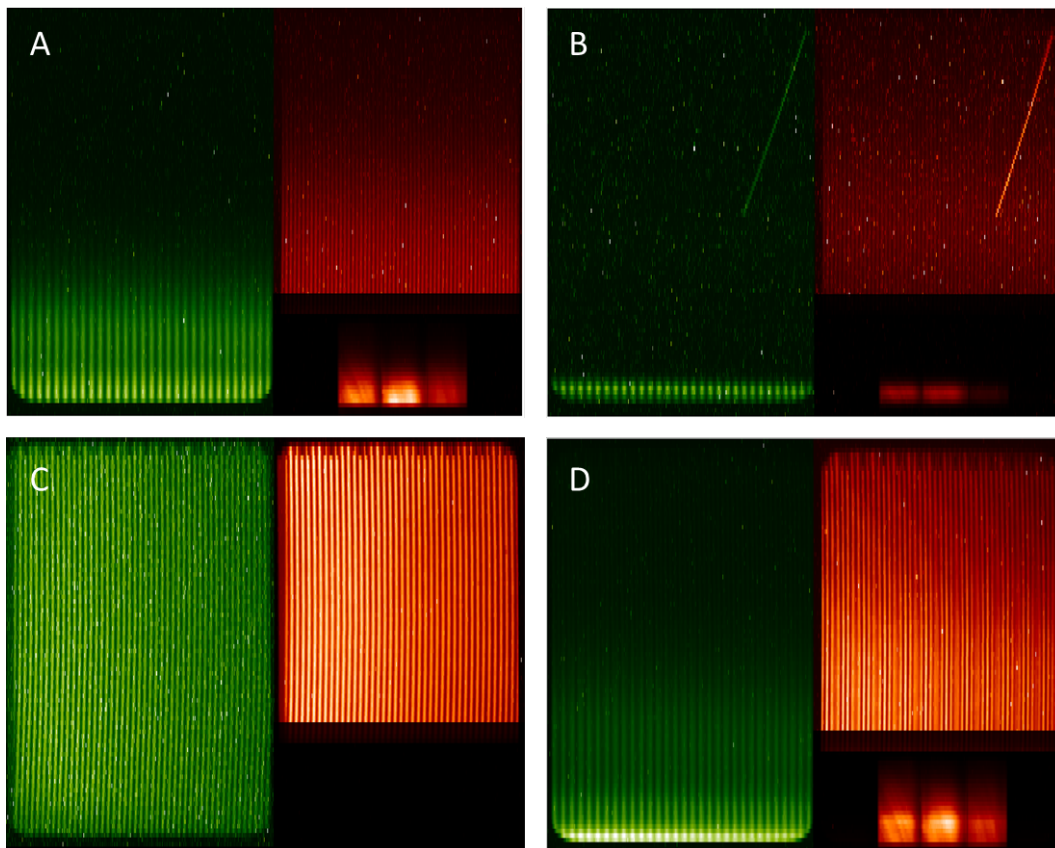


Figure 3.1.5.1: Sample on-orbit exposures. (A) MIGHTI-A, daytime, atmosphere signal only; (B) MIGHTI-A, nighttime, atmosphere signal only, with signature of a bright star; (C) MIGHTI-B, calibration signal only; (D) MIGHTI-A, daytime, atmosphere and calibration signals.

The information on the Doppler wind speed at the tangent point height is contained in the phase of the interference fringe at the respective row [Englert et al., 2007, 2017; Harding et al., 2017]. However, instrumental effects such as thermal drifts can also shift the fringe phase, so great care must be taken to isolate the wind speed information in the observed phase shift.

The Doppler shift of the airglow signal results in only a small change in phase. For the red line it is about 1.8 mrad for every 1 m/s in wind speed, or one thousandths of a fringe for every 3.5 m/s. Therefore, small thermal changes in the instrument, which can result in phase changes of similar magnitude have to be monitored and removed in the data processing [Englert et al., 2017, 2022].

3.2 Ion Velocity Meter (IVM)

3.2.1 Instrument Measurement Requirements

This subsection summarizes the required measurement parameters of the instrument.

Table 3.2.1.1 describes the key observable quantities that IVM must observe, the ranges and times over which these observations must be made. These describe the in situ observations needed to meet the L1 observation requirements described in Section 3.2.3.

Measurement Parameter	Value
Parameter Measured	Arrival angle and in-track velocity of in situ plasma
Geomagnetic Range	Within $\pm 10^\circ$ of the geomagnetic equator
In-track sampling	250 km
Temporal sampling	32 seconds
Temporal Coverage	Over a range from local sunrise to local midnight

Table 3.2.1.1 – Summary of the IVM Instrument Measurement Requirements

3.2.2 Instrument Description

This subsection describes the primary scientific objectives of the instrument, its hardware, physical configuration, etc.

The Ionospheric Connections Explorer (ICON) mission is poised to discover fundamental connections between the dynamics of the neutral atmosphere at altitudes between 100 km and 300 km and the charged particle motions at low and middle latitudes, which are tied to the magnetic field that threads the entire region.

These measurements will be made from a circular orbit at an altitude near 575 km with 27° inclination using a unique ability to image, at higher latitudes on the limb, that part of the neutral atmosphere that drives the current, and is connected along the magnetic field to the satellite location where the resulting plasma motions can be observed. The in-situ ion drift motion can be translated to all points along a magnetic flux tube under the assumption that magnetic flux lines are electric equipotentials. The neutral winds however, must be measured as a function of altitude and weighted by the electric conductivity in order to determine their influence on the plasma motion. By making the required measurements of plasma drifts, neutral winds, neutral density and plasma density, their contribution to the observed plasma motions can be resolved utilizing a suite of ionosphere and thermosphere models.

In-situ determination of the plasma density and plasma drift are made by an Ion Velocity Meter (IVM), a planar detector that views approximately along the spacecraft velocity vector and measures the energy and the angle of arrival of the thermal ions that move supersonically with respect to the spacecraft. Two IVM sensors, one that views along the ram and another along the anti-ram, allow measurement of the ion drift when the remote instrument suite either views the limb perpendicular to the satellite track to the north or the south.

The ICON IVM instrument performance is bolstered by design advancements that include the following. The inclusion of a proven sensor potential (SenPot) reference plate and circuit ensures that instrument-sensing circuits operate near the plasma potential, providing protection against the effects of spacecraft ground bias. The current sensing circuit resolution is improved by a factor of 4 over the previous design. Noise levels are reduced by a number of circuit design improvements. A number of command and configuration advancements provide additional on-orbit flexibility and capability, including fully programmable retarding voltage sweep levels, on-orbit electrometer gain calibration and improved drift meter switch modes.

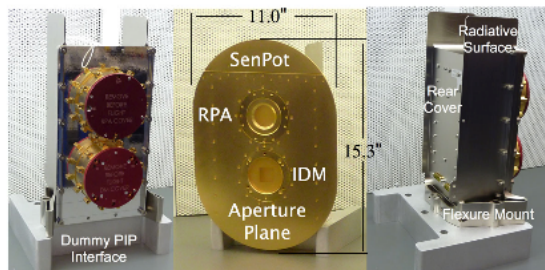


Figure 3.2.2.1 Photographs of the ICON IVM show the mounting configuration of the RPA and IDM and a segment of the aperture plane (SenPot) utilized to establish a floating ground reference potential with respect to the plasma. The aperture plane is removed in the photographs to the *left* and *right*

This subsection lists the major elements of the instrument and provides a schematic of the conceptual design.

The two sensors of IVM are shown in Figure 3.2.2.2. The key elements include the RPA, IDM and a repeller grid, each of which is outlined below.

Figure 3.2.2.1 has three panels showing a photograph of the flight IVM sensor and projections that detail the major mechanical systems. The ICON IVM consists of two planar sensors. A retarding potential analyzer (RPA) and an ion drift meter (IDM) are mounted to view approximately along the spacecraft velocity vector and are optimally configured to accomplish the separate functions of constituent ion energy determination and ion arrival angle respectively. The sensors are attached to a baseplate to which the electronics compartment is affixed at the rear. The rear cover is attached to a flexure mount that provides a mechanical interface to the spacecraft payload interface plate (PIP). The rear cover also contains passive radiator surfaces. In low earth orbit the spacecraft velocity V_s , is in excess of 7 km s^{-1} and provides the constituent ions with mass dependent ram energies $\frac{1}{2} m V_s^2$, of about 0.3 eV/amu and thermal energy widths $m V_s V_{t h}$, where $V_{t h}$ is the ion thermal speed, of about $0.4 \text{ eV/amu}^{1/2}$ with respect to the sensor.

In order to minimize the effects of the sensors themselves on the plasma, it is important that the local electrostatic environment present small and planar potentials parallel to the instrument aperture plane so that the ion arrival angle and energy distribution are modified in a predictable way by electric fields that are parallel to the sensor look direction. A planar conducting aperture plane, which surrounds the instrument apertures, is utilized to accomplish this task. It is attached to the sensors from the front and also provides key radiative surfaces to dissipate instrument and solar heat inputs. Optimum sensitivity to arrival angle and incident energy is also obtained if the sensor ground reference is maintained near the plasma potential.

The spacecraft reference ground with respect to the plasma is dependent on the conducting properties of the spacecraft exposed surfaces and to exposed potentials that may be part of the solar power system. While best practices are employed to maintain a spacecraft ground close to the plasma potential, the IVM sensors are electrically isolated from the spacecraft to provide an independent ground reference that is established by a section of the aperture plane called the SenPot surface, which is maintained at the floating potential.

Figure 3.2.2.2 shows schematic cross-sections of the RPA and IDM sensors. Each is constructed similarly, consisting of a gridded aperture plane and a series of internal planar grids that are precisely positioned using ceramic spacers to maintain parallel potential planes that are biased to provide the appropriate functionality. In both sensors the woven grids are $0.001''$ diameter gold-plated tungsten wire with a density of 50/inch or 100/inch.

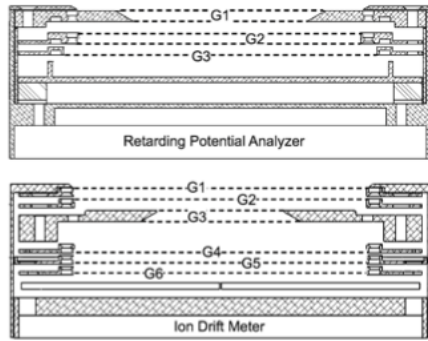


Figure 3.2.2.2 Schematic cross sections showing grid configurations for the Retarding Potential Analyzer and the Ion Drift Meter

Referring to Fig. 3.2.2.2 the RPA presents a gridded circular entrance aperture G1, of radius 2 cm, tied to the sensor ground and a solid collector at which the ion flux is measured as a current. The grid G2 is a double retarding grid that is stepped through a series of positive potentials to control the energy of incoming ions that have access to the collector. A suppressor grid, G3, is negatively biased with respect to the sensor ground to reject thermal electrons incident on the grid and to suppress photoemission currents that are produced from the collector. The grid stack transparency is $\approx 48\%$ giving an effective collection area of $\approx 6 \text{ cm}^2$.

Retarding Potential Analyzer (RPA)

The RPA views approximately along the spacecraft velocity vector and has a small entrance aperture compared to the collector size. Within the instrument a retarding grid is stepped through a sequence of potentials between 0 and 25.5 volts, which determine the energy of the incoming ions that have access to the collector. For the low inclination ICON orbit near 600 km altitude, the plasma drift velocities are expected to be less than 500 m s^{-1} and the total plasma density will usually be above 10^3 cm^{-3} except perhaps in equatorial plasma bubbles. Further, during normal operations the spacecraft will maintain a look direction for the IVM that is within 3° of the ram velocity. Under such conditions we do not expect any departures from thermal equilibrium in the plasma and the angle of arrival of the ions will be small ($<10^\circ$) compared to the angular acceptance of the sensor ($>30^\circ$). Thus, the current collected may be simply obtained by integrating the one-dimensional flowing Maxwellian distribution function along the instrument look direction from infinity to the velocity of the ions that will be stopped by the potential on the grid as seen by the plasma. The current for a single ion species of mass m and number density N_i is given by

$$I(\phi) = q A_{\text{eff}} \frac{N_i}{2} V_r \left(1 + \text{erf}(\beta f) + \frac{1}{\sqrt{\pi} \beta V_r} \exp(-\beta^2 f^2) \right)$$

where A_{eff} is the effective area of the collector, $f = V_r - (2q\phi/m)^{0.5}$, with q the electron charge, represents the average velocity of the ions that have access to the collector and $\beta = (m/2kT_i)^{0.5}$ is the reciprocal of the thermal velocity of the ions. Here, $V_r = (\mathbf{V}_d + \mathbf{V}_s) \cdot \hat{n}$ is the total velocity of the ions given by the sum of the ambient ion drift \mathbf{V}_d and the spacecraft velocity \mathbf{V}_s and \hat{n} is the unit vector along the sensor look direction. $\phi = R_V + \psi_s$, is the potential on the grid as seen by the plasma and is thus the sum of the retarding potential with respect to the sensor ground and the sensor ground potential with respect to the plasma ψ_s . The measured current will be the sum of currents for all constituent ions that are present. The current at zero retarding potential provides the total plasma number density and a least-squares fitting procedure, applied to the normalized current-voltage characteristic, yields a common temperature, a bulk flow velocity for the ions and the fractional population of the major constituent ions. In addition, the sensor plane potential with respect to the plasma is also retrieved. Corrections to account for the lack of perfect potential planes produced by wire grids are also included in the fitting procedure.

Ion Drift Meter (IDM)

The IDM also views approximately along the spacecraft velocity vector and uses a simple geometric relationship between the arrival angle of the incoming ion beam and the area illuminated, and thus the current collected, at the collector segments. During their transit from the ambient medium to the collector the ions change their energy due to the aperture plane potential and are displaced from straight-line trajectories by the negative suppressor potential. Since both the entrance aperture and the collector are at the same potential, no change in the ion arrival angle occurs. However a displacement in the beam that is dependent on the arrival angle is produced by the potential on the suppressor grid. The collector quadrant dividing lines and aperture edges are aligned with the local horizontal and the local vertical so that by appropriately configuring collector halves, the arrival angle in each of these planes containing the unit vectors \hat{h} and \hat{z} respectively, can be measured. If the arrival angle of the plasma in one of these planes is given by α , then the ratio of the collector currents, which are each proportional to the area illuminated, is given in terms of the sensor dimensions and the arrival angle by

$$\frac{I_1}{I_2} = \frac{W/2 + D \tan \alpha}{W/2 - D \tan \alpha}$$

where W is the length of the square aperture and D is the depth from the external aperture face to the collector. Thus by measuring the current ratio we may determine the ion arrival angle. The corresponding transverse drift velocity is given by

$$(\mathbf{V}_d + \mathbf{V}_s) \cdot \hat{\mathbf{t}} = \sqrt{V_r^2 - \frac{2q\psi_s}{m} \tan \alpha}$$

where $\hat{\mathbf{t}}$ is the unit vector along the selected transverse direction. The arrival angle is corrected for the displacement of the beam produced by the suppressor grid by accounting for the acceleration and deceleration of the ions during their transit to the collector. In addition, the suppression of photoemission currents from the collector can lead to some current exchange between the collector halves and correction procedures to account for this effect are also applied.

The IVM provides the ion drift with respect to the sensor in the sensor frame of reference. In order to translate this measurement into an inertial frame of geophysical significance, it is necessary to remove the spacecraft velocity in the instrument reference frame and to translate the instrument reference frame to an inertial frame. This procedure requires knowledge of the instrument pointing with respect to the spacecraft reference frame and knowledge of the inertial attitude of the spacecraft reference frame. Precise mounting knowledge to within 0.01° is achieved using a laser tracker and spherical mounted reflectors, while the spacecraft attitude control system maintains a ram pointing configuration within 3° for IVM during normal operations. A sophisticated spacecraft attitude determination system provides the inertial pointing directions of the spacecraft reference axes with an accuracy of 0.01° .

The IDM presents a square aperture, with side length 2.8 cm, to the incoming plasma. The grids G3 and G4/G5 are grounded, providing a field-free region through which the supersonic ions flow before forming an image of the aperture on a segmented collector. A suppressor grid G6 is negatively biased between 0 and -10.5 volts with respect to the sensor ground to reject thermal electrons incident on the grid and to suppress photoemission currents that are produced from the collector surfaces. The collector, located 1.65 cm from the aperture edge, is divided into four quadrants with the dividing lines parallel to the aperture edges allowing currents to collector halves to be measured along two mutually perpendicular axes. The grid stack transparency is $\approx 49\%$.

Repeller grid

The grid G1 forms a grounded plane across the aperture while a repeller grid G2 is positively biased between 0 and $+3.5$ volts with respect to the sensor ground. This grid serves to reject the admission of H^+ ions prior to the collimation of the beam produced by the entrance aperture. The removal of this signal allows the arrival angle associated with the bulk flow of all the species to be determined by the signal from the supersonic O^+ ions.

Known issues due to external factors that could impact any long-term comparison or analysis (e.g., optical distortion due to gradual radiation degradation) should be captured.

IVM does not use any consumables other than electric power. Long-term changes in instrument electronics from spaceflight have yet to impact the instrument in any level that can be seen in the data. Issues related to low densities and photoelectrons described in Section 2.2 do vary with time, and generally decrease with increasing solar UV flux. It is thus expected that the data from IVM will continue to improve as we move towards solar maximum. Long term offsets to the drifts, applied as a calibration step between Levels 1 and 2 described in the CMAD keep track of the instrument’s calibration, and are suitable for such long-term analysis.

3.2.3 Instrument Observation Requirements

This subsection summarizes the required observation parameters of the instrument. Not applicable for in situ measurements.

Table 3.2.3.1 describes the Observation Requirements that IVM must meet, the ranges and times over which these must be met in order to meet the L1 requirements in the PLRA.

Attribute	Value
Geophysical Quantity	In situ motion of the ionospheric O ⁺ plasma perpendicular to the local magnetic field in the local magnetic meridional plane (vertical ion drifts)
Geomagnetic Range	Within ±10° of the geomagnetic equator
In-track sampling	250 km
Temporal sampling	32 seconds
Temporal Coverage	Over a range from local sunrise to local midnight
Precision	10 m/s
Dynamic Range	±500 m/s

Table 3.2.3.1 – Summary of the L1 IVM Observation Requirements

3.2.4 Instrument Observation Capabilities

This subsection summarizes specific instrument parameters, such as number of detectors, field of view, wavelengths measured, time resolution, data rate, etc. Specify measurement capabilities for in situ instruments.

Table 3.2.4.1 describes key characteristics of the IVM instrument and the observations it provides. Additional details can be found in Heelis *et al.*, 2017 (DOI 10.1007/s11214-017-0383-3).

Observation Parameter	Value
Retarding Potential Analyzer	
Observables	Ion current as a function of retarding potential

Observation Parameter	Value
Retarding Potential Analyzer	
Number of units	1 each in IVM A and B
Number and Type of Detectors	1 metallic cathode plate and linear electrometer
Field of View (angular acceptance)	30°
Effective Collection area	6 cm ²
Potential range, steps	32 steps over 0 – 25.5 V
Potential dwell time	32 milliseconds
RV uncertainty	3 mV
Ion Drift Meter	
Observables	Ratio of ion currents on four collectors
Number of units	1 each in IVM A and B
Number and Type of Detectors	4 metallic cathode plates and logarithmic electrometer
Field of View (angular acceptance)	30°
Sample rate	Variable 8 and 16 Hz
Arrival angle error	0.02°

Table 3.2.4.1 IVM Instrument Characteristics

Table 3.2.4.2 describes the measurement characteristics for IVM, in terms of the geophysical quantities it is used to derive (drifts, densities). For further details on the in-flight observations see Heelis *et al.*, [2022].

Attribute	Value
Vertical Ion Drifts	
Geophysical Quantity	In situ motion of the ionospheric O ⁺ plasma perpendicular to the local magnetic field in the local magnetic meridional plane (vertical ion drifts)
Geomagnetic Range	Within ±15° of the geomagnetic equator
In-track sampling	8 km
Temporal sampling	1 second
Temporal Coverage	Over a range from before local noon to after local midnight – see Section 2.2 for further details
Precision	7.5 m/s
Dynamic Range	±500 m/s
In Situ Ionospheric Density	
Geophysical Quantity	Total ion number density
In Situ Ion Composition	
Geophysical Quantity	O ⁺ / H ⁺ ratio

Dynamic Range (O ⁺ concentration)	0 – 100%
Accuracy	±2 %
In Situ Ion Temperature	
Geophysical Quantity	Ion Temperature
Dynamic Range	400 – 8000 K
Accuracy	±100 K

Table 3.2.4.2 Geophysical quantities derived from IVM observations.

3.2.5 Data Acquisition

This subsection describes what data is obtained by the instrument, how it's obtained, any variation in data acquisition modes, etc.

Data is collected by the two sensors (RPA and IDM). The IVM instrument collects data continuously while in science mode. There is no variation in data acquisition modes for IVM. The operation of both sensors does not change between any modes – both collect data continuously in their only operating mode. Voltage sweeps etc. are described in more detail above. The RPA produces current-voltage characteristics at a 1 Hz rate and the IDM alternates between horizontal and vertical components at 8 Hz. Drifts and densities are reported at a 1 second cadence in higher level products.

3.3 Far Ultraviolet imaging spectrograph (FUV)

3.3.1 Instrument Measurement Requirements

This subsection summarizes the required measurement parameters of the instrument.

Table 3.3.3.1 describes the key observable quantities that FUV must observe, the ranges and times over which these observations must be made. These provide the remote sensing observations needed to meet the L1 observation requirements described in Section 3.3.3.

Measurement Parameter	Value
Daytime	
Parameter Measured	Airglow brightness of the O 135.6 nm and a portion of the N ₂ Lyman Birge Hopfield bands (LBH)
Tangent Altitude Range	Column-integrated, including 135 – 300 km
Tangent Altitude Resolution	<10 km
In-track sampling	500 km
Temporal Cadence Required	1 minute
Temporal Coverage	From local sunrise to local sunset
Nighttime	
Parameter Measured	Altitude-resolved brightness of O 135.6 nm airglow

Tangent Altitude Range	200 – 400 km
Tangent Altitude Resolution	20 km
In-track sampling	500 km
Temporal Cadence Required	1 minute
Temporal Coverage	From local sunset to local midnight

Table 3.3.1.1 – Summary of the FUV Instrument Measurement Requirements

3.3.2 Instrument Description

This subsection describes the primary scientific objectives of the instrument, its hardware, physical configuration, etc.

Primary Science Objectives: The ICON FUV instrument is designed to satisfy the following two principal requirements: to determine the altitude profile of ionospheric O⁺ density at nighttime through spatial imaging of the oxygen 135.6-nm FUV emissions; and to determine the daytime column density ratio of thermospheric O and N₂ using measurements of daytime 135.6 nm OI and LBH N₂ band FUV emissions. ICON FUV measures limb and sub-limb (on disk) optical intensities. These measurements have to be converted into altitude profiles of Volume Emission Rates (VER) of the emitting constituents and then the volume emission rates have to be inverted to density profiles of nighttime O⁺ density. The ratio of the sub-limb brightness of 135.6 and N₂ LBH are inverted to provide the daytime O and N₂ ratio. The required horizontal spatial resolution of the measurements was 500 km and an integration time of 60 seconds was assumed in these calculations.

The ICON FUV instrument spectral resolution needs to be adequate to resolve the 135.6 nm spectral line and measure its intensity. In addition it needs to measure the intensity of the LBH emissions of N₂ somewhere in the FUV spectral region. A moderate wavelength resolution instrument cannot separate the LBH at 135.4 nm from the 135.6 nm OI line and therefore a combined measurement of the two is made and the O/N₂ retrieval accounts for this and other LBH lines within the spectrometer's triangular transmission profile of the SW channel (see the ICON CMAD for further details). Another important spectral requirement is to eliminate the 130.4 OI spectral feature. The limb 130.4 emission is several times brighter than 135.6. Nevertheless, the separation of the 130.4 from 135.6 nm cannot be achieved with current state of the art multi-layer reflective UV filters and the spectral resolution of a grating instrument is required.

Hardware and Physical Configuration: In Figure 3.3.2.1, we present a schematic illustration of a dual wavelength Spectrographic Imager (SI) concept using refractive optical elements for easier illustration. The diagram provides two illustrations of the ray-paths through the same instrument. The top is the ray path shown for spectral selection. Light enters at the slit and is collimated by the collimator optics that are placed one focal distance behind the entrance slit. This collimating optics has two basic functions, first it produces parallel light from the slit and

second, it focuses the viewed object on the grating. The parallel light is dispersed by the grating according to wavelength. By having two separate exit slits it is possible to have two separate wavelength channels in a single instrument. In Figure 3.3.2.1, the wavelength λ_2 illustrated in red dispersed upward and the other wavelength λ_1 illustrated in blue is dispersed downward. After passing the grating, the camera lens focuses the parallel blue light of wavelength λ_1 into the lower exit slit, while the red light of wavelength λ_2 is focused into the upper slit. The blue and red light reach separate detectors in our scheme. In terms of the upper diagram, the instrument can be regarded as a conventional monochromator with two exit slits and without imaging. The lower illustration of Figure 3.3.2.1 represents the same optical train, but shows how two dimensional imaging takes place. From each distant object point in the scene, parallel light enters the entrance slit. The collimator lens, which is placed one focal distance in front of the grating, focuses the parallel light on the grating, thus forming an intermediate image at the grating. The “camera lens”, following the grating in combination with the small lens placed behind each exit slit re-images the intermediate image on the detector. This instrument therefore produces two-dimensional spectrally filtered images of the same scene on two detectors simultaneously. These instruments were introduced in the ultraviolet for space use where narrowband filtering with multi-layer filters would have been otherwise insufficient.

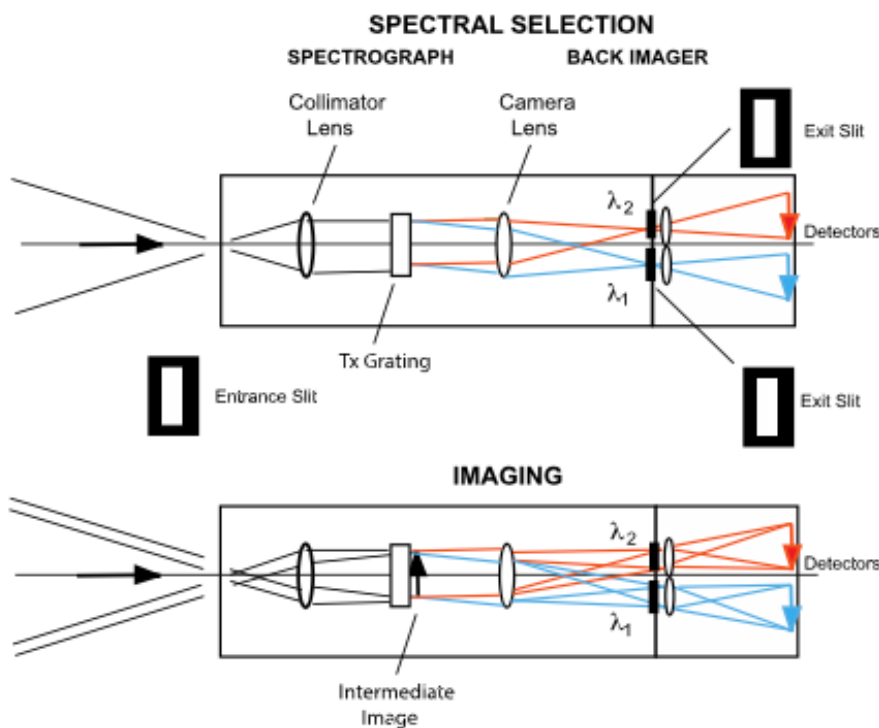


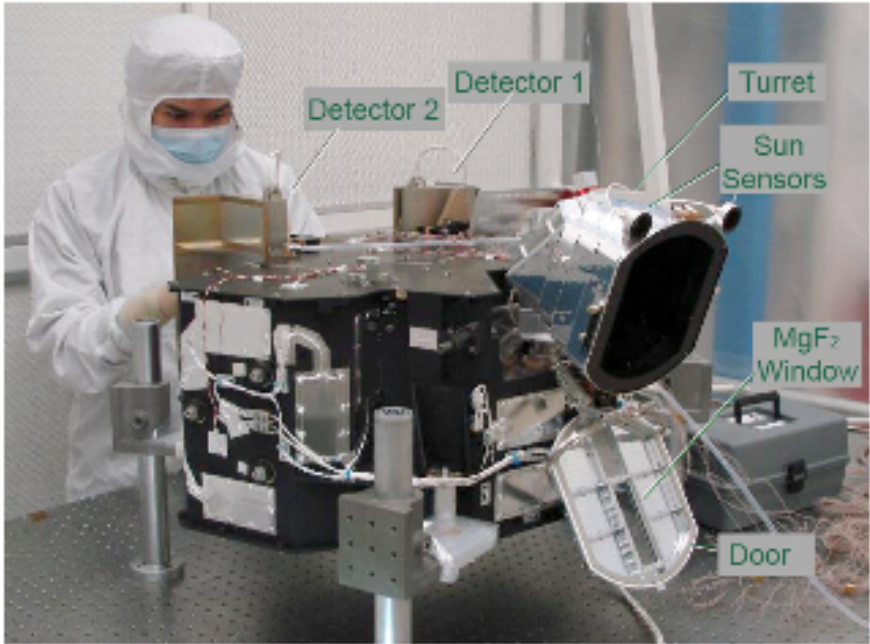
Figure 3.3.2.1 Schematic of the optical principle of a spectrographic imager designed to accept two wavelength channels using lenses (from Mende *et al.*, 2016).

The first example of a Spectrographic Imager was flown on the NASA IMAGE mission. In this instrument the grating spectrometer was a Wadsworth configuration instrument with a

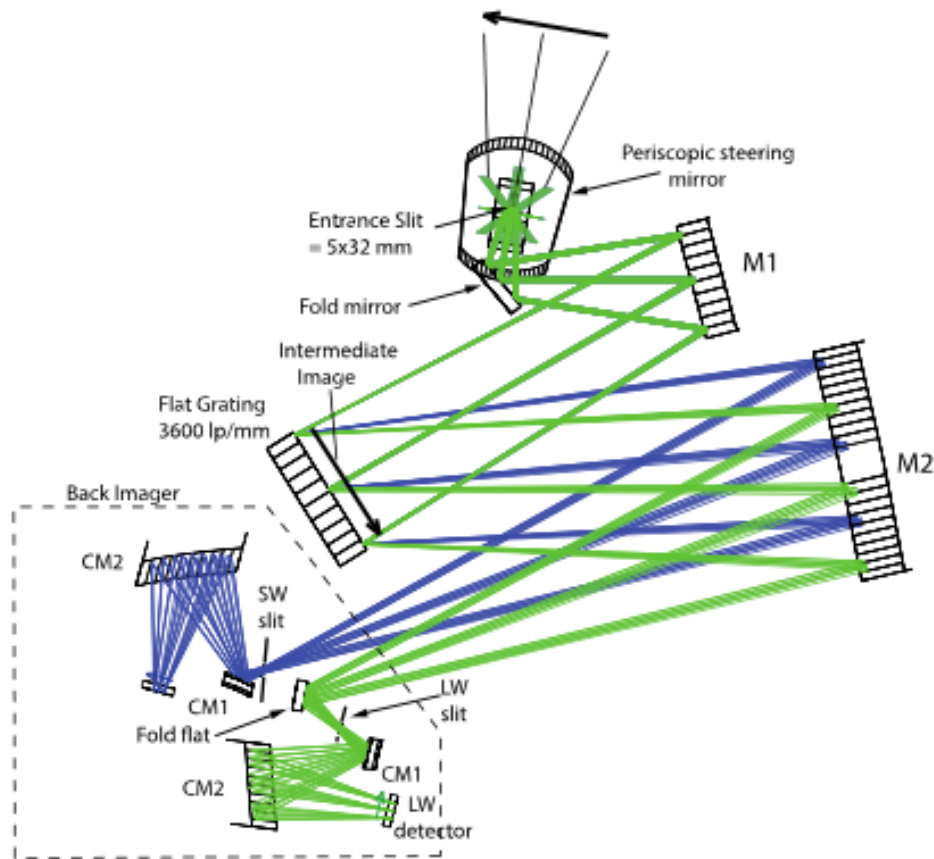
concave grating and with a hole in the grating center where the entrance slit was placed. This allowed the use of an axial collimator for improved spectral performance. However, this hole appeared as an obscured region at the center of the final image. For ICON it was considered highly desirable to remove the obscuration and a Czerny–Turner (CZT) spectrograph configuration was selected instead. With the ICON resolving requirements, this optical arrangement permitted the use of off-axis mirrors and eliminated the requirement for the central obscuration of the IMAGE Wadsworth type instrument. A disadvantage of the Czerny–Turner-based instrument is that it requires an additional mirror with the associated reflective losses and mass and cost penalties. Considerable progress has been made in producing highly-efficient UV mirrors since the IMAGE program and the additional reflection loss became a less crucial issue.

Optical elements/Spectrograph: A photograph of the ICON Spectrographic Imager is shown on Figure 3.3.2.2. A top view of the optical model is illustrated in Figure 3.3.2.3. The viewed object is schematically illustrated by an arrow on the top. Light enters the instrument at the top of the illustration and is reflected by the steering mirror. The periscopic steering mirror points the direction of the optic axis by rotating around a vertical (perpendicular to the page) axis. Actually there are two small 45° mirrors behind the entrance slit, one of them is to provide the second periscope mirror and the other to turn the image to ensure that the horizon is perpendicular to the slit when the turret is in its nominal (turret angle = 0) position. These two mirrors are not shown on the schematics. The spectrograph slits, grating and detectors are fixed in the instrument frame but if the scan mirror is not in its nominal position the projection of the slit on the outside view will appear to be rotated. Thus effectively the spectral slit will be superposed on the outside atmosphere at an angle with respect to the vertical depending on the position of the steering mirror.

All optical elements are reflective with the exception of the detector windows, which are MgF₂. The spectrograph mirrors M1 and M2 are both spherical. M1 acts as a spectroscopic collimator as well as a camera mirror to create the intermediate image of the scene at the grating acting the same as the collimating lens in Figure 3.3.2.1. M2 is the spectrograph's "camera mirror," which in combination with M1 focuses the image of the input slit at the output slits. Depending on the wavelength, the grating dispersion and the location of the output slits, light of the appropriate wavelength band is selected. One can regard M2 as a collimator for the imaging operation, creating near-parallel light for each image point on the grating to be re-focused on the detectors by the back imager aspheric mirrors CM1 and CM2. There is a separate set of back imager optics for each of the two wavelength channels (SW and LW) including the exit slits shown in black. In order to allow more room and accommodate the configuration, the LW channel has a flat turning mirror, which allows placing the LW detector out of the way of the other channel.



3.3.2.2 A view of the ICON FUV instrument on the bench



3.3.2.3 Top view schematic of the ICON FUV imager

Moveable turret: The plasma bubbles are strongly organized along the local magnetic field and good observing conditions from a low inclination limb-viewing satellite can only be achieved if the instrument can be pointed along the local magnetic field following its declination. Therefore a moveable turret was added in front of the Spectrographic Imager that can point the instrument in 10° steps up to $\pm 30^\circ$ around the nominal view direction. The ICON orbit is highly predictable and for each nighttime portion of any orbit the local magnetic field direction can be calculated using the IGRF model. The angle between the spacecraft velocity vector and the magnetic field direction is determined and commands are generated that move the turret so that it will point within $\pm 5^\circ$ to that field direction. Knowing the observation geometry then the observations can be mapped to the nominal emission altitude of 300 km in the Spacecraft Orbit-Aligned Position (SOAP) latitude-longitude coordinate space with $8 \times 8 \text{ km}^2$ pixel size. Then the TDI technique can be applied to the observations applying the known horizontal offset to each of the 100 frames to give the 12 second effective exposure time (Mende *et al.*, 2022; doi:10.1007/s11214-022-00928-w).

FUV Detectors and Electronics: The ICON FUV detectors consist of image tubes that are fiber-optically coupled to CCDs. The image tubes have MgF₂ windows and FUV photocathodes evaporated directly on to the microchannel plate (MCP). A stack of two MCPs are used, which arrangement provides sufficient charge multiplication gain to overcome readout or dark current noise downstream in the CCD.

CCD Detectors: ICON FUV requires modest spatial resolution in its FOV, which can be accomplished by a pixel raster of only 256 × 256. ICON detectors have to be sensitive in the spectral ranges around 135.6 and 157 nm and have the highest quantum efficiency possible consistent with high detectability of each resulting photo-electron. Although photo-conductive detectors like CCDs or CMOS are much simpler and require less resources to operate they could not be used in this application because of their residual sensitivity in the visible and near UV region. ICON has to view the dayside atmosphere and having a highly “solar blind” detector is of paramount importance. All of these requirements favor photo-emissive detectors with MCP electron amplification in the same manner as it was required for the IMAGE FUV instrument to view the aurora in the day-lit atmosphere. There are several ways to detect the FUV generated photo electron clouds from an MCP.

Dayglow limb emissions in the FUV can be quite intense, several kiloRayleighs, and can fill the entire FOV producing total counting rates that exceed the capabilities of cross delay line type detectors as used in the IMAGE SI instrument. To accommodate the large dynamic range we chose the type of detector, which was used in the IMAGE Wideband Imaging Camera (WIC), consisting of a photo-cathode on an MCP, an output phosphor, and a fiber-optics taper to couple the light from the phosphor to a CCD. ICON FUV optics produces a flat image unlike WIC so the ICON detector was considerably simpler. In-fact the front end was quite similar to a 25 mm conventional intensifier tube (Figure 3.3.2.4). The ICON intensifier has a dual stack MCP to provide enough gain to detect phosphor scintillations due to single photo-electron emission at the photocathode. One significant departure from the IMAGE WIC detector was the use of completely sealed tubes on ICON instead of the vented detectors of WIC. It was thought that the sealed tubes harbored less contamination risk during ground processing and allowed testing the entire detector chain without having to evacuate the detector.

In some ways the ICON detectors were also very similar to the detectors used in the spacecraft experiment named Imager of Sprites and Upper Atmospheric Lightning (ISUAL) designed and built at the Space Science Laboratory at UC Berkeley. This instrument had a camera with a 25 mm image tube that was fiber-optically coupled to a frame transfer CCD. These devices were space qualified including tests of their radiation tolerance to energetic proton bombardment. In ICON the same Teledyne DALSA FTT1010M 1024 × 1024 frame transfer CCDs were used. The CCD-s were binned on the chip 2 × 2 so the “native” readout provided a 512 × 512 image from the cameras.

The FUV converter tubes were built and characterized and their photocathode quantum efficiency was measured in Berkeley. The complete converters were integrated into the camera at Space Dynamics Laboratory (SDL) of the Utah State University in Logan Utah. The process

included bonding the converters to a fiber-optic taper and to the readout CCD. SDL assembled and tested the complete cameras, except the high voltage power supplies for the intensifiers, which were built by UC Berkeley. A completed camera is shown on Figure 3.3.2.4.

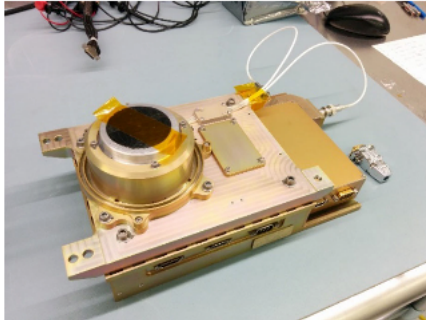


Figure 3.3.2.4 ICON flight camera shown integrated with the FUV image converter

Readout Electronics: The camera readout electronics provides video imagery to the ICP over a 21 bit serialized interface, nominally at 10 frames per second and in 512×512 format (2×2 pixel binning on chip). During science operations the pixels are further binned 2×2 by the processing electronics therefore the 1024×1024 CCD pixels are binned to 256×256 . The CCD and primary electronics assembly reside in separate thermal zones, to minimize dark current without active cooling. The CCD cameras were fully characterized with both visible light (prior to integration with the UV converter) and UV photons (following system integration). Measured parameters included camera dark current, dark signal non-uniformity, read noise, linearity, gain, pulse height distribution, dynamic range, charge transfer efficiency, resolution, relative efficiency, quantum efficiency, and full well capacity. UV characterization of the camera systems over a range of micro-channel plate (MCP) voltages during thermal vacuum testing demonstrated that camera performance met the critical on-orbit FUV dynamic range requirements.

Known issues due to external factors that could impact any long-term comparison or analysis (e.g., optical distortion due to gradual radiation degradation) should be captured.

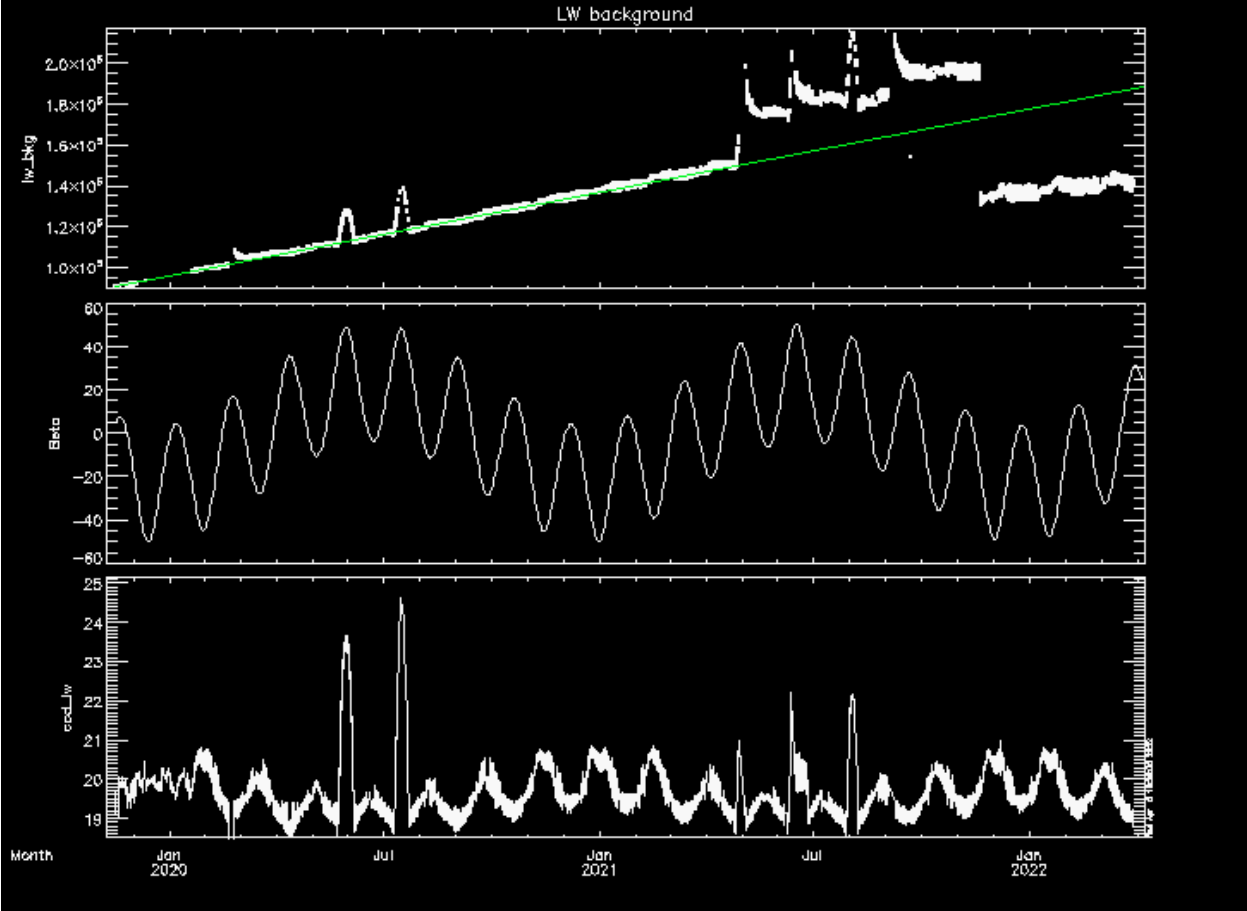
FUV does not use any consumables, other than electric power, so that consumable consumption is not a factor for instrument life expectancy, except the long term effect of S/C power generation.

The FUV instrument uses a combination of photocathode-MCP-phosphor-CCD detector system to convert incoming photons into output counts. The background signal of such a system is primarily created by the dark current of the CCD plus much smaller contributions from cosmic ray hits, scatter inside the instrument, out-of-band contributions, and bias electrons. The dark current in a semiconductor material is generated because the thermal motion of the electrons raises some electrons into the conduction band of the semiconductor and are indistinguishable

from signal in the CCD pixel . The amount of those knocked off electrons depends on the temperature of the silicon material and it accumulates linearly with exposure time.

ICON-FUV uses Teledyne Dalsa p/n FTT1010M frame transfer CCD sensors. Those CCD were selected because of very good experience with similar earlier type detectors on the Imager for Sprites and Upper Atmospheric Lightning (ISUAL) camera. The CCD has a 1024x1024 pixel imaging region and a similar size storage region. Photons are collected for 120 ms in the image section, the collected electrons are shifted into the storage section within 2.3 ms, and the readout takes 116.9 ms. During the 120 ms exposure time and the 2.3 ms frame transfer time dark current is mostly collected at a constant level over the whole image size. However, as the first line of the CCD is read out all other lines still accumulate dark current which leads to an increasing dark current signal from the bottom of the CCD to the top (Figure 2). Generally the background signal should increase linearly (within statistical fluctuations) from bottom to top but radiation damaged regions (hot pixels) can lead to increases (for instance at pixel=23 in Figure 3.3.2.5) which need to be determined and monitored.

The ICON satellite regularly flies through the South Atlantic Anomaly where the increased flux of energetic particles leads to increased signal fluctuations in all ICON science instruments. A data collection exclusion zone was defined where all remote sensing instruments turn off science data collection and set any high voltages to safe levels in order to prevent electric discharges. Without high voltage to the MCPs the FUV instrument still collects science data in order to determine the CCD background signal. Figure 3.3.2.5 shows the temporal change in the average background counts during the ICON science mission.



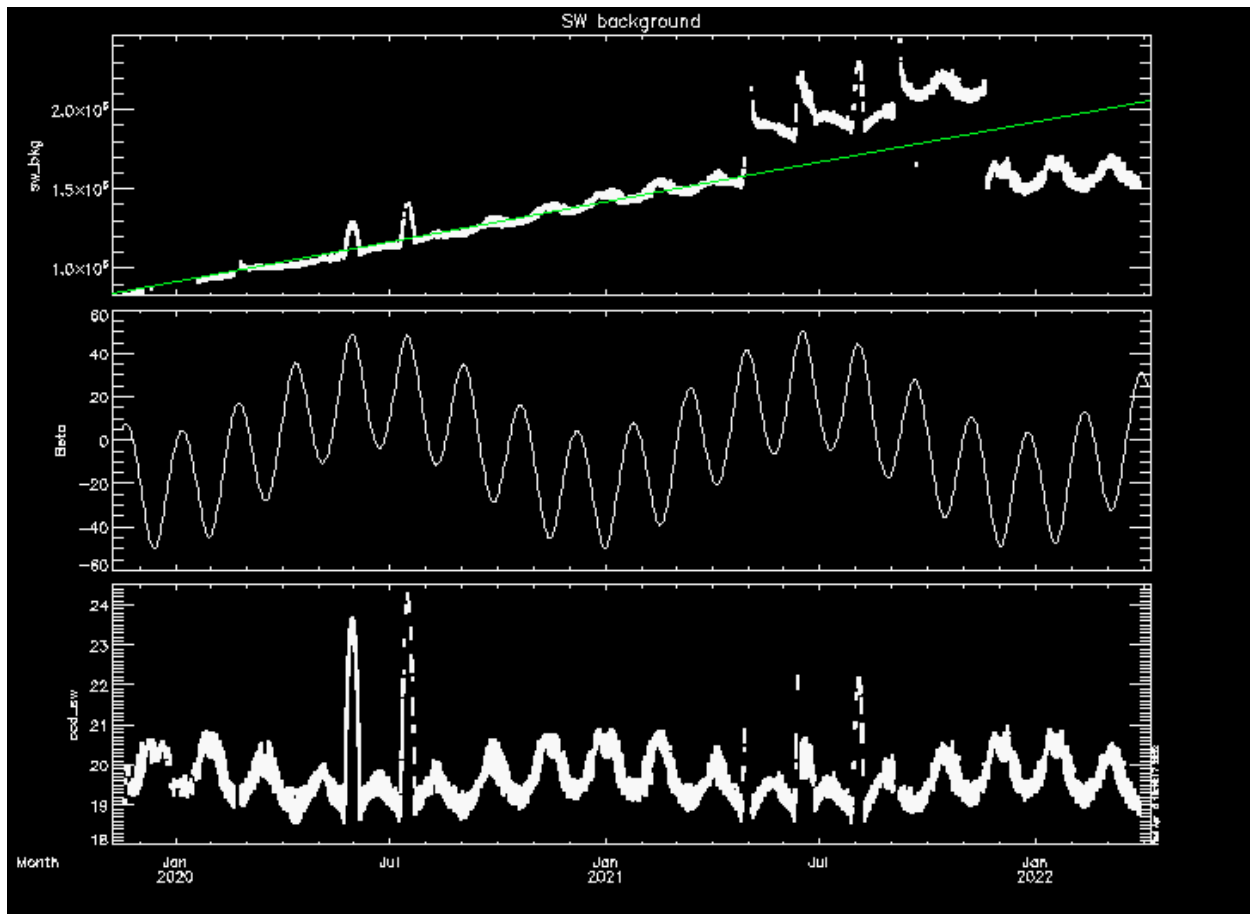


Figure 3.3.2.5: Average background counts in the central altitude profile for LW (top) and SW (bottom) since the beginning of the ICON science mission. The middle panels show the ICON orbit beta angle and the bottom shows the CCD temperature.

There is a general increase of the background signal with time with several strong excursions. Very strong excursions in summer of 2020 and 2021 coincide with peaks of the ICON orbit beta angle. The changed geometry during high beta angle puts sunlight onto radiator panels which cannot efficiently cool the detectors and the increased CCD temperature leads to an increase in the dark current and background signal. In order to slow the background signal increase the CCD bias was changed on November 20, 2021 which resulted in the strong decrease of the background counts. The further development will be closely monitored and the bias level potentially changed again to put it at roughly the level from the beginning of the mission. The instrument background is determined daily and monitored for each record with the collection of a column of pixels outside of the illuminated CCD chip. This “dynamic background determination” allows for a reliable background determination and subtraction before the science signal is transformed into reliable physical units.

3.3.3 Instrument Observation Requirements

This subsection summarizes the required observation parameters of the instrument. Not applicable for in situ measurements.

Table 3.3.3.1 describes the Observation Requirements that FUV must meet, the ranges and times over which these must be met in order to meet the L1 requirements in the PLRA.

Attribute	Value
Daytime O/N₂	
Geophysical Quantity	Thermospheric column-integrated density ratio of O to N ₂
Tangent Altitude Range	Column integrated, including 135 – 300 km
In-track sampling	500 km
Temporal Cadence Required	1 minute
Temporal Coverage	From local sunrise to local sunset
Precision	16.6 %
Nighttime O⁺	
Geophysical Quantity	O ⁺ plasma density
Tangent Altitude Range	200 - 400 km
Tangent Altitude Resolution	20 km
In-track sampling	500 km
Temporal Cadence Required	1 minute
Temporal Coverage	From local sunset to local midnight
Precision	33% for nmF2

Table 3.3.3.1 – Summary of the L1 FUV Observation Requirements

3.3.4 Instrument Observation Capabilities

This subsection summarizes specific instrument parameters, such as number of detectors, field of view, wavelengths measured, time resolution, data rate, etc. Specify measurement capabilities for in situ instruments.

Table 3.3.4.1 describes key characteristics of the FUV instrument and the observations it provides. Additional details can be found in Mende et al., [2017] (<https://doi.org/10.1007/s11214-017-0386-0>) and Frey et al., [2022].

Observation Parameter	Value
Observables	Brightness of O 135.6 nm airglow day and night Brightness of a portion of the N ₂ LBH band airglow during day
Number and Type of Detectors	2 CCD detectors, 1024x1024, binned to 256 x 6 science pixels on orbit (vertical x horizontal) during nominal science operations

Observation Parameter	Value
Field of View	24° vertical x 18° horizontal, divided into 6 vertical stripes in nominal science operations
Etendu AΩ per science pixel	1.3x10 ⁻⁴ cm ² str
Geometric photon collection rate at input aperture	10.9 Photons/s/science pixel/Rayleigh
Pass-bands	SW 4.73 nm Full-width half maximum centered on 135.6 nm LW 5.99 nm Full-width half maximum centered on 157 nm
Exposure time	12 seconds

Table 3.3.4.1 FUV Instrument Characteristics

Table 3.3.4.2 describes the measurement characteristics for FUV, in terms of the geophysical quantities it is used to derive (O/N₂ and nighttime O⁺). For further details on the in-flight observations of the O/N₂ see England *et al.*, 2021 (<https://doi.org/10.1029/2021JA029575>). For further details on the in-flight observations of nighttime O⁺ see Wautelet *et al.*, 2021 (<https://doi.org/10.1029/2021JA029360>) and Frey *et al.*, 2022.

Attribute	In-flight Performance (Prime Mission)
Daytime O/N₂	
Geophysical Quantity	Thermospheric column-integrated density ratio of O to N ₂
Tangent Altitude Range	Column integrated, from ~130 – 500 km
Tangent Altitude Resolution	4 km
In-track sampling	100 km
Temporal Cadence Required	12 seconds
Temporal Coverage	From local sunrise to local sunset
Precision	10 %
Nighttime O⁺	
Geophysical Quantity	O ⁺ plasma density
Tangent Altitude Range	150 – 500 km
Tangent Altitude Resolution	8 km
In-track sampling	100 km
Temporal Cadence Required	12 seconds
Temporal Coverage	From local sunset to local midnight
Precision	10% for nmF2

Table 3.3.4.2 Geophysical quantities derived from FUV observations

3.3.5 Data Acquisition

This subsection describes what data is obtained by the instrument, how it's obtained, any variation in data acquisition modes, etc.

The CCDs operate in a fast scan mode at 8.33 frames per second (fps). 100 video frames are co-added digitally in memory in the ICON Instrument Control Processor (ICP) to produce images of 12-second integration. The data from the 12-second exposures are downlinked to the ground. Because the satellite moves substantially during 12 seconds, two types of motion compensation schemes are used. In type one, six horizontally co-added vertical altitude profiles are generated for the measurements of the altitude distribution of the emission intensity (Figure 3.3.5.1). In this figure the image of the limb is shown to be projected on the detector between tangent heights of about 150 and 507 km. The data is co-added horizontally into six stripes as shown in blue. These strips represent the primary data source for taking vertical profiles of the thermosphere/ionosphere. The image can be regarded as having "resolution cells" of 4×4 km at the tangent height of 155 km representing an angular region of 0.093×0.093 degrees. Approximately 32 of these resolution cells are co-added in one stripe and each stripe represents 3 degrees in horizontal width. The resolution cells nominally would translate to a 4×4 binned CCD pixel on a 256×256 matrix of the detector however the imager optics has substantial non-linearity that has to be accounted for. A single strip is illustrated on the right and the limb view region is shown in red. Below 130 km tangent height the instrument is viewing a region where all FUV emissions in the background are absorbed by O_2 and this "sublimb" or "disc" region is illustrated in blue. The six profiles are generated by summing pixels horizontally in the direction of satellite motion without smearing in the vertical direction. The co-adding process is relatively straight forward when the turret is in its baseline (0°) position and the horizontal direction in the image of the limb is parallel with the pixel x-coordinate in the image. When the turret is at another angle, the co-adding of pixels has to take place along a slant path in the imager frame of reference. This is accomplished by transposing the images and modifying the pixel addresses during the transposition, thereby removing the geometric distortion and applying an x and y pixel shift to facilitate co-adding along contours that represent horizontal paths. The pixel addresses for the transposition use an address matrix stored in a Look-Up-Table (LUT).

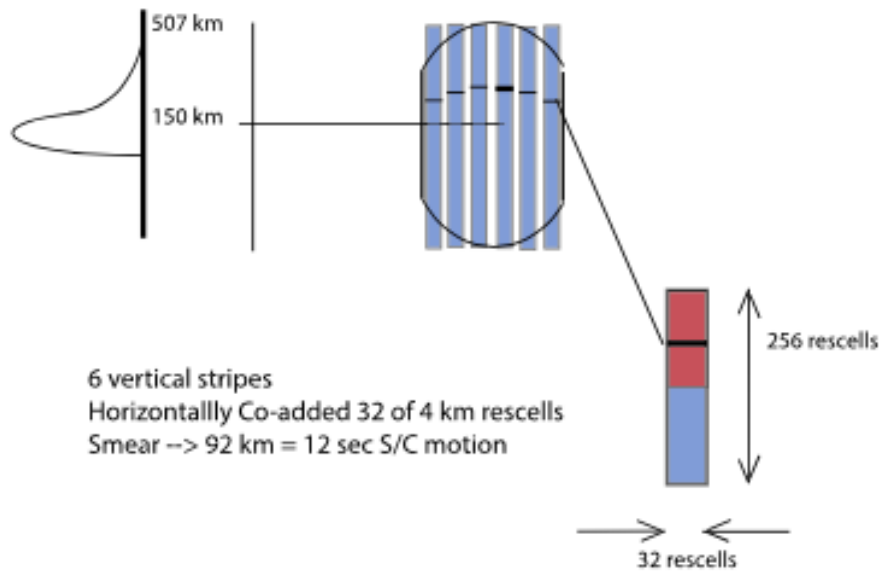


Figure 3.3.5.1 Illustration of limb altitude profiles. There are 6 vertical strips. In each strip the pixels are co-added horizontally. During daytime data is taken for both channels while during nighttime only for the 135.6 nm channel. Below 150 km altitude there is substantial O₂ absorption in the FUV and it is not possible to get limb views of the atmosphere. The linear dimension of a “resolution element” or “rescell” is 0.093° or 1/256 of the 24° vertical FOV

During nighttime a second type of motion compensation scheme is used which produces a data stream containing Time Delay Integrated (TDI) images reproducing a mapped view of a two dimensional horizontal intensity distribution (Wilkins et al. 2017; DOI 10.1007/s11214-017-0410-4).). In this mode, the individual frames are digitally co-added in the ICP memory as two dimensional images while compensating for the satellite motion (Figure 3.3.5.2). During the co-adding process, a constant offset is applied to the address of each pixel in each frame to shift the image. This offset is computed from the orbital speed of the satellite so that it compensates for the satellite motion.

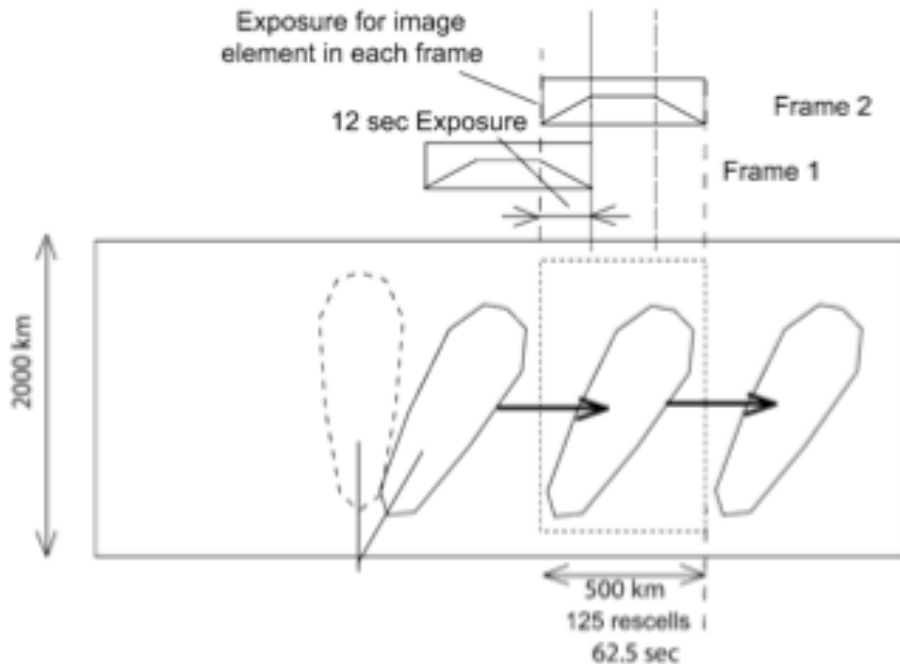


Figure 3.3.5.2 A schematic of TDI co-adding of limb or sub-limb images as the satellite is moving from left to right. The turret angle is illustrated to be 30° forward. In consecutive exposures some pixels near the edges of the FOV are only partially exposed whereas pixels in the middle receive full exposures. The exposure time of each image element, depending on their position in the field, is shown with the small trapezoidal illustration. Adjacent frames fill in the exposure time of regions near the edge of the FOV. The complete sequence of exposures with appropriate superposition of the images can be used to reproduce all pixels at their full exposure.

During nighttime the 135.6 nm emission maps will be treated as two dimensional images viewed from above. The 135.6 nm emission is produced by recombination of O^+ and its intensity is expected to peak at the bottom of the F region at an altitude of approximately 300 km. We divided the view of the atmosphere into two regions. Imaging at elevation angles corresponding to ray tangent height of 300 km or higher we map the emissions to the appropriate limb tangent because we expect the greatest intensity to be seen there and these images are called as "limb view" images. At elevation angles lower than the limb tangent of 300 km, we map the layer to a constant altitude of 300 km below the satellite as "sub-limb" views. We recognize that there is a confusion in the region from tangent heights of 150 to 300 km between structures originating nearer than the tangent point and structures further away from the tangent point. Both of the limb view and sub-limb models define an altitude and a range distance from the satellite and therefore can be mapped as a function of their horizontal position.

This TDI technique provides high-resolution images in spite of the substantial motion of the satellite platform during the 12-second exposure. It should be noted that these techniques

require sophisticated real-time image manipulations onboard the satellite. This is accomplished in ICP resident Field Programmable Gate Arrays (FPGAs) using firmware because of the high processing speeds needed. This technique is an evolution of the TDI motion compensation that was used in the FUV instrument on the NASA IMAGE satellite, with a much more detailed set of performance requirements (Wilkins et al. 2017; DOI 10.1007/s11214-017-0410-4).

Finally, engineering images are obtained from the FUV instrument by reading out the full resolution CCD image (1024 x 1024) for varying exposure times. These form the basic data from which the FUV calibrations are determined.

3.4 Extreme Ultraviolet Spectrograph (EUV)

3.4.1 Instrument Measurement Requirements

This subsection summarizes the required measurement parameters of the instrument.

Table 3.4.1.1 describes the key observable quantities that EUV must observe, the ranges and times over which these observations must be made. These provide the remote sensing observations needed to meet the Level 1 observation requirements described in Section 3.4.3.

Measurement Parameter	Value
Parameter Measured	Altitude-resolved measurements of the ultraviolet emissions from O ⁺ at 83.4 and 61.7 nm on the limb
Tangent Altitude Range	100 – 500 km
Tangent Altitude Resolution	20 km
In-track sampling	500 km
Temporal Cadence Required	1 minute
Temporal Coverage	From local sunrise to local sunset

Table 3.4.1.1 – Summary of the EUV Instrument Measurement Requirements

3.4.2 Instrument Description

This subsection describes the primary scientific objectives of the instrument, its hardware, physical configuration, etc.

The existence of EUV emission from singly ionized oxygen (O⁺) in the ionosphere of the Earth has long been known and is a useful diagnostic of the ionization state and density of the lower ionosphere. The brightest of the OII dayglow line complexes in the EUV is the 83.4 nm resonance triplet resulting from transition from the 2s2p⁴ 4P excited states to the 2p³ 4S^o ground state. The high population of nearby ions in the ground state causes a high probability that an emitted photon from this transition will be reabsorbed, resulting in a high optical depth

in this transition. This can make it difficult to disentangle ionospheric scattering effects from solar-source illumination changes when attempting to determine density of the O^+ ion. The nearby triplet at 61.6 nm from the $3s\ 2P$ state to the $2p^3\ 2D^0$ state, is optically thin. In principle, the two taken together can be used to more directly obtain the ion density and illumination source function than the 83.4 nm emission alone. Similar transitions at 67.3 nm and 71.8 nm could be used to supplement this analysis.

The *ICON EUV* spectrometer has been designed to perform wide field altitude profilometry of the region surrounding the peak O^+ densities in the lower ionosphere, at tangent altitudes between 100 and 500 km with a vertical resolution of 20 km, and a horizontal resolution of 500 km. In normal observing mode, *ICON EUV* will be pointed generally north perpendicular to the spacecraft velocity vector and take 12 s exposures. Each observation will image a 12° wide (spectral) by 17° high (imaging) wedge of the atmosphere from which daytime ion density altitude profiles from 100 to 500 km can be determined. Because the spacecraft motion during 12 s results in a shift of only $0^\circ.76$ along the orbit (small compared to the 12° field of view), each exposure is effectively a snapshot. Required sensitivity of 7.4 Rayleigh at 61.7 nm and 30 Rayleigh at 83.4 nm were determined based simulated model inversions of the altitude profiles to derive the O^+ density versus altitude (see *ICON CMAD* for further details). The primary design requirements relate to obtaining the sensitivity and angular resolution necessary to determine the maximum ion density of the F2 layer and the altitude of the maximum density using the 61.6 nm and 83.4 nm emission while rejecting interference from scattered $H\ I\ \alpha$ and the nearby $He\ I\ 58.4\ \text{nm}$ line.

Instrument Hardware: The *ICON EUV* instrument is a diffuse imaging spectrograph consisting of an entrance aperture, a diffraction grating, and a microchannel plate (MCP) detector.

Grating: The grating was manufactured by Horiba Jobin Yvon and delivered with a 40 nm thick coating of Cr. To enhance reflectivity in the EUV additional layers of Ir (20 nm) and B4C (10 nm) were applied by Reflective X-ray Optics LLC.

Detector: The MCP detector and spectrograph were both designed and assembled at the Space Sciences Laboratory (SSL) at the University of California Berkeley Campus. The design is patterned after the successful *SPEAR* mission.

Housing: The spectrograph housing is a hermetic enclosure measuring ~ 38 by 21 by 34 cm and has a mass of 10 kg. Figure 3.4.2.1 is a side view of the instrument including its mounting feet. Because contamination is a significant concern for EUV instruments, the entire instrument housing is built as a vacuum cavity. A sealed one-shot door in front of the instrument was successfully opened in orbit during experiment initialization in October 2019 to allow evacuation and allow light to enter.

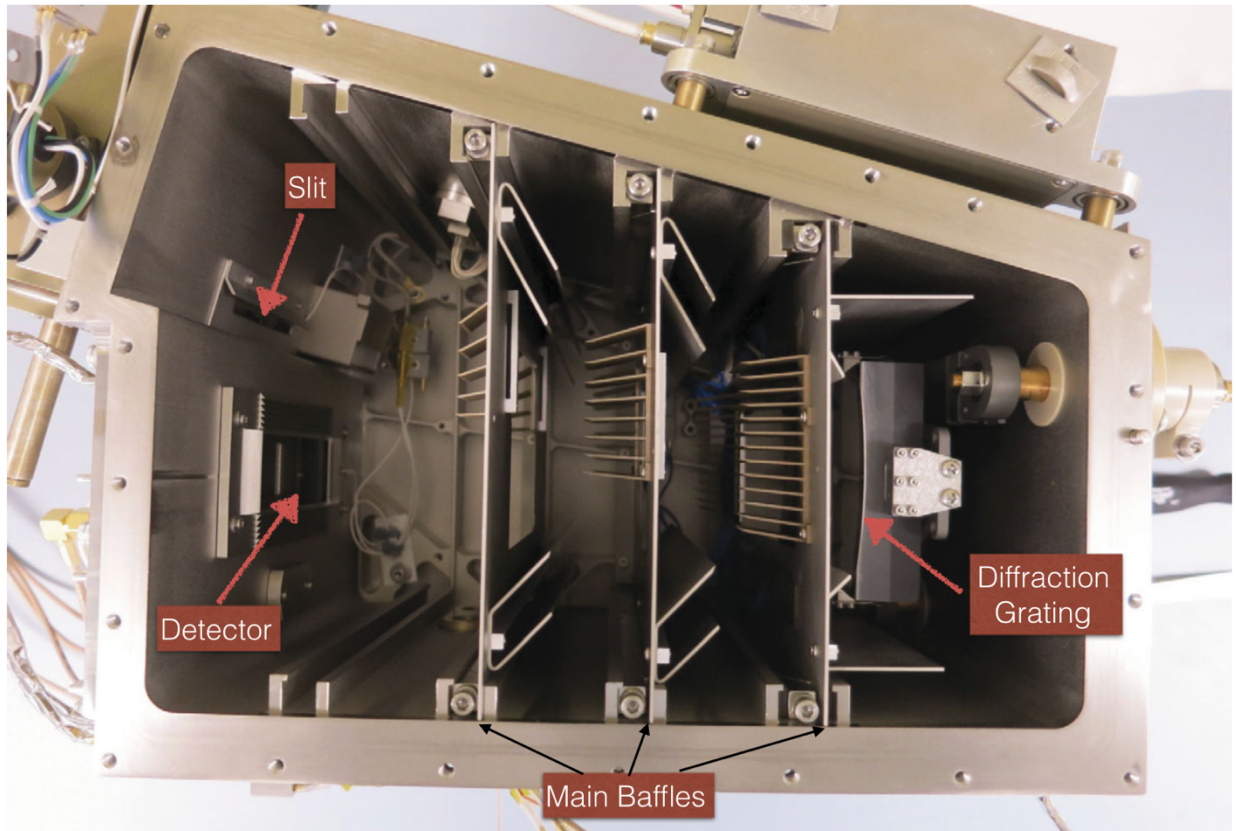


Figure 3.4.2.1 Top view into the *ICON EUV* housing showing relative location of principle components. Entrance slit and detector are at *upper, and lower left*, respectively. Grating is at *right*. Three of the four baffle sets are installed. The chevrons directed toward the grating are knife-edged to prevent glints and trap light from unwanted orders in the spectral direction. The knife-edged vanes directed towards the detector shadow the main baffle plates (*vertical sheets* seen nearly edge-on) from direct illumination in the imaging direction.

Optical design concept: EUV radiation from the sky enters the 0.90 by 40.0 mm slit, illuminates a 50 by 95 mm toroidal figure, ion-blazed (lamellar profile), holographically ruled diffraction grating, and is then focused by the grating onto a 19 by 54 mm cross delay line MCP detector with a spatial resolution of 90 μm in the spectral direction, and 160 μm in the imaging direction. On-board electronics digitize the photon events into an image 160 pixels wide in the spectral dimension, and 101 pixels tall in the imaging dimension. The field of view is determined by internal and external baffles, and the grating dimensions. The optical scheme provides imaging without using a separate telescope optic. In the spectral direction, the toroidal grating focuses an image of the slit onto the detector while in the imaging direction the toroid focuses at infinity resulting in a spectral image where each row is a spectrum from a horizontal slice of the sky 12° wide, and each column a vertical angular intensity profile at a given wavelength. A

schematic of the optical path is shown in Figure 3.4.2.2. The grating is coated with a special EUV-optimized, low stress B4C/Ir/Cr multilayer.

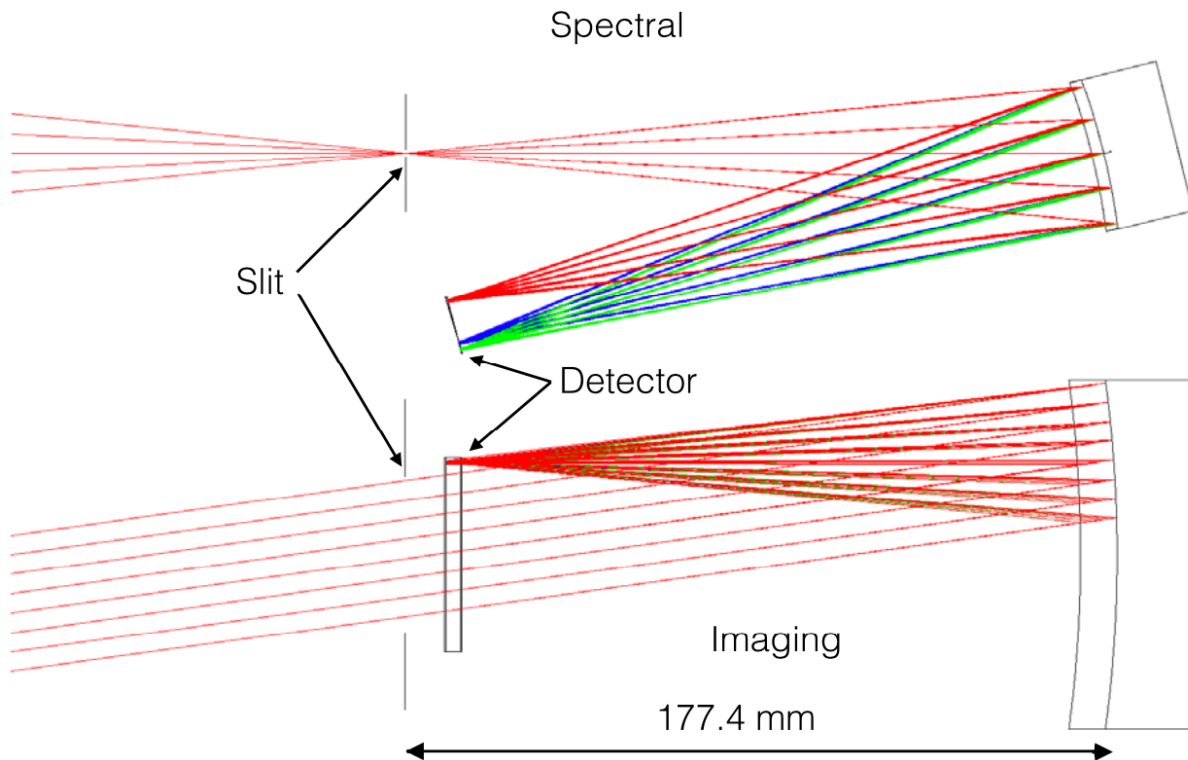


Figure 3.4.2.2 Schematic diagram showing how light of three wavelengths (58.4, 61.6, and 83.4 nm, *green, blue, and red, respectively*) from the entire 12° wide spectral field of view is focused onto detector along the dispersion direction (*top*), and how collimated, in-band light from a particular altitude angle is focused onto one row on the detector in the imaging direction (*bottom*). Slit width is exaggerated by a factor of 2 in *top panel*

Known issues due to external factors that could impact any long-term comparison or analysis (e.g., optical distortion due to gradual radiation degradation) should be captured.

EUV does not use any consumables, other than electric power, so that consumable consumption is not a factor for instrument life expectancy, except the long term effect of S/C power generation, which are discussed elsewhere. The nature of the MCP detector used for the EUV instrument is such that its gain changes over time with exposure to the airglow lines of interest – especially the 83.4 nm airglow. The calibration of the instrument (both flatfield and absolute sensitivity) are maintained through a combination of nadir calibration and lunar calibrations, discussed in Section 2.2. In addition, operations for the instrument changed after it had completed its goal for the prime mission, in response to this change in the detector performance. This is described below. From March 2022 onwards, these operations also include

full orbits of engineering data that are collected weekly, in order to identify any future changes in the detector prior to its impact on the data quality.

The EUV instrument collected 16 months of data with baseline performance, meeting all Level 1 requirements for the instrument. Beyond that window of time the instrument began producing data that raised questions related to the natural gain changes that were identified through the routine evaluation of the quality of the retrievals, and was powered down on July 28 2021. In March 2022, the ICON EUV imager has been restored to operating at a higher gain but reduced cadence that is calculated to extend the lifetime of the instrument for at least several years.

The gain and cadence changes address the issues of detector gain loss and related changes in flatfield. There are more rapid changes in sensitivity of the instrument (and the related flatfield) to the bright 83.4 nm line than elsewhere in the spectrum due to detector charge depletion. The monthly cadence of nadir-viewing flatfield determinations is the cadence for this determination, and it was determined that between March-July, 2021 large changes in the flatfield between monthly calibrations were observed. This was likely because the pulse height distribution (PHD) was changing faster than early in the mission as events became much less effective in driving measurable charge onto the XDL detector from the multi-channel plate (MCP), in part moving observable photons below the on-board PHD threshold used to discriminate photon events from undesired particle events. Therefore, in July of 2021 the EUV instrument was commanded off, pending an investigation of the PHD though collection of data in engineering mode, where the XDL readout was downloaded in full (see Figure 3.4.2.3). Additionally, the data from March – July 2021 are reported with larger uncertainties (consistent with best estimates) than the data taken at other times in the mission.

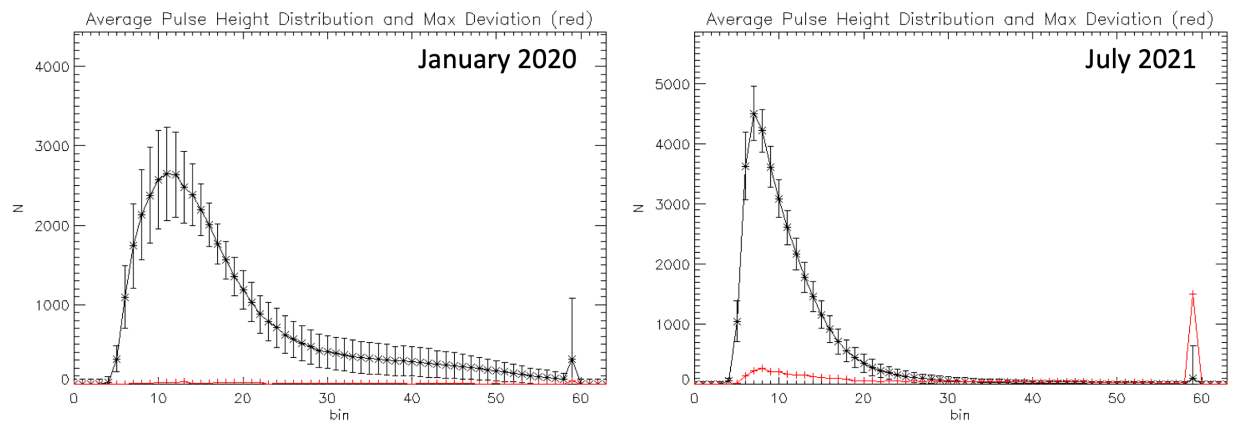


Figure 3.4.2.3 – Pulse height distributions in the region of 83.4-nm measurements from early in Phase E (left) and late in Phase E (right).

After an investigation of instrument performance, this issue is now being mitigated in three ways: increasing the gain of the MCP (through a high voltage increase from 4200 to 4450V); reducing data collection periods to focus on the equatorial ionosphere (when the spacecraft is within $\pm 5^\circ$ of the geomagnetic equator) in afternoon times (operation begin 10 minutes after local sunrise to 5 minutes prior to local sunset at the spacecraft); implementation of weekly engineering mode monitoring of the pulse height distributions. The reduced cadence of

observation extends the longevity of the EUV instrument. Further the current operating voltage of 4450 V leaves sufficient headroom for the high voltage to be increased again in the future, should the need arise. EUV operations will therefore continue to support focused science questions. Further, EUV can be operated in campaign modes where full orbital daytime coverage data will support future efforts such as campaigns involving ground-based Incoherent Scatter Radars (e.g. Wautelet *et al.*, 2022). These operations are subject to adjustment in response to emerging new science questions that future observations may answer.

3.4.3 Instrument Observation Requirements

This subsection summarizes the required observation parameters of the instrument. Not applicable for in situ measurements.

Table 3.4.3.1 describes the Observation Requirements that EUV must meet, the ranges and times over which these must be met in order to meet the L1 requirements in the PLRA.

Attribute	Value
Geophysical Quantity	Altitude profile of ionospheric O+ plasma density
Tangent Altitude Range	200 – 400 km
Tangent Altitude Resolution	20 km
In-track sampling	500 km
Temporal Cadence Required	1 minute
Temporal Coverage	From local sunrise to local sunset
Precision	33 %

Table 3.4.3.1 – Summary of the L1 EUV Observation Requirements

3.4.4 Instrument Observation Capabilities

This subsection summarizes specific instrument parameters, such as number of detectors, field of view, wavelengths measured, time resolution, data rate, etc. Specify measurement capabilities for in situ instruments.

Table 3.4.4.1 describes key characteristics of the EUV instrument and the observations it provides. Additional details can be found in Sirk *et al.*, 2017 (DOI 10.1007/s11214-017-0384-2).

Observation Parameter	Value
Observables	O+ 61.7 nm airglow O+ 83.4 nm airglow
Number and Type of Detectors	1 cross delay line detector, 101 x 160 pixels (imaging, spectral)
Field of View	17.3° vertical x 12° horizontal
Spectral resolution	2.4 nm

Observation Parameter	Value
Angular imaging resolution	0.26°
Exposure time	12 seconds

Table 3.4.4.1 EUV Instrument Characteristics

Table 3.4.4.2 describes the measurement characteristics for EUV, in terms of the geophysical quantities it is used to derive (O⁺ density). For further details on the instrument design, see Sirk *et al.*, [2017] (DOI 10.1007/s11214-017-0384-2). For more details on the inversion of the observations, see the ICON CMAD and Stephan *et al.*, [2017] (DOI 10.1007/s11214-017-0385-1). For further details on the in-flight observations, see Stephan *et al.*, [2022] and Wautelet *et al.*, [2022].

Attribute	In-flight Performance (Prime Mission)
Geophysical Quantity	Altitude profile of ionospheric O ⁺ plasma density
Tangent Altitude Range	200 – 400 km
Tangent Altitude Resolution	20 km
In-track sampling	100 km
Temporal Cadence Required	12 seconds
Temporal Coverage	From local sunrise to local sunset*
Precision	20 %

Table 3.4.4.2 Geophysical quantities derived from EUV observations.

*For further details on EUV operations after completing goals for the prime mission, See Sections 3.4.2 and 3.4.5.

3.4.5 Data Acquisition

This subsection describes what data is obtained by the instrument, how it's obtained, any variation in data acquisition modes, etc.

In science mode, the EUV instrument obtains its regular Level 0 spectral data at a 12 second cadence, with no other variation. Engineering data, which consists of pulse heights etc. are not used to determine the Level 1 science data, but are used for calibration and instrument health monitoring only.

The data acquisition prior to March 2022 is as follows. Science data were collected continuously, except when the spacecraft was in the South Atlantic Anomaly, during spacecraft outages noted in Section 2, or during some other instrument calibrations (again noted in Section 2).

The data acquisition following March 2022 is as follows. The duty cycle is reduced to focus on the primary science targets for ICON - reducing data collection periods to focus on the

equatorial ionosphere (when the spacecraft is within $\pm 5^\circ$ of the geomagnetic equator) in afternoon times (operation begin 10 minutes after local sunrise to 5 minutes prior to local sunset at the spacecraft – thus avoiding regions near the terminators where the L2 ionospheric inversions are generally of lower precision). During these times, the data are collected every 12 seconds, except when the spacecraft is in the South Atlantic Anomaly or during certain other instrument calibrations (see Section 2). In addition, 1 orbit of engineering mode data is collected every week. Further, EUV is operated in campaign modes, where full coverage data will support future efforts such as campaigns involving ground-based Incoherent Scatter Radars (e.g. Wautelet *et al.*, 2022).

4. Data Products

A summary table of data products, mapped by data level and instrument, shall be included.

The summary table of all ICON data products by level and instrument is given in Table 4.1. The relationship of these is shown at a high level in Figure 4.1. Full details of the products by instrument, their flow etc. is given in Sections 4.1 through 4.6. Data products are grouped according to which of the 4 ICON instruments they are associated with. The instruments – MIGHTI, IVM, FUV and EUV are described in detail in Sections 3.1 – 3.4, respectively.

All ICON data follow the data levels outlined below, which is adapted from the data levels given in “*Earth Science Reference Handbook—A Guide to NASA’s Earth Science Program and Earth Observing Satellite Missions*, NASA 2006, p 31”. These closely mirror those in the template PDMP.

Level 0 – Level 0 data are raw CCSDS telemetry packets processed by the MOC into 24-hour packet files per CCSDS APID, along with data quality statistics. Spacecraft and instrument housekeeping data, instrument science, ephemeris, observatory attitude and orbital state vector data are included.

Level 0’ – Reproduce the full contents of the L0, but are saved into netCDF format for easier reading. In addition to GPS time (used on the spacecraft), all time-stamps are additionally reported in UTC time.

Ancillary data - These are georeferencing parameters, coordinates, the observatory state vector, housekeeping data etc. that are used, along with the ICON observations to produce the Level 1 and higher-level data products.

Level 1 – All Level 1 data are calibrated instrument observations, in physical units (such as brightness in Rayleighs, rather than instrument count rates). These data are at the same instrument resolution as the Level 0 data. Level 1 data are in instrument coordinates, and are not generally georeferenced.

Level 2 –Level 2 data are inverted geophysical parameters (plasma motions in m/s, ionospheric densities in m^{-3} etc) specified at locations in geographic coordinates. These are at the highest possible resolution as determined by the instrument and inversion algorithm constraints.

Level 3 – Geophysical variables mapped on uniform space-time grids, at a common sampling rate. Not currently used for any ICON data product.

Level 4 – Level 4 data are outputs from numerical models.

All Level 1 ICON data products are produced from the Level 0 instrument files. Level 2 and 4 data products are produced from either Level 1 or Level 2 data products. Figure 4.1 shows this flow of the ICON data products, which are color-coded by instrument or model.

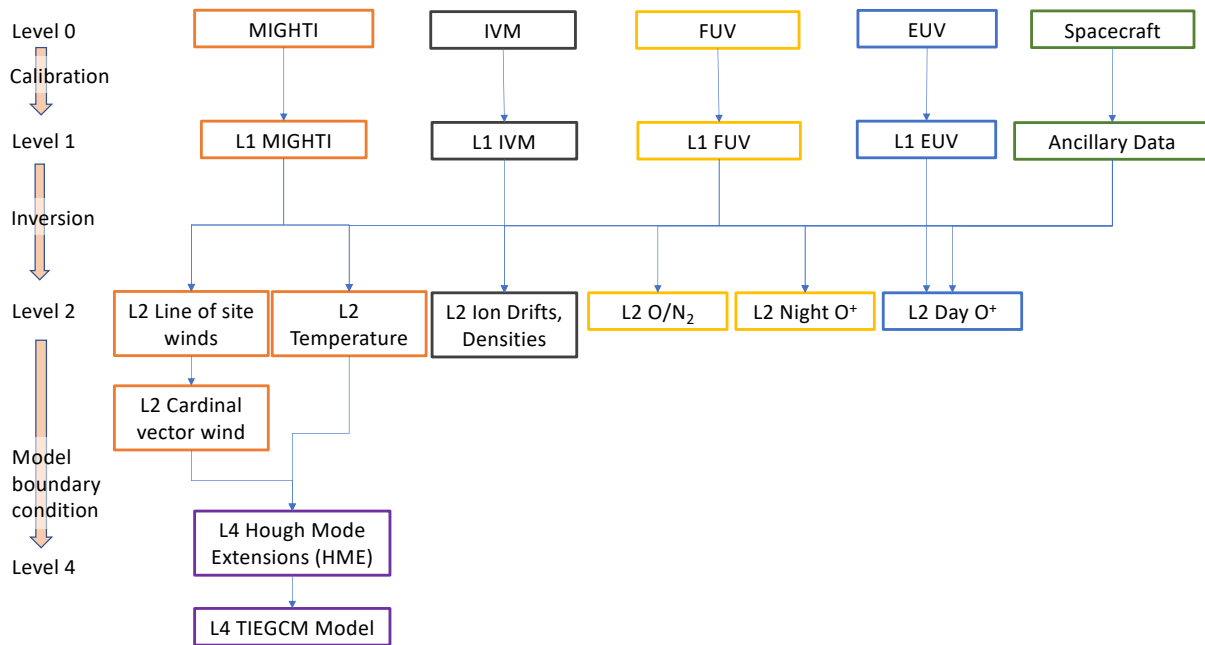


Figure 4.1 – High-level overview of ICON data products by Level. For further details, see Sections 4.1 – 4.4.

Data Level	MIGHTI	IVM	FUV	EUV
L0	Time -ordered raw data, with communication artifacts removed. UTC time included.	Time -ordered raw data, with communication artifacts removed. UTC time included.	Time -ordered raw data, with communication artifacts removed. UTC time included.	Time -ordered raw data, with communication artifacts removed. UTC time included.
L1	Calibrated interferograms of 557.7 and 630.0 nm observations vs time and view angle. O ₂ A-band and out-of-band brightness vs time and view	Calibrated incoming ion current and arrival angle vs time. Daily netCDF files. 1 file for IVM A, one for IVM B as applicable.	Calibrated shortwave and longwave Far UV images (6 horizontal bins, 256 vertical bins) vs time. Time-delay-integrated motion-	Calibrated extreme UV spectra vs time and view angle. Daily netCDF files.

	angle. Daily netCDF files. 1 file for MIGHTI A, one for MIGHTI B.		compensated images of the limb and sublimb in the shortwave channel. Daily netCDF files.	
Ancillary	Remote viewing geometry, instrument & spacecraft geometry at time of each observation. 1 file for MIGHTI A, one for MIGHTI B.	Instrument & spacecraft geometry at time of each observation. Spacecraft magneto torquer status at time of each observation. 1 file for IVM A, one for IVM B as applicable.	Remote viewing geometry, instrument & spacecraft geometry at time of each observation. Geophysical indices at time of each observation. One file for shortwave, one for longwave.	Remote viewing geometry, instrument & spacecraft geometry at time of each observation. Geophysical indices at time of each observation.
L2	Inverted line of site winds vs tangent altitude and time. Inverted vector (cardinal) horizontal winds vs altitude and time. Neutral temperatures vs altitude and time. All quantities georeferenced. Daily netCDF files. 1 file for MIGHTI A and B for the line of site and temperature, combined file for cardinal winds.	In situ ion density, composition, temperature and velocity in instrument, spacecraft and geomagnetic coordinates vs time. Daily netCDF files.	Inverted column O/N2 ratio vs time (daytime). O+ density vs altitude (nighttime). All quantities georeferenced. Daily netCDF files.	Inverted O+ density (daytime) vs altitude and time. All quantities georeferenced. Daily netCDF files.

L4	Hough Mode Extension fits to the MIGHTI L2 temperatures and winds vs altitude and time. Hough Mode Extension lower boundary files for the TIEGCM model. TIEGCM model output using the Hough Mode Extension lower boundary and a control run that does not use this lower boundary. Each as daily netCDF file	N/A	N/A	N/A
----	--	-----	-----	-----

Table 4.1 – List of ICON data products by level.

4.1 ICON Science Data Products

This section includes a summary list of the mission's instruments

Instrument Name	Parameters Measured [Baseline performance]	Instrument Type	Instrument Status
MIGHTI	Altitude resolved interferograms of 557.7 and 630.0 nm airglow, taken every 30s during daytime, 60s during nighttime. Altitude resolved brightness of 3 IR channels in-band and 2 out-of-band channels around the 762 nm O ₂ band. Two near orthogonally mounted units used to provide vector wind observations.	Visible imaging interferometer; IR imaging photometer	Green
IVM	In situ ion density, arrival angle, ram velocity, ion composition and	In situ plasma instrument – retarding	Green

	temperature. Measured every 4s day and night.	potential analyzer and drift meter	
FUV	2D images of the Far ultraviolet airglow centered on 135.6 and 155 nm O and N ₂ emissions taken every 12s during daytime. 2D images of the ultraviolet airglow centered on 135.6 nm O emission every 12s during nighttime. Time delay integration images of the limb and sublimb airglow centered on 135.6 nm O emission every 12s during nighttime.	Far ultraviolet spectrographic imager	Green
EUV	Altitude-resolved spectra of the extreme ultraviolet from 58.4 to 87.8 nm every 12s during daytime.	Extreme ultraviolet imaging spectrometer	Green, operating at reduced cadence – see Section 3.4.2

Table 4.1.1 summary list of the ICON instruments.

4.1.1 MIGHTI Data Products Functional Description

This subsection details the science data products produced by a particular mission instrument or ground system element (e.g., SOC).

Following this brief overview, details of the data products are provided for L1, L2 and Ancillary products. L0 are instrument level (voltages, modes, instrument codes etc.) and not interpretable for anyone without intimate knowledge of the instrumentation.

The mission-specific data levels should be defined, and the steps needed to process each level of data shall be described.

The introduction to Section 4 describes the overall data levels for ICON. Table 4.1.1.1 lists the MIGHTI products by level. The L0, Ancillary, L1 and L2 Line of Site and Temperatures have separate files for MIGHTI A and B. The L2 Vector Wind is made of the combination of both MIGHTI A and B line of site observations. The MIGHTI Ancillary file provides the geometry relevant to the observations, using knowledge of the spacecraft position and pointing derived from the spacecraft telemetry.

Level	Source (Instrument/Model)	Data Product
0	MIGHTI	L0 MIGHTI Science Data

0	MIGHTI	L0 MIGHTI Engineering Data
Anc.	Ground	MIGHTI Ancillary Data
1	MIGHTI	L1 MIGHTI
2	MIGHTI	Line of sight wind
2	MIGHTI	Cardinal vector wind
2	MIGHTI	Temperature

Table 4.1.1.1 – List of MIGHTI data products by level.

At a high level, the flow of the MIGHTI data products is shown in Figure 4.1.1.1 This also indicates how the MIGHTI winds and temperatures are used to produce the L4 Hough Mode Extension product, which in turn is used to drive the lower boundary of the TIEGCM model. Those L4 products are discussed in Sections 4.5 and 4.6, respectively.

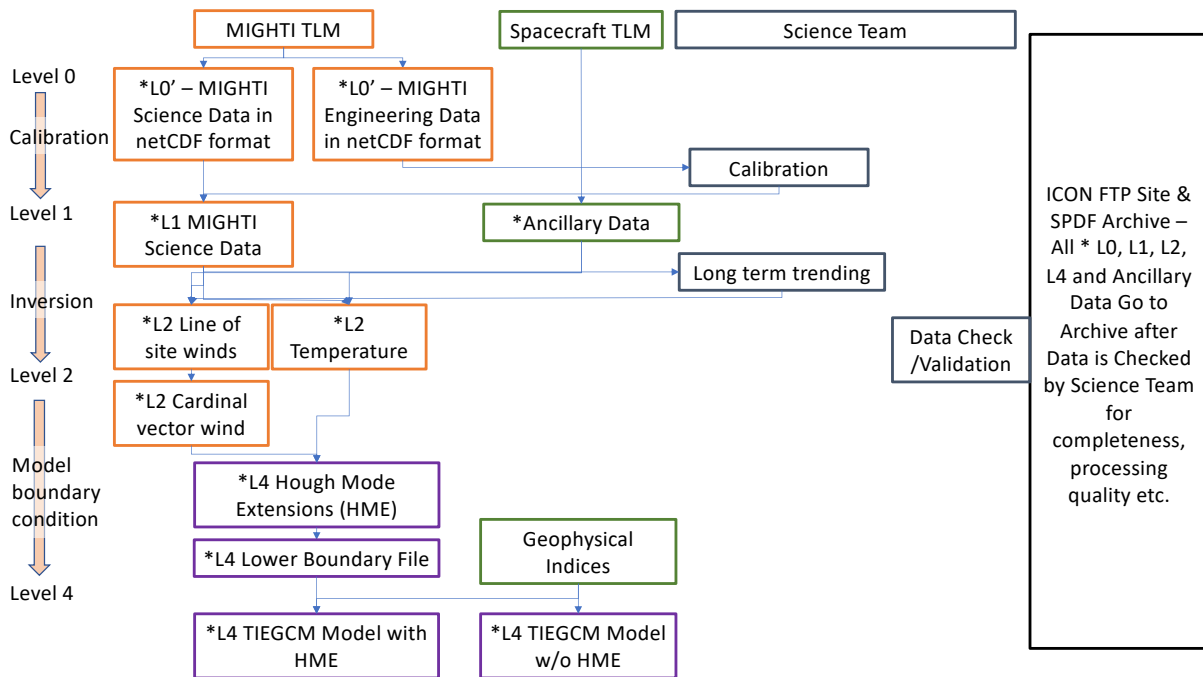


Figure 4.1.1.1 – Schematic of the MIGHTI Data Products and their Flow.

The overall concept for producing the L2 wind products are as follows: the MIGHTI instrument measures the line of sight Doppler shifts of the 557.7 and 630.0 nm airglow lines. These Doppler shifts are measured from changes in the phase of the peaks in two interferograms created within the image. From these line of sight Doppler shifts, winds can be inferred at Level 2. The L1 product includes the calibrated Doppler shifts across the redline and greenline images taken by MIGHTI. MIGHTI makes 2 such measurements on the horizon, with views that are 90° apart, in order to reconstruct the horizontal wind velocity. Daytime images are taken every 30s (approximately 250 km along the orbit track) during normal operations. Nighttime images are

taken every 60s (approximately 500 km along the orbit track) during normal operations. The overall process of producing MIGHTI L1 is shown in Figure 4.1.1.2.

MIGHTI L0 to MIGHTI L1 Interferometer – Algorithm & Output

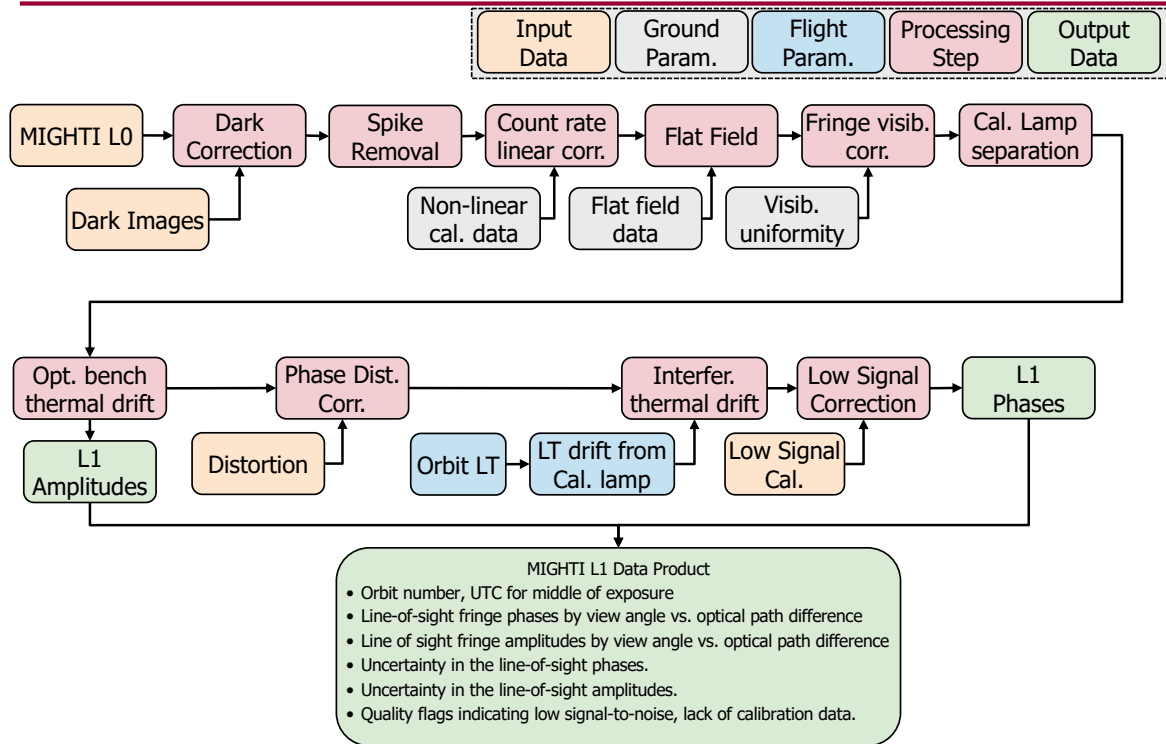


Figure 4.1.1.2 – Overall process for producing MIGHTI L1 Data Product.

L2 line of sight winds are then produced from the MIGHTI L1 and Ancillary data products. The L2 line of sight product includes the calibrated line of sight winds as a function of tangent altitude. These are done separately for each color and both of the MIGHTI channels. The LOS winds are attributed to the remote locations on the tangent (latitude, longitude, altitude etc.) using the MIGHTI Ancillary data. The overall process of producing MIGHTI L2 Line of sight Wind Product is shown in Figure 4.1.1.3.

MIGHTI L1 to 2 LOS Winds - Algorithm

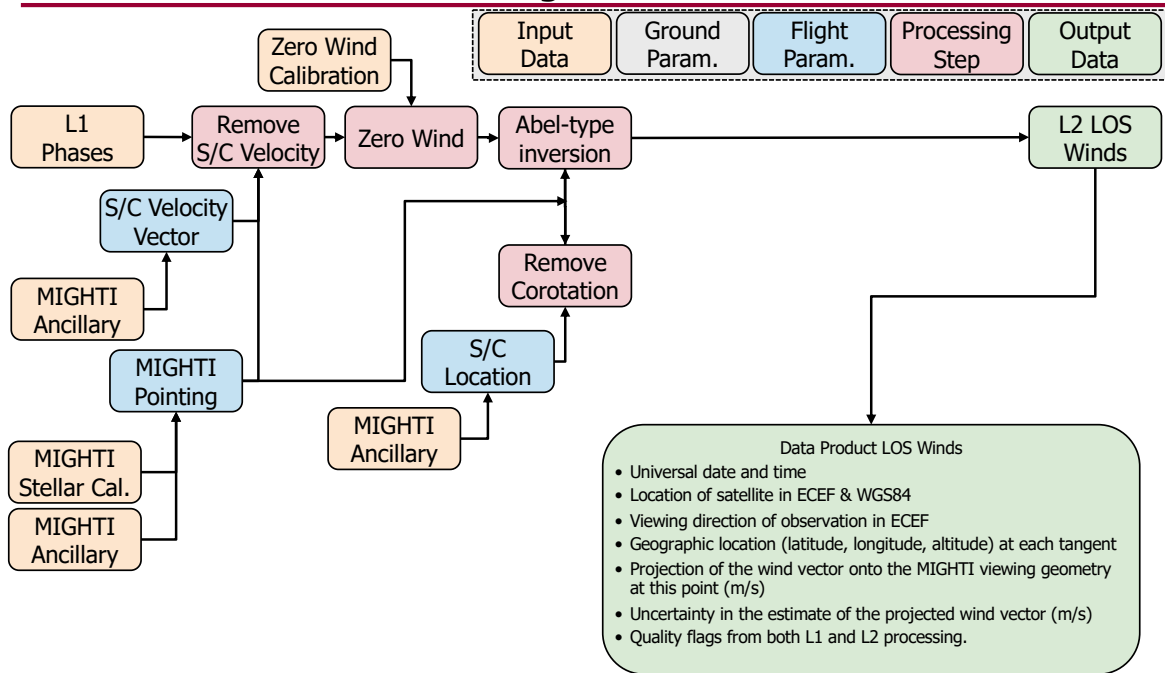


Figure 4.1.1.3 – Overall process for producing MIGHTI L2 Line of Site Wind Data Product.

L2 vector winds are then produced from the MIGHTI L2 Line of sight products for both MIGHTI A and B. The L2 vector product the calibrated vector winds (zonal and meridional) as a function of tangent altitude. These are produced by combining the line of sight measurements from both MIGHTI channels, but is done separately for each color. The vector winds are attributed to the remote locations on the tangent (latitude, longitude, altitude etc.). The overall process of producing MIGHTI L2 vector Wind Product is shown in Figure 4.1.1.4.

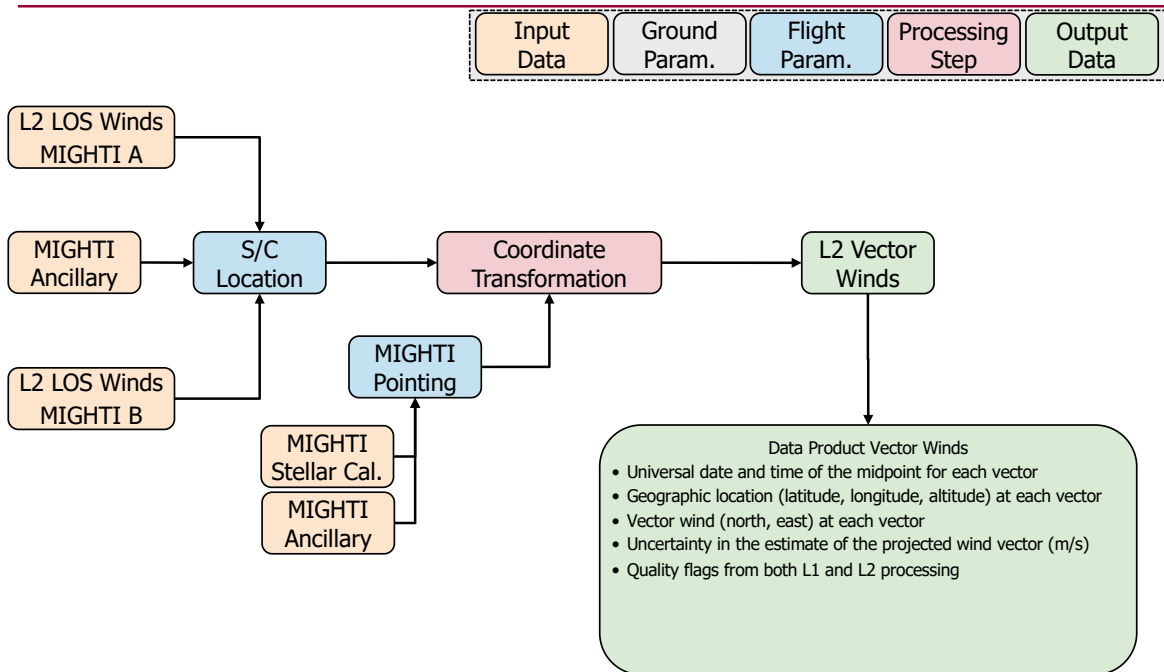


Figure 4.1.1.4 – Overall process for producing MIGHTI L2 Vector Wind Data Product.

The overall concept for producing the L2 temperature products are as follows: The MIGHTI instrument measures the brightness of the O₂ A-band in 3 bandpasses, plus 2 background channels. From these, the shape of the O₂ A Band is determined. The L1 product includes the relative brightness of the O₂ A band in these 3 wavelength ranges. The shape of the O₂ A Band can be used to infer neutral temperature (at Level 2). MIGHTI makes 2 such measurements on the horizon from MIGHTI-A and MIGHTI-B, with views that are 9 minutes apart with orthogonal look directions. Each view provides an independent measure of temperature (the 2 are not combined). Daytime images are taken every 30s (approximately 250 km along the orbit track) during normal operations. Nighttime images are taken every 60s (approximately 500 km along the orbit track) during normal operations. The tangent points associated with the image are quoted, but interpretation of what contribution comes from different remote locations is determined at Level 2. The overall process of producing MIGHTI L1 (O₂ A-band processing steps) are shown in Figure 4.1.1.5, although it is worth noting that this data is in the same file as the L1 interferometer data described above.

MIGHTI L0 to MIGHTI 1 O₂ Brightness - Algorithm

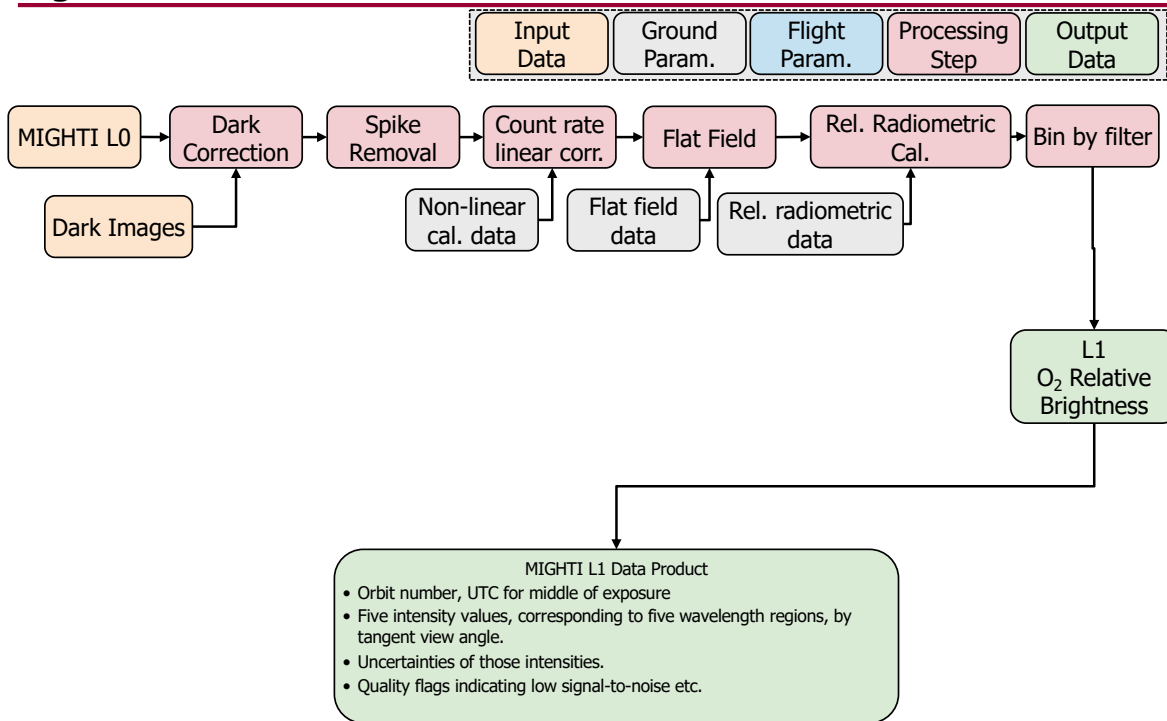


Figure 4.1.1.5 – Overall process for producing MIGHTI L1 Data Product relevant to O₂ A-band.

L2 temperatures are then produced from the MIGHTI L1 and Ancillary data products. The overall process of producing MIGHTI L2 Temperature Product is shown in Figure 4.1.1.6.

MIGHTI 1 to MIGHTI 2 Temperature - Algorithm

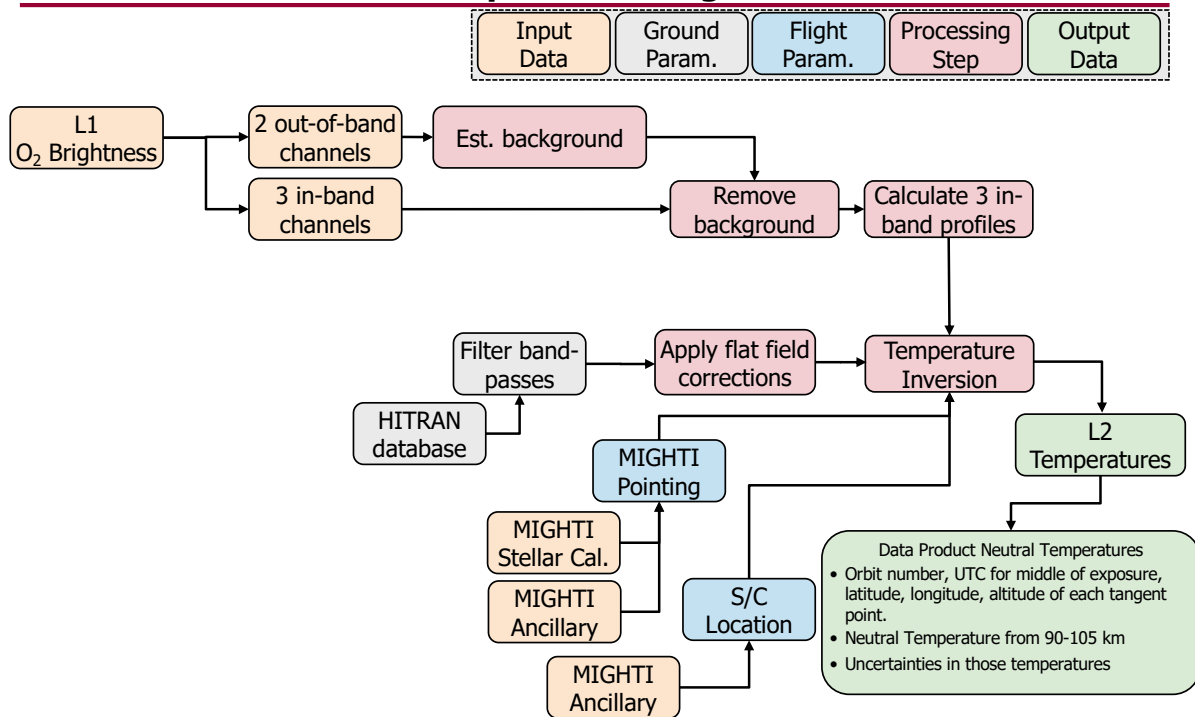


Figure 4.1.1.6 – Overall process for producing MIGHTI L2 Temperature Data Product.

For more details on the data processing, the reader is directed to the ICON Calibration and Measurement Algorithms Document and to relevant publications [Englert et al., 2022, Harding et al., 2017, Stevens et al., 2022].

A reference to the general data level definitions located in the Heliophysics Science Data Management Policy should be included.

The Heliophysics Science Data Management Policy, HPD-SDMP version 2.0, effective February 14, 2022 does not describe data levels. The ICON data levels closely follow those in the PDMP Template.

Any associated metadata products to be generated and maintained shall also be described.

Following this brief overview, full details of the metadata for each product are provided.

Details should also include the cadence (e.g., hourly, daily, etc.) for processing of data products.

The lowest level MIGHTI data (L0) has one file per image (nominally 30s daytime, 60s nighttime per MIGHTI Channel). Dark images, calibration images etc. are also saved as one file per image. These are processed as they arrive on the ground, until an entire day of data has arrived at the Science Data Center (SDC). The SDC processes the L0 into L1 and L2, and produces the Ancillary Data Products. The L1, Ancillary and L2 files all correspond to 1 file for 1 day. For L1, Ancillary and L2 Line of Sight Winds and Temperatures, there is 1 such file per day for MIGHTI A and another for MIGHTI B corresponding to each product. The L2 Vector Wind product requires both MIGHTI A and B as inputs, and produces just a single file per day for this product. The cadence for production of all products beyond L0 is daily, once all inputs are available. As one example, the ancillary products use the definitive ephemeris, which is generated by the Mission Operations Center approximately 1 week after real-time.

The following section contains detailed descriptions of each of the MIGHTI Data Products, the data and metadata contained within.

ICON Data Product 1.1,1.2: MIGHTI Calibrated LOS Winds and Temperature Array

This document describes the data product for ICON MIGHTI-B Level 1.1, 1.2 Calibrated Science Image File, which is in NetCDF4 format.

This file contains MIGHTI fringe information for wind retrieval and uncalibrated IR intensities (in electrons/s) for temperature retrieval.

The MIGHTI image is separated into three regions corresponding to the atmospheric emission collected: the red side (630.0 nm), the green side (557.7 nm), and the IR mosaic (760 - 765 nm).

For the wind retrieval the fringes are analyzed for envelope (fringe amplitude) and phase delta as compared to the previously determined phase of a fringe representing zero motion of the atmosphere.

Various instrument and spacecraft parameters are provided by or derived from information in an ancillary file which includes housekeeping data (thermal sensors, pointing data, etc) from the entire day.

ECEF stands for Earth Centered Earth Fixed and ECI for Earth Centered Inertial.

Further information on the instrument and analysis processes can be found in <https://doi.org/10.1364/FTS.2015.FM4A.1> by C. Englert, et. al., OSA 2015.

History

MIGHTI L1 Processing Code. Written by K. Marr, et al. Began 1/1/17.

Initial release: Version 1.3.0. Provides: Red and green line of sight fringe phases (less zero wind phase), red and green amplitudes, IR counts per second, red and green line of sight brightness profiles, tangent point geophysical data, and associated uncertainties. Processing includes: Spike correction, flatfield correction, fringe visibility correction, phase distortion correction, thermal effect correction, and image transfer pickup correction.

2nd release: Version 2.0.0. Includes sensor lateral shift calculation (notches) and correction. Update to zero wind determination.

Dimensions

NetCDF files contain **variables** and the **dimensions** over which those variables are defined. First, the dimensions are defined, then all variables in the file are described.

The dimensions used by the variables in this file are given below, along with nominal sizes. Note that the size may vary from file to file. For example, the "Epoch" dimension, which describes the number of time samples contained in this file, will have a varying size.

Dimension Name	Nominal Size
Epoch	1
ICON_L1_MIGHTI_B_IR_Array_Pixel_Index	413
ICON_L1_MIGHTI_B_IR_Array_Altitudes	20
ICON_L1_MIGHTI_B_Green_Array_OPD	362

Dimension Name	Nominal Size
ICON_L1_MIGHTI_B_Red_Array_OPD	323
ICON_L1_MIGHTI_B_Green_Array_Altitudes	82
ICON_L1_MIGHTI_B_Red_Array_Altitudes	60
ICON_L1_MIGHTI_B_Vector_LLA	3
ICON_L1_MIGHTI_B_Vector_XYZ	3
ICON_L1_MIGHTI_B_Vector_Roll	3
ICON_L1_MIGHTI_B_Time_Channel	3
ICON_L1_MIGHTI_B_IR_Channel	5
ICON_L0_MIGHTI_B_Image_ROI_Columns	92
ICON_L0_MIGHTI_B_Image_ROI_Rows	929

Variables

Variables in this file are listed below. First, "data" variables are described, followed by the "support_data" variables, and finally the "metadata" variables. The variables classified as "ignore_data" are not shown.

data

Variable Name	Description	Units	Dimensions
ICON_L1_MIGHTI_B_IR_Array	<p>CCD response per second to incident photons corresponding to the five IR filters</p> <p>CCD response per second to incident photons corresponding to the five IR filters by OPD and altitude.</p> <p>Raw CCD counts have been gain normalized and divided by integration time.</p>	Rel. R (Electrons/s)	Epoch, ICON_L1_MIGHTI_B_IR_Array_Altitudes, ICON_L1_MIGHTI_B_IR_Array_Pixel_Index
ICON_L1_MIGHTI_B_IR_Array_Tangent_LatLonAlt	<p>Tangent point latitudes, longitudes, and altitudes for IR altitudes - middle of FoV, all altitudes</p> <p>Tangent point latitudes, longitudes, and altitudes for IR side.</p> <p>Taken at middle of FoV for all altitudes at start, middle, and end of integration.</p>	degrees, degrees, km	Epoch, ICON_L1_MIGHTI_B_Time_Channel, ICON_L1_MIGHTI_B_Vector_LLA, ICON_L1_MIGHTI_B_IR_Array_Altitudes
ICON_L1_MIGHTI_B_IR_Array_Tangent_Local_Solar_Time	<p>Tangent point local solar time for IR altitudes at middle of FoV</p> <p>Tangent point local solar times for IR array.</p> <p>Taken at middle of FoV for all altitudes at start, middle, and end of integration.</p>	hr	Epoch, ICON_L1_MIGHTI_B_Time_Channel, ICON_L1_MIGHTI_B_IR_Array_Altitudes
ICON_L1_MIGHTI_B_IR_Array_Tangent_Azimuth_Angle	<p>Tangent point azimuth angle for IR altitudes at middle of FoV</p> <p>Azimuth angle (between line of sight and local north) at tangent points for IR array.</p> <p>Taken at middle of FoV for all altitudes at start, middle, and end of integration.</p> <p>Line of sight is the vector pointing from the spacecraft to the tangent point. At the tangent point, this vector is parallel to the ground. This variable follows the typical geophysical convention of degrees East of North (North=0, East=90, South=180, West=270). It can vary by a few degrees from the top of the profile to the bottom, so one value is reported per altitude. MIGHTI-A and MIGHTI-B will have values approximately 90 degrees apart.</p>	degrees	Epoch, ICON_L1_MIGHTI_B_Time_Channel, ICON_L1_MIGHTI_B_IR_Array_Altitudes
ICON_L1_MIGHTI_B_IR_Array_Tangent_Solar_Zenith_Angle	<p>Tangent point solar zenith angle for IR altitudes at middle of FoV</p> <p>Tangent point solar zenith angle for IR array.</p> <p>Taken at middle of FoV for all altitudes at start, middle, and end of integration.</p>	degrees	Epoch, ICON_L1_MIGHTI_B_Time_Channel, ICON_L1_MIGHTI_B_IR_Array_Altitudes

Variable Name	Description	Units	Dimensions
ICON_L1_MIGHTI_B_IR_Array_Tangent_Magnetic_Latitude	<p>Tangent point magnetic latitude</p> <p>Tangent point magnetic latitude for IR array.</p> <p>Taken at middle of FoV for all altitudes at start, middle, and end of integration.</p> <p>Quasi-dipole latitude and longitude are calculated using the fast implementation developed by Emmert et al. (2010, doi:10.1029/2010JA015326) and the Python wrapper apexpy (doi.org/10.5281/zenodo.1214207).</p> <p>Quasi-dipole longitude is defined such that zero occurs where the geodetic longitude is near 285 deg east (depending on latitude).</p>	degrees	Epoch, ICON_L1_MIGHTI_B_Time_Channel, ICON_L1_MIGHTI_B_IR_Array_Altitudes
ICON_L1_MIGHTI_B_IR_Array_Tangent_Magnetic_Longitude	<p>Tangent point magnetic longitude</p> <p>Tangent point magnetic longitude for IR array.</p> <p>Taken at middle of FoV for all altitudes at start, middle, and end of integration.</p> <p>Quasi-dipole latitude and longitude are calculated using the fast implementation developed by Emmert et al. (2010, doi:10.1029/2010JA015326) and the Python wrapper apexpy (doi.org/10.5281/zenodo.1214207).</p> <p>Quasi-dipole longitude is defined such that zero occurs where the geodetic longitude is near 285 deg east (depending on latitude).</p>	degrees	Epoch, ICON_L1_MIGHTI_B_Time_Channel, ICON_L1_MIGHTI_B_IR_Array_Altitudes
ICON_L1_MIGHTI_B_SC_Altitude	<p>Spacecraft Altitude</p> <p>Spacecraft altitude at start, middle, and end of integration.</p>	km	Epoch, ICON_L1_MIGHTI_B_Time_Channel
ICON_L1_MIGHTI_B_SC_Latitude	<p>Spacecraft latitude</p> <p>Spacecraft latitude at start, middle, and end of integration.</p>	degrees	Epoch, ICON_L1_MIGHTI_B_Time_Channel
ICON_L1_MIGHTI_B_SC_Longitude	<p>Spacecraft longitude</p> <p>Spacecraft longitude at start, middle, and end of integration.</p>	degrees	Epoch, ICON_L1_MIGHTI_B_Time_Channel
ICON_L1_MIGHTI_B_Total_Boresight_Sun_Angle	<p>Total angle between the MIGHTI boresight and the sun</p> <p>Total (not component) angle between the MIGHTI boresight and the sun at start, middle, and end of integration.</p>	degrees	Epoch, ICON_L1_MIGHTI_B_Time_Channel
ICON_L1_MIGHTI_B_Green_Phase	<p>Phase difference between the green atmospheric line and the associated calibration line minus the corresponding Zero Wind delta - by optical path difference (OPD) and altitude</p> <p>Phase difference between the green atmospheric line and the associated calibration line minus the corresponding Zero Wind delta - by optical path difference (OPD) and altitude.</p>	rad	Epoch, ICON_L1_MIGHTI_B_Green_Array_Altitudes, ICON_L1_MIGHTI_B_Green_Array_OPD

Variable Name	Description	Units	Dimensions
ICON_L1_MIGHTI_B_Green_Envelope	<p>Envelopes of the green atmospheric fringes by optical path difference (OPD) and altitude</p> <p>Envelopes (fringe amplitudes) of the green atmospheric interferograms by optical path difference (OPD) and altitude.</p>	Rel R	Epoch, ICON_L1_MIGHTI_B_Green_Array_Altitudes, ICON_L1_MIGHTI_B_Green_Array_OPD
ICON_L1_MIGHTI_B_Green_Relative_Brightness	<p>Relative brightness of green emission by altitude</p> <p>Relative brightness of green emission by altitude.</p> <p>Average of signal + DC for each altitude.</p> <p>SDL calibration used to convert counts to brightness.</p>	Rayleighs	Epoch, ICON_L1_MIGHTI_B_Green_Array_Altitudes
ICON_L1_MIGHTI_B_Green_Phase_Uncertainties	<p>Uncertainties of the phases of the green atmospheric line by altitude</p> <p>Uncertainties of the phase deltas of the green atmospheric line by altitude.</p> <p>Calculated from total signal, modulated signal, and first principles based on assumption of shot noise dominance.</p>	rad	Epoch, ICON_L1_MIGHTI_B_Green_Array_Altitudes
ICON_L1_MIGHTI_B_Green_Envelope_Uncertainties	<p>Uncertainties of the envelopes of the green atmospheric fringes by altitude</p> <p>Uncertainties of the envelopes of the green atmospheric fringes by altitude.</p> <p>Calculated from total signal, modulated signal, and first principles based on assumption of shot noise dominance.</p>	Rel R	Epoch, ICON_L1_MIGHTI_B_Green_Array_Altitudes
ICON_L1_MIGHTI_B_Green_Tangent_LatLonAlt	<p>Tangent point latitudes, longitudes, and altitudes for green side - middle of FoV, all altitudes</p> <p>Tangent point latitudes, longitudes, and altitudes for green side.</p> <p>Taken at middle of FoV for all altitudes at start, middle, and end of integration.</p>	degrees, degrees, km	Epoch, ICON_L1_MIGHTI_B_Time_Channel, ICON_L1_MIGHTI_B_Vector_LLA, ICON_L1_MIGHTI_B_Green_Array_Altitudes
ICON_L1_MIGHTI_B_Green_Tangent_Local_Solar_Time	<p>Tangent point local solar time for green side altitudes at middle of FoV</p> <p>Tangent point local solar times for green side.</p> <p>Taken at middle of FoV for all altitudes at start, middle, and end of integration.</p>	hr	Epoch, ICON_L1_MIGHTI_B_Time_Channel, ICON_L1_MIGHTI_B_Green_Array_Altitudes

Variable Name	Description	Units	Dimensions
ICON_L1_MIGHTI_B_Green_Tangent_Magnetic_Latitude	<p>Tangent point magnetic latitudes for green side altitudes at middle of FoV</p> <p>Tangent point magnetic latitudes for green side.</p> <p>Taken at middle of FoV for all altitudes at start, middle, and end of integration.</p> <p>Quasi-dipole latitude and longitude are calculated using the fast implementation developed by Emmert et al. (2010, doi:10.1029/2010JA015326) and the Python wrapper apexpy (doi.org/10.5281/zenodo.1214207).</p> <p>Quasi-dipole longitude is defined such that zero occurs where the geodetic longitude is near 285 deg east (depending on latitude).</p>	degrees	Epoch, ICON_L1_MIGHTI_B_Time_Channel, ICON_L1_MIGHTI_B_Green_Array_Altitudes
ICON_L1_MIGHTI_B_Green_Tangent_Magnetic_Longitude	<p>Tangent point magnetic longitudes for green side altitudes at middle of FoV</p> <p>Tangent point magnetic longitudes for green side.</p> <p>Taken at middle of FoV for all altitudes at start, middle, and end of integration.</p> <p>Quasi-dipole latitude and longitude are calculated using the fast implementation developed by Emmert et al. (2010, doi:10.1029/2010JA015326) and the Python wrapper apexpy (doi.org/10.5281/zenodo.1214207).</p> <p>Quasi-dipole longitude is defined such that zero occurs where the geodetic longitude is near 285 deg east (depending on latitude).</p>	degrees	Epoch, ICON_L1_MIGHTI_B_Time_Channel, ICON_L1_MIGHTI_B_Green_Array_Altitudes
ICON_L1_MIGHTI_B_Green_Tangent_Solar_Zenith_Angle	<p>Tangent point solar zenith angle for green side altitudes at middle of FoV</p> <p>Tangent point solar zenith angles for green side.</p> <p>Taken at middle of FoV for all altitudes at start, middle, and end of integration.</p>	degrees	Epoch, ICON_L1_MIGHTI_B_Time_Channel, ICON_L1_MIGHTI_B_Green_Array_Altitudes
ICON_L1_MIGHTI_B_Red_Phase	<p>Phase difference between the red atmospheric line and the associated calibration line minus the corresponding Zero Wind delta - by optical path difference (OPD) and altitude</p> <p>Phase difference between the red atmospheric line and the associated calibration line minus the corresponding Zero Wind delta - by optical path difference (OPD) and altitude.</p>	rad	Epoch, ICON_L1_MIGHTI_B_Red_Array_Altitudes, ICON_L1_MIGHTI_B_Red_Array_OPD
ICON_L1_MIGHTI_B_Red_Envelope	<p>Envelopes of the red atmospheric fringes by optical path difference (OPD) and altitude</p> <p>Envelopes (fringe amplitudes) of the red atmospheric interferograms by optical path difference (OPD) and altitude.</p>	Rel R	Epoch, ICON_L1_MIGHTI_B_Red_Array_Altitudes, ICON_L1_MIGHTI_B_Red_Array_OPD

Variable Name	Description	Units	Dimensions
ICON_L1_MIGHTI_B_Red_Relative_Brightness	<p>Relative brightness of the red emission by altitude</p> <p>Relative brightness of the red emission by altitude.</p> <p>Average of signal + DC for each altitude.</p> <p>SDL calibration used to convert counts to brightness.</p>	Rayleighs	Epoch, ICON_L1_MIGHTI_B_Red_Array_Altitudes
ICON_L1_MIGHTI_B_Red_Phase_Uncertainties	<p>Uncertainties of the phase deltas of the red atmospheric line by altitude</p> <p>Uncertainties of the phase deltas of the red atmospheric line by altitude.</p> <p>Calculated from total signal, modulated signal, first principles based on assumption of shot noise dominance.</p>	rad	Epoch, ICON_L1_MIGHTI_B_Red_Array_Altitudes
ICON_L1_MIGHTI_B_Red_Envelope_Uncertainties	<p>Uncertainties of the envelopes of the red atmospheric fringes by altitude</p> <p>Uncertainties of the envelopes of the red atmospheric fringes by altitude.</p> <p>Calculated from total signal, modulated signal, and first principles based on assumption of shot noise dominance.</p>	Relative R	Epoch, ICON_L1_MIGHTI_B_Red_Array_Altitudes
ICON_L1_MIGHTI_B_Red_Tangent_LatLonAlt	<p>Tangent point latitudes, longitudes, and altitudes for red side - middle of FoV, all altitudes</p> <p>Tangent point latitudes, longitudes, and altitudes for red side.</p> <p>Taken at middle of FoV for all altitudes at start, middle, and end of integration.</p>	degrees, degrees, km	Epoch, ICON_L1_MIGHTI_B_Time_Channel, ICON_L1_MIGHTI_B_Vector_LLA, ICON_L1_MIGHTI_B_Red_Array_Altitudes
ICON_L1_MIGHTI_B_Red_Tangent_Local_Solar_Time	<p>Tangent point local solar time for red side altitudes at middle of FoV</p> <p>Tangent point local solar times for red side.</p> <p>Taken at middle of FoV for all altitudes at start, middle, and end of integration.</p>	hr	Epoch, ICON_L1_MIGHTI_B_Time_Channel, ICON_L1_MIGHTI_B_Red_Array_Altitudes
ICON_L1_MIGHTI_B_Red_Tangent_Magnetic_Latitude	<p>Tangent point magnetic latitudes for red side altitudes at middle of FoV</p> <p>Tangent point magnetic latitudes for red side.</p> <p>Taken at middle of FoV for all altitudes at start, middle, and end of integration.</p> <p>Quasi-dipole latitude and longitude are calculated using the fast implementation developed by Emmert et al. (2010, doi:10.1029/2010JA015326) and the Python wrapper apexpy (doi.org/10.5281/zenodo.1214207).</p> <p>Quasi-dipole longitude is defined such that zero occurs where the geodetic longitude is near 285 deg east (depending on latitude).</p>	degrees	Epoch, ICON_L1_MIGHTI_B_Time_Channel, ICON_L1_MIGHTI_B_Red_Array_Altitudes

Variable Name	Description	Units	Dimensions
ICON_L1_MIGHTI_B_Red_Tangent_Magnetic_Longitude	<p>Tangent point magnetic longitudes for red side altitudes at middle of FoV</p> <p>Tangent point magnetic longitudes for red side.</p> <p>Taken at middle of FoV for all altitudes at start, middle, and end of integration.</p> <p>Quasi-dipole latitude and longitude are calculated using the fast implementation developed by Emmert et al. (2010, doi:10.1029/2010JA015326) and the Python wrapper apexpy (doi.org/10.5281/zenodo.1214207).</p> <p>Quasi-dipole longitude is defined such that zero occurs where the geodetic longitude is near 285 deg east (depending on latitude).</p>	degrees	Epoch, ICON_L1_MIGHTI_B_Time_Channel, ICON_L1_MIGHTI_B_Red_Array_Altitudes
ICON_L1_MIGHTI_B_Red_Tangent_Solar_Zenith_Angle	<p>Tangent point solar zenith angle for red side altitudes at middle of FoV</p> <p>Tangent point solar zenith angles for red side.</p> <p>Taken at middle of FoV for all altitudes at start, middle, and end of integration.</p>	degrees	Epoch, ICON_L1_MIGHTI_B_Time_Channel, ICON_L1_MIGHTI_B_Red_Array_Altitudes
ICON_L1_MIGHTI_B_Green_ECEF_Unit_Vectors	<p>ECEF Unit Vectors per pixel representing the green lines of sight</p> <p>ECEF Unit Vectors per pixel representing the green lines of sight.</p> <p>Calculated from the boresight ECEF vector and pixel-to-view-angle ground calibrations, as documented in the MIGHTI alignment report.</p> <p>By OPD and altitude at start, middle and end of the integration.</p>		Epoch, ICON_L1_MIGHTI_B_Vector_XYZ, ICON_L1_MIGHTI_B_Green_Array_Altitudes, ICON_L1_MIGHTI_B_Green_Array_OPD
ICON_L1_MIGHTI_B_Red_ECEF_Unit_Vectors	<p>ECEF Unit Vectors per pixel representing the red lines of sight</p> <p>ECEF Unit Vectors per pixel representing the red lines of sight.</p> <p>Calculated from the boresight ECEF vector and pixel-to-view-angle ground calibrations, as documented in the alignment report.</p> <p>By OPD and altitude at start, middle and end of the integration.</p>		Epoch, ICON_L1_MIGHTI_B_Vector_XYZ, ICON_L1_MIGHTI_B_Red_Array_Altitudes, ICON_L1_MIGHTI_B_Red_Array_OPD
ICON_L0_MIGHTI_B_Image_ROI_Pixels	<p>MIGHTI region of interest pixel values layed out [ROWS]x[COLUMNS].</p> <p>The entire unrotated imaged region from MIGHTI. Typically 92 x 929 pixels (altitude x optical path difference). During processing this image is rotated ninety degrees clockwise and then split into red, green, and IR regions.</p>	Count	Epoch, ICON_L0_MIGHTI_B_Image_ROI_Rows, ICON_L0_MIGHTI_B_Image_ROI_Columns

support_data

Variable Name	Description	Units	Dimensions
Epoch	<p>Milliseconds since 1970-01-01 00:00:00 UTC at middle of image integration</p> <p>Milliseconds since 1970-01-01 00:00:00 UTC at middle of image integration.</p>	ms	Epoch
ICON_L1_MIGHTI_B_IR_Array_Pixel_Index	<p>Pixel indices corresponding to the IR filter mosaic</p> <p>Pixel (OPD) indices corresponding to the IR filter mosaic (1st dimension).</p>		Epoch, ICON_L1_MIGHTI_B_IR_Array_Pixel_Index
ICON_L1_MIGHTI_B_IR_Array_Altitudes	<p>Tangent altitudes corresponding to the five IR filters</p> <p>Tangent altitudes corresponding to the rows of the IR filter mosaic (2nd dimension).</p>	km	Epoch, ICON_L1_MIGHTI_B_IR_Array_Altitudes
ICON_L1_MIGHTI_B_Green_Quality_Factor	<p>Data quality Factor by altitude for 557nm</p> <p>Data quality Factor by altitude for green line.</p> <p>0: unable to analyze data</p> <p>0.5: data has one or more of the issues listed below</p> <p>1.0: good data</p> <p>Reasons for 0.5 setting: Thermal Drift calibration file greater than 3 days old, uncertainty in green phases greater than 0.35.</p>		Epoch, ICON_L1_MIGHTI_B_Green_Array_Altitudes
ICON_L1_MIGHTI_B_Green_Array_OPD	<p>Optical path differences corresponding to the L1 green side pixels (along fringe pattern)</p> <p>Optical path differences corresponding to the L1 green side pixels (along fringe pattern).</p> <p>The OPD increases from left to right in L1 rotated coordinates and is used to convert phase deltas to atmospheric winds as demonstrated in https://doi.org/10.1364/FTS.2015.FM4A.1 by C. Englert, et. al., OSA 2015.</p> <p>OPD range is roughly 4.9 - 5.9 cm depending on region of interest.</p>	cm	Epoch, ICON_L1_MIGHTI_B_Green_Array_OPD
ICON_L1_MIGHTI_B_Green_Array_Altitudes	<p>Tangent altitudes corresponding to the green fringes - middle of integration, middle of FoV</p> <p>Tangent altitudes corresponding to the rows of the green fringes.</p> <p>Taken from middle of integration time at middle of FoV.</p>	km	Epoch, ICON_L1_MIGHTI_B_Green_Array_Altitudes
ICON_L1_MIGHTI_B_Red_Quality_Factor	<p>Data quality Factor by altitude for 630nm</p> <p>Data quality Factor by altitude for red line.</p> <p>0.0: unable to analyze data</p> <p>0.5: data has one or more of the issues listed below</p> <p>1.0: good data</p> <p>Reasons for 0.5 setting: Thermal Drift calibration file greater than 3 days old, uncertainty in red phases greater than 0.35.</p>		Epoch, ICON_L1_MIGHTI_B_Red_Array_Altitudes

Variable Name	Description	Units	Dimensions
ICON_L1_MIGHTI_B_Red_Array_OPD	<p>Optical path differences corresponding to the L1 red side pixels (along fringe pattern)</p> <p>Optical path differences corresponding to the L1 red side pixels (along fringe pattern).</p> <p>The OPD increases from left to right in L1 rotated coordinates and is used to convert phase deltas to atmospheric winds as demonstrated in https://doi.org/10.1364/FTS.2015.FM4A.1 by C. Englert, et. al., OSA 2015.</p> <p>OPD range is roughly 4.9 - 5.9 cm depending on region of interest.</p>	cm	Epoch, ICON_L1_MIGHTI_B_Red_Array_OPD
ICON_L1_MIGHTI_B_Red_Array_Altitudes	<p>Tangent altitudes corresponding to the red fringes - middle of integration, middle of FoV</p> <p>Tangent altitudes corresponding to the rows for the red fringes</p> <p>Taken from middle of integration time at middle of FoV.</p>	km	Epoch, ICON_L1_MIGHTI_B_Red_Array_Altitudes
ICON_L1_MIGHTI_B_SC_Position_ECEF	<p>Spacecraft Position Vector in ECEF</p> <p>Spacecraft Position Vector in ECEF as given in the MIGHTI ancillary file.</p>	km	Epoch, ICON_L1_MIGHTI_B_Time_Channel, ICON_L1_MIGHTI_B_Vector_XYZ
ICON_L1_MIGHTI_B_SC_Velocity_ECEF	<p>ECEF Vector for spacecraft velocity</p> <p>ECEF Vector for spacecraft velocity as given in the MIGHTI ancillary file.</p>	m/s	Epoch, ICON_L1_MIGHTI_B_Time_Channel, ICON_L1_MIGHTI_B_Vector_XYZ
ICON_L1_MIGHTI_B_Image_Times	<p>Epochs corresponding to the Start, Middle, and Stop of the integration</p> <p>Epochs corresponding to the start, middle, and end of the integration.</p>	ms	Epoch, ICON_L1_MIGHTI_B_Time_Channel
ICON_L1_MIGHTI_B_Roll_Angles	<p>Roll angles of the field of view</p> <p>Roll angles of the field of view.</p> <p>Order: Boresight angle, CCD_Limb angle, CCD_Altitudes angle.</p>	degrees, degrees, degrees	Epoch, ICON_L1_MIGHTI_B_Vector_Roll
ICON_L1_MIGHTI_B_Quality_Flag_Low_Signal_To_Noise_Red	<p>Quality Flag indicating low signal to noise in red signal</p> <p>Quality Flag indicating low signal to noise for red signal by altitude. Half up means the uncertainty is above 0.35rad. Full up means single-row analysis was impossible.</p>		Epoch, ICON_L1_MIGHTI_B_Red_Array_Altitudes
ICON_L1_MIGHTI_B_Quality_Flag_Low_Signal_To_Noise_Green	<p>Quality Flag indicating low signal to noise in green signal</p> <p>Quality Flag indicating low signal to noise for green signal by altitude. Half up means the uncertainty is above 0.35rad. Full up means single-row analysis was impossible.</p>		Epoch, ICON_L1_MIGHTI_B_Green_Array_Altitudes

Variable Name	Description	Units	Dimensions
ICON_L1_MIGHTI_B_Quality_Flag_SAA	<p>Quality Flag indicating that the spacecraft is within the South Atlantic Anomaly</p> <p>Quality Flag indicating that the spacecraft is within the South Atlantic Anomaly based on the spacecraft status register.</p>		Epoch
ICON_L1_MIGHTI_B_Quality_Flag_Bad_Calibration	<p>Quality Flag indicating an inappropriate calibration file has been used or was missing</p> <p>Quality Flag indicating a thermal drift file older than three days has been used.</p>		Epoch
ICON_L1_MIGHTI_B_Quality_Flag_Sun_Moon_in_FoV	<p>Quality Flag indicating that either the Sun or Moon is in or near the field of view.</p> <p>Quality Flag indicating either the Sun or Moon is in or near the field of view.</p> <p>Half up means the moon was within 5 degrees of the field of view for this image.</p> <p>Full up means the Sun is within 7 degrees of the field of view at some point during the day.</p> <p>For both cases the quality factors are set to zero for the whole image.</p>		Epoch
ICON_L1_MIGHTI_B_SC_Attitude_Control_Register	<p>Spacecraft Attitude Control Register</p> <p>Spacecraft Attitude Control Register.</p> <p>Bit 0: LVLH NORMAL</p> <p>Bit 1: LVLH Reverse Mode</p> <p>Bit 2: Earth Limb Pointing</p> <p>Bit 3: Inertial Pointing</p> <p>Bit 4: Stellar Pointing</p> <p>Bit 5: Attitude Slew</p> <p>Bit 6: Conjugate Maneuver</p> <p>Bit 7: Nadir Calibration</p> <p>Bit 8: Lunar Calibration</p> <p>Bit 9: Stellar Calibration</p>		Epoch
ICON_L1_MIGHTI_B_SC_Pointing_Jitter	<p>Spacecraft Pointing Jitter</p> <p>Spacecraft pointing jitter.</p> <p>On the basis of the ECEF quaternion ephemeris, a 60-second window is found.</p> <p>Over that window a linear fit is found.</p> <p>A residual between the actual values and linear fit is calculated.</p> <p>The standard deviation of that residual is reported as the jitter.</p> <p>The closest ephemeris time to the MIGHTI middle time is used in this variable.</p>	degrees	Epoch

Variable Name	Description	Units	Dimensions
ICON_LO_MIGHTI_B_Time.UTC	<p>ISO 9601 formatted UTC timestamp (at middle of image integration).</p> <p>ISO 9601 formatted UTC timestamp (at middle of image integration).</p> <p>Derived from original GPS values reported from spacecraft (Time_GPS_Seconds and Time_GPS_Subseconds).</p> <p>Time calculation is offset by 615ms (flush time) for the first image in the series and for all other images are adjusted by subtracting (integration time + 308 milliseconds) from the reported GPS time then adding the difference between the readout FRT and the header FRT.</p> <p>Time may be delayed by up to 10 ms due to FSW polling delay.</p> <p>Minimum allowed value for this variable is 1970-01-01 00:00:00 UTC and maximum allowed value is 2150-01-01 00:00:00 UTC.</p> <p>All character arrays are NULL terminated (size includes NULL).</p>		Epoch
ICON_LO_MIGHTI_B_Time.GPS	<p>Milliseconds since 1980-01-06 00:00:00 TAI (coincident with UTC) at middle of image integration.</p> <p>Milliseconds since 1980-01-06 00:00:00 TAI (coincident with UTC) at middle of image integration.</p> <p>Derived from original GPS values reported from spacecraft (Time_GPS_Seconds and Time_GPS_Subseconds).</p> <p>Time calculation is offset by 615ms (flush time) for the first image in the series and for all other images are adjusted by subtracting (integration time + 308 milliseconds) from the reported GPS time then adding the difference between the readout FRT and the header FRT.</p> <p>Time may be delayed by up to 10 ms due to FSW polling delay.</p> <p>Minimum allowed value for this variable is a long integer corresponding to 1980-01-06 00:00:00 UTC and maximum allowed value is a long integer corresponding to a time in year 2154 UTC.</p>	milliseconds	Epoch

Variable Name	Description	Units	Dimensions
ICON_LO_MIGHTI_B_Time.UTC_Start	<p>Milliseconds since 1970-01-01 00:00:00 UTC at start of image integration.</p> <p>Milliseconds since 1970-01-01 00:00:00 UTC at start of image integration.</p> <p>Derived from original GPS values reported from spacecraft (Time_GPS_Seconds and Time_GPS_Subseconds).</p> <p>Time calculation is offset by 615ms (flush time) for the first image in the series and for all other images are adjusted by subtracting (integration time + 308 milliseconds) from the reported GPS time then adding the difference between the readout FRT and the header FRT.</p> <p>Time may be delayed by up to 10 ms due to FSW polling delay.</p> <p>Minimum allowed value for this variable is a long integer corresponding to 1970-01-01 00:00:00 UTC and maximum allowed value is a long integer corresponding to a time in year 2160 UTC.</p>	milliseconds	Epoch
ICON_LO_MIGHTI_B_Time.UTC_Stop	<p>Milliseconds since 1970-01-01 00:00:00 UTC at end of image integration.</p> <p>Milliseconds since 1970-01-01 00:00:00 UTC at end of image integration.</p> <p>Derived from original GPS values reported from spacecraft (Time_GPS_Seconds and Time_GPS_Subseconds).</p> <p>Time calculation is offset by 615ms (flush time) for the first image in the series and for all other images are adjusted by subtracting (integration time + 308 milliseconds) from the reported GPS time then adding the difference between the readout FRT and the header FRT.</p> <p>Time may be delayed by up to 10 ms due to FSW polling delay.</p> <p>Minimum allowed value for this variable is a long integer corresponding to 1970-01-01 00:00:00 UTC and maximum allowed value is a long integer corresponding to a time in year 2160 UTC.</p>	milliseconds	Epoch
ICON_LO_MIGHTI_B_Time.GPS_Seconds	<p>GPS seconds count when FSW received image packet header.</p> <p>GPS seconds count when FSW received image packet header.</p> <p>The FSW received the header of the first image in a series 615ms after start of image processing. Following headers are adjusted by subtracting (integration time + 308 milliseconds) from the reported GPS time then adding the difference between the readout FRT and the header FRT.</p> <p>Time may be delayed by up to 10 ms due to FSW polling delay.</p>	Seconds	Epoch

Variable Name	Description	Units	Dimensions
ICON_L0_MIGHTI_B_Time_GPS_Subseconds	<p>FSW 20MHz clock (50 nanosecond) offset from GPS seconds.</p> <p>FSW 20MHz clock (50 nanosecond) offset from GPS seconds.</p> <p>The FSW received the header of the first image in a series 615ms after start of image processing. Following headers are adjusted by subtracting (integration time + 308 milliseconds) from the reported GPS time then adding the difference between the readout FRT and the header FRT.</p> <p>The offset may be more than 1 second but never 2 or more seconds.</p> <p>Time may be delayed by up to 10 ms due to FSW polling delay.</p>	50 Nanoseconds	Epoch
ICON_L0_MIGHTI_B_Time_Integration	Time to integrate MIGHTI-B region of interest (ROI) image.	milliseconds	Epoch
ICON_L0_MIGHTI_B_Time_Header_Free_Running_Timer	<p>Free running timer reading for MIGHTI image header.</p> <p>The FRTs are millisecond free running timers used to calculate the time offset for this image's integration from the observatory GPS time tag. This is only used when it is not the first image in the integration sequence. When the prior image FRT is not known a timing error is generated as a calculation cannot be performed. The base GPS time is used as the start time.</p>	milliseconds	Epoch
ICON_L0_MIGHTI_B_Time_Readout_Free_Running_Timer	<p>Free running timer reading for MIGHTI image data readout start.</p> <p>The FRTs are millisecond free running timers used to calculate the time offset for this image's integration from the observatory GPS time tag. This is only used when it is not the first image in the integration sequence. When the prior image FRT is not known a timing error is generated as a calculation cannot be performed. The base GPS time is used as the start time.</p>	milliseconds	Epoch
ICON_L0_MIGHTI_B_Time_Prior_Readout_Free_Running_Timer	<p>Free running timer reading for MIGHTI prior image data readout start.</p> <p>The FRTs are millisecond free running timers used to calculate the time offset for this image's integration from the observatory GPS time tag. This is only used when it is not the first image in the integration sequence. When the prior image FRT is not known a timing error is generated as a calculation cannot be performed. The base GPS time is used as the start time.</p>	milliseconds	Epoch
ICON_L0_MIGHTI_B_Time_Prior_Known	<p>Flag indicating prior image's free running timer known.</p> <p>The FRTs are millisecond free running timers used to calculate the time offset for this image's integration from the observatory GPS time tag. This is only used when it is not the first image in the integration sequence. When the prior image FRT is not known a timing error is generated as a calculation cannot be performed. The base GPS time is used as the start time.</p>	Flag	Epoch

Variable Name	Description	Units	Dimensions
ICON_L0_MIGHTI_B_MT_Device_ID	MIGHTI camera instrument ID (0=MIGHTI-A, 1=MIGHT-B).	Flag	
ICON_L0_MIGHTI_B_MT_Device_Current_Sense	MIGHTI camera current (power) monitor count.	Count	Epoch
ICON_L0_MIGHTI_B_Calibration_Lamp_1	MIGHTI camera calibration lamp 1 setting (0=OFF, 1=ON). MIGHTI krypton (557.03 nm) camera calibration lamp 1 setting (0=OFF, 1=ON).	Flag	Epoch
ICON_L0_MIGHTI_B_Calibration_Lamp_2	MIGHTI camera calibration lamp 2 setting (0=OFF, 1=ON). MIGHTI neon (630.48 nm) camera calibration lamp 1 setting (0=OFF, 1=ON).	Flag	Epoch
ICON_L0_MIGHTI_B_Calibration_Lamp_Current	MIGHTI camera calibration lamp combined current monitor sense count.	Count	Epoch
ICON_L0_MIGHTI_B_Calibration_Lamp_Temperature	MIGHTI camera calibration lamp combined temperature monitor sense count.	Count	Epoch
ICON_L0_MIGHTI_B_Interferometer_1_Temperature_Sense	MIGHTI interferometer 1 fine temperature sense count.	Count	Epoch
ICON_L0_MIGHTI_B_Interferometer_2_Temperature_Sense	MIGHTI interferometer 2 fine temperature sense count.	Count	Epoch
ICON_L0_MIGHTI_B_Optics_Bench_Temperature_Forward	MIGHTI optics bench forward temperature sense count.	Count	Epoch
ICON_L0_MIGHTI_B_Optics_Bench_Temperature_Rear	MIGHTI optics bench rear temperature sense count.	Count	Epoch
ICON_L0_MIGHTI_B_Optics_Temperature_Aft	MIGHTI optics aft temperature sense count.	Count	Epoch
ICON_L0_MIGHTI_B_TEC_Current_Input_Count	MIGHTI thermo-electric cooler combined (TEC-A + TEC-B) input current count.	Count	Epoch
ICON_L0_MIGHTI_B_TEC_Temperature_Cold_Count	MIGHTI thermo-electric cooler cold-side temperature sense count.	Count	Epoch
ICON_L0_MIGHTI_B_TEC_Temperature_Hot_Count	MIGHTI thermo-electric cooler hot-side temperature sense count.	Count	Epoch

Variable Name	Description	Units	Dimensions
ICON_L0_MIGHTI_B_MTA_Aperture1_Position	MIGHTI-A camera aperture 1 position sense flag. 0=OPEN, 1=CLOSED, 2=15% OPEN, 3=UNKNOWN	Flag	Epoch
ICON_L0_MIGHTI_B_MTA_Aperture2_Position	MIGHTI-A camera aperture 2 position sense flag. 0=OPEN, 1=CLOSED, 2=15% OPEN, 3=UNKNOWN	Flag	Epoch
ICON_L0_MIGHTI_B_MTA_Aperture1	MIGHTI-A camera aperture 1 switch setting (0=OPEN, 1=CLOSED).	Flag	Epoch
ICON_L0_MIGHTI_B_MTA_Aperture2	MIGHTI-A camera aperture 2 switch setting (0=OPEN, 1=CLOSED).	Flag	Epoch
ICON_L0_MIGHTI_B_MTB_Aperture1_Position	MIGHTI-B camera aperture 1 position sense flag. 0=OPEN, 1=CLOSED, 2=15% OPEN, 3=UNKNOWN	Flag	Epoch
ICON_L0_MIGHTI_B_MTB_Aperture2_Position	MIGHTI-B camera aperture 2 position sense flag. 0=OPEN, 1=CLOSED, 2=15% OPEN, 3=UNKNOWN	Flag	Epoch
ICON_L0_MIGHTI_B_MTB_Aperture1	MIGHTI-B camera aperture 1 switch setting (0=OPEN, 1=CLOSED).	Flag	Epoch
ICON_L0_MIGHTI_B_MTB_Aperture2	MIGHTI-B camera aperture 2 switch setting (0=OPEN, 1=CLOSED).	Flag	Epoch
ICON_L0_MIGHTI_B_Error_Compression	Error count during compression (per packet). Error count during compression (per packet). Should be zero (for no error) but if it is a non-zero number then the number indicates the number of packets that contained an overflow in the delta bit field during compression.	Count	Epoch
ICON_L0_MIGHTI_B_Error_Time	Error finding prior image readout FRT (0=GOOD, 1=ERROR). Error finding prior image readout FRT (0=GOOD, 1=ERROR). The prior image read out FRT was missing so proper time offset couldn't be calculated correctly. The time will indicate later than the actual time. This only occurs when not the first image of the series.	Flag	Epoch
ICON_L0_MIGHTI_B_CCD_CS_Register	CCD CS register value from image header at end of integration. CCD CS register value from image header at end of integration. See ICN-ICD-002 (MIGHTI) for more details on this parameter.	Flag	Epoch

Variable Name	Description	Units	Dimensions
ICON_L0_MIGHTI_B_Horizontal_Charge_Transfer_Efficiency_Count	Horizontal charge transfer efficiency register count indicating the horizontal overscan pixel configuration per MIGHTI ICD. Horizontal charge transfer efficiency register count indicating the horizontal overscan pixel configuration per MIGHTI ICD. See ICN-ICD-002 (MIGHTI) for more details on this parameter.	Count	Epoch
ICON_L0_MIGHTI_B_Image_BIN_Parameters	MIGHTI binning parameters (BINCOUNTS). MIGHTI binning parameters (BINCOUNTS). See ICN-ICD-002 (MIGHTI) for more details on this parameter. Bitwise register. Typical binning is 16 x 2 in unrotated coordinates.	Flag	Epoch
ICON_L0_MIGHTI_B_Image_First	First image in MIGHTI integration sequence (0=NOT FIRST, 1=FIRST).	Flag	Epoch
ICON_L0_MIGHTI_B_Image_ROI_Column_Count	MIGHTI region of interest (ROI) pixel column count.	Count	Epoch
ICON_L0_MIGHTI_B_Image_ROI_Column_Start	MIGHTI region of interest (ROI) pixel starting column.	Count	Epoch
ICON_L0_MIGHTI_B_Image_ROI_Row_Count	MIGHTI region of interest (ROI) pixel row count.	Count	Epoch
ICON_L0_MIGHTI_B_Image_ROI_Row_Start	MIGHTI region of interest (ROI) pixel starting row.	Count	Epoch

metadata

Variable Name	Description	Units	Dimensions
ICON_L1_MIGHTI_B_Vector_LLA	Vector labels corresponding to the tangent latitude, longitude, and altitude Vector labels corresponding to the tangent latitude, longitude, and altitude.		ICON_L1_MIGHTI_B_Vector_LLA
ICON_L1_MIGHTI_B_Vector_XYZ	Vector labels corresponding to the ECEF lines of sight Vector labels corresponding to the ECEF lines of sight.		ICON_L1_MIGHTI_B_Vector_XYZ
ICON_L1_MIGHTI_B_Vector_Roll	Vector labels corresponding to the field of view roll angles Vector labels corresponding to the field of view roll angles.		ICON_L1_MIGHTI_B_Vector_Roll
ICON_L1_MIGHTI_B_Time_Channel	Vector labels corresponding to the time channels Vector labels corresponding to the time channels.		ICON_L1_MIGHTI_B_Time_Channel

Acknowledgement

This is a data product from the NASA Ionospheric Connection Explorer mission, an Explorer launched at 21:59:45 EDT on October 10, 2019, from Cape Canaveral AFB in the USA. Guidelines for the use of this product are described in the ICON Rules of the Road (<http://icon.ssl.berkeley.edu/Data>).

Responsibility for the mission science falls to the Principal Investigator, Dr. Thomas Immel at UC Berkeley: Immel, T.J., England, S.L., Mende, S.B. et al. Space Sci Rev (2018) 214: 13. <https://doi.org/10.1007/s11214-017-0449-2>

Responsibility for the validation of the L1 data products falls to the instrument lead investigators/scientists.

- * EUV: Dr. Eric Korpela : <https://doi.org/10.1007/s11214-017-0384-2>
- * FUV: Dr. Harald Frey : <https://doi.org/10.1007/s11214-017-0386-0>
- * MIGHTI: Dr. Christoph Englert : <https://doi.org/10.1007/s11214-017-0358-4>, and <https://doi.org/10.1007/s11214-017-0374-4>
- * IVM: Dr. Roderick Heelis : <https://doi.org/10.1007/s11214-017-0383-3>

Responsibility for the validation of the L2 data products falls to those scientists responsible for those products.

- * Daytime O and N2 profiles: Dr. Andrew Stephan : <https://doi.org/10.1007/s11214-018-0477-6>
- * Daytime (EUV) O+ profiles: Dr. Andrew Stephan : <https://doi.org/10.1007/s11214-017-0385-1>
- * Nighttime (FUV) O+ profiles: Dr. Farzad Kamalabadi : <https://doi.org/10.1007/s11214-018-0502-9>
- * Neutral Wind profiles: Dr. Jonathan Makela : <https://doi.org/10.1007/s11214-017-0359-3>
- * Neutral Temperature profiles: Dr. Christoph Englert : <https://doi.org/10.1007/s11214-017-0434-9>
- * Ion Velocity Measurements : Dr. Russell Stoneback : <https://doi.org/10.1007/s11214-017-0383-3>

Responsibility for Level 4 products falls to those scientists responsible for those products.

- * Hough Modes : Dr. Chihoko Yamashita : <https://doi.org/10.1007/s11214-017-0401-5>
- * TIEGCM : Dr. Astrid Maute : <https://doi.org/10.1007/s11214-017-0330-3>
- * SAMI3 : Dr. Joseph Huba : <https://doi.org/10.1007/s11214-017-0415-z>

Pre-production versions of all above papers are available on the ICON website.
<http://icon.ssl.berkeley.edu/Publications>

Overall validation of the products is overseen by the ICON Project Scientist, Dr. Scott England.

NASA oversight for all products is provided by the Mission Scientist, Dr. Jeffrey Klenzing.

Users of these data should contact and acknowledge the Principal Investigator Dr. Immel and the party directly responsible for the data product (noted above) and acknowledge NASA funding for the collection of the data used in the research with the following statement : "ICON is supported by NASA's Explorers Program through contracts NNG12FA45C and NNG12FA42I".

These data are openly available as described in the ICON Data Management Plan available on the ICON website (<http://icon.ssl.berkeley.edu/Data>).

This document was automatically generated on 2020-10-01 09:55 using the file:

ICON_L1_MIGHTI-B_Science_2019-12-11_000131_v98r001.nc

Software version: ICON_SDC > MIGHTI L1 Processor v2.0.0

ICON Data Product L0P: MIGHTI Ancillary Products

This document describes the data product for Ancillary Products for MIGHTI Data Processing, which is in NetCDF4 format.

The MIGHTI ancillary data file contains information on the ICON observatory as well as MIGHTI specific information. This includes the pointing, position, and velocity of the ICON observatory. It also includes information on the status of the observatory such as maneuvers, being in or out of the Earth's shadow, and calibrations. Pertinent information for the MIGHTI instrument is included such as locations and details at the MIGHTI tangent points. These files are combined with the MIGHTI Level 1 data to produce Level 2 data. For clarification, variables named 'MIGHTI_A' are for MIGHTI-A, variables named 'MIGHTI_B' are for MIGHTI-B, and variables named MIGHTI are either for the spacecraft or the MIGHTI instrument indicated in the file name. The TIMETABLE dimension refers to the start, middle, and end of the MIGHTI integration time. ECEF is Earth-centered, Earth-fixed reference frame. ECI is Earth-centered inertial reference frame. We use the J2000 ECI frame. LVLH is local-vertical, local-horizontal. We have two LVLH modes: normal and reverse. LVLH Normal is when the spacecraft is looking north with latitude tangent locations between ~12 S and ~42 N. LVLH Reverse is when the spacecraft is looking south with latitude tangent locations between ~42 S and ~12 N.

History

Version 03, Created by MIGHTI Ancillary Processor v3.0.2 on Thu, 08 Oct 2020, 2020-10-08T16:38:25.000 UTC

Dimensions

NetCDF files contain **variables** and the **dimensions** over which those variables are defined. First, the dimensions are defined, then all variables in the file are described.

The dimensions used by the variables in this file are given below, along with nominal sizes. Note that the size may vary from file to file. For example, the "Epoch" dimension, which describes the number of time samples contained in this file, will have a varying size.

Dimension Name	Nominal Size
Epoch	2119
HORIZONTAL	3
VERTICAL	3
VECTORS	3
TIMETABLE	3

Variables

Variables in this file are listed below. First, "data" variables are described, followed by the "support_data" variables, and finally the "metadata" variables. The variables classified as "ignore_data" are not shown.

support_data

Variable Name	Description	Units	Dimensions
Epoch	<p>Milliseconds since 1970-01-01 00:00:00 UTC at middle of measurement integration.</p> <p>Number of milliseconds since 1970-01-01 00:00:00 UTC at the middle of the measurement integration.</p>	milliseconds	Epoch, TIMETABLE
ICON Ancillary MIGHTI Time GPS	<p>Milliseconds since 1980-01-06 00:00:00 TAI (coincident with UTC) at middle of reading.</p> <p>Number of milliseconds since 1980-01-06 00:00:00 TAI at the middle of the measurement integration. Taken from LOP MIGHTI data file.</p>	milliseconds	Epoch
ICON Ancillary MIGHTI Time UTC String	<p>Date and Time in UTC format</p> <p>ISO 8601 formatted UTC timestamp (at middle of reading). E.g., 2017-05-27 00:00:00.380Z</p>	UTC	Epoch, TIMETABLE
ICON Ancillary MIGHTI SC Position ECEF	<p>Spacecraft Position in ECEF Coordinates</p> <p>Position of spacecraft in ECEF at the start, middle, and end of each exposure.</p>	km	Epoch, TIMETABLE, VECTORS
ICON Ancillary MIGHTI SC Velocity ECEF	<p>Spacecraft Velocity in ECEF</p> <p>Spacecraft velocity in ECEF coordinates at the start, middle, and end of each exposure.</p>	m/s	Epoch, TIMETABLE, VECTORS
ICON Ancillary MIGHTI Latitude	<p>WGS84 Latitude of Spacecraft Position (Geodetic)</p> <p>Geodetic Latitude of Spacecraft in WGS84 at the start, middle, and end of each exposure.</p>	degrees	Epoch, TIMETABLE
ICON Ancillary MIGHTI Longitude	<p>WGS84 Longitude of Spacecraft Position (Geodetic)</p> <p>Geodetic Longitude of Spacecraft in WGS84 at the start, middle, and end of each exposure.</p>	degrees	Epoch, TIMETABLE
ICON Ancillary MIGHTI Altitude	<p>WGS84 Altitude of Spacecraft Position (Geodetic)</p> <p>Geodetic altitude of the spacecraft in WGS84 at the start, middle, and end of each exposure.</p>	km	Epoch, TIMETABLE
ICON Ancillary MIGHTI VNorth	<p>North Velocity of Spacecraft</p> <p>North component of the spacecraft velocity in WGS84 at the start, middle and end of each exposure</p>	m/s	Epoch, TIMETABLE

Variable Name	Description	Units	Dimensions
ICON_ANCILLARY_MIGHTI_VEAST	<p>East Velocity of Spacecraft</p> <p>East component of the spacecraft velocity in WGS84 at the start, middle, and end of each exposure.</p>	m/s	Epoch, TIMETABLE
ICON_ANCILLARY_MIGHTI_VDOWN	<p>Down (perpendicular to local Earth surface) velocity of Spacecraft</p> <p>Down component of the spacecraft velocity in WGS84 at the start, middle, and end of each exposure.</p>	m/s	Epoch, TIMETABLE
ICON_ANCILLARY_MIGHTI_TANGENTPOINTS_MAGNETIC_LATITUDE	<p>Magnetic Latitude at Tangent Points</p> <p>Quasi-Dipole Magnetic Latitude at the tangent points for 9 points that define the center & outside edges (sides and corners). at the start, middle, and end of each exposure. These values are obtained from passing the geodectic latitudes, longitudes, and altitudes from ICON_ANCILLARY_MIGHTI_TANGENTPOINTS_LATLONALT into apexpy Python module. For details on apexpy see: https://apexpy.readthedocs.org/</p>	degrees	Epoch, TIMETABLE, VERTICAL, HORIZONTAL
ICON_ANCILLARY_MIGHTI_TANGENTPOINTS_MAGNETIC_LONGITUDE	<p>Magnetic Longitude at Tangent Points</p> <p>Quasi-Dipole Magnetic Longitude at the tangent points for 9 points that define the center & outside edges (side and corners).at the start, middle, and end of each exposure. These values are obtained from passing the geodectic latitudes, longitudes, and altitudes from ICON_ANCILLARY_MIGHTI_TANGENTPOINTS_LATLONALT into apexpy Python module.For details on apexpy see: https://apexpy.readthedocs.org/</p>	degrees	Epoch, TIMETABLE, VERTICAL, HORIZONTAL
ICON_ANCILLARY_MIGHTI_SC_SZA	<p>Spacecraft Solar Zenith Angle</p> <p>Solar zenith angle at the spacecraft at the start, middle, and end of each exposure.</p>	degrees	Epoch, TIMETABLE
ICON_ANCILLARY_MIGHTI_LST	<p>Local Solar Time</p> <p>Local solar time at the spacecraft at the start, middle, and end of each exposure</p>	hours, decimal	Epoch, TIMETABLE
ICON_ANCILLARY_MIGHTI_SC_XHAT	<p>Spacecraft X-unit Vector in ECEF Components (Ram Direction)</p> <p>Unit vector in ECEF for the spacecraft x-axis (nominal Ram direction) at the start, middle, and end of each exposure.</p>	dimensionless	Epoch, TIMETABLE, VECTORS
ICON_ANCILLARY_MIGHTI_SC_YHAT	<p>Spacecraft Y-unit Vector in ECEF Components (Starboard Direction)</p> <p>Unit vector in ECEF for the spacecraft y-axis (nominal Starboard direction) at the start, middle, and end of each exposure.</p>	dimensionless	Epoch, TIMETABLE, VECTORS

Variable Name	Description	Units	Dimensions
ICON_ANCILLARY_MIGHTI_SC_ZHAT	Spacecraft Z-unit Vector in ECEF Components (Nadir Direction) Unit vector in ECEF for the spacecraft z-axis (nominal Nadir direction) at the start, middle, and end of each exposure.	dimensionless	Epoch, TIMETABLE, VECTORS
ICON_ANCILLARY_MIGHTI_SUN_STATUS	Spacecraft Sun/Shadow Status Code Spacecraft sun/shadow status code (1 = shadow, 0 = sun) at the start, middle, and end of each exposure.	binary	Epoch, TIMETABLE
ICON_ANCILLARY_MIGHTI_ORBIT_NUMBER	Orbit Number Integer Orbit Number at the start, middle, and end of each exposure.	integer	Epoch, TIMETABLE
ICON_ANCILLARY_MIGHTI_SLEW_STATUS	MIGHTI Attitude System Status Code Binary Coded Integer where 1: LVLH Normal Mode 2: LVLH Reverse Mode 4: Earth Limb Pointing 8: Inertial Pointing 16: Stellar Pointing 32: Attitude Slew 64: Conjugate Maneuver 128: Nadir Calibration 256: Lunar Calibration 512: Stellar Calibration 1024: Zero Wind Calibration 2048-32768: SPARE	binary	Epoch
ICON_ANCILLARY_MIGHTI_TANGENTPOINTS_LATLONALT	Tangent Locations in WGS84 (Latitude, Longitude, Altitude) Latitude, longitude and altitude in WGS84 of tangent points for 9 points that define the center & outside edges (sides and corners) of the field of view at the start, middle, and end of each exposure.	mixed	Epoch, TIMETABLE, VECTORS, VERTICAL, HORIZONTAL
ICON_ANCILLARY_MIGHTI_TANGENTPOINTS_ECEF	Tangent Locations in ECEF Locations in ECEF of tangent points for 9 points that define the center & outside edges (sides and corners) of the field of view at the start, middle, and end of each exposure.	km	Epoch, TIMETABLE, VECTORS, VERTICAL, HORIZONTAL
ICON_ANCILLARY_MIGHTI_TANGENTPOINTS_SZA	Tangent Points Solar Zenith Angle Solar zenith angle at the tangent points for the 9 points that define the center & outside edges (sides and corners) of the field of view at the start, middle, and end of each exposure.	degrees	Epoch, TIMETABLE, VERTICAL, HORIZONTAL
ICON_ANCILLARY_MIGHTI_TANGENTPOINTS_LOS_COROTATION	Tangent Points LOS Corotation Velocity Corotation velocity at the tangent points projection into the line of sight for the 9 points that define the center & outside edges (sides and corners) of the field of view at the start, middle, and end of each exposure.	m/s	Epoch, TIMETABLE, VERTICAL, HORIZONTAL

Variable Name	Description	Units	Dimensions
ICON_ANCILLARY_MIGHTI_SC_LOS_VELOCITY	Spacecraft LOS Velocity in ECI Spacecraft velocity in ECI, J2000, projected into the line of sight for 9 points that define the center & outside edges (sides and corners) of the field of view at the start, middle, and end of each exposure.	m/s	Epoch, TIMETABLE, VERTICAL, HORIZONTAL
ICON_ANCILLARY_MIGHTI_FOV_UNITVECTORS_ECEF	FOV Unit Vectors in ECEF Unit look vectors in ECEF for the 9 look directions that define the center & outside edges (sides and corners) of the field of view at the start, middle, and end of each exposure.	dimensions	Epoch, TIMETABLE, VECTORS, VERTICAL, HORIZONTAL
ICON_ANCILLARY_MIGHTI_TANGENTPOINT_DISTANCE	Distance to Tangent Points Line of sight distance to the tangent points for the 9 points that define the center & outside edges (sides and corners) of the field of view at the start, middle, and end of each exposure.	km	Epoch, TIMETABLE, VERTICAL, HORIZONTAL
ICON_ANCILLARY_MIGHTI_HORIZONTAL_BORESIGHT_SUN_ANGLE	Horizontal Boresight to Sun Angle Angle between the Sun and the image horizontal direction (perpendicular to the boresight) at the start, middle, and end of each exposure.	degrees	Epoch, TIMETABLE
ICON_ANCILLARY_MIGHTI_VERTICAL_BORESIGHT_SUN_ANGLE	Vertical Boresight to Sun Angle Angle between the Sun and the image vertical direction (perpendicular to the boresight) at the start, middle, and end of each exposure.	degrees	Epoch, TIMETABLE
ICON_ANCILLARY_MIGHTI_TOTAL_BORESIGHT_SUN_ANGLE	Total Boresight to Sun Angle Magnitude of the angle between the Sun and the boresight of the instrument at the start, middle, and end of each exposure.	degrees	Epoch, TIMETABLE
ICON_ANCILLARY_MIGHTI_FOV_AZIMUTH_ANGLE	FOV Celestial Azimuth Celestial Azimuth angle for the 9 points that define the center & outside edges (sides and corners) of the field of view at the start, middle, and end of each exposure.	degrees	Epoch, TIMETABLE, VERTICAL, HORIZONTAL

Variable Name	Description	Units	Dimensions
ICON Ancillary MIGHTI Space Environment Region Status TI_SPACE_ENVIRONMENT_REGION_STATUS	<p>Space Environment Region Status</p> <p>Standardized for several missions, not all codes are relevant to ICON. Binary Coded Integer where</p> <ul style="list-style-type: none"> 1: Earth Shadow 2: Lunar Shadow 4: Atmospheric Absorption Zone 8: South Atlantic Anomaly 16: Northern Auroral Zone 32: Southern Auroral Zone 64: Periapsis Passage 128: Inner & Outer Radiation Belts 256: Deep Plasma Sphere 512: Foreshock Solar Wind 1024: Solar Wind Beam 2048: High Magnetic Field 4096: Average Plasma Sheet 8192: Bowshock Crossing 16384: Magnetopause Crossing 32768: Ground Based Observatories 65536: 2-Day Conjunctions 131072: 4-Day Conjunctions 262144: Time Based Conjunctions 524288: Radial Distance Region 1 1048576: Orbit Outbound 2097152: Orbit Inbound 4194304: Lunar Wake 8388608: Magnetotail 16777216: Magnetosheath 33554432: Science 67108864: Low Magnetic Latitude 134217728: Conjugate Observation 	binary	Epoch
ICON Ancillary MIGHTI-A Status TI_A_STATUS	<p>MIGHTI-A Status</p> <p>Binary Coded Integer for view status of MIGHTI-A where</p> <ul style="list-style-type: none"> 1: Earth Day View 2: Earth Night View 4: Calibration Target View 8: Off-target View 16: Sun Proximity View 32: Moon Proximity View 64: North Magnetic Footpoint View 128: South Magnetic Footpoint View 256: Science Data Collection View 512: Calibration Data Collection View 1024: RAM Proximity View 2048-32768: SPARE <p>Activity is what the spacecraft was commanded to do while status is the spacecraft's natural state of operations. This means that activity should always be used over status if they differ, but will almost always be the same.</p>	binary	Epoch

Variable Name	Description	Units	Dimensions
ICON Ancillary Mighti-B Status ICON Ancillary Mighti-B Status	MIGHTI-B Status Binary Coded Integer for view status of MIGHTI-B where 1: Earth Day View 2: Earth Night View 4: Calibration Target View 8: Off-target View 16: Sun Proximity View 32: Moon Proximity View 64: North Magnetic Footpoint View 128: South Magnetic Footpoint View 256: Science Data Collection View 512: Calibration Data Collection View 1024: RAM Proximity View 2048-32768: SPARE Activity is what the spacecraft was commanded to do while status is the spacecraft's natural state of operations. This means that activity should always be used over status if they differ, but will almost always be the same.	binary	Epoch
ICON Ancillary Mighti-A Activity ICON Ancillary Mighti-A Activity	MIGHTI-A Activity Binary Coded Integer for activity in MIGHTI-A where 1: Earth Day Activity 2: Earth Night Activity 4: Calibration Target Activity 8: Off-target Activity 16: Sun Proximity Activity 32: Moon Proximity Activity 64: North Magnetic Footpoint Activity 128: South Magnetic Footpoint Activity 256: Science Data Collection Activity 512: Calibration Data Collection Activity 1024: RAM Proximity Activity 2048-32768: SPARE Activity is what the spacecraft was commanded to do while status is the spacecraft's natural state of operations. This means that activity should always be used over status if they differ, but will almost always be the same.	binary	Epoch

Variable Name	Description	Units	Dimensions
ICON Ancillary_MIGHTI_B_Activity	<p>MIGHTI-B Activity</p> <p>Binary Coded Integer for activity in MIGHTI-B where</p> <p>1: Earth Day Activity 2: Earth Night Activity 4: Calibration Target Activity 8: Off-target Activity 16: Sun Proximity Activity 32: Moon Proximity Activity 64: North Magnetic Footpoint Activity 128: South Magnetic Footpoint Activity 256: Science Data Collection Activity 512: Calibration Data Collection Activity 1024: RAM Proximity Activity 2048-32768: SPARE</p> <p>Activity is what the spacecraft was commanded to do while status is the spacecraft's natural state of operations. This means that activity should always be used over status if they differ, but will almost always be the same.</p>	binary	Epoch
ICON Ancillary_MIGHTI_Horizontal_Boresight_ECEF	<p>Horizontal Boresight in ECEF</p> <p>Unit look vector for the image horizontal direction (perpendicular to the boresight) in ECEF at the start, middle, and end of each exposure.</p>	dimensionless	Epoch, TIMETABLE, VECTORS
ICON Ancillary_MIGHTI_Vertical_Boresight_ECEF	<p>Vertical Boresight in ECEF</p> <p>Unit look vector for the image vertical direction (perpendicular to the boresight) in ECEF at the start, middle, and end of each exposure.</p>	dimensionless	Epoch, TIMETABLE, VECTORS
ICON Ancillary_MIGHTI_Boresight_ECEF	<p>Boresight in ECEF</p> <p>Unit vector of the nominal boresight (center of instrument FOV) in ECEF at the start, middle, and end of each exposure.</p>	dimensionless	Epoch, TIMETABLE, VECTORS
ICON Ancillary_MIGHTI_Horizontal_Boresight_ECI	<p>Horizontal Boresight in ECI</p> <p>Unit look vector for the image horizontal direction (perpendicular to the boresight) in ECI, J2000, at the start, middle, and end of each exposure.</p>	dimensionless	Epoch, TIMETABLE, VECTORS
ICON Ancillary_MIGHTI_Vertical_Boresight_ECI	<p>Vertical Boresight in ECI</p> <p>Unit look vector for the image vertical direction (perpendicular to the boresight) in ECI, J2000, at the start, middle, and end of each exposure.</p>	dimensionless	Epoch, TIMETABLE, VECTORS
ICON Ancillary_MIGHTI_Boresight_ECI	<p>Boresight in ECI</p> <p>Unit vector of the nominal boresight (center of instrument FOV) in ECI, J2000, at the start, middle, and end of each exposure.</p>	dimensionless	Epoch, TIMETABLE, VECTORS

Variable Name	Description	Units	Dimensions
ICON Ancillary_MIGHTI_Earth_Shadow_Transition_Seconds	<p>Number of Seconds Since Transitioning From Shadow to Sun.</p> <p>Number of seconds since the last spacecraft transition from Earth's shadow into sunlight has occurred at the start, middle, and end of each exposure.</p>	seconds	Epoch, TIMETABLE
ICON Ancillary_MIGHTI_Instrument_Status	<p>Instrument Calibration Status Code</p> <p>Binary Coded Integer for Instrument Calibration Status where 1: MIGHTI A/B Red Lamp Calibration 2: MIGHTI A/B Green Lamp Calibration 4: MIGHTI A Stellar Calibration 8: MIGHTI B Stellar Calibration 16: MIGHTI A Zero Wind Calibration 32: MIGHTI B Zero Wind Calibration 64: FUV Lamp Calibration 128: FUV Stellar Calibration 256: EUV Lunar Calibration 512: FUV Nadir Flat Field Calibration 1024: EUV Nadir Flat Field Calibration 2048-32768: SPARE</p>	binary	Epoch
ICON Ancillary_MIGHTI_A_Radiator_Temperature	<p>MIGHTI-A Radiator Temperature</p> <p>Temperature of MIGHTI-A radiator as reported by the spacecraft housekeeping</p>	degrees Celsius	Epoch
ICON Ancillary_MIGHTI_B_Radiator_Temperature	<p>MIGHTI-B Radiator Temperature</p> <p>Temperature of MIGHTI-B radiator as reported by the spacecraft housekeeping</p>	degrees Celsius	Epoch
ICON Ancillary_MIGHTI_Camera_Electronics_Temperature	<p>MIGHTI Camera Electronics Temperature</p> <p>Temperature of MIGHTI camera electronics as reported by the spacecraft housekeeping</p>	degrees Celsius	Epoch
ICON Ancillary_MIGHTI_SC_Voltage	<p>Spacecraft Bus Voltage</p> <p>Spacecraft bus voltage as reported by the spacecraft housekeeping</p>	Volts	Epoch
ICON Ancillary_MIGHTI_TangentPoint_Scattering_Angle	<p>Solar Scattering Angle of Tangent Points</p> <p>Angle between the (1) a vector from the Sun to the tangent point(s) and (2) a vector from the spacecraft to the tangent point(s). Found for the 9 points that define the center & outside edges (sides and corners) of the field of view at the start, middle, and end of each exposure.</p>	degrees	Epoch, TIMETABLE, VERTICAL, HORIZONTAL
ICON Ancillary_MIGHTI_TangentPoints_Local_Solar_Time	<p>Tangent Points Local Solar Time</p> <p>Local solar time at the tangent points for the 9 points that define the center & outside edges (sides and corners) of the field of view at the start, middle, and end of each exposure.</p>	hours, decimal	Epoch, TIMETABLE, VERTICAL, HORIZONTAL

Variable Name	Description	Units	Dimensions
ICON_ANCILLARY_MIGHTI_JITTER	<p>Jitter Around Middle Time</p> <p>On the basis of the ECEF quaternion ephemeris, a 60-second window is found. Over that window a linear fit of the corresponding Euler angles is found. A residual between the actual values and linear fit is calculated. The standard deviation of that residual is reported as the jitter. The closest ephemeris time to the MIGHTI middle time is used in this variable.</p>	degrees	Epoch

Variable Name	Description	Units	Dimensions
ICON Ancillary_Mighty Quality Flag TI_QUALITY_FLAG	<p>Quality Flag</p> <p>Binary Coded Integer where</p> <p>1: STATE_NO_DATA 2: STATE_UNCONVERGED 4: STATE_LOW 8: STATE_MED 16: STATE_HIGH 32: AD_NO_DATA 64: AD_DIVERGING 128: AD_NOT_STARTED 256: AD_CONVERGING 512: AD_COARSE_CONVERGED 1024: AD_FINE_CONVERGED 2048-32768: SPARE</p> <p>STATE_NO_DATA: No telemetry available for this time period. States are propagated from the last valid solution.</p> <p>STATE_UNCONVERGED: The GOODS KF solution is unconverged and should not be used. States are propagated from the last valid solution.</p> <p>STATE_LOW: The GPSR solution is better than the GOODS solution (The position accuracy is worse than 150 m, 1-sigma)</p> <p>STATE_MEDIUM: The GOODS solution is better than the GPSR solution (The position accuracy is better than 150 m, 1-sigma)</p> <p>STATE_HIGH: The GOODS solution is better than the GPSR solution, and meets its performance requirements (20 m position and 0.02 m/sec velocity, 1-sigma).</p> <p>AD_NO_DATA: No telemetry available for this time period. Attitude is copied from the last valid solution.</p> <p>AD_DIVERGING: Tolerances on the diagonal elements of the covariance matrix diverging and exceeds 9.9e9 asec² for attitude sigma and 9.9e9 asec²/sec² for rate sigma or negative values</p> <p>AD_NOT_STARTED: KF has not started processing measurements</p> <p>AD_CONVERGING: KF is in state of updating measurements and filter started to converge</p> <p>AD_COARSE_CONVERGED: Tolerances on the diagonal elements of the covariance matrix converging and below 200K asec² for x, y and 1000K for z in tracker frame for attitude and 10 asec²/sec² for x, y and z for rate</p> <p>AD_FINE_CONVERGED: Tolerances on the diagonal elements of the covariance matrix converging and below 1000 asec² for x, y and z in tracker frame for attitude and 1 asec²/sec² x, y and z for rate</p> <p>Nominal value of 1040: STATE_HIGH (16) and AD_FINE_CONVERGED (1024). All values are a combination of a STATE value and an AD (attitude determination) value. It is up to the user to determine if data outside 1040 is usable. AD values NOT AD_FINE_CONVERGED should be suspect. STATE_HIGH is expected, but STATE_MED is possible during maneuvers.</p>	binary	Epoch

Variable Name	Description	Units	Dimensions
ICON_ANCILLARY_MIGH TI_TOTAL_BORESIGHT_ MOON_ANGLE	Total Boresight to Moon Angle Magitude of the angle between the Moon and the boresight for the instrument at the start,middle, and end of each exposure.	degree s	Epoch, TIMETABLE

Acknowledgement

This is a data product from the NASA Ionospheric Connection Explorer mission, an Explorer launched at 21:59:45 EDT on October 10, 2019. Guidelines for the use of this product are described in the ICON Rules of the Road (<https://icon.ssl.berkeley.edu/Data>)

Responsibility for the mission science falls to the Principal Investigator, Dr. Thomas Immel at UC Berkeley: Immel, T.J., England, S.L., Mende, S.B. et al. Space Sci Rev (2018) 214: 13. <https://doi.org/10.1007/s11214-017-0449-2>

Responsibility for the validation of the L1 data products falls to the instrument lead investigators/scientists.

- * EUV: Dr. Eric Korpela : <https://doi.org/10.1007/s11214-017-0384-2>
- * FUV: Dr. Harald Frey : <https://doi.org/10.1007/s11214-017-0386-0>
- * MIGHTI: Dr. Christoph Englert : <https://doi.org/10.1007/s11214-017-0358-4>, and <https://doi.org/10.1007/s11214-017-0374-4>
- * IVM: Dr. Roderick Heelis : <https://doi.org/10.1007/s11214-017-0383-3>

Responsibility for the validation of the L2 data products falls to those scientists responsible for those products.

- * Daytime O and N2 profiles: Dr. Andrew Stephan : <https://doi.org/10.1007/s11214-018-0477-6>
- * Daytime (EUV) O+ profiles: Dr. Andrew Stephan : <https://doi.org/10.1007/s11214-017-0385-1>
- * Nighttime (FUV) O+ profiles: Dr. Farzad Kamalabadi : <https://doi.org/10.1007/s11214-018-0502-9>
- * Neutral Wind profiles: Dr. Jonathan Makela : <https://doi.org/10.1007/s11214-017-0359-3>
- * Neutral Temperature profiles: Dr. Christoph Englert : <https://doi.org/10.1007/s11214-017-0434-9>
- * Ion Velocity Measurements : Dr. Russell Stoneback : <https://doi.org/10.1007/s11214-017-0383-3>

Responsibility for Level 4 products falls to those scientists responsible for those products.

- * Hough Modes : Dr. Chihoko Yamashita : <https://doi.org/10.1007/s11214-017-0401-5>
- * TIEGCM : Dr. Astrid Maute : <https://doi.org/10.1007/s11214-017-0330-3>
- * SAMI3 : Dr. Joseph Huba : <https://doi.org/10.1007/s11214-017-0415-z>

Pre-production versions of all above papers are available on the ICON website.

Overall validation of the products is overseen by the ICON Project Scientist, Dr. Scott England.

NASA oversight for all products is provided by the Mission Scientist, Dr. Jeffrey Klenzing.

Users of these data should contact and acknowledge the Principal Investigator Dr. Immel and the party directly responsible for the data product (noted above) and acknowledge NASA funding for the collection of the data used in the research with the following statement : "ICON is supported by NASA's Explorers Program through contracts NNG12FA45C and NNG12FA42I"

These data are openly available as described in the ICON Data Management Plan available on the ICON website (<http://icon.ssl.berkeley.edu/Data>).

This document was automatically generated on 2020-10-08 10:09 using the file:

ICON_L0P_MIGHTI-A_Ancillary_2020-02-15_v03r099.NC

Software version: ICON_SDC > MIGHTI Prime Generator 3.0.2

ICON Data Product 2.1: Line-of-sight Wind Profiles

This document describes the data product for ICON MIGHTI Line-of-sight Winds (DP 2.1), which is in NetCDF4 format.

This data product contains altitude profiles of the line-of-sight winds (inverted wind profiles in the direction of the sensor's line of sight) for 24 hours of data taken by MIGHTI. In addition to the line-of-sight wind data and the corresponding ancillary data, such as time and location, this product contains supporting data, such as fringe amplitude profiles and relative volume emission rate profiles. Absolute calibration and MIGHTI-A/B cross calibration of these data is not necessary to obtain the wind data, and therefore any direct analysis of these supporting data requires caution.

There is one file for each sensor (A or B), for each color (red or green) and for each day. The profile spans from an altitude of ~90 km (for green) or ~150 km (for red) to ~300 km, though altitudes with low signal levels are masked out. This data product is generated from the Level 1 MIGHTI product, which comprises calibrated interference fringe amplitudes and phases. The effect of spacecraft velocity is removed from the interferogram phase, then (optionally) the data are binned from their native altitude sampling (~2.5 km) to improve statistics. An onion-peeling inversion is performed to remove the effect of the line-of-sight integration. After the inversion, each row (i.e., altitude) is analyzed to extract the phase, and thus the line-of-sight wind. Level 2.1 files from MIGHTI-A and MIGHTI-B are combined during the Level 2.2 processing (not discussed here). See Harding et al. [2017, doi:10.1007/s11214-017-0359-3] for more details of the inversion algorithm. Further discussion of the calibration and performance of MIGHTI after launch can be found in a forthcoming paper in Space Science Reviews [Englert et al., 2022, in preparation].

Known issues with the v05 data release are listed below. Work is in progress to resolve or mitigate these issues in future data releases.

Known issues with v05:

- * When ICON is in the South Atlantic Anomaly (SAA), radiation effects on the detector cause poor data quality. The quality control algorithm adequately flags and masks most of the affected samples, but some outliers remain, especially near the edge of the SAA. Other uncaught outliers are rare but can occur due to cosmic rays, stars in the field of view, moonlight, etc.

- * The bottom row of data (corresponding to an altitude of ~88 km) is masked out as the signal is rarely strong enough to permit a wind estimate, and calibrations have large uncertainties. It is unlikely but possible that this altitude will be reported in future releases, pending further investigation.

- * Airglow brightness observations are not a required mission product, and no effort was yet made to absolutely calibrate the brightness observations for MIGHTI-A and MIGHTI-B, and thus the Relative_VER variable should be treated with caution. In v05, MIGHTI-A and B are cross-calibrated using a conversion factor derived from on-orbit data. However, there are some indications that this cross-calibration may be changing with time, which is not accounted for in v05.

- * As discussed in the variable notes below, a new zero wind phase determination has been implemented in v05. However, during the period from 2021 Apr 26 to Aug 14, data gaps and one period of southward ("Reverse LVLH") pointing cause errors in this determination. The accuracy is estimated to be degraded by a factor of two. See the *_Accuracy variable.

- * During the one orbit per day when the calibration lamp is on, the wind data can be noisier and have a slight bias. Although this issue is much improved since v04, for the sake of conservatism, these orbits are still labeled with quality=0.5 (i.e., caution).

- * Some data gaps appear on days when the sun passes near MIGHTI's field of view. Most of these gaps are located near the terminator, but some are longer lasting.

- * In some cases, there are indications that the *_Precision_1_Sample variables are underestimating the true sample-to-sample noise, suggesting that, in addition to shot noise, there is a second source of noise. It is recommended that any quantitative use of the reported error estimates (i.e., precision and accuracy) should treat those estimates as uncertain. It is believed that most error estimates are correct to within a factor of 2. The largest problems with error reporting occur where the airglow signal is weakest.

- * Imperfect daily calibration data lead to small discontinuities in the zero wind phase at the boundaries between days (i.e., between 23:59:59 and 00:00:00 UT), which are not accounted for by the reported error variables.

This was estimated to be a 2-5 m/s (root-mean-square) error early in the mission, but is growing over time, possibly reaching 5-10 m/s by mid-2022.

* A signal-dependent phase shift is seen in atmospheric and calibration lamp fringes, possibly caused by a charge trapping effect in the CCD. This is the subject of ongoing investigation, but a first-order correction is implemented in the v05 dataset. The correction increases linearly with time to match the effect seen in on-orbit calibration data. The variable *_Precision_Low_Signal_Effect is an estimate of the remaining uncertainty due to an imperfect correction. Where this uncertainty is large, caution is recommended. For example, for winds in the core science region (90-105 km altitude, away from the terminator), the magnitude of the correction is small or zero, but data in the red channel during the night and twilight are subject to a large correction (many tens of m/s) and the uncertainty is correspondingly large. A goal for future releases is to characterize and correct this effect more accurately.

* Data near the solar terminators are subject to a variety of errors, including those described above and others related to the rapidly varying illumination. Not all errors near the terminator are accounted for by the reported error. Users are encouraged to use extra caution with these data.

See the documentation below for more information.

History

v1.0: First release of MIGHTI L2.1/L2.2 software, B. J. Harding, 05 Mar 2018

v2.0: First run of on-orbit data, using external zero wind reference and smooth daily-averaged profiles, B. J. Harding, 01 May 2020

v3.0: Correction for long-term mechanical drift, B. J. Harding, 04 Jun 2020

v4.0: Updated correction for long-term mechanical drift to handle settling after ~May 2020 and precession cycle variation. LoS winds have changed by a bulk offset of up to 30 m/s. Studies using only perturbations from the mean (e.g., non-migrating tidal retrievals) are unlikely to be affected. B. J. Harding, 21 Oct 2020

v5.0: The ad-hoc, HWM-based correction for the zero wind phase has been replaced with a self-calibration based on comparing data from the ascending and descending orbits (see the notes for the wind variables below for details). Long-term trends in the zero wind phase degraded the accuracy of version 4 over time, and the accuracy of version 4 data was tied to the accuracy of HWM. In version 5, errors on these long time scales (>100-150 days) are now accounted for, improving the accuracy to 10-25 m/s (see the "Accuracy" variable for more details) and removing the dependence on external models. A long window of data is required to implement this self-calibration, so v05 data are processed at least 100 days behind real time. For errors on precession-cycle time scales (48 days), the previous ad-hoc correction using initial red-vs-green comparisons has been replaced with a more comprehensive red-green cross-calibration (165-185 km altitude during the day) that accounts for the time-dependence of mechanical drifts of the optics. This result is consistent with a first-principles analysis of the fiducial notch positions (see Marr et al., 2020 and subsequent publications). A mission-average fiducial notch analysis is also used to correct mechanical drifts on an orbital time scale (97 minutes, or 24 hours of local time), which could affect migrating tide estimates. The RMS difference due to this effect is estimated at 5-10 m/s (root mean square). Analysis of waves with periods that do not coincide with these new corrections are not likely to be different than in version 4 (e.g., nonmigrating tides, planetary waves, and gravity waves). New variables related to error (i.e., uncertainty) estimates from various sources are now included, whereas version 4 error estimates only included the effects of shot, read, and dark noise. MIGHTI-A and MIGHTI-B variables related to emission brightness are now cross-calibrated, though not absolutely calibrated. Exposures affected by solar and lunar stray light are now flagged. Some data during periods in May and July 2020 when the sun approached the MIGHTI field of view was marked as unavailable in v04, but is now available in v05 with the exception of a few days. The data from the second row in the green channel (~91 km) is now available when the signal strength permits a wind estimate. An error in the local time calculation has been corrected, which changes the local time by up to 20 min. A new algorithm to identify cosmic ray spikes has been implemented, improving precision. A preliminary algorithm has been implemented to correct a wind bias associated with low signal levels, and associated uncertainties are estimated (see the "Precision_Low_Signal_Effect" variable for more details). Finally, various quality control parameters have been optimized. More description is provided in the notes below. A full history of software changes can be found on

Github: https://github.com/bharding512/airglowrsss/commits/master/Python/modules/MIGHTI_L2.py B. J. Harding 08 Sep 2022

Dimensions

NetCDF files contain **variables** and the **dimensions** over which those variables are defined. First, the dimensions are defined, then all variables in the file are described.

The dimensions used by the variables in this file are given below, along with nominal sizes. Note that the size may vary from file to file. For example, the "Epoch" dimension, which describes the number of time samples contained in this file, will have a varying size.

Dimension Name	Nominal Size
Epoch	unlimited
Altitude	82
Vector	3
Start_Mid_Stop	3
N_Flags	12
Row	82

Variables

Variables in this file are listed below. First, "data" variables are described, followed by the "support_data" variables, and finally the "metadata" variables. The variables classified as "ignore_data" are not shown.

data

Variable Name	Description	Units	Dimensions
ICON_L21_Line_of_Sight_Wind	<p>Line-of-sight horizontal wind profile. A positive wind is towards MIGHTI.</p> <p>The wind is the primary data product in this file. This variable contains the projection of the horizontal wind (at the tangent point) onto the line of sight direction. An entire altitude profile is observed simultaneously. An onion-peeling inversion is used on the raw observations to remove the effects of the integration along the line of sight. The line-of-sight wind is defined such that a positive value indicates motion towards the spacecraft. This direction is given by the Line_of_Sight_Azimuth variable. It is assumed that the vertical wind is zero, but even large vertical winds (~100 m/s) do not significantly affect this data product, since the line of sight is nearly horizontal everywhere. It should be noted that while this measurement is ascribed to a particular latitude, longitude and altitude, it is actually an average over many hundreds of kilometers horizontally, and 2.5-30 kilometers vertically (depending on the binning). See Harding et al. [2017, doi:10.1007/s11214-017-0359-3] for a more complete discussion of the inversion algorithm.</p> <p>Knowledge of the "zero wind phase" is needed for any instrument using Doppler shifts to determine winds. The zero wind phase is defined as the measured interference fringe phase that corresponds to the rest wavelength of the emission. For the v05 data release, the zero wind phase has been determined by considering a window of LoS wind data spanning two precession cycles (96 days). Assuming that on average the real zonal and meridional winds do not depend on the aspect angle with which MIGHTI observes the atmosphere (an angle which is significantly different between the ascending and descending portions of the orbit), a matrix equation can be constructed which combines data from both MIGHTI-A and MIGHTI-B and both the ascending and descending orbits. This equation is solved for the average zonal and meridional wind, and the zero wind phase for MIGHTI-A and MIGHTI-B. This window is moved in time to determine the appropriate zero wind phase for each date. The value of the zero wind phase depends on emission color (red or green), aperture mode (day or night), calibration lamp status (on or off) and row (i.e., altitude). An additional zero-mean signal is added to this result to ensure that 48-day (i.e., 1 precession cycle) average winds are smooth in altitude. Adjustments are smaller than the reported accuracy, so this adjustment is not expected to change any scientific conclusions, although it does ensure more realistic wind profiles. This is a less restrictive assumption than the smoothness criterion used in v04, which relied on the Horizontal Wind Model 2014 and also enforced smoothness on 1-day averages. It is thus expected that the amplitude of tidal structures in the lower thermosphere are subject to less suppression in v05+ than in v04. This version of the MIGHTI zero wind phase is independent of any external data or models (such as the Horizontal Wind Model 2014, which was used in v04 and earlier versions). The zero wind phase used for each wind sample is saved in the _Zero_Wind_Phase variable below. The 1-sigma uncertainty in the winds incurred by the inaccuracy in the zero wind phase is estimated and reported in the *_Wind_Accuracy variable below.</p>	m/s	Epoch, Altitude

Variable Name	Description	Units	Dimensions
ICON_L21_Line_of_Sight_Wind_Precision_1_Sample	<p>Line-of-sight wind precision (1 sample)</p> <p>Various sources of error in MIGHTI winds are quantified with 1-sigma estimates and organized by their temporal persistence. These error sources are nearly uncorrelated with each other and can thus be added in quadrature. Users are encouraged to contact the MIGHTI team for assistance with error propagation.</p> <p>The "1 sample" error variable quantifies errors that are uncorrelated from one exposure to the next, dominated by shot and dark noise in the detectors. The correlation time of this error source is 30-60 seconds (i.e., the measurement cadence). The reported error is estimated from the fringe intensity and background. This is the recommended variable to use for analyses of wind fluctuations within a single day and a single altitude (e.g., gravity waves). Because the Level 2.2 data include interpolation of Level 2.1 data, some correlation remains between consecutive samples. Errors are slightly correlated across small altitude gaps as a result of the inversion.</p>	m/s	Epoch, Altitude
ICON_L21_Line_of_Sight_Wind_Precision_1_Day	<p>Line-of-sight wind precision (1 day)</p> <p>Various sources of error in MIGHTI winds are quantified with 1-sigma estimates and organized by their temporal persistence. These error sources are nearly uncorrelated with each other and can thus be added in quadrature. Users are encouraged to contact the MIGHTI team for assistance with error propagation.</p> <p>The "1 Day" error variable quantifies the error introduced by daily calibrations, which is correlated for an entire 24-hour period (00:00 - 23:59 UT). This is estimated from the magnitude of fluctuations in the daily-averaged phase, propagated through the inversion. Errors in day mode and night mode are nearly uncorrelated. For studies pertaining to atmospheric tidal modes that combine data from many days, this error can be treated as uncorrelated across time.</p>	m/s	Epoch, Altitude

Variable Name	Description	Units	Dimensions
ICON_L21_Line_of_Sight_Wind_Precision_Low_Signal_Effect	<p>Line-of-sight wind precision (from low signal effect)</p> <p>Various sources of error in MIGHTI winds are quantified with 1-sigma estimates and organized by their temporal persistence. These error sources are nearly uncorrelated with each other and can thus be added in quadrature. Users are encouraged to contact the MIGHTI team for assistance with error propagation.</p> <p>The "Low Signal Effect" error variable quantifies the error introduced by the imperfect correction for the signal-dependent phase shift, which is an effect seen in atmospheric and calibration-lamp fringes where the phase of the fringes is biased at very low signal levels. This is under investigation but could be caused by a charge trapping effect in the CCD. A correction has been implemented based upon the empirical relationship between measured phase and signal level of the calibration lamps for the first ~30 months of the mission. However, especially for cases with low signal levels, this correction is uncertain. The uncertainty in the resulting winds is estimated from the signal level and reported in this variable. It is likely to be correlated across samples nearby in time and space, but the correlation between different channels (red and green), sensors (MIGHTI-A and MIGHTI-B), and operating modes (Day and Night) is not known. Depending on the analysis being used, it could be treated as a systematic error or as a statistical error. Where this uncertainty is large, caution is recommended. For example, for winds in the core science region (90-105 km altitude), the magnitude of the correction is small or zero, but data in the red channel during the night and twilight are subject to a large correction (many tens of m/s) and the uncertainty is correspondingly large. A goal for future releases is to characterize and correct this effect more accurately.</p>	m/s	Epoch, Altitude
ICON_L21_Line_of_Sight_Wind_Accuracy	<p>Line-of-sight wind accuracy</p> <p>Various sources of error in MIGHTI winds are quantified with 1-sigma estimates and organized by their temporal persistence. These error sources are nearly uncorrelated with each other and can thus be added in quadrature. Users are encouraged to contact the MIGHTI team for assistance with error propagation.</p> <p>The "Accuracy" variable quantifies the error introduced by the zero-wind phase estimate. It is strongly correlated across time lags of days to weeks and becomes increasingly decorrelated for time lags longer than 2 precession cycles (96 days). This error is estimated from the discrepancy between various techniques of determining the zero-wind phase. This error source is irrelevant for most users studying perturbations from the mean (e.g., tides, waves), but may be important for studies of zonal mean winds, point comparisons with other data sets, and seasonal/long-term trends thereof. Errors are moderately correlated across small altitude gaps. Errors in day mode and night mode are nearly uncorrelated, implying there could be different offsets for day mode and night mode. This could be important for error propagation of odd-numbered migrating tides (e.g., DW1).</p>	m/s	Epoch, Altitude

Variable Name	Description	Units	Dimensions
ICON_L21_Line_of_Sight_Wind_Error	<p>Line-of-sight horizontal wind error profile</p> <p>For robust error propagation, users are encouraged to consider the individual error variables: "Precision_1_Sample," "Precision_1_Day," and "Accuracy." The "Wind_Error" variable is included for backwards compatibility and is equal to the quadrature sum of the "1 Sample" error and the "1 Day" error. This is the recommended uncertainty to use for analyses that collect data from several weeks and compute perturbations from the mean (e.g., for estimating tides and planetary waves). This error is uncorrelated across time lags larger than 24 hours. Errors are slightly correlated across small altitude gaps. Errors in day mode and night mode are nearly uncorrelated.</p>	m/s	Epoch, Altitude
ICON_L21_Wind_Quality	<p>A quantification of the wind quality, from 0 (Bad) to 1 (Good)</p> <p>A quantification of the overall quality of the wind data. While the intent is that the variable ICON_...Line_of_Sight_Wind_Error accurately characterizes the statistical error in the wind data, it is possible that systematic errors are present, or that the statistical error estimation is not accurate. If it is suspected that this is the case, the quality will be less than 1.0. If the data are definitely unusable, the quality will be 0.0 and the sample will be masked. Users should exercise caution when the quality is less than 1.0.</p> <p>This parameter can currently take 3 values: 0.0 (Bad), 0.5 (Caution), 1.0 (Good)</p>		Epoch, Altitude
ICON_L21_Fringe_Amplitude	<p>Fringe amplitude profile</p> <p>An approximate volume emission rate (VER) profile in arbitrary units. Technically this a profile of the amplitude of the fringes, which has a dependence on thermospheric temperature and background emission. Thus, it does not truly represent volume emission rate. However, it is a useful proxy. The units are arbitrary, but an attempt has been made to cross-calibrate MIGHTI-A with MIGHTI-B. In contrast to the wind inversion, which is nonlinear due to the phase extraction step, the amplitude inversion is purely linear. The Level 1 interferogram is analyzed to obtain a single brightness value per zenith angle, and this is inverted with the distance matrix to obtain a value of the amplitude per altitude.</p>	arb	Epoch, Altitude
ICON_L21_Fringe_Amplitude_Error	<p>Fringe amplitude error profile</p> <p>The statistical (1-sigma) error in the fringe amplitude. As with the wind, systematic errors are not included, but can arise from sources such as horizontal gradients and inaccurate calibration.</p>	arb	Epoch, Altitude

Variable Name	Description	Units	Dimensions
ICON_L21_Relative_VER	<p>Relative volume emission rate profile</p> <p>The volume emission rate (VER) obtained by scaling the fringe amplitude by a calibration factor. Pre-flight calibrations and on-orbit comparisons with ground-based instruments are used to determine the best possible calibration. The fringe amplitude has a dependence on temperature, which is corrected using the MSIS model. Because the on-orbit calibration is uncertain, and because the MSIS temperature correction is not perfect, caution should be exercised when absolute calibration is required, or when comparisons are being made between samples at different temperatures. Please contact the MIGHTI team before performing any studies that require absolute calibration. The statistical (1-sigma) error for this variable is provided in the variable ICON_..._Relative_VER_Error, though it is expected that systematic calibration errors dominate the total error. See the Fringe_Amplitude variable for a discussion of the inversion.</p>	ph/cm ³ /s	Epoch, Altitude
ICON_L21_Relative_VER_Error	<p>Relative volume emission rate error profile</p> <p>The statistical (1-sigma) error in the relative VER estimate. This error arises mostly from shot noise. Importantly, it is expected that systematic errors (e.g., calibration errors) dominate the total error, but they are not included in this variable.</p>	ph/cm ³ /s	Epoch, Altitude
ICON_L21_VER_Quality	<p>A quantification of the VER quality, from 0 (Bad) to 1 (Good)</p> <p>A quantification of the overall quality of the VER data. While the intent is that the variable VER_Error accurately characterizes the statistical error in the wind data, it is possible that systematic errors are present, or that the statistical error estimation is not accurate. If it is suspected that this is the case, the quality will be less than 1.0. If the data are definitely unusable, the the quality will be 0.0 and the sample will be masked. Users should exercise caution when the quality is less than 1.0.</p> <p>This parameter can currently take 3 values: 0.0 (Bad), 0.5 (Caution), 1.0 (Good)</p>		Epoch, Altitude

support_data

Variable Name	Description	Units	Dimensions
Epoch	<p>Sample time, midpoint of exposure. Number of msec since Jan 1, 1970.</p> <p>This variable contains the time corresponding to the wind profiles reported in this file, taken at the midpoint of the exposure time. It is in UTC and has units of milliseconds since Jan 1, 1970. A human-readable version of the time can be found in the variable ICON_..._UTC_Time</p>	ms	Epoch
ICON_L21_Time	<p>Sample time at start, mid, stop of exposure. Number of msec since Jan 1, 1970.</p> <p>This variable is the same as Epoch, except it has another dimension which holds the start time, middle time, and stop time of each exposure.</p>	ms	Epoch, Start_Mid_Stop

Variable Name	Description	Units	Dimensions
ICON_L21_UTC_Time	<p>Sample time, midpoint of exposure.</p> <p>This variable is the same as Epoch but is formatted as a human-readable string.</p>		Epoch
ICON_L21_Altitude	<p>WGS84 altitude of each wind sample</p> <p>The altitudes of each point in the wind profile, evaluated using the WGS84 ellipsoid. If the variable Integration_Order=0 (which is the default value), then these altitudes are one half sample above the tangent altitudes of each pixel's line of sight (consistent with the assumption implicit in the inversion that the wind and emission rate are constant within the layer between tangent altitudes). If Integration_Order=1, this variable contains the tangent altitudes.</p>	km	Epoch, Altitude
ICON_L21_Latitude	<p>WGS84 latitude of each wind sample</p> <p>The latitudes of each point in the wind profile, evaluated using the WGS84 ellipsoid. The latitude only varies by several degrees from the bottom of the profile to the top. It should be noted that while a single latitude value (the tangent latitude) is given for each point, the observation is inherently a horizontal average over many hundreds of kilometers.</p>	deg	Epoch, Altitude
ICON_L21_Longitude	<p>WGS84 longitude of each wind sample</p> <p>The longitudes (0-360) of each point in the wind profile, evaluated using the WGS84 ellipsoid. The longitude only varies by several degrees from the bottom of the profile to the top. It should be noted that while a single longitude value (the tangent longitude) is given for each point, the observation is inherently a horizontal average over many hundreds of kilometers.</p>	deg	Epoch, Altitude
ICON_L21_Magnetic_Latitude	<p>Magnetic quasi-dipole latitude of each wind sample</p> <p>A two-dimensional array defining the magnetic quasi-dipole latitude of the two-dimensional data grid. The latitude varies only slightly (a few deg) with altitude, but this variation is included. It should be noted that while a single latitude value is given for each point, the observation is inherently a horizontal average over many hundreds of kilometers. Quasi-dipole latitude and longitude are calculated using the fast implementation developed by Emmert et al. (2010, doi:10.1029/2010JA015326) and the Python wrapper apexpy (doi.org/10.5281/zenodo.1214207).</p>	deg	Epoch, Altitude
ICON_L21_Magnetic_Longitude	<p>Magnetic quasi-dipole longitude of each wind sample</p> <p>A two-dimensional array defining the magnetic quasi-dipole longitude of the two-dimensional data grid. The longitude varies only slightly (a few deg) with altitude, but this variation is included. It should be noted that while a single longitude value is given for each point, the observation is inherently a horizontal average over many hundreds of kilometers. Quasi-dipole latitude and longitude are calculated using the fast implementation developed by Emmert et al. (2010, doi:10.1029/2010JA015326) and the Python wrapper apexpy (doi.org/10.5281/zenodo.1214207). Quasi-dipole longitude is defined such that zero occurs where the geodetic longitude is near 285 deg east (depending on latitude).</p>	deg	Epoch, Altitude

Variable Name	Description	Units	Dimensions
ICON_L21_Line_of_Sight_Azimuth	<p>Azimuth angle of the line of sight at the tangent point. Deg East of North.</p> <p>Consider the vector pointing from the spacecraft to the tangent point (i.e., the line of sight). At the tangent point, this vector is parallel to the ground. This variable contains the azimuth angle of this vector, evaluated at the tangent point. It follows the typical geophysical convention of degrees East of North (North=0, East=90, South=180, West=270). It can vary by a few degrees from the top of the profile to the bottom, so one value is reported per altitude. MIGHTI-A and MIGHTI-B will have values approximately 90 degrees apart.</p>	deg	Epoch, Altitude
ICON_L21_Low_Signal_Effect_Correction	<p>Correction for low-signal effect</p> <p>This is the correction used for the "low signal effect" in the lower-level processing. This correction has already been applied to the data, but is included here for reference. It was taken directly from the Level 1 file but has been converted from rad to m/s. For the red channel, it has also been binned to match the data. It has not been modified by the inversion. The uncertainty of this correction is captured by the Line_of_Sight_Wind_Precision_Low_Signal_Effect variable. See the notes for that variable for more information.</p>	m/s	Epoch, Altitude
ICON_L21_Solar_Zenith_Angle	<p>Solar zenith angle of each wind sample</p> <p>Angle between the vectors towards the sun and towards zenith, at the location of each wind sample.</p>	deg	Epoch, Altitude
ICON_L21_Local_Solar_Time	<p>Local solar time of each wind sample</p> <p>Local solar time at the location and time of each wind sample, calculated using the equation of time.</p>	hour	Epoch, Altitude

metadata

Variable Name	Description	Units	Dimensions
ICON_L21_Exposure_Time	<p>The exposure time for each profile</p> <p>The exposure time (i.e., integration time) for each sample. Nominally this is 30 seconds during the day and 60 seconds at night.</p>	s	Epoch
ICON_L21_Chi2	<p>Variance of the phase in each (unwrapped) row: (std of phase)²</p> <p>In consolidating each row of the unwrapped interferogram into a single phase value, the variance of the phase is saved in this variable. Ideally this should provide no new information beyond what is provided by the wind uncertainty, but it is a useful diagnostic.</p>	rad ²	Epoch, Altitude

Variable Name	Description	Units	Dimensions
ICON_L21_Observatory_Velocity_Vector	<p>ICON S/C velocity vector in Earth-centered, Earth-fixed coordinates</p> <p>At each time, this is a length-3 vector [vx,vy,vz] of the ICON spacecraft's velocity in Earth-centered Earth-fixed (ECEF) coordinates at the midpoint time of the observation. The effect of spacecraft velocity has already been removed from the ICON_..._Line_of_Sight_Wind variable.</p>	m/s	Epoch, Vector
ICON_L21_Observatory_Latitude	<p>The WGS84 latitude of the ICON S/C</p> <p>The latitude of the ICON spacecraft at the midpoint time of the observation, using the WGS84 ellipsoid.</p>	deg	Epoch
ICON_L21_Observatory_Longitude	<p>The WGS84 longitude of the ICON S/C</p> <p>The longitude (0-360) of the ICON spacecraft at the midpoint time of the observation, using the WGS84 ellipsoid.</p>	deg	Epoch
ICON_L21_Observatory_Altitude	<p>The WGS84 altitude of the ICON S/C</p> <p>The altitude of the ICON spacecraft at the midpoint time of the observation, using the WGS84 ellipsoid.</p>	km	Epoch
ICON_L21_Line_of_Sight_Vector	<p>The look direction of each MIGHTI line of sight, as a vector in ECEF</p> <p>The vector from the spacecraft to the tangent point (i.e., along MIGHTI's line of sight), as a unit vector in Earth-centered Earth-fixed (ECEF) coordinates. A vector is provided for each tangent point for each time. If this vector is transformed to an azimuth and zenith angle at the tangent point, the zenith angle will be 90 deg, and the azimuth angle will be the same as the ICON_..._Line_of_Sight_Azimuth variable.</p>		Epoch, Altitude, Vector
ICON_L21_Orbit_Number	<p>Orbit Number</p> <p>Integer ICON orbit number</p>		Epoch
ICON_L21_Orbit_Node	<p>Orbit Ascending/Descending Node Flag</p> <p>Orbit Ascending/Descending Node Flag.</p> <p>0 = Latitude of ICON is increasing.</p> <p>1 = Latitude of ICON is decreasing.</p>		Epoch
ICON_L21_Binning_Size	<p>How many raw samples were binned vertically for each reported sample</p> <p>To improve statistics, adjacent rows of the interferogram can be averaged together before the inversion. This improves precision at the cost of vertical resolution. If no binning is performed, this value will be 1, corresponding to ~2.5 km sampling. A value of 2 corresponds to ~5 km sampling, etc.</p>		

Variable Name	Description	Units	Dimensions
ICON_L21_Integration_Order	<p>Order used to discretize the integral for inversion: 0=Riemann, 1=Trapezoidal</p> <p>In formulating the inversion, an assumption must be made regarding the choice of basis functions, which can be thought of as an assumption regarding the behavior of the wind and fringe amplitude (airglow volume emission rate) within each altitude layer. The most basic assumption is that these quantities are constant within each altitude layer, which corresponds to Integration_Order=0. However, if it is assumed that the variation within each layer is linear, Integration_Order=1. This sacrifices precision to improve vertical resolution.</p>		Epoch
ICON_L21_Top_Layer_Model	<p>How the top altitudinal layer is handled in the inversion: "exp" or "thin"</p> <p>In formulating the inversion, an assumption must be made about the shape of the emission rate profile above the top measured altitude, since this shape is not measured. It can be assumed to go to zero (Top_Layer_Model="thin") or assumed to fall off exponentially with a scale height of 26 km, a value extracted from running a variety of airglow models (Top_Layer_Model="exp"). Usually this choice will not affect the inversion significantly. In cases where it does, the quality variable will be decreased.</p>		Epoch
ICON_L21_Attitude_LVLH_Normal	<p>Attitude status bit 0: LVLH Normal</p> <p>LVLH Normal pointing. This variable is taken from bit 0 of the Level 1 variable ICON_L1_MIGHTI_X_SC_Attitude_Control_Register. 0=False, 1=True</p>		Epoch
ICON_L21_Attitude_LVLH_Reverse	<p>Attitude status bit 1: LVLH Reverse</p> <p>LVLH Reverse pointing. This variable is taken from bit 1 of the Level 1 variable ICON_L1_MIGHTI_X_SC_Attitude_Control_Register. 0=False, 1=True</p>		Epoch
ICON_L21_Attitude_Limb_Pointing	<p>Attitude status bit 2: Earth Limb Pointing</p> <p>Earth limb pointing. This variable is taken from bit 2 of the Level 1 variable ICON_L1_MIGHTI_X_SC_Attitude_Control_Register. 0=False, 1=True</p>		Epoch
ICON_L21_Attitude_Conjugate_Maneuver	<p>Attitude status bit 6: Conjugate Maneuver</p> <p>Conjugate Maneuver. This variable is taken from bit 6 of the Level 1 variable ICON_L1_MIGHTI_X_SC_Attitude_Control_Register. 0=False, 1=True. If it is 1, then the S/C is performing a conjugate maneuver during this exposure.</p>		Epoch
ICON_L21_Attitude_Zero_Wind_Maneuver	<p>Attitude status bit 10: Zero Wind Maneuver</p> <p>Zero Wind Maneuver. This variable is taken from bit 10 of the Level 1 variable ICON_L1_MIGHTI_X_SC_Attitude_Control_Register. 0=False, 1=True. If it is 1, then the S/C is performing a zero wind maneuver during this exposure.</p>		Epoch

Variable Name	Description	Units	Dimensions
ICON_L21_Quality_Flags	<p>Quality flags</p> <p>This variable provides information on why the Wind_Quality and VER_Quality variables are reduced from 1.0. Many quality flags can exist for each grid point, each either 0 or 1. More than one flag can be raised per point. This variable is a two-dimensional array with dimensions of altitude and number of flags.</p> <p>0 : (From L1) SNR too low to reliably perform L1 processing</p> <p>1 : (From L1) Proximity to South Atlantic Anomaly</p> <p>2 : (From L1) Bad calibration</p> <p>3 : (From L1) Calibration lamps are on</p> <p>4 : (From L1) Solar/lunar contamination</p> <p>5 : Not enough valid points in profile</p> <p>6 : SNR is very low after inversion</p> <p>7 : Significant airglow above 300 km</p> <p>8 : Line of sight crosses the terminator</p> <p>9 : Thermal drift correction is uncertain</p> <p>10: S/C pointing is not stable</p> <p>11: SNR is low after inversion, but maybe still usable</p>		Epoch, Altitude, N_Flags
ICON_L21_Relative_VER_DC	<p>Relative volume emission rate profile derived from DC value</p> <p>The MIGHTI team recommends that users utilize the Relative_VER variable instead of this variable. This is the same as Relative_VER, except it is derived from the DC value of the interferogram rather than the fringe amplitude. The DC value is susceptible to contamination by stray light and background emission, but is not sensitive to atmospheric temperature like the fringe amplitude.</p>	ph/cm ³ /s	Epoch, Altitude
ICON_L21_Zero_Wind_Phase	<p>The phase subtracted from Level 1 data</p> <p>See notes for _Line_of_Sight_Wind above. This variable is reported as a function of Row (Level 1 coordinates) instead of Altitude (Level 2 coordinates).</p>	rad	Epoch, Row

Acknowledgement

This is a data product from the NASA Ionospheric Connection Explorer mission, an Explorer launched at 21:59:45 EDT on October 10, 2019, from Cape Canaveral AFB in the USA. Guidelines for the use of this product are described in the ICON Rules of the Road (<http://icon.ssl.berkeley.edu/Data>).

Responsibility for the mission science falls to the Principal Investigator, Dr. Thomas Immel at UC Berkeley: Immel, T.J., England, S.L., Mende, S.B. et al. Space Sci Rev (2018) 214: 13. <https://doi.org/10.1007/s11214-017-0449-2>

Responsibility for the validation of the L1 data products falls to the instrument lead investigators/scientists.

- * EUV: Dr. Eric Korpela : <https://doi.org/10.1007/s11214-017-0384-2>
- * FUV: Dr. Harald Frey : <https://doi.org/10.1007/s11214-017-0386-0>
- * MIGHTI: Dr. Christoph Englert : <https://doi.org/10.1007/s11214-017-0358-4>, and <https://doi.org/10.1007/s11214-017-0374-4>
- * IVM: Dr. Roderick Heelis : <https://doi.org/10.1007/s11214-017-0383-3>

Responsibility for the validation of the L2 data products falls to those scientists responsible for those products.

- * Daytime O and N2 profiles: Dr. Andrew Stephan : <https://doi.org/10.1007/s11214-018-0477-6>
- * Daytime (EUV) O+ profiles: Dr. Andrew Stephan : <https://doi.org/10.1007/s11214-017-0385-1>
- * Nighttime (FUV) O+ profiles: Dr. Farzad Kamalabadi : <https://doi.org/10.1007/s11214-018-0502-9>
- * Neutral Wind profiles: Dr. Jonathan Makela : <https://doi.org/10.1007/s11214-017-0359-3>
- * Neutral Temperature profiles: Dr. Christoph Englert : <https://doi.org/10.1007/s11214-017-0434-9>
- * Ion Velocity Measurements : Dr. Russell Stoneback : <https://doi.org/10.1007/s11214-017-0383-3>

Responsibility for Level 4 products falls to those scientists responsible for those products.

- * Hough Modes : Dr. Chihoko Yamashita : <https://doi.org/10.1007/s11214-017-0401-5>
- * TIEGCM : Dr. Astrid Maute : <https://doi.org/10.1007/s11214-017-0330-3>
- * SAMI3 : Dr. Joseph Huba : <https://doi.org/10.1007/s11214-017-0415-z>

Pre-production versions of all above papers are available on the ICON website.
<http://icon.ssl.berkeley.edu/Publications>

Overall validation of the products is overseen by the ICON Project Scientist, Dr. Scott England.

NASA oversight for all products is provided by the Mission Scientist, Dr. Jeffrey Klenzing.

Users of these data should contact and acknowledge the Principal Investigator Dr. Immel and the party directly responsible for the data product (noted above) and acknowledge NASA funding for the collection of the data used in the research with the following statement : "ICON is supported by NASA's Explorers Program through contracts NNG12FA45C and NNG12FA42I".

These data are openly available as described in the ICON Data Management Plan available on the ICON website (<http://icon.ssl.berkeley.edu/Data>).

This document was automatically generated on 2022-10-18 10:25 using the file:

ICON_L2-1_MIGHTI-A_LOS-Wind-Green_2022-01-01_v05r000.NC

Software version: ICON SDC > ICON UIUC MIGHTI L2.1 Processor v5.05

ICON Data Product 2.2: Cardinal Vector Winds

This document describes the data product for ICON MIGHTI Cardinal Vector Winds (DP 2.2), which is in NetCDF4 format.

This data product contains cardinal (i.e., zonal and meridional) thermospheric winds obtained by combining Level 2.1 (line-of-sight winds) from MIGHTI A and MIGHTI B. The cardinal winds are given as a function of time (spanning 24 hours) and altitude (spanning nominally 90-300 km). In addition to the cardinal vector wind data and the corresponding ancillary data, such as time and location, this product contains supporting data, such as fringe amplitude profiles and relative volume emission rate profiles. Absolute calibration and MIGHTI-A/B cross calibration of these data is not necessary to obtain the wind data, and therefore any direct analysis of these supporting data requires caution. There is one file per emission color (red or green).

Cardinal wind observations are enabled by the ~90-degree offset between the two MIGHTI sensors. First, MIGHTI A measures a wind component along its line of sight. Five to eight minutes later, depending on tangent point altitude, the spacecraft has moved to a position such that MIGHTI B measures a nearly orthogonal wind component at approximately the same location. A coordinate rotation is performed on the two line-of-sight components to obtain the northward and eastward components reported in this file. The assumption is that the thermospheric wind has not changed during this time interval. Because the Level 2.1 data are naturally on an irregular grid, they are first interpolated to a regular, pre-defined grid of longitude and altitude before the coordinate rotation is performed. See Harding et al. [2017, doi:10.1007/s11214-017-0359-3] for more details of the Level 2.2 algorithm. Further discussion of the calibration and performance of MIGHTI after launch can be found in a forthcoming paper in Space Science Reviews [Englert et al., 2022, in preparation].

Known issues with the v05 data release are listed below. Work is in progress to resolve or mitigate these issues in future data releases.

Known issues with v05:

- * When ICON is in the South Atlantic Anomaly (SAA), radiation effects on the detector cause poor data quality. The quality control algorithm adequately flags and masks most of the affected samples, but some outliers remain, especially near the edge of the SAA. Other uncaught outliers are rare but can occur due to cosmic rays, stars in the field of view, moonlight, etc.

- * The bottom row of data (corresponding to an altitude of ~88 km) is masked out as the signal is rarely strong enough to permit a wind estimate, and calibrations have large uncertainties. It is unlikely but possible that this altitude will be reported in future releases, pending further investigation.

- * Airglow brightness observations are not a required mission product, and no effort was yet made to absolutely calibrate the brightness observations for MIGHTI-A and MIGHTI-B, and thus the Relative_VER variable should be treated with caution. In v05, MIGHTI-A and B are cross-calibrated using a conversion factor derived from on-orbit data. However, there are some indications that this cross-calibration may be changing with time, which is not accounted for in v05.

- * As discussed in the variable notes below, a new zero wind phase determination has been implemented in v05. However, during the period from 2021 Apr 26 to Aug 14, data gaps and one period of southward ("Reverse LVLH") pointing cause errors in this determination. The accuracy is estimated to be degraded by a factor of two. See the *_Accuracy variable.

- * During the one orbit per day when the calibration lamp is on, the wind data can be noisier and have a slight bias. Although this issue is much improved since v04, for the sake of conservatism, these orbits are still labeled with quality=0.5 (i.e., caution).

- * Some data gaps appear on days when the sun passes near MIGHTI's field of view. Most of these gaps are located near the terminator, but some are longer lasting.

- * In some cases, there are indications that the *_Precision_1_Sample variables are underestimating the true sample-to-sample noise, suggesting that, in addition to shot noise, there is a second source of noise. It is recommended that any quantitative use of the reported error estimates (i.e., precision and accuracy) should treat those estimates as uncertain. It is believed that most error estimates are correct to within a factor of 2. The largest problems with error reporting occur where the airglow signal is weakest.

- * Imperfect daily calibration data lead to small discontinuities in the zero wind phase at the boundaries between days (i.e., between 23:59:59 and 00:00:00 UT), which are not accounted for by the reported error variables.

This was estimated to be a 2-5 m/s (root-mean-square) error early in the mission, but is growing over time, possibly reaching 5-10 m/s by mid-2022.

* A signal-dependent phase shift is seen in atmospheric and calibration lamp fringes, possibly caused by a charge trapping effect in the CCD. This is the subject of ongoing investigation, but a first-order correction is implemented in the v05 dataset. The correction increases linearly with time to match the effect seen in on-orbit calibration data. The variable *_Precision_Low_Signal_Effect is an estimate of the remaining uncertainty due to an imperfect correction. Where this uncertainty is large, caution is recommended. For example, for winds in the core science region (90-105 km altitude, away from the terminator), the magnitude of the correction is small or zero, but data in the red channel during the night and twilight are subject to a large correction (many tens of m/s) and the uncertainty is correspondingly large. A goal for future releases is to characterize and correct this effect more accurately.

* Data near the solar terminators are subject to a variety of errors, including those described above and others related to the rapidly varying illumination. Not all errors near the terminator are accounted for by the reported error. Users are encouraged to use extra caution with these data.

See the documentation below for more information.

History

v1.0: First release of MIGHTI L2.1/L2.2 software, B. J. Harding, 05 Mar 2018

v2.0: First run of on-orbit data, using external zero wind reference and smooth daily-averaged profiles, B. J. Harding, 01 May 2020

v3.0: Correction for long-term mechanical drift, B. J. Harding, 04 Jun 2020

v4.0: Updated correction for long-term mechanical drift to handle settling after ~May 2020 and precession cycle variation. LoS winds have changed by a bulk offset of up to 30 m/s. Studies using only perturbations from the mean (e.g., non-migrating tidal retrievals) are unlikely to be affected. B. J. Harding 21 Oct 2020

v5.0: The ad-hoc, HWM-based correction for the zero wind phase has been replaced with a self-calibration based on comparing data from the ascending and descending orbits (see the notes for the wind variables below for details). Long-term trends in the zero wind phase degraded the accuracy of version 4 over time, and the accuracy of version 4 data was tied to the accuracy of HWM. In version 5, errors on these long time scales (>100-150 days) are now accounted for, improving the accuracy to 10-25 m/s (see the "Accuracy" variable for more details) and removing the dependence on external models. A long window of data is required to implement this self-calibration, so v05 data are processed at least 100 days behind real time. For errors on precession-cycle time scales (48 days), the previous ad-hoc correction using initial red-vs-green comparisons has been replaced with a more comprehensive red-green cross-calibration (165-185 km altitude during the day) that accounts for the time-dependence of mechanical drifts of the optics. This result is consistent with a first-principles analysis of the fiducial notch positions (see Marr et al., 2020 and subsequent publications). A mission-average fiducial notch analysis is also used to correct mechanical drifts on an orbital time scale (97 minutes, or 24 hours of local time), which could affect migrating tide estimates. The RMS difference due to this effect is estimated at 5-10 m/s (root mean square). Analysis of waves with periods that do not coincide with these new corrections are not likely to be different than in version 4 (e.g., nonmigrating tides, planetary waves, and gravity waves). New variables related to error (i.e., uncertainty) estimates from various sources are now included, whereas version 4 error estimates only included the effects of shot, read, and dark noise. MIGHTI-A and MIGHTI-B variables related to emission brightness are now cross-calibrated, though not absolutely calibrated. Exposures affected by solar and lunar stray light are now flagged. Some data during periods in May and July 2020 when the sun approached the MIGHTI field of view was marked as unavailable in v04, but is now available in v05 with the exception of a few days. The data from the second row in the green channel (~91 km) is now available when the signal strength permits a wind estimate. An error in the local time calculation has been corrected, which changes the local time by up to 20 min. A new algorithm to identify cosmic ray spikes has been implemented, improving precision. A preliminary algorithm has been implemented to correct a wind bias associated with low signal levels, and associated uncertainties are estimated (see the "Precision_Low_Signal_Effect" variable for more details). Finally, various quality control parameters have been optimized. More description is provided in the notes below. A full history of software changes can be found on

Github: https://github.com/bharding512/airglowrsss/commits/master/Python/modules/MIGHTI_L2.py B. J. Harding 08 Sep 2022

Dimensions

NetCDF files contain **variables** and the **dimensions** over which those variables are defined. First, the dimensions are defined, then all variables in the file are described.

The dimensions used by the variables in this file are given below, along with nominal sizes. Note that the size may vary from file to file. For example, the "Epoch" dimension, which describes the number of time samples contained in this file, will have a varying size.

Dimension Name	Nominal Size
Epoch	unlimited
ICON_L22_Altitude	84
N_Flags	34

Variables

Variables in this file are listed below. First, "data" variables are described, followed by the "support_data" variables, and finally the "metadata" variables. The variables classified as "ignore_data" are not shown.

data

Variable Name	Description	Units	Dimensions
ICON_L22_Zonal_Wind	<p>Zonal component of the horizontal wind. Positive Eastward.</p> <p>The zonal (positive eastward) and meridional (positive northward) winds are the primary data product in this file. They are defined on a grid with dimensions of time and altitude, spanning 24 hours and nominally 90-300 km (150-300 km for the red channel). The altitude, time, latitude and longitude corresponding to each point in the grid are given by other variables in this file. It should be noted that while each measurement is ascribed to a particular latitude, longitude, altitude, and time, it is actually an average over many hundreds of kilometers horizontally and 2.5-30 kilometers vertically (depending on the binning). It also assumes stationarity over the 5-8 minutes between the MIGHTI-A and B measurements used for each point. See Harding et al. [2017, doi:10.1007/s11214-017-0359-3] for a more complete discussion of the inversion algorithm.</p> <p>Knowledge of the "zero wind phase" is needed for any instrument using Doppler shifts to determine winds. The zero wind phase is defined as the measured interference fringe phase that corresponds to the rest wavelength of the emission. For the v05 data release, the zero wind phase has been determined by considering a window of LoS wind data spanning two precession cycles (96 days). Assuming that on average the real zonal and meridional winds do not depend on the aspect angle with which MIGHTI observes the atmosphere (an angle which is significantly different between the ascending and descending portions of the orbit), a matrix equation can be constructed which combines data from both MIGHTI-A and MIGHTI-B and both the ascending and descending orbits. This equation is solved for the average zonal and meridional wind, and the zero wind phase for MIGHTI-A and MIGHTI-B. This window is moved in time to determine the appropriate zero wind phase for each date. The value of the zero wind phase depends on emission color (red or green), aperture mode (day or night), calibration lamp status (on or off) and row (i.e., altitude). An additional zero-mean signal is added to this result to ensure that 48-day (i.e., 1 precession cycle) average winds are smooth in altitude. Adjustments are smaller than the reported accuracy, so this adjustment is not expected to change any scientific conclusions, although it does ensure more realistic wind profiles. This is a less restrictive assumption than the smoothness criterion used in v04, which relied on the Horizontal Wind Model 2014 and also enforced smoothness on 1-day averages. It is thus expected that the amplitude of tidal structures in the lower thermosphere are subject to less suppression in v05+ than in v04. This version of the MIGHTI zero wind phase is independent of any external data or models (such as the Horizontal Wind Model 2014, which was used in v04 and earlier versions). The zero wind phase used for each wind sample is saved in the <code>_Zero_Wind_Phase</code> variable below. The 1-sigma uncertainty in the winds incurred by the inaccuracy in the zero wind phase is estimated and reported in the <code>*_Wind_Accuracy</code> variable below.</p>	m/s	Epoch, ICON_L22_Altitude

Variable Name	Description	Units	Dimensions
ICON_L22_Meridional_Wind	<p data-bbox="397 262 1088 325">Meridional component of the horizontal wind. Positive Northward.</p> <p data-bbox="397 357 1088 766">The zonal (positive eastward) and meridional (positive northward) winds are the primary data product in this file. They are defined on a grid with dimensions of time and altitude, spanning 24 hours and nominally 90-300 km (150-300 km for the red channel). The altitude, time, latitude and longitude corresponding to each point in the grid are given by other variables in this file. It should be noted that while each measurement is ascribed to a particular latitude, longitude, altitude, and time, it is actually an average over many hundreds of kilometers horizontally and 2.5-30 kilometers vertically (depending on the binning). It also assumes stationarity over the 5-8 minutes between the MIGHTI-A and B measurements used for each point. See Harding et al. [2017, doi:10.1007/s11214-017-0359-3] for a more complete discussion of the inversion algorithm.</p> <p data-bbox="397 787 1088 1816">Knowledge of the "zero wind phase" is needed for any instrument using Doppler shifts to determine winds. The zero wind phase is defined as the measured interference fringe phase that corresponds to the rest wavelength of the emission. For the v05 data release, the zero wind phase has been determined by considering a window of LoS wind data spanning two precession cycles (96 days). Assuming that on average the real zonal and meridional winds do not depend on the aspect angle with which MIGHTI observes the atmosphere (an angle which is significantly different between the ascending and descending portions of the orbit), a matrix equation can be constructed which combines data from both MIGHTI-A and MIGHTI-B and both the ascending and descending orbits. This equation is solved for the average zonal and meridional wind, and the zero wind phase for MIGHTI-A and MIGHTI-B. This window is moved in time to determine the appropriate zero wind phase for each date. The value of the zero wind phase depends on emission color (red or green), aperture mode (day or night), calibration lamp status (on or off) and row (i.e., altitude). An additional zero-mean signal is added to this result to ensure that 48-day (i.e., 1 precession cycle) average winds are smooth in altitude. Adjustments are smaller than the reported accuracy, so this adjustment is not expected to change any scientific conclusions, although it does ensure more realistic wind profiles. This is a less restrictive assumption than the smoothness criterion used in v04, which relied on the Horizontal Wind Model 2014 and also enforced smoothness on 1-day averages. It is thus expected that the amplitude of tidal structures in the lower thermosphere are subject to less suppression in v05+ than in v04. This version of the MIGHTI zero wind phase is independent of any external data or models (such as the Horizontal Wind Model 2014, which was used in v04 and earlier versions). The zero wind phase used for each wind sample is saved in the <code>_Zero_Wind_Phase</code> variable below. The 1-sigma uncertainty in the winds incurred by the inaccuracy in the zero wind phase is estimated and reported in the <code>*_Wind_Accuracy</code> variable below.</p>	m/s	Epoch, ICON_L22_Altitude

Variable Name	Description	Units	Dimensions
ICON_L22_Zonal_Wind_Precision_1_Sample	<p>1-sample precision in the zonal wind estimate.</p> <p>Various sources of error in MIGHTI winds are quantified with 1-sigma estimates and organized by their temporal persistence. These error sources are nearly uncorrelated with each other and can thus be added in quadrature. Users are encouraged to contact the MIGHTI team for assistance with error propagation.</p> <p>The "1 sample" error variable quantifies errors that are uncorrelated from one exposure to the next, dominated by shot and dark noise in the detectors. The correlation time of this error source is 30-60 seconds (i.e., the measurement cadence). The reported error is estimated from the fringe intensity and background. This is the recommended variable to use for analyses of wind fluctuations within a single day and a single altitude (e.g., gravity waves). Because the Level 2.2 data include interpolation of Level 2.1 data, some correlation remains between consecutive samples. Errors are slightly correlated across small altitude gaps as a result of the inversion.</p>	m/s	Epoch, ICON_L22_Altitude
ICON_L22_Zonal_Wind_Precision_1_Day	<p>1-day precision in the zonal wind estimate.</p> <p>Various sources of error in MIGHTI winds are quantified with 1-sigma estimates and organized by their temporal persistence. These error sources are nearly uncorrelated with each other and can thus be added in quadrature. Users are encouraged to contact the MIGHTI team for assistance with error propagation.</p> <p>The "1 Day" error variable quantifies the error introduced by daily calibrations, which is correlated for an entire 24-hour period (00:00 - 23:59 UT). This is estimated from the magnitude of fluctuations in the daily-averaged phase, propagated through the inversion. Errors in day mode and night mode are nearly uncorrelated. For studies pertaining to atmospheric tidal modes that combine data from many days, this error can be treated as uncorrelated across time.</p>	m/s	Epoch, ICON_L22_Altitude

Variable Name	Description	Units	Dimensions
ICON_L22_Zonal_Wind_Precision_Low_Signal_Effect	<p>Low-signal precision in the zonal wind estimate.</p> <p>Various sources of error in MIGHTI winds are quantified with 1-sigma estimates and organized by their temporal persistence. These error sources are nearly uncorrelated with each other and can thus be added in quadrature. Users are encouraged to contact the MIGHTI team for assistance with error propagation.</p> <p>The "Low Signal Effect" error variable quantifies the error introduced by the imperfect correction for the signal-dependent phase shift, which is an effect seen in atmospheric and calibration-lamp fringes where the phase of the fringes is biased at very low signal levels. This is under investigation but could be caused by a charge trapping effect in the CCD. A correction has been implemented based upon the empirical relationship between measured phase and signal level of the calibration lamps for the first ~30 months of the mission. However, especially for cases with low signal levels, this correction is uncertain. The uncertainty in the resulting winds is estimated from the signal level and reported in this variable. It is likely to be correlated across samples nearby in time and space, but the correlation between different channels (red and green), sensors (MIGHTI-A and MIGHTI-B), and operating modes (Day and Night) is not known. Depending on the analysis being used, it could be treated as a systematic error or as a statistical error. Where this uncertainty is large, caution is recommended. For example, for winds in the core science region (90-105 km altitude), the magnitude of the correction is small or zero, but data in the red channel during the night and twilight are subject to a large correction (many tens of m/s) and the uncertainty is correspondingly large. A goal for future releases is to characterize and correct this effect more accurately.</p>	m/s	Epoch, ICON_L22_Altitude
ICON_L22_Zonal_Wind_Accuracy	<p>Accuracy of the zonal wind estimate.</p> <p>Various sources of error in MIGHTI winds are quantified with 1-sigma estimates and organized by their temporal persistence. These error sources are nearly uncorrelated with each other and can thus be added in quadrature. Users are encouraged to contact the MIGHTI team for assistance with error propagation.</p> <p>The "Accuracy" variable quantifies the error introduced by the zero-wind phase estimate. It is strongly correlated across time lags of days to weeks and becomes increasingly decorrelated for time lags longer than 2 precession cycles (96 days). This error is estimated from the discrepancy between various techniques of determining the zero-wind phase. This error source is irrelevant for most users studying perturbations from the mean (e.g., tides, waves), but may be important for studies of zonal mean winds, point comparisons with other data sets, and seasonal/long-term trends thereof. Errors are moderately correlated across small altitude gaps. Errors in day mode and night mode are nearly uncorrelated, implying there could be different offsets for day mode and night mode. This could be important for error propagation of odd-numbered migrating tides (e.g., DW1).</p>	m/s	Epoch, ICON_L22_Altitude

Variable Name	Description	Units	Dimensions
ICON_L22_Zonal_Wind_Error	<p>Error in the zonal wind estimate.</p> <p>For robust error propagation, users are encouraged to consider the individual error variables: "Precision_1_Sample," "Precision_1_Day," and "Accuracy." The "Wind_Error" variable is included for backwards compatibility and is equal to the quadrature sum of the "1 Sample" error and the "1 Day" error. This is the recommended uncertainty to use for analyses that collect data from several weeks and compute perturbations from the mean (e.g., for estimating tides and planetary waves). This error is uncorrelated across time lags larger than 24 hours. Errors are slightly correlated across small altitude gaps. Errors in day mode and night mode are nearly uncorrelated.</p>	m/s	Epoch, ICON_L22_Altitude
ICON_L22_Meridional_Wind_Precision_1_Sample	<p>1-sample precision in the meridional wind estimate.</p> <p>Various sources of error in MIGHTI winds are quantified with 1-sigma estimates and organized by their temporal persistence. These error sources are nearly uncorrelated with each other and can thus be added in quadrature. Users are encouraged to contact the MIGHTI team for assistance with error propagation.</p> <p>The "1 sample" error variable quantifies errors that are uncorrelated from one exposure to the next, dominated by shot and dark noise in the detectors. The correlation time of this error source is 30-60 seconds (i.e., the measurement cadence). The reported error is estimated from the fringe intensity and background. This is the recommended variable to use for analyses of wind fluctuations within a single day and a single altitude (e.g., gravity waves). Because the Level 2.2 data include interpolation of Level 2.1 data, some correlation remains between consecutive samples. Errors are slightly correlated across small altitude gaps as a result of the inversion.</p>	m/s	Epoch, ICON_L22_Altitude
ICON_L22_Meridional_Wind_Precision_1_Day	<p>1-day precision in the meridional wind estimate.</p> <p>Various sources of error in MIGHTI winds are quantified with 1-sigma estimates and organized by their temporal persistence. These error sources are nearly uncorrelated with each other and can thus be added in quadrature. Users are encouraged to contact the MIGHTI team for assistance with error propagation.</p> <p>The "1 Day" error variable quantifies the error introduced by daily calibrations, which is correlated for an entire 24-hour period (00:00 - 23:59 UT). This is estimated from the magnitude of fluctuations in the daily-averaged phase, propagated through the inversion. Errors in day mode and night mode are nearly uncorrelated. For studies pertaining to atmospheric tidal modes that combine data from many days, this error can be treated as uncorrelated across time.</p>	m/s	Epoch, ICON_L22_Altitude

Variable Name	Description	Units	Dimensions
ICON_L22_Meridional_Wind_Precision_Low_Signal_Effect	<p>Low-signal precision in the meridional wind estimate.</p> <p>Various sources of error in MIGHTI winds are quantified with 1-sigma estimates and organized by their temporal persistence. These error sources are nearly uncorrelated with each other and can thus be added in quadrature. Users are encouraged to contact the MIGHTI team for assistance with error propagation.</p> <p>The "Low Signal Effect" error variable quantifies the error introduced by the imperfect correction for the signal-dependent phase shift, which is an effect seen in atmospheric and calibration-lamp fringes where the phase of the fringes is biased at very low signal levels. This is under investigation but could be caused by a charge trapping effect in the CCD. A correction has been implemented based upon the empirical relationship between measured phase and signal level of the calibration lamps for the first ~30 months of the mission. However, especially for cases with low signal levels, this correction is uncertain. The uncertainty in the resulting winds is estimated from the signal level and reported in this variable. It is likely to be correlated across samples nearby in time and space, but the correlation between different channels (red and green), sensors (MIGHTI-A and MIGHTI-B), and operating modes (Day and Night) is not known. Depending on the analysis being used, it could be treated as a systematic error or as a statistical error. Where this uncertainty is large, caution is recommended. For example, for winds in the core science region (90-105 km altitude), the magnitude of the correction is small or zero, but data in the red channel during the night and twilight are subject to a large correction (many tens of m/s) and the uncertainty is correspondingly large. A goal for future releases is to characterize and correct this effect more accurately.</p>	m/s	Epoch, ICON_L22_Altitude
ICON_L22_Meridional_Wind_Accuracy	<p>Accuracy of the meridional wind estimate.</p> <p>Various sources of error in MIGHTI winds are quantified with 1-sigma estimates and organized by their temporal persistence. These error sources are nearly uncorrelated with each other and can thus be added in quadrature. Users are encouraged to contact the MIGHTI team for assistance with error propagation.</p> <p>The "Accuracy" variable quantifies the error introduced by the zero-wind phase estimate. It is strongly correlated across time lags of days to weeks and becomes increasingly decorrelated for time lags longer than 2 precession cycles (96 days). This error is estimated from the discrepancy between various techniques of determining the zero-wind phase. This error source is irrelevant for most users studying perturbations from the mean (e.g., tides, waves), but may be important for studies of zonal mean winds, point comparisons with other data sets, and seasonal/long-term trends thereof. Errors are moderately correlated across small altitude gaps. Errors in day mode and night mode are nearly uncorrelated, implying there could be different offsets for day mode and night mode. This could be important for error propagation of odd-numbered migrating tides (e.g., DW1).</p>	m/s	Epoch, ICON_L22_Altitude

Variable Name	Description	Units	Dimensions
ICON_L22_Meridional_Wind_Error	<p>Error in the meridional wind estimate.</p> <p>For robust error propagation, users are encouraged to consider the individual error variables: "Precision_1_Sample," "Precision_1_Day," and "Accuracy." The "Wind_Error" variable is included for backwards compatibility and is equal to the quadrature sum of the "1 Sample" error and the "1 Day" error. This is the recommended uncertainty to use for analyses that collect data from several weeks and compute perturbations from the mean (e.g., for estimating tides and planetary waves). This error is uncorrelated across time lags larger than 24 hours. Errors are slightly correlated across small altitude gaps. Errors in day mode and night mode are nearly uncorrelated.</p>	m/s	Epoch, ICON_L22_Altitude
ICON_L22_Wind_Quality	<p>A quantification of the quality, from 0 (Bad) to 1 (Good)</p> <p>A quantification of the overall quality of the wind data. While the intent is that the XXX_Wind_Error variable accurately characterizes the statistical error in the wind data, it is possible that systematic errors are present, or that the statistical error estimation is not accurate. If this is suspected to be the case, the quality will be less than 1.0. If the data are definitely unusable, the quality will be 0.0 and the sample will be masked. Users should exercise caution when the quality is less than 1.0.</p> <p>Currently, the quality can take values of 0 (Bad), 0.5 (Caution), or 1 (Good).</p>		Epoch, ICON_L22_Altitude
ICON_L22_Fringe_Amplitude	<p>Fringe Amplitude</p> <p>An approximate volume emission rate (VER) profile in arbitrary units, estimated by combining MIGHTI-A and MIGHTI-B data. Technically this is not the VER, but rather the amplitude of the fringes, which has a dependence on thermospheric temperature and background emission. Thus, it does not truly represent volume emission rate. However, it is a useful proxy. The units are arbitrary, as the fringe amplitudes are not calibrated. See also variables Fringe_Amplitude_Relative_Difference, Fringe_Amplitude_A, and Fringe_Amplitude_B.</p>	arb	Epoch, ICON_L22_Altitude
ICON_L22_Fringe_Amplitude_Error	<p>Error in the fringe amplitude estimate</p> <p>The statistical (1-sigma) error in the fringe amplitude estimate, propagated from error in the MIGHTI-A and MIGHTI-B inversions. The units are arbitrary, as the fringe amplitudes are not absolutely calibrated. Systematic errors, such as those arising from airglow gradients or cross-calibration, are not included in this variable, but are probably the dominant source of total error.</p>	arb	Epoch, ICON_L22_Altitude

Variable Name	Description	Units	Dimensions
ICON_L22_Relative_VER	<p>Relative volume emission rate</p> <p>The volume emission rate (VER) obtained by averaging the VER from MIGHTI-A and MIGHTI-B, which is obtained by scaling the fringe amplitude by a calibration factor, as described in Data Product 2.1. Pre-flight calibrations and on-orbit comparisons with ground-based instruments are used to determine the best possible calibration. The fringe amplitude has a dependence on temperature, which is corrected using the MSIS model. Because the on-orbit calibration is uncertain, and because the MSIS temperature correction is not perfect, caution should be exercised when absolute calibration is required, or when precise comparisons are being made between samples at very different temperatures. Please contact the MIGHTI team before performing any studies that require absolute calibration. The statistical (1-sigma) error for this variable is provided in the variable ICON_..._Relative_VER_Error, though it is expected that systematic calibration errors dominate the total error.</p>	ph/cm ³ /s	Epoch, ICON_L22_Altitude
ICON_L22_Relative_VER_Error	<p>Error in VER estimate (statistical)</p> <p>The statistical (1-sigma) error in the relative VER estimate, propagated from error in the MIGHTI-A and MIGHTI-B inversions. This error arises mostly from shot noise. Importantly, it is expected that systematic errors (e.g., calibration errors) dominate the total error, but they are not included in this variable.</p>	ph/cm ³ /s	Epoch, ICON_L22_Altitude
ICON_L22_VER_Quality	<p>A quantification of the quality, from 0 (Bad) to 1 (Good)</p> <p>A quantification of the overall quality of the VER data. While the intent is that the XXX_VER_Error variable accurately characterizes the statistical error in the VER data, it is possible that systematic errors are present, or that the statistical error estimation is not accurate. If it is suspected that this is the case, the quality will be less than 1.0. If the data are definitely unusable, the quality will be 0.0 and the sample will be masked. Users should exercise caution when the quality is less than 1.0.</p> <p>Currently, the quality can take values of 0 (Bad), 0.5 (Caution), or 1 (Good).</p>		Epoch, ICON_L22_Altitude
ICON_L22_Magnetic_Field_Aligned_Wind	<p>Magnetic field-aligned component of the wind</p> <p>The component of the wind in the direction of the magnetic field line, assuming vertical winds are negligible. This variable is calculated by taking the geographic zonal and meridional wind (the primary data products in this file) and expressing the wind vector in a local magnetic coordinate system defined using the Python package OMMBV (https://github.com/rstoneback/OMMBV). The coordinate system used here is orthogonal and is identical to the coordinate system used to express the ion drifts in the ICON IVM data product 2.7 (i.e., the variables ICON_L27_Ion_Velocity_Meridional, ICON_L27_Ion_Velocity_Zonal, and ICON_L27_Ion_Velocity_Field_Aligned).</p>	m/s	Epoch, ICON_L22_Altitude

Variable Name	Description	Units	Dimensions
ICON_L22_Magnetic_Meridional_Wind	<p>Magnetic meridional component of the wind</p> <p>The component of the wind in the magnetic meridional direction, assuming vertical winds are negligible. This variable is calculated by taking the geographic zonal and meridional wind (the primary data products in this file) and expressing the wind vector in a local magnetic coordinate system defined using the Python package OMMBV (https://github.com/rstoneback/OMMBV). The magnetic meridional unit vector is orthogonal to the magnetic field line but within the plane of the magnetic meridian (defined by the apex of the field line and its footpoint). At the magnetic equator, the meridional direction points up, while away from the equator it has a poleward component (north in the northern hemisphere, south in the southern hemisphere). Note that in some ion-neutral coupling models, a definition of magnetic meridional is often used that is horizontal (i.e., perpendicular to gravity) and generally northward. The definition used here is perpendicular to B and thus has primarily a vertical component at ICON latitudes. Note also that the definition of magnetic meridional and zonal used here differs from quasi-dipole and apex coordinate bases. The coordinate system used here is orthonormal and is identical to the coordinate system used to express the ion drifts in the ICON IVM data product 2.7 (i.e., the variables ICON_L27_Ion_Velocity_Meridional, ICON_L27_Ion_Velocity_Zonal, and ICON_L27_Ion_Velocity_Field_Aligned).</p>	m/s	Epoch, ICON_L22_Altitude
ICON_L22_Magnetic_Zonal_Wind	<p>Magnetic zonal component of the wind</p> <p>The component of the wind in the magnetic zonal direction, assuming vertical winds are negligible. This variable is calculated by taking the geographic zonal and meridional wind (the primary data products in this file) and expressing the wind vector in a local magnetic coordinate system defined using the Python package OMMBV (https://github.com/rstoneback/OMMBV). At the magnetic equator, the zonal direction points horizontally, while away from the equator it can have a slightly vertical component. Note that the definition of magnetic meridional and zonal used here differs from quasi-dipole and apex coordinate bases. The coordinate system used here is orthonormal and is identical to the coordinate system used to express the ion drifts in the ICON IVM data product 2.7 (i.e., the variables ICON_L27_Ion_Velocity_Meridional, ICON_L27_Ion_Velocity_Zonal, and ICON_L27_Ion_Velocity_Field_Aligned).</p>	m/s	Epoch, ICON_L22_Altitude
ICON_L22_Orbit_Number	<p>ICON orbit number</p> <p>The ICON orbit number corresponding to each grid point. This is usually an integer, but when samples from two different orbits are used, an interpolated (fractional) value is used.</p>		Epoch, ICON_L22_Altitude
ICON_L22_Orbit_Node	<p>ICON orbit ascending/descending flag</p> <p>A flag indicating whether ICON is in the ascending (0) or descending (1) part of the orbit. For some grid points, samples from MIGHTI-A are on the descending part of the orbit, while samples from MIGHTI-B are ascending. In these cases an interpolated value is used (between 0 and 1).</p>		Epoch, ICON_L22_Altitude

support_data

Variable Name	Description	Units	Dimensions
Epoch	<p>Sample time, average of A and B measurements. Number of msec since Jan 1, 1970.</p> <p>A one-dimensional array defining the time dimension of the two-dimensional data grid (the other dimension being altitude). This is the average of the MIGHTI-A and MIGHTI-B sample times, which differ by 5-8 minutes. Where MIGHTI-A or MIGHTI-B samples are missing, data are reported as missing, but gaps in Epoch are interpolated over to adhere to the netCDF4 standard that coordinate variables should have no missing values. The matchup between MIGHTI-A and B happens at slightly different times at different altitudes, a complication which is ignored by this variable. The effect is small (plus or minus 30-60 seconds), but in cases where it is important, it is recommended to use the alternative time variable Epoch_Full, which is two dimensional and captures the variation with altitude.</p>	ms	Epoch
Epoch_Full	<p>Sample time, midpoint of A and B measurements. Number of msec since Jan 1, 1970.</p> <p>See the notes for the variable Epoch. This variable is the same as Epoch but contains a second dimension, which captures the small (30-60 second) variation of time with altitude. For most applications this is expected to be negligible, and Epoch can be used instead of this variable. Also see the variable Time_Delta, which contains the difference between the MIGHTI-A and MIGHTI-B times that contributed to each point. Epoch_Full contains the average time.</p>	ms	Epoch, ICON_L22_Altitude
ICON_L22_UTC_Time	<p>Sample time, average of A and B measurements.</p> <p>This variable is the same as Epoch but is formatted as a human-readable string. Missing grid points are labeled with empty strings.</p>		Epoch
ICON_L22_Altitude	<p>WGS84 altitude of each wind sample</p> <p>A one-dimensional array defining the altitude dimension of the data grid (the other dimension being time). Altitude is defined using the WGS84 ellipsoid.</p>	km	ICON_L22_Altitude
ICON_L22_Longitude	<p>WGS84 longitude of each wind sample</p> <p>A two-dimensional array defining the longitude (0-360 deg) of the two-dimensional data grid. In the initial implementation, the longitude is constant with altitude, but this may change in the future to capture the slight (few deg) variation with altitude. Longitude is defined using the WGS84 ellipsoid. It should be noted that while a single longitude value is given for each point, the observation is inherently a horizontal average over many hundreds of kilometers.</p>	deg	Epoch, ICON_L22_Altitude

Variable Name	Description	Units	Dimensions
ICON_L22_Latitude	<p>WGS84 latitude of each wind sample</p> <p>A two-dimensional array defining the latitude of the two-dimensional data grid. The latitude varies only slightly (a few deg) with altitude, but this variation is included. Latitude is defined using the WGS84 ellipsoid. It should be noted that while a single latitude value is given for each point, the observation is inherently a horizontal average over many hundreds of kilometers.</p>	deg	Epoch, ICON_L22_Altitude
ICON_L22_Magnetic_Latitude	<p>Magnetic quasi-dipole latitude of each wind sample</p> <p>A two-dimensional array defining the magnetic quasi-dipole latitude of the two-dimensional data grid. The latitude varies only slightly (a few deg) with altitude, but this variation is included. It should be noted that while a single latitude value is given for each point, the observation is inherently a horizontal average over many hundreds of kilometers. Quasi-dipole latitude and longitude are calculated using the fast implementation developed by Emmert et al. (2010, doi:10.1029/2010JA015326) and the Python wrapper apexpy (doi.org/10.5281/zenodo.1214207).</p>	deg	Epoch, ICON_L22_Altitude
ICON_L22_Magnetic_Longitude	<p>Magnetic quasi-dipole longitude of each wind sample</p> <p>A two-dimensional array defining the magnetic quasi-dipole longitude of the two-dimensional data grid. The longitude varies only slightly (a few deg) with altitude, but this variation is included. It should be noted that while a single longitude value is given for each point, the observation is inherently a horizontal average over many hundreds of kilometers. Quasi-dipole latitude and longitude are calculated using the fast implementation developed by Emmert et al. (2010, doi:10.1029/2010JA015326) and the Python wrapper apexpy (doi.org/10.5281/zenodo.1214207). Quasi-dipole longitude is defined such that zero occurs where the geodetic longitude is near 285 deg east (depending on latitude).</p>	deg	Epoch, ICON_L22_Altitude
ICON_L22_Solar_Zenith_Angle	<p>Solar zenith angle of each wind sample</p> <p>Angle between the vectors towards the sun and towards zenith, for each point in the grid.</p>	deg	Epoch, ICON_L22_Altitude
ICON_L22_Local_Solar_Time	<p>Local solar time of each wind sample</p> <p>Local solar time at each point in the grid, calculating using the equation of time.</p>	hour	Epoch, ICON_L22_Altitude
ICON_L22_Time_Delta	<p>Difference between MIGHTI-A and B times contributing to each point</p> <p>To determine the cardinal wind at each point, a MIGHTI-A line-of-sight wind is combined with a MIGHTI-B line-of-sight wind from several minutes later. This variable contains this time difference for every point. During standard operations (LVLH Normal), this variable should be positive, but can potentially become negative during conjugate operations or when ICON is observing to the south (LVLH Reverse).</p>	s	Epoch, ICON_L22_Altitude

metadata

Variable Name	Description	Units	Dimensions
ICON_L22_Fringe_Amplitude_A	<p>Fringe Amplitude from MIGHTI-A</p> <p>See Fringe_Amplitude. This variable contains the fringe amplitude measured by MIGHTI-A, interpolated to the reconstruction grid. This is one of two variables used to create Fringe_Amplitude.</p>	arb	Epoch, ICON_L22_Altitude
ICON_L22_Fringe_Amplitude_B	<p>Fringe Amplitude from MIGHTI-B</p> <p>See Fringe_Amplitude. This variable contains the fringe amplitude measured by MIGHTI-B, interpolated to the reconstruction grid. This is one of two variables used to create Fringe_Amplitude.</p>	arb	Epoch, ICON_L22_Altitude
ICON_L22_Relative_VER_A	<p>Relative VER from MIGHTI-A</p> <p>See Relative_VER. This variable contains the VER measured by MIGHTI-A, interpolated to the reconstruction grid. This is one of two variables used to create Relative_VER. When A and B are significantly different, large horizontal gradients are suspected, and the quality is reduced.</p>	ph/cm ³ /s	Epoch, ICON_L22_Altitude
ICON_L22_Relative_VER_B	<p>Relative VER from MIGHTI-B</p> <p>See Relative_VER. This variable contains the VER measured by MIGHTI-B, interpolated to the reconstruction grid. This is one of two variables used to create Relative_VER. When A and B are significantly different, large horizontal gradients are suspected, and the quality is reduced.</p>	ph/cm ³ /s	Epoch, ICON_L22_Altitude
ICON_L22_VER_Relative_Difference	<p>Difference in MIGHTI A and B's VER estimates, divided by the mean</p> <p>The absolute value of the difference between Relative_VER_A and Relative_VER_B, divided by the average. Ideally, MIGHTI A and B should measure the same VER. When they do not, this is an indication of potential violations of the spherical symmetry assumption inherent to the inversion. This is the parameter used to determine if the spherical asymmetry flag is raised.</p>		Epoch, ICON_L22_Altitude

Variable Name	Description	Units	Dimensions
ICON_L22_Quality_Flags	<p>Quality flags</p> <p>This variable provides information on why the Quality variable is reduced from 1.0. Many quality flags can be raised for each grid point, and each flag takes values 0 or 1. More than one flag can be raised per point. This variable is a three-dimensional array with dimensions time, altitude, and number of flags. Each entry is 0 or 1. Most quality flags are passed through from the L1 and L2.1 algorithms (after interpolation to the L2.2 grid). Some additional quality flags are created in L2.2. The N_Flags dimension is defined below:</p> <ul style="list-style-type: none"> * 0 : (From L1 A) SNR too low to reliably perform L1 processing * 1 : (From L1 A) Proximity to South Atlantic Anomaly * 2 : (From L1 A) Bad calibration * 3 : (From L1 A) Calibration lamps are on * 4 : (From L1 A) Solar/lunar contamination * 5 : (From L2.1 A) Not enough valid points in profile * 6 : (From L2.1 A) SNR too low after inversion * 7 : (From L2.1 A) Significant airglow above 300 km * 8 : (From L2.1 A) Line of sight crosses the terminator * 9 : (From L2.1 A) Thermal drift correction is uncertain * 10: (From L2.1 A) S/C pointing is not stable * 11: (From L2.1 A) SNR is low after inversion, but maybe usable * 12: (From L1 B) SNR too low to reliably perform L1 processing * 13: (From L1 B) Proximity to South Atlantic Anomaly * 14: (From L1 B) Bad calibration * 15: (From L1 B) Calibration lamps are on <p>NOTE: Var_Notes truncated. See NC file for full description.</p>		Epoch, ICON_L22_Altitude, N_Flags

Acknowledgement

This is a data product from the NASA Ionospheric Connection Explorer mission, an Explorer launched at 21:59:45 EDT on October 10, 2019, from Cape Canaveral AFB in the USA. Guidelines for the use of this product are described in the ICON Rules of the Road (<http://icon.ssl.berkeley.edu/Data>).

Responsibility for the mission science falls to the Principal Investigator, Dr. Thomas Immel at UC Berkeley: Immel, T.J., England, S.L., Mende, S.B. et al. Space Sci Rev (2018) 214: 13. <https://doi.org/10.1007/s11214-017-0449-2>

Responsibility for the validation of the L1 data products falls to the instrument lead investigators/scientists.

* EUV: Dr. Eric Korpela : <https://doi.org/10.1007/s11214-017-0384-2>

* FUV: Dr. Harald Frey : <https://doi.org/10.1007/s11214-017-0386-0>

* MIGHTI: Dr. Christoph Englert : <https://doi.org/10.1007/s11214-017-0358-4>, and <https://doi.org/10.1007/s11214-017-0374-4>

* IVM: Dr. Roderick Heelis : <https://doi.org/10.1007/s11214-017-0383-3>

Responsibility for the validation of the L2 data products falls to those scientists responsible for those products.

* Daytime O and N2 profiles: Dr. Andrew Stephan : <https://doi.org/10.1007/s11214-018-0477-6>

* Daytime (EUV) O+ profiles: Dr. Andrew Stephan : <https://doi.org/10.1007/s11214-017-0385-1>

* Nighttime (FUV) O+ profiles: Dr. Farzad Kamalabadi : <https://doi.org/10.1007/s11214-018-0502-9>

* Neutral Wind profiles: Dr. Jonathan Makela : <https://doi.org/10.1007/s11214-017-0359-3>

* Neutral Temperature profiles: Dr. Christoph Englert : <https://doi.org/10.1007/s11214-017-0434-9>

* Ion Velocity Measurements : Dr. Russell Stoneback : <https://doi.org/10.1007/s11214-017-0383-3>

Responsibility for Level 4 products falls to those scientists responsible for those products.

* Hough Modes : Dr. Chihoko Yamashita : <https://doi.org/10.1007/s11214-017-0401-5>

* TIEGCM : Dr. Astrid Maute : <https://doi.org/10.1007/s11214-017-0330-3>

* SAMI3 : Dr. Joseph Huba : <https://doi.org/10.1007/s11214-017-0415-z>

Pre-production versions of all above papers are available on the ICON website.

<http://icon.ssl.berkeley.edu/Publications>

Overall validation of the products is overseen by the ICON Project Scientist, Dr. Scott England.

NASA oversight for all products is provided by the Mission Scientist, Dr. Jeffrey Klenzing.

Users of these data should contact and acknowledge the Principal Investigator Dr. Immel and the party directly responsible for the data product (noted above) and acknowledge NASA funding for the collection of the data used in the research with the following statement : "ICON is supported by NASA's Explorers Program through contracts NNG12FA45C and NNG12FA42I".

These data are openly available as described in the ICON Data Management Plan available on the ICON website (<http://icon.ssl.berkeley.edu/Data>).

This document was automatically generated on 2022-10-18 10:25 using the file:

ICON_L2-2_MIGHTI_Vector-Wind-Green_2022-01-01_v05r001.NC

Software version: ICON_SDC > ICON_UIUC_MIGHTI_L2.2_Processor_v5.05

ICON Data Product 2.3: MIGHTI Retrieved Temperatures and Brightnesses

This document describes the data product for ICON MIGHTI-A Level 2.3 Retrieved Temperature File, which is in NetCDF4 format.

MIGHTI samples the O₂ A band spectral region at five different wavelengths in order to both measure the shape of the band and to specify a background radiance that is subtracted from the signal. The wavelengths of the filter passbands are selected to maximize the sensitivity to lower thermospheric temperature variations. Two filter channels sample either end of the band to define a background (754.1 nm and 780.1 nm) and three more sample its shape (760.0 nm, 762.8 nm and 765.2 nm). Using three filters that sample the band shape allows the simultaneous retrieval of the atmospheric temperature and common shifts in the center wavelengths of the pass bands due to thermal drifts of the filters [Stevens et al., 2018; Englert et al., 2017]. MIGHTI has two identical sensor units: MIGHTI-A and MIGHTI-B. The operations are conducted such that MIGHTI-B measures the same volume of air as MIGHTI-A but approximately 8 minutes later.

History

v03: First public release of MIGHTI L2.3 Temperature software and retrievals, M.H. Stevens, 04 Jun 2020. This release uses a fixed common wavenumber offset of 7.5 cm⁻¹ and retrieves temperatures using only the 760 nm channel and the 763 nm. This offset and channel pair are used for all retrievals. Although the images sample ~90-140 km, all temperature profiles in v03 are for altitudes between 90-115 km. MIGHTI-A temperatures are available for both daytime and nighttime. MIGHTI-B temperatures are available only for daytime and only between 99-115 km.

v04: Second public release of L2.3 Temperature software and retrievals, M.H. Stevens, 21 Sep 2020. For daytime retrievals, v04 uses the same 7.5 cm⁻¹ wavenumber offset and 760 nm and 763 nm channel pair as v03. For nighttime retrievals, v04 uses a 3.0 cm⁻¹ wavenumber offset and the 763 nm and 765 nm channel pair. These changes produce a more distinct mesopause from nighttime images. The MIGHTI-A (day and night) and MIGHTI-B (day only) minimum/maximum altitudes are the same as for v03.

v05: Third public release of L2.3 Temperature software and retrievals, M.H. Stevens, 3 Aug 2021. The most significant change in v05 is the modification of the flat fields and these changes are informed by on-orbit data. The flat fields describe the response of the instrument to the O₂ A Band emission and were measured in the lab prior to launch. The modifications include small changes to both the transmittance at each channel as well as the channel center wavenumbers. These modifications are contained in new calibration files: `delta_filter_transm_X.sav` and `delta_filter_waven_X.sav`, where X is A or B. Delta transmittances for the detectors multiply the lab flat fields and delta channel center wavenumbers are added to the convolved HITRAN spectra. With these changes the MIGHTI-A and MIGHTI-B daytime data are now both available between 90-127 km. MIGHTI-A nighttime data are available between 90-108 km. MIGHTI-B nighttime data are available between 90-106 km. Terminator data between 90-105 degrees solar zenith angle now included. Retrievals for MIGHTI-A and MIGHTI-B now use all three signal channels to maximize constraints to temperatures. Reduced bias uncertainty for MIGHTI-A and MIGHTI-B based on differences between common volume observations at 90 km. They are also now separately defined for day and night so that this bias can be positive or negative for day and positive or negative for night. Epoch and altitude dimensions have been swapped to conform to existing standards.

Dimensions

NetCDF files contain **variables** and the **dimensions** over which those variables are defined. First, the dimensions are defined, then all variables in the file are described.

The dimensions used by the variables in this file are given below, along with nominal sizes. Note that the size may vary from file to file. For example, the "Epoch" dimension, which describes the number of time samples contained in this file, will have a varying size.

Dimension Name	Nominal Size
Epoch	unlimited
Altitude	18
Wavelength	5

Variables

Variables in this file are listed below. First, "data" variables are described, followed by the "support_data" variables, and finally the "metadata" variables. The variables classified as "ignore_data" are not shown.

data

Variable Name	Description	Units	Dimensions
ICON_L23_MIGHTI_A_T emperature	<p>Derived temperatures from A band by altitude</p> <p>Derived temperatures from A band by altitude. Temperatures are retrieved from the rotational distribution of emission lines in the O2 A band. The measurement is made at 5 spectral channels. 3 channels measure the A band and 2 others on either side of the band measure a background, which is subtracted from the 3 signal channels. An entire altitude profile is observed simultaneously. An onion-peeling inversion is used on the raw observations to remove the effects of the integration along the line of sight. See Stevens et al. (Space Science Reviews (2018) 214:4. https://doi.org/10.1007/s11214-017-0434-9). O2 A band spectra are pre-calculated from 100-400 K in 20 K increments based on the HITRAN 2016 database [Gordon et al., JQSRT (2017), 203:3-69.https://doi.org/10.1016/j.jqsrt.06.038] and smoothed filter functions with FWHM of ~2.0 nm. The filter functions are based on Gaussian fits to laboratory measurements and are a function of channel, row (altitude), and column. The fits are separately done for each pixel as a function of peak wavenumber (wavelength), width, and transmittance. For each of the three signal channels the fitted Gaussians are co-added over 51 pixels where the transmittance is largest for a representative filter function for that channel. The transmittances are not absolutely calibrated in photometric units, but the relative transmittance between channels and between detectors is maintained, which allows for the retrieval of temperature at the tangent altitude.</p>	K	Epoch, Altitude
ICON_L23_MIGHTI_A_T emperature_Statisti cal_Uncertainty	<p>Statistical uncertainties in derived temperatures by altitude</p> <p>Statistical uncertainties (one sigma) in derived temperatures by altitude</p>	K	Epoch, Altitude

Variable Name	Description	Units	Dimensions
ICON_L23_MIGHTI_A_T emperature_Bias_Unc ertainty	<p>Bias uncertainties in derived temperatures by altitude</p> <p>Estimated bias uncertainties in derived temperatures by altitude; aka systematic uncertainties. These uncertainties are present in each temperature profile and are primarily due to 1) uncertainty in the common shift applied to pre-flight laboratory determined filter positions. This uncertainty is determined by comparing MIGHTI-A and MIGHTI-B temperature retrievals for the same day at 90 km and averaging the absolute difference over 3 different days. a derived fixed uncertainty of 3 K is propagated at all altitudes and 2) the lack of measurements above the top altitude sampled, and altitude dependent, with the topmost altitudes of the retrieval affected the most. The temperature bias uncertainty is found by a root sum square of these two. At most altitudes the estimated bias uncertainty is dominated by the uncertainty in the common shift. The systematic bias is the same at all altitudes for daytime images or nighttime images. However, the bias can be different for daytime images and nighttime images.</p>	K	Epoch, Altitude
ICON_L23_MIGHTI_A_T emperature_Total_Un certainty	<p>Total uncertainties in derived temperatures by altitude</p> <p>Total uncertainties in derived temperatures by altitude: Here the statistical temperature uncertainty has been linearly added to the estimated temperature bias.</p>	K	Epoch, Altitude
ICON_L23_MIGHTI_A_F ilter_Wavenumber_Sh ift	<p>Common shift of all filter center wavenumbers.</p> <p>Common shift of all filter center wavenumbers due to thermal drift that is added to laboratory measured filter center wavenumbers. The three channels measuring the A band overdetermines the temperature such that the wavenumber registration due to any thermal drift of the instrument can be additionally inferred. This is typically fixed with altitude and determined (along with temperature) from the signal originating from the O2 A band as measured from 3 signal channels.</p>	cm ⁻¹	Epoch, Altitude
ICON_L23_MIGHTI_A_F ilter_Wavenumber_Sh ift_Uncertainty	<p>Uncertainties in the shift of all filter center wavenumbers.</p> <p>Uncertainties (1-sigma) in the shift of all filter center wavenumbers. If the common wavenumber shift is fixed with altitude and prescribed, then this uncertainty is zero everywhere.</p>	cm ⁻¹	Epoch, Altitude
ICON_L23_MIGHTI_A_A Band_Intensity_Scal ed	<p>Derived scaling of O2 A Band to Radiances by altitude</p> <p>Derived common scaling of O2 A Band radiances in the 3 signal channels by altitude. Calculated forward radiances are fit to the observations from each of the three signal channels. The scaling is done at each tangent altitude separately and iteratively until a best fit solution is found. The intensity of each signal channel relative to the other two determines the temperature, so the scale factor is unitless. The scaling is derived using pre-calculated spectra from the HITRAN 2016 database [Gordon et al., JQSRT, 203, 3-69 (2017)].</p>		Epoch, Altitude

Variable Name	Description	Units	Dimensions
ICON_L23_MIGHTI_A_A Band_Intensity_Scaled_Uncertainty	<p>Uncertainty in Scaling of O2 A Band to Radiances by altitude</p> <p>Derived uncertainty (1-sigma) in derived common scaling of O2 A Band to emergent intensity by altitude.</p>		Epoch, Altitude
ICON_L23_MIGHTI_A_R relative_Radiance	<p>Relative radiance by filter and altitude</p> <p>Observed relative radiance by filter and altitude. The retrieval is based on a forward modeling approach to these observed radiances as reported in electrons/s from the MIGHTI L1 product. These are converted to electrons based on the integration time during day (30 s) or night (60 s).</p>	Electrons	Epoch, Altitude, Wavelength
ICON_L23_MIGHTI_A_R relative_Radiance_Uncertainty	<p>Uncertainties in relative radiance by filter and altitude</p> <p>Uncertainty (1-sigma) in relative radiance by filter by altitude and filter. These are calculated by taking the square root of the total number of electrons in each of the three signal channels, which are 51 pixels wide for MIGHTI-A or MIGHTI-B (day or night).</p>	Electrons	Epoch, Altitude, Wavelength
ICON_L23_MIGHTI_A_B background_Signal	<p>Background Signal Subtracted</p> <p>Background Signal by altitude and filter. This background is interpolated across the 3 signal channels from two background channels located spectrally on either side of the O2 A band.</p>	Electrons	Epoch, Altitude, Wavelength
ICON_L23_MIGHTI_A_B background_Slope	<p>Slope of background</p> <p>Derived slope of subtracted background. The slope of the background is saved here for diagnostic purposes. It is calculated by taking the difference of the flatfielded signal from the two background channels and dividing by the difference of the the channel center wavelengths (in nm) of the two background channels (approximately 780 nm - 754 nm). This is done explicitly by $[bg2 - bg1]/flatfield/[wavelength2 - wavelength1]$, where $bg2$ and $bg1$ are the observed background signals in electrons.</p>	/nm	Epoch, Altitude

support_data

Variable Name	Description	Units	Dimensions
Epoch	<p>ms since 1970-01-01 00:00:00 UTC at middle of image integration</p> <p>This variable contains the time corresponding to the temperature profiles reported in this file. The variable is in ms since 1970-01-01 00:00:00 UTC at middle of image integration. A human-readable version of the time can be found in the variable ICON_...UTC_Time.</p>	ms	Epoch

Variable Name	Description	Units	Dimensions
ICON_L23_MIGHTI_A_Tangent_Altitude	<p>Tangent point altitudes</p> <p>The tangent altitudes of each point in the temperature profile, which are evaluated using the WGS84 ellipsoid. The MIGHTI L23 tangent point altitudes are identical to the MIGHTI L1 tangent altitudes: ICON_L1_MIGHTI_X_IR_ARRAY_ALTITUDES, where "X" is "A" or "B". These altitudes correspond to the center of each IR altitude sample.</p>	km	Epoch, Altitude
ICON_L23_MIGHTI_A_Filter_Center_Wavenumber	<p>Filter Center Wavenumber</p> <p>Filter Center Wavenumber used in temperature retrieval as measured in the laboratory and fitted by a Gaussian. These filter center wavenumbers vary with detector (MIGHTI A and MIGHTI B), with altitude as well as with channel. They are also difference for daytime and nighttime operations. It is from these center wavenumbers that the common wavenumber shift (across all channels) is calculated.</p>	cm ⁻¹	Epoch, Wavelength, Altitude
ICON_L23_MIGHTI_A_Filter_Center_Wavelength	<p>Filter Center Wavelength</p> <p>Filter Center Wavelength used in temperature retrieval (=1e7/FilterCWN).</p>	nm	Epoch, Wavelength, Altitude
ICON_L23_MIGHTI_A_Tangent_Latitude	<p>Tangent point latitudes by altitude</p> <p>Tangent point latitudes by altitude. Note that these are a function of both epoch and altitude. Note also that due to the nature of the limb observations these latitudes are typically an average over many hundreds of kilometers.</p>	degrees North	Epoch, Altitude
ICON_L23_MIGHTI_A_Tangent_Longitude	<p>Tangent point longitudes by altitude</p> <p>Tangent point longitudes (0-360) by altitude. Note that these are a function of both epoch and altitude. Note also that due to the nature of the limb observations these longitudes are typically an average over many hundreds of kilometers.</p>	degrees East	Epoch, Altitude
ICON_L23_MIGHTI_A_Tangent_Magnetic_Latitude	<p>Tangent point magnetic latitudes by altitude</p> <p>Tangent point magnetic latitudes by altitude. Quasi-dipole latitude and longitude are calculated using the fast implementation developed by Emmert et al. (2010, doi:10.1029/2010JA015326) and the Python wrapper apexpy (doi.org/10.5281/zenodo.1214207). Quasi-dipole longitude is defined such that zero occurs where the geodetic longitude is near 285 deg east (depending on latitude). Note that these are a function of both epoch and altitude. Note also that due to the nature of the limb observations these latitudes are typically an average over many hundreds of kilometers.</p>	degrees North	Epoch, Altitude

Variable Name	Description	Units	Dimensions
ICON_L23_MIGHTI_A_Tangent_Magnetic_Longitude	Tangent point magnetic longitudes by altitude Tangent point magnetic longitudes by altitude. Quasi-dipole latitude and longitude are calculated using the fast implementation developed by Emmert et al. (2010, doi:10.1029/2010JA015326) and the Python wrapper apexpy (doi.org/10.5281/zenodo.1214207). Quasi-dipole longitude is defined such that zero occurs where the geodetic longitude is near 285 deg east (depending on latitude). Note that these are a function of both epoch and altitude. Note also that due to the nature of the limb observations these longitudes are typically an average over many hundreds of kilometers.	degrees East	Epoch, Altitude
ICON_L23_MIGHTI_A_Tangent_Local_Solar_Time	Local solar time at tangent point Local solar time (0-24 h) at tangent point calculated using the equation of time. LST is a function of both epoch and altitude.	hour	Epoch, Altitude
ICON_L23_MIGHTI_A_Tangent_Solar_Zenith_Angle	Solar zenith angle at tangent point Solar zenith angle at tangent point. SZA is a function of both epoch and altitude.	degrees	Epoch, Altitude
ICON_L23_MIGHTI_A_Field_of_View_Azimuth_Angle	Field of view azimuth angle Field of view azimuth angle	degrees	Epoch, Altitude
ICON_L23_MIGHTI_A_Total_Boresight_Sun_Angle	Total boresight to sun angle Total boresight to sun angle	degrees	Epoch
ICON_L23_MIGHTI_A_Thermal_Electric_Cooler_Cold_Temperature	Cold-side temperature of the thermoelectric cooler attached to the camera head Cold-side temperature of the thermoelectric cooler attached to the camera head	C	Epoch
ICON_L23_Orbit_Number	Integer orbit number at middle of exposure Integer orbit number at middle of exposure		Epoch
ICON_L23_Observatory_Latitude	Spacecraft latitude at middle of exposure Spacecraft latitude at middle of exposure	degrees North	Epoch
ICON_L23_Observatory_Longitude	Spacecraft longitude at middle of exposure Spacecraft longitude (0-360) at middle of exposure	degrees East	Epoch
ICON_L23_Observatory_Altitude	Spacecraft altitude at middle of exposure Spacecraft altitude at middle of exposure	km	Epoch
ICON_L23_Observatory_Local_Solar_Time	Spacecraft local solar time at middle of exposure Spacecraft local solar time (0-24) at middle of exposure	hour	Epoch
ICON_L23_Observatory_Solar_Zenith_Angle	Spacecraft solar zenith angle at middle of exposure Spacecraft solar zenith angle at middle of exposure	degrees	Epoch

Variable Name	Description	Units	Dimensions
ICON_L23_MIGHTI_Aperture_1_Position	MIGHTI-A camera aperture 1 position sense flag. Aperture Position 1: 0=OPEN, 1=CLOSED, 2=15% OPEN, 3=UNKNOWN. Note that when OPEN (0) the integration time is 60 s for nighttime observations and when 15% OPEN (2) the integration time is 30 s for daytime observations.		Epoch
ICON_L23_MIGHTI_Aperture_2_Position	MIGHTI-A camera aperture 2 position sense flag. Aperture Position 2: 0=OPEN, 1=CLOSED, 2=15% OPEN, 3=UNKNOWN. Note that when OPEN (0) the integration time is 60 s for nighttime observations and when 15% OPEN (2) the integration time is 30 s for daytime observations.		Epoch
ICON_L23_Orbit_Node	Flag indicating that the spacecraft is ascending (0) or descending (1) node Flag indicating that the spacecraft is ascending (0) or descending (1) node.		Epoch
ICON_L1_MIGHTI_A_Quality_Flag_South_Atlantic_Anomaly	Quality Flag indicating that the spacecraft is within the South Atlantic Anomaly Quality Flag indicating that the spacecraft is within the South Atlantic Anomaly (0 = not in SAA)		Epoch
ICON_L1_MIGHTI_A_Quality_Flag_Bad_Calibration	Quality Flag indicating an inappropriate calibration file has been used or was missing Quality Flag indicating an inappropriate calibration file has been used or was missing		Epoch
ICON_L23_MIGHTI_A_UTC_Time	ISO 9601 formatted UTC timestamp (at middle of image integration). This variable is the same as Epoch but is formatted as a human-readable string.		Epoch
ICON_L23_MIGHTI_A_UTC_Time_Start	ms since 1970-01-01 00:00:00 UTC at start of image integration. ms since 1970-01-01 00:00:00 UTC at start of image integration. Derived from original GPS values reported from spacecraft (Time_GPS_Seconds and Time_GPS_Subseconds). Time calculation is offset by 615ms (flush time) for the first image in the series and for all other images are adjusted by subtracting (integration time + 308 ms) from the reported GPS time.		Epoch
ICON_L23_MIGHTI_A_UTC_Time_Stop	ms since 1970-01-01 00:00:00 UTC at end of image integration. ms since 1970-01-01 00:00:00 UTC at end of image integration. Derived from original GPS values reported from spacecraft (Time_GPS_Seconds and Time_GPS_Subseconds). Time calculation is offset by 615ms (flush time) for the first image in the series and for all other images are adjusted by subtracting (integration time + 308 ms) from the reported GPS time.		Epoch

Variable Name	Description	Units	Dimensions
ICON_L23_MIGHTI_A_GPS_Time	<p>ms since 1980-01-06 00:00:00 TAI (coincident with UTC) at middle of image integration.</p> <p>ms since 1980-01-06 00:00:00 TAI (coincident with UTC) at middle of image integration. Derived from original GPS values reported from spacecraft (Time_GPS_Seconds and Time_GPS_Subseconds). Time calculation is offset by 615ms (flush time) for the first image in the series and for all other images are adjusted by subtracting (integration time + 308 ms) from the reported GPS time.</p>		Epoch
ICON_L23_MIGHTI_A_GPS_Time_Seconds	<p>GPS seconds count when FSW received image packet header.</p> <p>The header of the first image received in a series 615 ms after start of image processing. Following headers are adjusted by subtracting (integration time + 308 ms) from the reported GPS time.</p>		Epoch
ICON_L23_MIGHTI_A_GPS_Time_Subseconds	<p>20MHz clock (50 nanosecond) offset from GPS seconds.</p> <p>GPS Time in sub seconds, 50 nanosecond offset from GPS seconds from 20 MHz clock.</p>	50 Nanoseconds	Epoch
ICON_L23_MIGHTI_A_Integration_Time	<p>Time to integrate MIGHTI-A region of interest (ROI) image.</p> <p>MIGHTI Integration Time in milliseconds</p>	ms	Epoch

metadata

Variable Name	Description	Units	Dimensions
ICON_L23_MIGHTI_A_Filter_Wavelengths	<p>Wavelength labels corresponding to the five filters</p> <p>Wavelength labels corresponding to the five filters. These are for guidance. Actual values used in retrieval for MIGHTI-A and MIGHTI-B (day/night) are in ICON_L23_MIGHTI_(A or B)_Filter_Center_Wavelength.</p>		Wavelength

Acknowledgement

This is a data product from the NASA Ionospheric Connection Explorer mission, an Explorer launched at 21:59:45 EDT on October 10, 2019, from Cape Canaveral AFB in the USA. Guidelines for the use of this product are described in the ICON Rules of the Road (<http://icon.ssl.berkeley.edu/Data>).

Responsibility for the mission science falls to the Principal Investigator, Dr. Thomas Immel at UC Berkeley: Immel, T.J., England, S.L., Mende, S.B. et al. *Space Sci Rev* (2018) 214: 13. <https://doi.org/10.1007/s11214-017-0449-2>

Responsibility for the validation of the L1 data products falls to the instrument lead investigators/scientists.

- * EUV: Dr. Eric Korpela : <https://doi.org/10.1007/s11214-017-0384-2>
- * FUV: Dr. Harald Frey : <https://doi.org/10.1007/s11214-017-0386-0>
- * MIGHTI: Dr. Christoph Englert : <https://doi.org/10.1007/s11214-017-0358-4>, and <https://doi.org/10.1007/s11214-017-0374-4>
- * IVM: Dr. Roderick Heelis : <https://doi.org/10.1007/s11214-017-0383-3>

Responsibility for the validation of the L2 data products falls to those scientists responsible for those products.

- * Daytime O and N2 profiles: Dr. Andrew Stephan : <https://doi.org/10.1007/s11214-018-0477-6>
- * Daytime (EUV) O+ profiles: Dr. Andrew Stephan : <https://doi.org/10.1007/s11214-017-0385-1>
- * Nighttime (FUV) O+ profiles: Dr. Farzad Kamalabadi : <https://doi.org/10.1007/s11214-018-0502-9>
- * Neutral Wind profiles: Dr. Jonathan Makela : <https://doi.org/10.1007/s11214-017-0359-3>
- * Neutral Temperature profiles: Dr. Christoph Englert : <https://doi.org/10.1007/s11214-017-0434-9>
- * Ion Velocity Measurements : Dr. Russell Stoneback : <https://doi.org/10.1007/s11214-017-0383-3>

Responsibility for Level 4 products falls to those scientists responsible for those products.

- * Hough Modes : Dr. Chihoko Yamashita : <https://doi.org/10.1007/s11214-017-0401-5>
- * TIEGCM : Dr. Astrid Maute : <https://doi.org/10.1007/s11214-017-0330-3>
- * SAMI3 : Dr. Joseph Huba : <https://doi.org/10.1007/s11214-017-0415-z>

Pre-production versions of all above papers are available on the ICON website.
<http://icon.ssl.berkeley.edu/Publications>

Overall validation of the products is overseen by the ICON Project Scientist, Dr. Scott England.

NASA oversight for all products is provided by the Mission Scientist, Dr. Jeffrey Klenzing.

Users of these data should contact and acknowledge the Principal Investigator Dr. Immel and the party directly responsible for the data product (noted above) and acknowledge NASA funding for the collection of the data used in the research with the following statement : "ICON is supported by NASA's Explorers Program through contracts NNG12FA45C and NNG12FA42I".

These data are openly available as described in the ICON Data Management Plan available on the ICON website (<http://icon.ssl.berkeley.edu/Data>).

This document was automatically generated on 2021-09-07 07:52 using the file:

ICON_L2-3_MIGHTI-A_Temperature_2020-04-08_v05r000.nc

Software version: ICON_SDC > MIGHTI L2 Temperature Retrieval v5.00

4.1.2 IVM Data Products Functional Description

This subsection details the science data products produced by a particular mission instrument or ground system element (e.g., SOC).

Following this brief overview, details of the data products are provided for L1, L2 and Ancillary products. L0 are instrument level (voltages, currents, instrument codes etc.) and not interpretable for anyone without intimate knowledge of the instrumentation.

The mission-specific data levels should be defined, and the steps needed to process each level of data shall be described.

The introduction to Section 4 describes the overall data levels for ICON. Table 4.1.2.1 lists the IVM products by level. The L0, Ancillary, L1 and L2 data have separate files for IVM A and B, but it is worth noting that only IVM A or B is in science mode at any time. The IVM Ancillary file provides the geometry relevant to the observations, using knowledge of the spacecraft position and pointing derived from the spacecraft telemetry.

Level	Source (Instrument/Model)	Data Product
0	IVM	L0 IVM Data
Anc.	Ground	IVM Ancillary Data
1	IVM	L1 IVM
2	IVM	Ion densities, drifts

Table 4.1.2.1 – List of IVM data products by level.

At a high level, the flow of the IVM data products is shown in Figure 4.1.2.1.

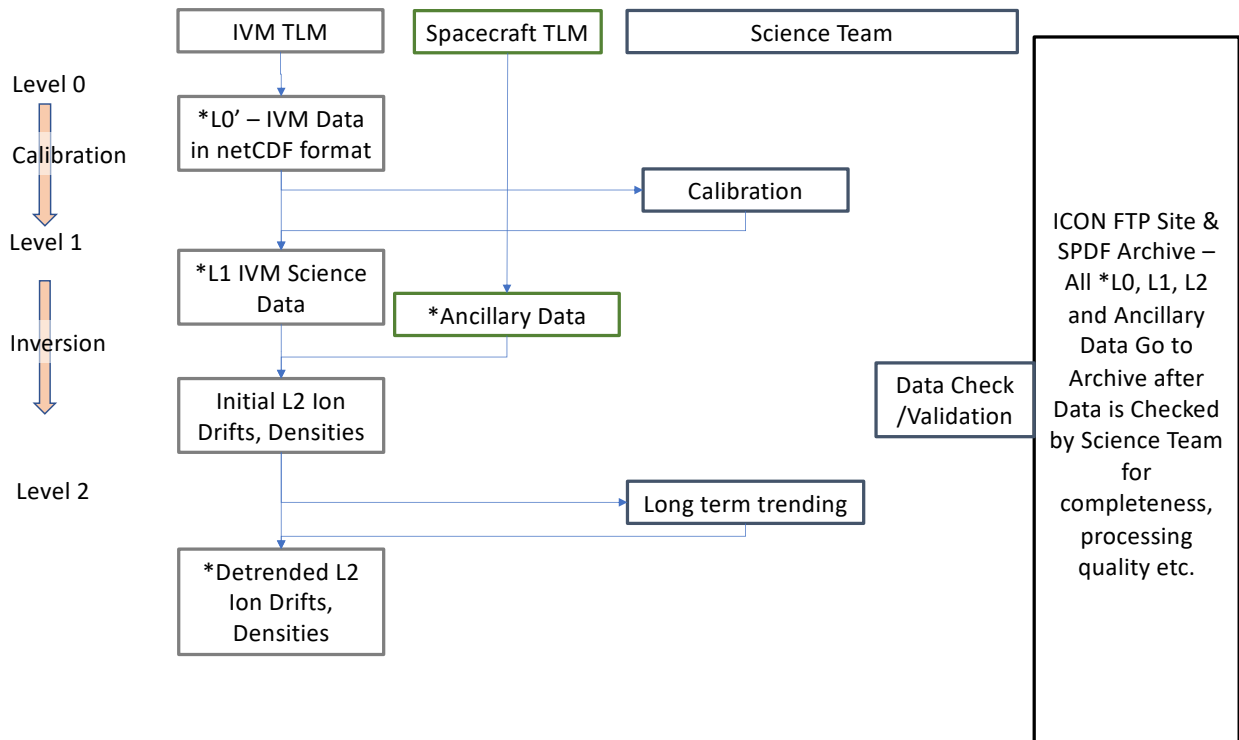


Figure 4.1.2.1 – Schematic of the IVM Data Products and their Flow.

The overall concept for producing the L2 density and drift products are as follows: the IVM instrument measures the arrival angle of positively charged ions relative to spacecraft ram, and the number of ions arriving in spacecraft ram. By increasing a retarding voltage, the instrument measures the number of ions arriving as a function of this voltage. From the arrival angle, the velocity of the ions perpendicular to the instrument can be found (Level 2 product). From the number of ions arriving as a function of retarding voltage, the ion composition, temperature and velocity in the spacecraft track can be found (Level 2 product). Together, this gives the 3 dimensional velocity vector of the ions *in situ*. The Level 1 product includes calibrated arrival angles and ion current as a function of retarding voltage. The nominal view direction of the IVM instrument is along the spacecraft track (either IVM A or B). The second IVM instrument is mounted in nominal spacecraft wake (either IVM B or A). Whenever the spacecraft is turned around, this second instrument continues the same observation as the first. Measurements are taken every second, but some fraction can potentially be impacted by the operation of spacecraft magneto-torquers. At least 3 measurements every 32s completely avoid the times when these spacecraft components are turned on during nominal operations (equivalent to around 250 km of spacecraft motion). Any measurements impacted by these are flagged. Operations are identical during day and night. The overall process of producing IVM L1 is shown in Figure 4.1.2.2.

IVM L0 to L1 Calibrated Arrival Angles and I-V Characteristics - Algorithm

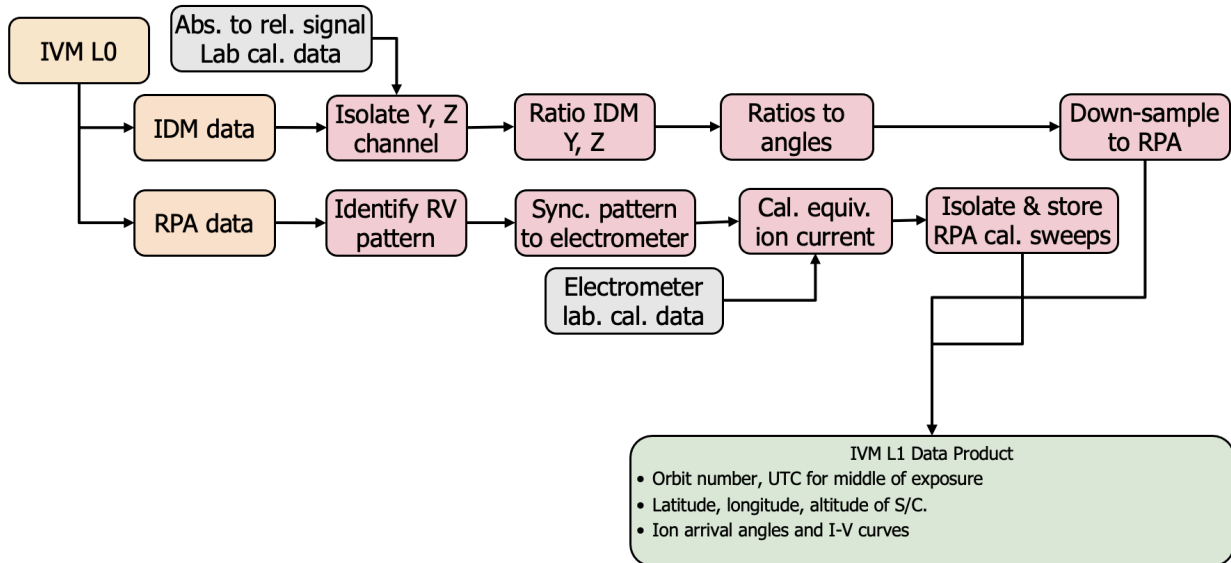


Figure 4.1.2.2 – Overall process for producing IVM L1 Data Product.

L2 ion density and drifts are then produced from the IVM L1 and Ancillary data products. The L2 product includes the calibrated ion density and drift velocity. From the arrival angle, the velocity of the ions perpendicular to the instrument can be found (2 components of the ion drift). From the number of ions arriving as a function of retarding voltage, the ion composition, temperature and velocity in the spacecraft track can be found (3rd component of the ion drift and density). Together, this gives the 3 dimensional velocity vector of the ions *in situ*. The Level 2 product includes calibrated ion drifts parallel and perpendicular to the local magnetic field, the ion density, the O⁺/He⁺ ratio and the ion temperature *in situ*. The overall process of producing IVM L2 Vector drift and density Product is shown in Figure 4.1.2.3.

IVM L1 to L2 In Situ Ion Parameters - Algorithm

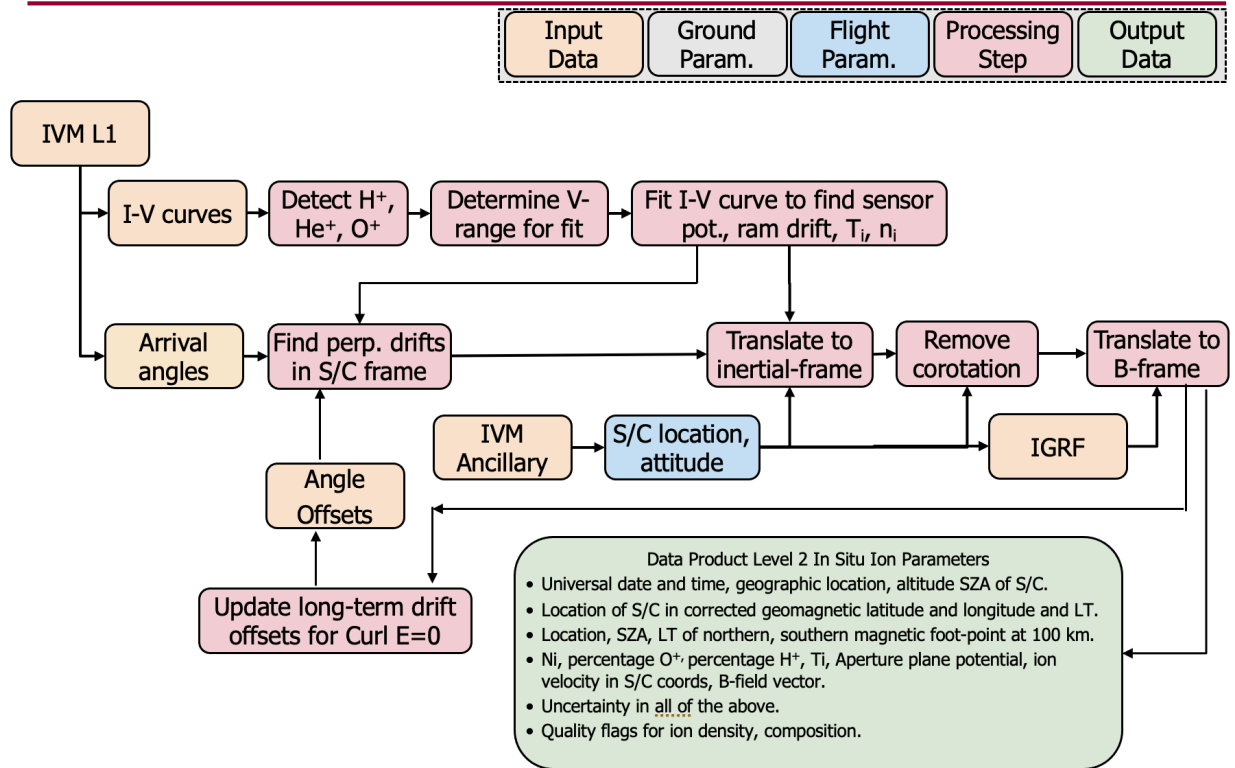


Figure 4.1.2.3 – Overall process for producing IVM L2 Ion density and drifts Data Product.

For more details on the data processing, the reader is directed to the ICON Calibration and Measurement Algorithms Document (CMAD).

A reference to the general data level definitions located in the Heliophysics Science Data Management Policy should be included.

The Heliophysics Science Data Management Policy, HPD-SDMP version 2.0, effective February 14, 2022 does not describe data levels. The ICON data levels closely follow those in the PDMP Template.

Any associated metadata products to be generated and maintained shall also be described.

Following this brief overview, full details of the metadata for each product are provided.

Details should also include the cadence (e.g., hourly, daily, etc.) for processing of data products.

The lowest level IVM data (L0) has one file per 4s. These are processed as they arrive on the ground, until an entire day of data has arrived at the Science Data Center (SDC). The SDC

processes the L0 into L1 and L2, and produces the Ancillary Data Products. The L1, Ancillary and L2 files all correspond to 1 file for 1 day. For L1, Ancillary and L2, there is 1 such file per day for IVM A and another for IVM B corresponding to each product. However, as in general only IVM A or B is in science mode on any given day, only one set of files exist. On days during which the spacecraft changes orientation and both IVM A and B files exist for parts of the day, both IVM A and B L0 through L2 files exist. The cadence for production of all products beyond L0 is daily, and beings once all inputs are available. As one example, the ancillary products use the definitive ephemeris, which is generated by the Mission Operations Center approximately 1 week after real-time.

The following section contains detailed descriptions of each of the IVM Data Products, the data and metadata contained within.

ICON Data Product 1.7: IVM Engineering Parameters

This document describes the data product for IVM L1 file, which is in NetCDF4 format.

This is a preliminary release of the NASA Ionospheric Connections Explorer Ion Velocity Meter (IVM) Level-1 file. This file contains a calibrated translation of the raw IVM engineering parameters into relevant raw physical values. For example, digital counts transmitted by the instrument are translated into actual voltages, or measured currents. This file also contains the fusion of the IVM parameters with satellite ephemeris and other ancillary data provided by the satellite team. The values within this file are not immediately valuable for scientific research however they may be useful for researchers seeking to perform their own translations of raw physical measurements into geophysical characterizations of the ionosphere.

History

Version 001, R. A. Stoneback, 2019-08-06T00:00:00, Initial Release

Version 002, R. A. Stoneback, 2020-06-19T00:00:00, Update for public release, adds quality flags

Version 003, R. A. Stoneback, 2020-04-10T00:00:00, Adds first order photoemission correction

Version 004, R. A. Stoneback, 2020-12-03T00:00:00, Adjustments to IVM offsets

Version 005, R. A. Stoneback, 2021-03-21T00:00:00, Improvements to RPA Fit noise, Drifts in East, North, Up. Data between 0500 and 1200 should be rejected at this time due to poor S/N and contaminant signals from internally generated photocurrents that have not been removed.

The V05 data product has been corrected for long-term systematic offsets produced by uncertainties in the electrostatic environment of the spacecraft. The corrected variables are:

ICON_L27_Ion_Velocity_X

ICON_L27_Ion_Velocity_Y

ICON_L27_Ion_Velocity_Z

They are used to compute the plasma drifts in magnetic coordinates.

The uncorrected data may be accessed directly in the variables

ICON_L27_Raw_Ion_Velocity_X

ICON_L27_Raw_Ion_Velocity_Y

ICON_L27_Raw_Ion_Velocity_Z

Short term variations with periods less than 10 days have not been removed but may be accurately assessed from examination of the zonal (daily) average of the meridional drift `ICON_L27_Ion_Velocity_Meridional` within 1 hour of 1800 MLT. Zonal averages in excess of 5 m/s over this local time range provide a reliable estimate of the short-term offset.

Version 006, TBD, The V06 data product has been improved to handle large O+ fractions and to include cross-track ion drifts derived by neglecting inputs from the RPA. Data products has been corrected for long-term systematic offsets produced by uncertainties in the electrostatic environment of the spacecraft. The corrected variables are: `ICON_L27_Ion_Velocity_X`, `ICON_L27_Ion_Velocity_Y`, `ICON_L27_Ion_Velocity_Z`. They are used to compute the plasma drifts in magnetic coordinates. The uncorrected data may be accessed directly in the variables `ICON_L27_Raw_Ion_Velocity_X`, `ICON_L27_Raw_Ion_Velocity_Y`, `ICON_L27_Raw_Ion_Velocity_Z`. Transverse ion drifts derived by neglecting RPA inputs may be accessed directly in the variables `ICON_L27_Original_Velocity_Y`, `ICON_L27_Original_Velocity_Z`. Short term variations with periods less than 10 days have not been removed but may be accurately assessed from examination of the zonal (daily) average of the meridional drift `ICON_L27_Ion_Velocity_Meridional` within 1 hour of 1800 MLT. Zonal averages in excess of 5 m/s over this local time range provide a reliable estimate of the short-term offset.

Dimensions

NetCDF files contain **variables** and the **dimensions** over which those variables are defined. First, the dimensions are defined, then all variables in the file are described.

The dimensions used by the variables in this file are given below, along with nominal sizes. Note that the size may vary from file to file. For example, the "Epoch" dimension, which describes the number of time samples contained in this file, will have a varying size.

Dimension Name	Nominal Size
Epoch	unlimited
ICON_L1_IVM_A_RPA	32
ICON_L1_IVM_A_DM	32
ICON_L1_IVM_A_LLA	16
ICON_L1_IVM_A_LLB	16
ICON_L1_IVM_A_RV_MEM	32
ICON_L1_IVM_A_RV_MON	32

Variables

Variables in this file are listed below. First, "data" variables are described, followed by the "support_data" variables, and finally the "metadata" variables. The variables classified as "ignore_data" are not shown.

data

Variable Name	Description	Units	Dimensions
Epoch	<p>Universal Time (UTC)</p> <p>Time at the midpoint of the IVM measurements.</p>	<p>Milliseconds since 1970-01-01 00:00:00</p>	Epoch
ICON_L1_IVM_A_RPA_currents	<p>RPA Ion Current</p> <p>The value of RPA currents varies as a function of plasma parameters (density, composition, temperature, motion) and the value of the Retarding Voltage (RV). The RV setting creates an energy barrier such that only ions with energy above the barrier are measured. By varying the RV setting in time the energy distribution of the ions is recorded in the changing value of the RPA currents.</p>	A	Epoch, ICON_L1_IVM_A_RPA
ICON_L1_IVM_A_RPA_digitalval	<p>RPA Ion current A/D sample value</p> <p>Sample value is used with lab determined range parameters to reconstruct the value of currents recorded by the RPA.</p>		Epoch, ICON_L1_IVM_A_RPA
ICON_L1_IVM_A_RPA_range	<p>Instrument measurement range (index) used to digitize current sample</p> <p>To maintain accuracy and precision the RPA employs multiple current measurement scales. These scales are indicated by number (0-7). The smallest currents are recorded on range 0, the largest currents on range 7.</p>		Epoch, ICON_L1_IVM_A_RPA
ICON_L1_IVM_A_RPA_source	<p>Bipolar/Unipolar transistor flag</p> <p>The RPA employs two different transistor types. Setting 0, for the bipolar transistor, allows for a determination of both positive and negative currents. This setting is limited to range 0. The unipolar setting is restricted to positive currents only. The unipolar setting is typical for currents interpreted geophysically.</p>		Epoch, ICON_L1_IVM_A_RPA
ICON_L1_IVM_A_RPA_voltage	<p>Electrometer voltage value recorded by RPA</p> <p>The ion plasma currents produced in the RPA are converted into measurable voltages using an electrometer. The range of voltages produced is controlled by the range setting. This voltage is digitized, and used to reconstruct the measured current in ground software.</p>	V	Epoch, ICON_L1_IVM_A_RPA

Variable Name	Description	Units	Dimensions
ICON_L1_IVM_A_RPA	<p>RPA Voltages</p> <p>Dimension variable for storing Retarding Potential Analyzer (RPA) measurements. The RPA is one half of the Ion Velocity Meter (IVM), and provides information on ion density, composition (O+/H+ fractions), ion temperature, and ion motion along the look direction of the instrument. The RPA uses a variable Retarding Voltage (RV) to create an energy barrier that limits the collection of ions to those with an energy greater than the barrier. The RV values used for a given sweep are stored here.</p>	V	Epoch, ICON_L1_IVM_A_RPA
ICON_L1_IVM_A_DM_angle	<p>DM arrival angle determined from current ratio</p> <p>The Drift Meter (DM) has an entrance aperture that projects an ion beam onto a collector plate divided into 4 equal sections. The angle of the beam determines the beam location, and thus the amount of current recorded by each collector plate. The ratio of currents is recorded on-orbit by the DM. The value of this angle can be reconstructed using the measured ratio of currents. The angle reported here is reconstructed using current ratios measured on-orbit.</p>	Degrees	Epoch, ICON_L1_IVM_A_DM
ICON_L1_IVM_A_DM_axis	<p>Direction (axis) of measurement</p> <p>The DM is capable of measuring ion drifts along two orthogonal directions. The axis flag (0,1) indicates direction. At a hardware level, the axis flag indicates which pairings of collector plates are used when measuring currents and forming a current ratio. For collector plates labeled 1,2,3, and 4, the groupings could be 1,2 and 3,4 or 1,3 and 2,4.</p>		Epoch, ICON_L1_IVM_A_DM
ICON_L1_IVM_A_DM_digital	<p>DM measurement A/D sample value</p> <p>Digital value corresponding to the current ratios across pairs of collector plates.</p>		Epoch, ICON_L1_IVM_A_DM
ICON_L1_IVM_A_DM_polarity	<p>Electrical polarity of measurement</p> <p>The DM operates by measuring collector plate current ratios. The ratio may be formed as current levels A/B (0 polarity) or B/A (1 polarity).</p>		Epoch, ICON_L1_IVM_A_DM
ICON_L1_IVM_A_DM_ratio	<p>Ratio of plasma currents recorded by DM</p> <p>The ratio of currents between two pairs of collector plates within the DM is driven by the arrival angle of plasma within the instrument.</p>		Epoch, ICON_L1_IVM_A_DM
ICON_L1_IVM_A_DM_voltage	<p>Voltage value recorded by log difference amp</p> <p>The DM current ratios are electronically determined by measuring the currents with log electrometers and then forming the difference between two log electrometers. $\log(A)/\log(B) = \log(A) - \log(B)$. This is the difference between the two electrometers.</p>	V	Epoch, ICON_L1_IVM_A_DM

Variable Name	Description	Units	Dimensions
ICON_L1_IVM_A_DM	<p>DM Measurements</p> <p>Dimension variable for storing measurements from the Drift Meter (DM). The DM measures the cross-track velocities of ions, the ion motion perpendicular to the satellite track. The DM varies between measuring two orthogonal directions over its 1-second measurement cadence. The DM produces geophysical ion velocities by directly measuring the arrival angle of plasma and using knowledge of spacecraft motion and orientation to produce a measure of ion motion relative to co-rotation. Stores the times at native DM sampling rate. Each 32 sample sweep is donwsampled onto a 1-Hz sampling rate reporting drifts in two directions. Times are UTC milliseconds since 1970-01-01 00:00:00.</p>	<p>Millisecons since 1970-1-1 00:00:00</p>	<p>Epoch, ICON_L1_IVM_A_DM</p>
ICON_L1_IVM_A_LLA_axis	<p>LLA Direction (axis) of measurement</p> <p>The direction of the DM measurement is determined by the grouping of collector plates used in forming the current ratio. The two possible combinations are indicated by a 0 and 1.</p>		<p>Epoch, ICON_L1_IVM_A_LLA</p>
ICON_L1_IVM_A_LLA_digval	<p>LLA measurement A/D sample value</p> <p>Sample reflects A/D value of the voltage produced by a plasma current flowing through a log electrometer. Half of the collector plates (two) are hooked up to a given electrometer. This sample value is converted on the ground back to a voltage using a lab calibration.</p>		<p>Epoch, ICON_L1_IVM_A_LLA</p>
ICON_L1_IVM_A_LLA_i	<p>Currents entering DM onto collector plate pairs measured by LLA</p> <p>Plasma entering the Drift Meter (DM) is projected onto a collector plate divided into 4 equal segments. The currents recorded here reflect the signal produced by half of these plates.</p>	<p>A</p>	<p>Epoch, ICON_L1_IVM_A_LLA</p>
ICON_L1_IVM_A_LLA_polarity	<p>Electrical polarity of LLA measurement</p> <p>The DM operates by measuring collector plate current ratios. The ratio may be formed as current levels A/B (0 polarity) or B/A (1 polarity).</p>		<p>Epoch, ICON_L1_IVM_A_LLA</p>
ICON_L1_IVM_A_LLA_v	<p>Voltage value recorded by log A electrometer</p> <p>Sample reflects the voltage produced by a plasma current flowing through a log electrometer. Half of the collector plates (two) are hooked up to a given electrometer. This reconstructed data is produced on the ground using a lab calibration to translate a digital sample made on-orbit into a voltage value.</p>	<p>V</p>	<p>Epoch, ICON_L1_IVM_A_LLA</p>
ICON_L1_IVM_A_LLA_currents	<p>Lab calibrated currents obtained from log electrometer A.</p> <p>The internal IVM temperature is used along with a lab calibration over temperature to construct a temperature compensated description of measured ion plasma currents.</p>	<p>A</p>	<p>Epoch, ICON_L1_IVM_A_LLA</p>

Variable Name	Description	Units	Dimensions
ICON_L1_IVM_A_LLA	<p>Log Level A Measurement Times</p> <p>Dimension variable for LLA measurements. The LLA is a log electrometer that performs the conversion from plasma generated currents within the Drift Meter (DM) to a measureable voltage. Times are UTC milliseconds since 1970-1-1 00:00:00.</p>	Milliseconds since 1970-1-1 00:00:00	Epoch, ICON_L1_IVM_A_LLA
ICON_L1_IVM_A_LLB_axis	<p>LLB Direction (axis) of measurement</p> <p>The direction of the DM measurement is determined by the grouping of collector plates used in forming the current ratio. The two possible combinations are indicated by a 0 and 1.</p>		Epoch, ICON_L1_IVM_A_LLB
ICON_L1_IVM_A_LLB_digitalval	<p>LLB measurement A/D sample value</p> <p>Sample reflects A/D value of the voltage produced by a plasma current flowing through a log electrometer. Half of the collector plates (two) are hooked up to a given electrometer. This sample value is converted on the ground back to a voltage using a lab calibration.</p>		Epoch, ICON_L1_IVM_A_LLB
ICON_L1_IVM_A_LLB_i	<p>Currents entering DM along axis measured by LLB</p> <p>Plasma entering the Drift Meter (DM) is projected onto a collector plate divided into 4 equal segments. The currents recorded here reflect the signal produced by half of these plates.</p>	A	Epoch, ICON_L1_IVM_A_LLB
ICON_L1_IVM_A_LLB_polarity	<p>Electrical polarity of LLB measurement</p> <p>The DM operates by measuring collector plate current ratios. The ratio may be formed as current levels A/B (0 polarity) or B/A (1 polarity).</p>		Epoch, ICON_L1_IVM_A_LLB
ICON_L1_IVM_A_LLB_v	<p>Voltage value recorded by log B electrometer</p> <p>Sample reflects the voltage produced by a plasma current flowing through a log electrometer. Half of the collector plates (two) are hooked up to a given electrometer. This reconstructed data is produced on the ground using a lab calibration to translate a digital sample made on-orbit into a voltage value.</p>	V	Epoch, ICON_L1_IVM_A_LLB
ICON_L1_IVM_A_LLB_currents	<p>Lab calibrated currents obtained from log electrometer B.</p> <p>The internal IVM temperature is used along with a lab calibration over temperature to construct a temperature compensated description of measured ion plasma currents.</p>	A	Epoch, ICON_L1_IVM_A_LLB
ICON_L1_IVM_A_LLB	<p>Log Level B Measurement Times</p> <p>Dimension variable for LLB measurements. The LLB is a log electrometer that performs the conversion from plasma generated currents within the Drift Meter (DM) to a measureable voltage. Times are UTC milliseconds since 1970-1-1 00:00:00.</p>	Milliseconds since 1970-1-1 00:00:00	Epoch, ICON_L1_IVM_A_LLB

Variable Name	Description	Units	Dimensions
ICON_L1_IVM_A_RV_MEM_digval	RV sample value used for measurement. The Retarding Voltage (RV) is monitored onboard. This is the A/D output value from that monitoring.		Epoch, ICON_L1_IVM_A_RV_MEM
ICON_L1_IVM_A_RV_MEM_v	Retarding voltage value obtained from memory lookup based on digval. The voltages produced by the Retarding Voltage (RV) circuitry were measured in the lab before launch and are used here to construct the nominally applied RV values.	V	Epoch, ICON_L1_IVM_A_RV_MEM
ICON_L1_IVM_A_RV_MEM	Retarding Voltage Memory Values Dimension variable for the Retarding Voltage (RV) memory values. The RV is varied to change the energy of plasma allowed within the RPA instrument. The RV values corresponding to the assigned state, as measured in the lab, are reported using this dimension. RV settings are fixed for a given 4-second instrument packet. Dimension data is a simple index.		Epoch, ICON_L1_IVM_A_RV_MEM
ICON_L1_IVM_A_RV_MON_digval	RV monitor measurement A/D sample value The Retarding Voltage (RV) value is monitored onboard the RPA. This monitor digitizes a voltage proportional to the RV. This variable stores the output of the D/A process.		Epoch, ICON_L1_IVM_A_RV_MON
ICON_L1_IVM_A_RV_MON_ppos	Location within IVM packet		Epoch, ICON_L1_IVM_A_RV_MON
ICON_L1_IVM_A_RV_MON_scaled_v	RV monitored voltage, obtained by scaling raw measurement. The Retarding Voltage (RV) value is monitored onboard the RPA. This monitor digitizes a voltage proportional to the RV. This variable reconstructs the applied RV value from the raw measurement voltage.	V	Epoch, ICON_L1_IVM_A_RV_MON
ICON_L1_IVM_A_RV_MON_src	Source of RV Monitored Voltage The Retarding Voltage (RV) value is monitored with one of two monitor circuits, based on its value. One circuit is for high RVs and one is for low RVs. This field indicates which monitor circuit was used. 1 = low RV, 0 = high RV		Epoch, ICON_L1_IVM_A_RV_MON
ICON_L1_IVM_A_RV_MON_v	Raw voltage value recorded by monitor The Retarding Voltage (RV) value is monitored onboard the RPA. This monitor digitizes a voltage proportional to the RV. This variable reconstructs the raw measured voltage as determined from the digital sample value.	V	Epoch, ICON_L1_IVM_A_RV_MON

Variable Name	Description	Units	Dimensions
ICON_L1_IVM_A_RV_MON	<p>Retarding Voltage Monitor Index</p> <p>Dimension variable for the Retarding Voltage (RV) Monitored values. The RV is varied to change the energy of plasma allowed within the RPA instrument. The RV values corresponding to the assigned state, as monitored on the s/c, are reported using this dimension. Dimension data is a simple index.</p>		Epoch, ICON_L1_IVM_A_RV_MON
ICON_L1_IVM_A_SENPOT	<p>Floating potential of instrument aperture sensor with respect to the plasma</p> <p>The SenPot reference surface is allowed to float electrically with respect to the spacecraft. The flux of ions (driven by s/c motion) must be balanced by the flux of electrons (driven by electron temperature). The value of the SenPot surface potential limits the collection of electrons such the net flux is zero.</p>	V	Epoch
ICON_L1_IVM_A_ALTITUDE	<p>WGS84 Altitude of Spacecraft Position (geodetic)</p> <p>Geodetic Altitude of Spacecraft in WGS84.</p>	km	Epoch
ICON_L1_IVM_A_COROTATION_X	<p>ECI Earth Corotation Velocity Components in IVM Coordinates</p> <p>Component of Earth's corotation velocity vector projected into the IVM instrument axes by taking the dot product of the corotation vector with the instrument's axes and multiplying the Y and Z components by negative 1 (but not the X component by convention).</p>	m/s	Epoch
ICON_L1_IVM_A_COROTATION_Y	<p>ECI Earth Corotation Velocity Components in IVM Coordinates</p> <p>Component of Earth's corotation velocity vector projected into the IVM instrument axes by taking the dot product of the corotation vector with the instrument's axes and multiplying the Y and Z components by negative 1 (but not the X component by convention).</p>	m/s	Epoch
ICON_L1_IVM_A_COROTATION_Z	<p>ECI Earth Corotation Velocity Components in IVM Coordinates</p> <p>Component of Earth's corotation velocity vector projected into the IVM instrument axes by taking the dot product of the corotation vector with the instrument's axes and multiplying the Y and Z components by negative 1 (but not the X component by convention).</p>	m/s	Epoch
ICON_L1_IVM_A_LATITUDE	<p>WGS84 Latitude of Spacecraft Position (geodetic)</p> <p>Geodetic latitude of spacecraft in WGS84</p>	degrees North	Epoch
ICON_L1_IVM_A_LONGITUDE	<p>WGS84 Longitude of Spacecraft Position (geodetic)</p> <p>Geodetic longitude of spacecraft in WGS84</p>	degrees East	Epoch

Variable Name	Description	Units	Dimensions
ICON_L1_IVM_A_SC_ML T	Magnetic Local Time at Spacecraft Magnetic Local Time at the spacecraft.	hour	Epoch
ICON_L1_IVM_A_SC_PO SITION_X	ECEF Spacecraft Position Position of spacecraft in ECEF coordinates.	km	Epoch
ICON_L1_IVM_A_SC_PO SITION_Y	ECEF Spacecraft Position Position of spacecraft in ECEF coordinates.	km	Epoch
ICON_L1_IVM_A_SC_PO SITION_Z	ECEF Spacecraft Position Position of spacecraft in ECEF coordinates.	km	Epoch
ICON_L1_IVM_A_SC_VE LOCITY_X	ECI Spacecraft Velocity Velocity of spacecraft in ECI, J2000, coordinates.	m/s	Epoch
ICON_L1_IVM_A_SC_VE LOCITY_Y	ECI Spacecraft Velocity Velocity of spacecraft in ECI, J2000, coordinates.	m/s	Epoch
ICON_L1_IVM_A_SC_VE LOCITY_Z	ECI Spacecraft Velocity Velocity of spacecraft in ECI, J2000, coordinates.	m/s	Epoch
ICON_L1_IVM_A_SC_XH AT_X	Instrument X Unit Vector in ECEF (Ram Direction) IVM x-axis (nominal Ram direction) unit vector in ECEF.	dimensi onless	Epoch
ICON_L1_IVM_A_SC_XH AT_Y	Instrument X Unit Vector in ECEF (Ram Direction) IVM x-axis (nominal Ram direction) unit vector in ECEF.	dimensi onless	Epoch
ICON_L1_IVM_A_SC_XH AT_Z	Instrument X Unit Vector in ECEF (Ram Direction) IVM x-axis (nominal Ram direction) unit vector in ECEF.	dimensi onless	Epoch
ICON_L1_IVM_A_SC_YH AT_X	Instrument Y Unit Vector in ECEF (Starboard Direction) IVM y-axis (nominal Starboard direction) unit vector in ECEF.	dimensi onless	Epoch
ICON_L1_IVM_A_SC_YH AT_Y	Instrument Y Unit Vector in ECEF (Starboard Direction) IVM y-axis (nominal Starboard direction) unit vector in ECEF.	dimensi onless	Epoch
ICON_L1_IVM_A_SC_YH AT_Z	Instrument Y Unit Vector in ECEF (Starboard Direction) IVM y-axis (nominal Starboard direction) unit vector in ECEF.	dimensi onless	Epoch
ICON_L1_IVM_A_SC_ZH AT_X	Instrument Z Unit Vector in ECEF (Nadir Direction) IVM z-axis (nominal Nadir direction) unit vector in ECEF.	dimensi onless	Epoch
ICON_L1_IVM_A_SC_ZH AT_Y	Instrument Z Unit Vector in ECEF (Nadir Direction) IVM z-axis (nominal Nadir direction) unit vector in ECEF.	dimensi onless	Epoch
ICON_L1_IVM_A_SC_ZH AT_Z	Instrument Z Unit Vector in ECEF (Nadir Direction) IVM z-axis (nominal Nadir direction) unit vector in ECEF.	dimensi onless	Epoch

Variable Name	Description	Units	Dimensions
ICON_L1_IVM_A_SUN_XY_PLANE_ANGLE	<p>Angle Between Sun and IVM XY Plane</p> <p>Angle between the Sun and IVM instrument XY plane.</p>	degrees	Epoch
ICON_L1_IVM_A_SUN_XZ_PLANE_ANGLE	<p>Angle Between Sun and IVM XZ Plane</p> <p>Angle between the Sun and IVM instrument XZ plane.</p>	degrees	Epoch
ICON_L1_IVM_A_ANGLE_0	<p>DM determined angle along axis 0</p> <p>The Drift Meter (DM) has an entrance aperture that projects an O+ ion beam onto a collector plate divided into 4 equal sections. The angle of the beam determines the beam location, and thus the amount of current recorded by each collector plate. The ratio of currents is recorded on-orbit by the DM. The value of this angle can be reconstructed using the measured ratio of currents. The angle reported here is reconstructed using current ratios measured on-orbit and downsampled onto 1-Hz cadence.</p>	degrees	Epoch
ICON_L1_IVM_A_ANGLE_1	<p>DM determined angle along axis 1</p> <p>The Drift Meter (DM) has an entrance aperture that projects an O+ ion beam onto a collector plate divided into 4 equal sections. The angle of the beam determines the beam location, and thus the amount of current recorded by each collector plate. The ratio of currents is recorded on-orbit by the DM. The value of this angle can be reconstructed using the measured ratio of currents. The angle reported here is reconstructed using current ratios measured on-orbit and downsampled onto 1-Hz cadence.</p>	degrees	Epoch
ICON_L1_IVM_A_LST	<p>Local Solar Time at Spacecraft</p> <p>Local Solar Time at spacecraft.</p>	hour	Epoch
ICON_L1_IVM_A_SZA	<p>Solar Zenith Angle at Spacecraft</p> <p>Solar Zenith Angle at the spacecraft.</p>	degrees	Epoch
ICON_L1_IVM_A_IVM_TEMPERATURE	<p>Internal IVM temperature</p> <p>Internally monitored temperature taken at board level.</p>	C	Epoch

Variable Name	Description	Units	Dimensions
ICON_L1_IVM_A_A_STATUS	<p>IVM-A Status</p> <p>Binary Coded Integer where</p> <ul style="list-style-type: none"> 1: Earth Day View 2: Earth Night View 4: Calibration Target View 8: Off-target View 16: Sun Proximity View 32: Moon Proximity View 64: North Magnetic Footpoint View 128: South Magnetic Footpoint View 256: Science Data Collection View 512: Calibration Data Collection View 1024: RAM Proximity View 2048-32768: SPARE <p>Activity is what the spacecraft was commanded to do while status is the spacecraft's natural state of operations. This means that activity should always be used over status if they differ, but will almost always be the same.</p>	binary	Epoch
ICON_L1_IVM_A_B_STATUS	<p>IVM-B Status</p> <p>Binary Coded Integer where</p> <ul style="list-style-type: none"> 1: Earth Day View 2: Earth Night View 4: Calibration Target View 8: Off-target View 16: Sun Proximity View 32: Moon Proximity View 64: North Magnetic Footpoint View 128: South Magnetic Footpoint View 256: Science Data Collection View 512: Calibration Data Collection View 1024: RAM Proximity View 2048-32768: SPARE <p>Activity is what the spacecraft was commanded to do while status is the spacecraft's natural state of operations. This means that activity should always be used over status if they differ, but will almost always be the same.</p>	binary	Epoch

Variable Name	Description	Units	Dimensions
ICON_L1_IVM_A_A_ACTIVITY	<p>IVM-A Activity</p> <p>Binary Coded Integer where:</p> <ul style="list-style-type: none"> 1: Earth Day View 2: Earth Night View 4: Calibration Target View 8: Off-target View 16: Sun Proximity View 32: Moon Proximity View 64: North Magnetic Footpoint View 128: South Magnetic Footpoint View 256: Science Data Collection View 512: Calibration Data Collection View 1024: RAM Proximity View 2048-32768: SPARE <p>Activity is what the spacecraft was commanded to do while status is the spacecraft's natural state of operations. This means that activity should always be used over status if they differ, but will almost always be the same.</p>	binary	Epoch
ICON_L1_IVM_A_B_ACTIVITY	<p>IVM-A Activity</p> <p>Binary Coded Integer where:</p> <ul style="list-style-type: none"> 1: Earth Day View 2: Earth Night View 4: Calibration Target View 8: Off-target View 16: Sun Proximity View 32: Moon Proximity View 64: North Magnetic Footpoint View 128: South Magnetic Footpoint View 256: Science Data Collection View 512: Calibration Data Collection View 1024: RAM Proximity View 2048-32768: SPARE <p>Activity is what the spacecraft was commanded to do while status is the spacecraft's natural state of operations. This means that activity should always be used over status if they differ, but will almost always be the same.</p>	binary	Epoch
ICON_L1_IVM_A_MTB_STATUS	<p>Magnetic Torquer Bar Firing Status</p> <p>If the magnetic torquers are active during any part of the measurement, it is recorded as active for whole measurement. Decoded from spacecraft housekeeping file: ICON_L0_Spacecraft_Housekeeping-MTB_2021-09-30_v01r001.CSV</p>	binary	Epoch
ICON_L1_IVM_A_SLEW_STATUS			Epoch
ICON_L1_IVM_A_SUN_STATUS	<p>Spacecraft Sun/Shadow Status Code</p> <p>Data is from predictive ephemeris. 0 = spacecraft in Sun, 1 = spacecraft in Earth Shadow.</p>	binary	Epoch

Variable Name	Description	Units	Dimensions
ICON_L1_IVM_A_ORBIT_NUMBER	Orbit Number Integer Orbit Number.	integer	Epoch
ICON_L1_IVM_A_ATTITUDE_STATUS	Slew or Off-Point Status Code Binary Coded Integer where 1: LVLH Normal Mode 2: LVLH Reverse Mode 4: Earth Limb Pointing 8: Inertial Pointing 16: Stellar Pointing 32: Attitude Slew 64: Conjugate Maneuver 128: Nadir Calibration 256: Lunar Calibration 512: Stellar Calibration 1024: Zero Wind Calibration 2048-32768: SPARE	binary	Epoch
ICON_L1_IVM_A_SPACE_ENVIRONMENT_REGION_STATUS	Space Environment Region Status Standardized for several missions, not all codes are relevant for ICON where 1: Earth Shadow 2: Lunar Shadow 4: Atmospheric Absorption Zone 8: South Atlantic Anomaly 16: Northern Auroral Zone 32: Southern Auroral Zone 64: Periapsis Passage 128: Inner & Outer Radiation Belts 256: Deep Plasma Sphere 512: Foreshock Solar Wind 1024: Solar Wind Beam 2048: High Magnetic Field 4096: Average Plasma Sheet 8192: Bowshock Crossing 16384: Magnetopause Crossing 32768: Ground Based Observatories 65536: 2-Day Conjunctions 131072: 4-Day Conjunctions 262144: Time Based Conjunctions 524288: Radial Distance Region 1 1048576: Orbit Outbound 2097152: Orbit Inbound 4194304: Lunar Wake 8388608: Magnetotail 16777216: Magnetosheath 33554432: Science 67108864: Low Magnetic Latitude 134217728: Conjugate Observation	binary	Epoch

Variable Name	Description	Units	Dimensions
ICON_L1_IVM_A_MAGNETIC_LATITUDE	<p>Magnetic Latitude of Spacecraft Position</p> <p>Quasi-dipole magnetic latitude of the spacecraft position. These values are obtained from passing the geodetic latitudes, longitudes, and altitudes from ICON Ancillary IVM Latitude, ICON Ancillary IVM Longitude, and ICON Ancillary IVM Altitude into apexpy Python module. For details on apexpy see: https://apexpy.readthedocs.org/</p>	degrees North	Epoch
ICON_L1_IVM_A_MAGNETIC_LONGITUDE	<p>Magnetic Longitude of Spacecraft Position</p> <p>Quasi-dipole magnetic longitude of the spacecraft position. These values are obtained from passing the geodetic latitudes, longitudes, and altitudes from ICON Ancillary IVM Latitude, ICON Ancillary IVM Longitude, and ICON Ancillary IVM Altitude into apexpy Python module. For details on apexpy see: https://apexpy.readthedocs.org/</p>	degrees East	Epoch
ICON_L1_IVM_A_TIME_UTC	<p>ISO 9601 formatted UTC timestamp (at middle of reading).</p> <p>ISO 9601 formatted UTC timestamp (at middle of reading).</p> <p>Time is generated from the time-code at byte 1015 of the IVM packet minus the time sync at byte 1019 of the IVM packet. This is the GPS time at the start of the integration period. The integration period is assumed to be 4 seconds so the center time is 2 seconds after that. The formula is $(\text{time-code} * 1000\text{ms}) + 2000\text{ms} - (16 * \text{time sync} / 1000)$ in GPS milliseconds then converted to UTC time. See the UTD 206-024 Rev A document.</p> <p>Time may be delayed by up to 10 ms due to FSW polling delay.</p> <p>Maximum time is ~2150 UTC and minimum time is ~1970 UTC.</p>		Epoch
ICON_L1_IVM_A_TIME_UTC_START	<p>Milliseconds since 1970-01-01 00:00:00 UTC at start of reading.</p> <p>Milliseconds since 1970-01-01 00:00:00 UTC at start of reading.</p> <p>Time is generated from the time-code at byte 1015 of the IVM packet minus the time sync at byte 1019 of the IVM packet. This is the GPS time at the start of the integration period. The integration period is assumed to be 4 seconds so the center time is 2 seconds after that. The formula is $(\text{time-code} * 1000\text{ms}) + 2000\text{ms} - (16 * \text{time sync} / 1000)$ in GPS milliseconds then converted to UTC time. See the UTD 206-024 Rev A document.</p> <p>Time may be delayed by up to 10 ms due to FSW polling delay.</p> <p>Maximum time is ~2150 UTC and minimum time is ~1970 UTC.</p>	milliseconds	Epoch

Variable Name	Description	Units	Dimensions
ICON_L1_IVM_A_TIME_UTC_STOP	<p>Milliseconds since 1970-01-01 00:00:00 UTC at end of reading.</p> <p>Milliseconds since 1970-01-01 00:00:00 UTC at end of reading.</p> <p>Time is generated from the time-code at byte 1015 of the IVM packet minus the time sync at byte 1019 of the IVM packet. This is the GPS time at the start of the integration period. The integration period is assumed to be 4 seconds so the center time is 2 seconds after that. The formula is (time-code * 1000ms) + 2000ms - (16 * time sync / 1000) in GPS milliseconds then converted to UTC time. See the UTD 206-024 Rev A document.</p> <p>Time may be delayed by up to 10 ms due to FSW polling delay.</p> <p>Maximum time is ~2150 UTC and minimum time is ~1970 UTC.</p>	milliseconds	Epoch
ICON_L1_IVM_A_NORTH_FOOTPOINT_ALT	<p>Altitude of North Footpoint of Geomagnetic Line at 150 km from IGRF</p> <p>Altitude location of the magnetic footpoint in the Northern Hemisphere at 150 km. These data were interpolated using a tricubic algorithm from IGRF and ephemeris data then linearly interpolated to IVM times.</p>	km	Epoch
ICON_L1_IVM_A_NORTH_FOOTPOINT_LAT	<p>Latitude of North Footpoint of Geomagnetic Line at 150 km from IGRF</p> <p>Latitude location of the magnetic footpoint in the Northern Hemisphere at 150 km. These data were interpolated using a tricubic algorithm from IGRF and ephemeris data then linearly interpolated to IVM times.</p>	degrees	Epoch
ICON_L1_IVM_A_NORTH_FOOTPOINT_LON	<p>Longitude of North Footpoint of Geomagnetic Line at 150 km from IGRF</p> <p>Longitude location of the magnetic footpoint in the Northern Hemisphere at 150 km. These data were interpolated using a tricubic algorithm from IGRF and ephemeris data then linearly interpolated to IVM times.</p>	degrees	Epoch
ICON_L1_IVM_A_NORTH_FOOTPOINT_FA_ECEF_X	<p>ECEF X-Component of Field Aligned Drift Direction at Northern Footpoint</p> <p>At the northern footpoint this is the x-component of the unit vector for field aligned ion drifts expressed in the ECEF frame.</p>	dimensionless	Epoch
ICON_L1_IVM_A_NORTH_FOOTPOINT_FA_ECEF_Y	<p>ECEF Y-Component of Field Aligned Drift Direction at Northern Footpoint</p> <p>At the northern footpoint this is the y-component of the unit vector for field aligned ion drifts expressed in the ECEF frame.</p>	dimensionless	Epoch
ICON_L1_IVM_A_NORTH_FOOTPOINT_FA_ECEF_Z	<p>ECEF Z-Component of Field Aligned Drift Direction at Northern Footpoint</p> <p>At the northern footpoint this is the z-component of the unit vector for field aligned ion drifts expressed in the ECEF frame.</p>	dimensionless	Epoch

Variable Name	Description	Units	Dimensions
ICON_L1_IVM_A_NORTH _FOOTPOINT_MER_DRIFT	Translating Scalars of Meridional Ion Drifts at Northern Footpoint Scalars for translating meridional ion drifts (zonal E fields) measured at the spacecraft down to the northern footpoint.	dimensionless	Epoch
ICON_L1_IVM_A_NORTH _FOOTPOINT_ZON_DRIFT	Translating Scalars of Zonal Ion Drifts at Northern Footpoint Scalars for translating zonal ion drifts (meridional E fields) measured at the spacecraft down to the northern footpoint.	dimensionless	Epoch
ICON_L1_IVM_A_NORTH _FOOTPOINT_QD_LAT	Quasi-dipole Latitude of Northern Footpoint Calculated value of quasi-dipole latitude of northern footpoint from IGRF.	degrees	Epoch
ICON_L1_IVM_A_NORTH _FOOTPOINT_QD_LON	Quasi-dipole Longitude of Northern Footpoint Calculated value of quasi-dipole longitude of northern footpoint from IGRF	degrees	Epoch
ICON_L1_IVM_A_NORTH _FOOTPOINT_MER_ECEF_X	ECEF X-Component of Meridional Drift Direction at Northern Footpoint At the northern footpoint this is the x-component of the unit vector for meridional ion drifts expressed in the ECEF frame.	dimensionless	Epoch
ICON_L1_IVM_A_NORTH _FOOTPOINT_MER_ECEF_Y	ECEF Y-Component of Meridional Drift Direction at Northern Footpoint At the northern footpoint this is the y-component of the unit vector for meridional ion drifts expressed in the ECEF frame.	dimensionless	Epoch
ICON_L1_IVM_A_NORTH _FOOTPOINT_MER_ECEF_Z	ECEF Z-Component of Meridional Drift Direction at Northern Footpoint At the northern footpoint this is the z-component of the unit vector for meridional ion drifts expressed in the ECEF frame.	dimensionless	Epoch
ICON_L1_IVM_A_NORTH _FOOTPOINT_ZON_ECEF_X	ECEF X-Component of Zonal Drift Direction at Northern Footpoint At the northern footpoint this is the x-component of the unit vector for zonal ion drifts expressed in the ECEF frame.	dimensionless	Epoch
ICON_L1_IVM_A_NORTH _FOOTPOINT_ZON_ECEF_Y	ECEF Y-Component of Zonal Drift Direction at Northern Footpoint At the northern footpoint this is the y-component of the unit vector for zonal ion drifts expressed in the ECEF frame.	dimensionless	Epoch
ICON_L1_IVM_A_NORTH _FOOTPOINT_ZON_ECEF_Z	ECEF Z-Component of Zonal Drift Direction at Northern Footpoint At the northern footpoint this is the z-component of the unit vector for zonal ion drifts expressed in the ECEF frame.	dimensionless	Epoch

Variable Name	Description	Units	Dimensions
ICON_L1_IVM_A_SOUTH _FOOTPOINT_ALT	Altitude of South Footpoint of Geomagnetic Line at 150 km from IGRF Altitude location of the magnetic footpoint in the Northern Hemisphere at 150 km. These data were interpolated using a tricubic algorithm from IGRF and ephemeris data then linearly interplotted to IVM times.	km	Epoch
ICON_L1_IVM_A_SOUTH _FOOTPOINT_LAT	Latitude of South Footpoint of Geomagnetic Line at 150 km from IGRF Latitude location of the magnetic footpoint in the Southern Hemisphere at 150 km. These data were interpolated using a tricubic algorithm from IGRF and ephemeris data then linearly interplotted to IVM times.	degrees	Epoch
ICON_L1_IVM_A_SOUTH _FOOTPOINT_LON	Longitude of South Footpoint of Geomagnetic Line at 150 km from IGRF Longitude location of the magnetic footpoint in the Southern Hemisphere at 150 km. These data were interpolated using a tricubic algorithm from IGRF and ephemeris data then linearly interplotted to IVM times.	degrees	Epoch
ICON_L1_IVM_A_SOUTH _FOOTPOINT_FA_ECEF_X	ECEF X-Component of Field Aligned Drift Direction at Southern Footpoint At the Southern footpoint this is the x-component of the unit vector for field aligned ion drifts expressed in the ECEF frame.	dimensionless	Epoch
ICON_L1_IVM_A_SOUTH _FOOTPOINT_FA_ECEF_Y	ECEF Y-Component of Field Aligned Drift Direction at Southern Footpoint At the Southern footpoint this is the y-component of the unit vector for field aligned ion drifts expressed in the ECEF frame.	dimensionless	Epoch
ICON_L1_IVM_A_SOUTH _FOOTPOINT_FA_ECEF_Z	ECEF Z-Component of Field Aligned Drift Direction at Southern Footpoint At the Southern footpoint this is the z-component of the unit vector for field aligned ion drifts expressed in the ECEF frame.	dimensionless	Epoch
ICON_L1_IVM_A_SOUTH _FOOTPOINT_MER_DRIFT	Translating Scalars of Meridional Ion Drifts at Southern Footpoint Scalars for translating meridional ion drifts (zonal E fields) measured at the spacecraft down to the southern footpoint.	dimensionless	Epoch
ICON_L1_IVM_A_SOUTH _FOOTPOINT_ZON_DRIFT	Translating Scalars of Zonal Ion Drifts at Southern Footpoint Scalars for translating zonal ion drifts (meridional E fields) measured at the spacecraft down to the southern footpoint.	dimensionless	Epoch
ICON_L1_IVM_A_SOUTH _FOOTPOINT_QD_LAT	Quasi-dipole Latitude of Southern Footpoint Calculated value of quasi-dipole latitude of southern footpoint from IGRF	degrees	Epoch

Variable Name	Description	Units	Dimensions
ICON_L1_IVM_A_SOUTH _FOOTPOINT_QD_LON	Quasi-dipole Longitude of Southern Footpoint Calculated value of quasi-dipole longitude of southern footpoint from IGRF	degrees	Epoch
ICON_L1_IVM_A_SOUTH _FOOTPOINT_MER_ECEF _X	ECEF X-Component of Meridional Drift Direction at Southern Footpoint At the Southern footpoint this is the x-component of the unit vector for meridional ion drifts expressed in the ECEF frame.	dimensionless	Epoch
ICON_L1_IVM_A_SOUTH _FOOTPOINT_MER_ECEF _Y	ECEF Y-Component of Meridional Drift Direction at Southern Footpoint At the Southern footpoint this is the y-component of the unit vector for meridional ion drifts expressed in the ECEF frame.	dimensionless	Epoch
ICON_L1_IVM_A_SOUTH _FOOTPOINT_MER_ECEF _Z	ECEF Z-Component of Meridional Drift Direction at Southern Footpoint At the Southern footpoint this is the z-component of the unit vector for meridional ion drifts expressed in the ECEF frame.	dimensionless	Epoch
ICON_L1_IVM_A_SOUTH _FOOTPOINT_ZON_ECEF _X	ECEF X-Component of Zonal Drift Direction at Southern Footpoint At the Southern footpoint this is the x-component of the unit vector for zonal ion drifts expressed in the ECEF frame.	dimensionless	Epoch
ICON_L1_IVM_A_SOUTH _FOOTPOINT_ZON_ECEF _Y	ECEF Y-Component of Zonal Drift Direction at Southern Footpoint At the Southern footpoint this is the y-component of the unit vector for zonal ion drifts expressed in the ECEF frame.	dimensionless	Epoch
ICON_L1_IVM_A_SOUTH _FOOTPOINT_ZON_ECEF _Z	ECEF Z-Component of Zonal Drift Direction at Southern Footpoint At the Southern footpoint this is the z-component of the unit vector for zonal ion drifts expressed in the ECEF frame.	dimensionless	Epoch
ICON_L1_IVM_A_SC_B_ X	X Component of the Magnetic Field at the Spacecraft X-component of the magnetic field from IGRF at the spacecraft position, expressed in the ECEF frame.	nT	Epoch
ICON_L1_IVM_A_SC_B_ Y	Y Component of the Magnetic Field at the Spacecraft Y-component of the magnetic field from IGRF at the spacecraft position, expressed in the ECEF frame.	nT	Epoch
ICON_L1_IVM_A_SC_B_ Z	Z Component of the Magnetic Field at the Spacecraft Z-component of the magnetic field from IGRF at the spacecraft position, expressed in the ECEF frame.	nT	Epoch
ICON_L1_IVM_A_APEX_ HEIGHT	Modified APEX Height Modified APEX height of the spacecraft position.	km	Epoch

Variable Name	Description	Units	Dimensions
ICON_L1_IVM_A_EQU_MER_DRIFT	<p>Translating Scalars of Meridional Ion Drifts at Equator</p> <p>Scalars for translating meridional ion drifts (zonal E fields) measured at the spacecraft down to the magnetic equator.</p>	dimensionless	Epoch
ICON_L1_IVM_A_EQU_ZON_DRIFT	<p>Translating Scalars of Zonal Ion Drifts at Equator</p> <p>Scalars for translating zonal ion drifts (meridional E fields) measured at the spacecraft down to the magnetic equator.</p>	dimensionless	Epoch
ICON_L1_IVM_A_TIME_GPS	<p>Milliseconds since 1980-01-06 00:00:00 TAI (coincident with UTC) at middle of reading.</p> <p>Milliseconds since 1980-01-06 00:00:00 TAI (coincident with UTC) at middle of reading.</p> <p>Time is generated from the time-code at byte 1015 of the IVM packet minus the time sync at byte 1019 of the IVM packet. This is the GPS time at the start of the integration period. The integration period is assumed to be 4 seconds so the center time is 2 seconds after that. The formula is (time-code * 1000ms) + 2000ms - (16 * time sync / 1000) in GPS milliseconds then converted to UTC time. See the UTD 206-024 Rev A document.</p> <p>Time may be delayed by up to 10 ms due to FSW polling delay.</p> <p>Maximum time is ~2150 UTC and minimum time is ~1970 UTC.</p>	milliseconds	Epoch
ICON_L1_IVM_A_DM_ANGLE_0	<p>DM determined angle along axis 0</p> <p>The Drift Meter (DM) has an entrance aperture that projects an O+ ion beam onto a collector plate divided into 4 equal sections. The angle of the beam determines the beam location, and thus the amount of current recorded by each collector plate. The ratio of currents is recorded on-orbit by the DM. The value of this angle can be reconstructed using the measured ratio of currents. The angle reported here is reconstructed using current ratios measured on-orbit and downsampled onto 1-Hz cadence.</p>	degrees	Epoch
ICON_L1_IVM_A_DM_ANGLE_1	<p>DM determined angle along axis 1</p> <p>The Drift Meter (DM) has an entrance aperture that projects an O+ ion beam onto a collector plate divided into 4 equal sections. The angle of the beam determines the beam location, and thus the amount of current recorded by each collector plate. The ratio of currents is recorded on-orbit by the DM. The value of this angle can be reconstructed using the measured ratio of currents. The angle reported here is reconstructed using current ratios measured on-orbit and downsampled onto 1-Hz cadence.</p>	degrees	Epoch
ICON_L1_IVM_A_DM_RATIO_0	<p>DM measured ratio along axis 0</p>	degrees	Epoch
ICON_L1_IVM_A_DM_RATIO_1	<p>DM measured ratio along axis 1</p>	degrees	Epoch

Variable Name	Description	Units	Dimensions
ICON_L1_IVM_A_LL_ANGLE_0	LL determined angle along axis 0 The Drift Meter (DM) has an entrance aperture that projects an O+ ion beam onto a collector plate divided into 4 equal sections. The angle of the beam determines the beam location, and thus the amount of current recorded by each collector plate. The ratio of collector plate currents is generated using the individual current levels recorded by the log level monitor. The angle reported here is generated using the log level current ratios. Generally speaking, the dm_ratios area a better source.	degrees	Epoch
ICON_L1_IVM_A_LL_ANGLE_1	LL determined angle along axis 0 The Drift Meter (DM) has an entrance aperture that projects an O+ ion beam onto a collector plate divided into 4 equal sections. The angle of the beam determines the beam location, and thus the amount of current recorded by each collector plate. The ratio of collector plate currents is generated using the individual current levels recorded by the log level monitor. The angle reported here is generated using the log level current ratios. Generally speaking, the dm_ratios area a better source.	degrees	Epoch
ICON_L1_IVM_A_LL_RATIO_0	Log level measured ratio along axis 0	degrees	Epoch
ICON_L1_IVM_A_LL_RATIO_1	Log level measured ratio along axis 1	degrees	Epoch
ICON_L1_IVM_A_LLA_MEDIAN_0	Log level A median ratio along axis 0 The log levels are used as an internal monitor of instrument performance. This is the median value of LLA over a packet.	A	Epoch
ICON_L1_IVM_A_LLA_MEDIAN_1	Log level A median ratio along axis 1 The log levels are used as an internal monitor of instrument performance. This is the median value of LLA over a packet.	A	Epoch
ICON_L1_IVM_A_LL_B_MEDIAN_0	Log level B median current level along axis 0 The log levels are used as an internal monitor of instrument performance. This is the median value of LLB over a packet.	A	Epoch
ICON_L1_IVM_A_LL_B_MEDIAN_1	Log level B median current level along axis 1 The log levels are used as an internal monitor of instrument performance. This is the median value of LLB over a packet.	A	Epoch
ICON_L1_IVM_A_RATIO_0	DM measured ratio along axis 0	degrees	Epoch
ICON_L1_IVM_A_RATIO_1	DM measured ratio along axis 1	degrees	Epoch

Variable Name	Description	Units	Dimensions
ICON_L1_IVM_A_ORIG_ANGLE_0	DM determined angle along axis 0 The Drift Meter (DM) has an entrance aperture that projects an O+ ion beam onto a collector plate divided into 4 equal sections. The angle of the beam determines the beam location, and thus the amount of current recorded by each collector plate. The ratio of currents is recorded on-orbit by the DM. The value of this angle can be reconstructed using the measured ratio of currents. The angle reported here is reconstructed using current ratios measured on-orbit and downsampled onto 1-Hz cadence.	degrees	Epoch
ICON_L1_IVM_A_ORIG_ANGLE_1	DM determined angle along axis 1 The Drift Meter (DM) has an entrance aperture that projects an O+ ion beam onto a collector plate divided into 4 equal sections. The angle of the beam determines the beam location, and thus the amount of current recorded by each collector plate. The ratio of currents is recorded on-orbit by the DM. The value of this angle can be reconstructed using the measured ratio of currents. The angle reported here is reconstructed using current ratios measured on-orbit and downsampled onto 1-Hz cadence.	degrees	Epoch
ICON_L1_IVM_A_ORIG_RATIO_0	DM measured ratio along axis 0	degrees	Epoch
ICON_L1_IVM_A_ORIG_RATIO_1	DM measured ratio along axis 1	degrees	Epoch
ICON_L1_IVM_A_DM_CURRENT_POSITIVE_0	Currents to plate pair along positive axis direction.		Epoch
ICON_L1_IVM_A_DM_CURRENT_NEGATIVE_0	Currents to plate pair along negative axis direction.		Epoch
ICON_L1_IVM_A_DM_CURRENT_POSITIVE_1	Currents to plate pair along positive axis direction.		Epoch
ICON_L1_IVM_A_DM_CURRENT_NEGATIVE_1	Currents to plate pair along negative axis direction.		Epoch
ICON_L1_IVM_A_ORIG_DM_CURRENT_POSITIVE_0	Currents to plate pair along positive axis direction.		Epoch
ICON_L1_IVM_A_ORIG_DM_CURRENT_NEGATIVE_0	Currents to plate pair along negative axis direction.		Epoch
ICON_L1_IVM_A_ORIG_DM_CURRENT_POSITIVE_1	Currents to plate pair along positive axis direction.		Epoch
ICON_L1_IVM_A_ORIG_DM_CURRENT_NEGATIVE_1	Currents to plate pair along negative axis direction.		Epoch

Variable Name	Description	Units	Dimensions
ICON_L1_IVM_A_DM_GRID_PHOTO_FLAG	Indicator for presence of illumination. 1 - area illuminated, 0 - no illumination. There are multiple indicators with a consistent naming scheme. inst_surface, where inst is dm or rpa, and the surface is either an internal grid or the instrument collector plate.		Epoch
ICON_L1_IVM_A_DM_COLLECTION_PHOTO_FLAG	Indicator for presence of illumination. 1 - area illuminated, 0 - no illumination. There are multiple indicators with a consistent naming scheme. inst_surface, where inst is dm or rpa, and the surface is either an internal grid or the instrument collector plate.		Epoch
ICON_L1_IVM_A_RPA_GRID_PHOTO_FLAG	Indicator for presence of illumination. 1 - area illuminated, 0 - no illumination. There are multiple indicators with a consistent naming scheme. inst_surface, where inst is dm or rpa, and the surface is either an internal grid or the instrument collector plate.		Epoch
ICON_L1_IVM_A_RPA_COLLECTION_PHOTO_FLAG	Indicator for presence of illumination. 1 - area illuminated, 0 - no illumination. There are multiple indicators with a consistent naming scheme. inst_surface, where inst is dm or rpa, and the surface is either an internal grid or the instrument collector plate.		Epoch
ICON_L1_IVM_A_RPA_RING_PHOTO_FLAG	Flag for when the ring on the edge of collector is illuminated. 0 - not illuminated. 1 - illuminated.	A	Epoch
ICON_L1_IVM_A_RPA_GRID_RING_PHOTO_FLAG	Flag for when the ring holder on the edge of a grid is illuminated. 0 - not illuminated. 1 - illuminated.	A	Epoch
ICON_L1_IVM_A_PHOTO_DM_GRID_AREA_0_POSITIVE	Fractional illuminated area along collector plate axis. Positive (negative) refers to collector half along positive (negative) axis direction.		Epoch
ICON_L1_IVM_A_PHOTO_DM_GRID_AREA_0_NEGATIVE	Fractional illuminated area along collector plate axis. Positive (negative) refers to collector half along positive (negative) axis direction.		Epoch
ICON_L1_IVM_A_PHOTO_DM_GRID_AREA_1_POSITIVE	Fractional illuminated area along collector plate axis. Positive (negative) refers to collector half along positive (negative) axis direction.		Epoch
ICON_L1_IVM_A_PHOTO_DM_GRID_AREA_1_NEGATIVE	Fractional illuminated area along collector plate axis. Positive (negative) refers to collector half along positive (negative) axis direction.		Epoch

Variable Name	Description	Units	Dimensions
ICON_L1_IVM_A_PHOTO_DM_GRID_CURRENT_0_POSITIVE	Photoemission estimated to be present on collector plate pair along axis (0,1). Positive (negative) refers to collector half along positive (negative) axis direction. Estimate obtained by scaling the observed negative currents at high RV in the RPA, illuminated areas, as well as the ratio of illuminated DM and RPA areas.	A	Epoch
ICON_L1_IVM_A_PHOTO_DM_GRID_CURRENT_0_NEGATIVE	Photoemission estimated to be present on collector plate pair along axis (0,1). Positive (negative) refers to collector half along positive (negative) axis direction. Estimate obtained by scaling the observed negative currents at high RV in the RPA, illuminated areas, as well as the ratio of illuminated DM and RPA areas.	A	Epoch
ICON_L1_IVM_A_PHOTO_DM_GRID_CURRENT_1_POSITIVE	Photoemission estimated to be present on collector plate pair along axis (0,1). Positive (negative) refers to collector half along positive (negative) axis direction. Estimate obtained by scaling the observed negative currents at high RV in the RPA, illuminated areas, as well as the ratio of illuminated DM and RPA areas.	A	Epoch
ICON_L1_IVM_A_PHOTO_DM_GRID_CURRENT_1_NEGATIVE	Photoemission estimated to be present on collector plate pair along axis (0,1). Positive (negative) refers to collector half along positive (negative) axis direction. Estimate obtained by scaling the observed negative currents at high RV in the RPA, illuminated areas, as well as the ratio of illuminated DM and RPA areas.	A	Epoch
ICON_L1_IVM_A_PHOTO_DM_ANLY_GRID_CURRENT_0_POSITIVE	Photoemission estimated to be present on collector plate pair along axis (0,1). Positive (negative) refers to collector half along positive (negative) axis direction. Estimate obtained by a simple first-order analytic model that uses the calculated illuminated DM areas, as well as the solar incidence angles.	A	Epoch
ICON_L1_IVM_A_PHOTO_DM_ANLY_GRID_CURRENT_0_NEGATIVE	Photoemission estimated to be present on collector plate pair along axis (0,1). Positive (negative) refers to collector half along positive (negative) axis direction. Estimate obtained by a simple first-order analytic model that uses the calculated illuminated DM areas, as well as the solar incidence angles.	A	Epoch
ICON_L1_IVM_A_PHOTO_DM_ANLY_GRID_CURRENT_1_POSITIVE	Photoemission estimated to be present on collector plate pair along axis (0,1). Positive (negative) refers to collector half along positive (negative) axis direction. Estimate obtained by a simple first-order analytic model that uses the calculated illuminated DM areas, as well as the solar incidence angles.	A	Epoch

Variable Name	Description	Units	Dimensions
ICON_L1_IVM_A_PHOTO_DM_ANLY_GRID_CURRENT_1_NEGATIVE	Photoemission estimated to be present on collector plate pair along axis (0,1). Positive (negative) refers to collector half along positive (negative) axis direction. Estimate obtained by a simple first-order analytic model that uses the calculated illuminated DM areas, as well as the solar incidence angles.	A	Epoch
ICON_L1_IVM_A_PHOTO_RPA_ANLY_GRID_CURRENT	Photoemission estimated to be present on RPA collector. Estimate obtained by a simple first-order analytic model that uses the calculated illuminated RPA areas, as well as the solar incidence angles.	A	Epoch
ICON_L1_IVM_A_PHOTO_SCALAR	Scalar maps the most negative of the modeled photoemission currents to the same current value measured by the RPA at high RV at the same time.		Epoch
ICON_L1_IVM_A_PHOTO_FLAG_Y	0 - no difference, 1 - small correction, 2 - medium correction, 3 - large correction		Epoch
ICON_L1_IVM_A_PHOTO_FLAG_Z	0 - no difference, 1 - small correction, 2 - medium correction, 3 - large correction		Epoch
ICON_L1_IVM_A_DM_GRID_ILLUMINATED_AREA	The net illuminated area that is incident upon all quadrants within the DM.	m ²	Epoch
ICON_L1_IVM_A_RPA_GRID_ILLUMINATED_AREA	The total illuminated area based upon projecting illumination from the aperture and accounting for the fact that portions of the projected aperture will travel off the projected surface, reducing the illuminated area.	m ²	Epoch
ICON_L1_IVM_A_DM_COLL_ILLUMINATED_AREA	The net illuminated area that is incident upon all quadrants within the DM.	m ²	Epoch
ICON_L1_IVM_A_RPA_COLL_ILLUMINATED_AREA	The total illuminated area based upon projecting illumination from the aperture and accounting for the fact that portions of the projected aperture will travel off the projected surface, reducing the illuminated area.	m ²	Epoch
ICON_L1_IVM_A_PHOTO_DM_RPA_RATIO	Ratio of the illuminated DM and RPA grid areas.		Epoch
ICON_L1_IVM_A_RPA_OFFSET_CURRENT	RPA negative current at maximum RV	A	Epoch
ICON_L1_IVM_A_PHOTO_DM_COLL_CURRENT_0_POSITIVE	Net photoemission estimated on each pair of DM collector plates due to inter-plate electrons, along with currents from lost electrons. The IVM axis is denoted by 0 or 1, and the plate pair along the positive or negative directions is also indicated. 0_positive is comprised of TR and TL currents.	A	Epoch

Variable Name	Description	Units	Dimensions
ICON_L1_IVM_A_PHOTO_DM_COLL_CURRENT_0_NEGATIVE	Net photoemission estimated on each pair of DM collector plates due to inter-plate electrons, along with currents from lost electrons. The IVM axis is denoted by 0 or 1, and the plate pair along the positive or negative directions is also indicated. 0_positive is comprised of TR and TL currents.	A	Epoch
ICON_L1_IVM_A_PHOTO_DM_COLL_CURRENT_1_POSITIVE	Net photoemission estimated on each pair of DM collector plates due to inter-plate electrons, along with currents from lost electrons. The IVM axis is denoted by 0 or 1, and the plate pair along the positive or negative directions is also indicated. 0_positive is comprised of TR and TL currents.	A	Epoch
ICON_L1_IVM_A_PHOTO_DM_COLL_CURRENT_1_NEGATIVE	Net photoemission estimated on each pair of DM collector plates due to inter-plate electrons, along with currents from lost electrons. The IVM axis is denoted by 0 or 1, and the plate pair along the positive or negative directions is also indicated. 0_positive is comprised of TR and TL currents.	A	Epoch
ICON_L1_IVM_A_SUN_TOTAX_ANGLE	Net solar incidence angle with respect to the IVM-X (boresight) axis, positive from IVM towards space	degrees	Epoch
ICON_L1_IVM_A_LOW_LOG_LEVEL_CURRENTS_0	When flag is 1, currents in the DM are too low for the measurement hardware to function. Currents in the DM are measured using log amps.		Epoch
ICON_L1_IVM_A_LOW_LOG_LEVEL_CURRENTS_1	When flag is 1, currents in the DM are too low for the measurement hardware to function. Currents in the DM are measured using log amps.		Epoch
ICON_L1_IVM_A_LOG_LEVEL_RPA_MISMATCH	When flag is 1, currents in the DM are too low for the measurement hardware to function. Currents in the DM are measured using log amps.		Epoch
ICON_L1_IVM_A_RPA_OPPLUS_CURRENT	RPA current closest to RV=3 Volts	A	Epoch
ICON_L1_IVM_A_DM_RPA_LL_CDP_0	Product of one minus the rolling correlation between RPA opplus current and the sum of the log level currents and the std dev of the DM angle. This serves as a combined measure of DM deviation and RPA/DM correlation. Currents in the DM are measured using log amps.		Epoch

Variable Name	Description	Units	Dimensions
ICON_L1_IVM_A_DM_RPA_LL_CDP_1	<p>Product of one minus the rolling correlation between RPA oplus current and the sum of the log level currents and the std dev of the DM angle. This serves as a combined measure of DM deviation and RPA/DM correlation.</p> <p>Currents in the DM are measured using log amps.</p>		Epoch
ICON_L1_IVM_A_RPA_LL_CORR_0	<p>The rolling correlation between RPA oplus current and the sum of the log level currents</p> <p>Currents in the DM are measured using log amps.</p>		Epoch
ICON_L1_IVM_A_RPA_LL_CORR_1	<p>The rolling correlation between RPA oplus current and the sum of the log level currents</p> <p>Currents in the DM are measured using log amps.</p>		Epoch

Acknowledgement

This is a data product from the NASA Ionospheric Connection Explorer mission, an Explorer launched at 21:59:45 EDT on October 10, 2019. Guidelines for the use of this product are described in the ICON Rules of the Road (<https://icon.ssl.berkeley.edu/Data>)

Responsibility for the mission science falls to the Principal Investigator, Dr. Thomas Immel at UC Berkeley: Immel, T.J., England, S.L., Mende, S.B. et al. Space Sci Rev (2018) 214: 13. <https://doi.org/10.1007/s11214-017-0449-2>

Responsibility for the validation of the L1 data products falls to the instrument lead investigators/scientists.

- * EUV: Dr. Eric Korpela : <https://doi.org/10.1007/s11214-017-0384-2>
- * FUV: Dr. Harald Frey : <https://doi.org/10.1007/s11214-017-0386-0>
- * MIGHTI: Dr. Christoph Englert : <https://doi.org/10.1007/s11214-017-0358-4>, and <https://doi.org/10.1007/s11214-017-0374-4>
- * IVM: Dr. Roderick Heelis : <https://doi.org/10.1007/s11214-017-0383-3>

Responsibility for the validation of the L2 data products falls to those scientists responsible for those products.

- * Daytime O and N2 profiles: Dr. Andrew Stephan : <https://doi.org/10.1007/s11214-018-0477-6>
- * Daytime (EUV) O+ profiles: Dr. Andrew Stephan : <https://doi.org/10.1007/s11214-017-0385-1>
- * Nighttime (FUV) O+ profiles: Dr. Farzad Kamalabadi : <https://doi.org/10.1007/s11214-018-0502-9>
- * Neutral Wind profiles: Dr. Jonathan Makela : <https://doi.org/10.1007/s11214-017-0359-3>
- * Neutral Temperature profiles: Dr. Christoph Englert : <https://doi.org/10.1007/s11214-017-0434-9>
- * Ion Velocity Measurements : Dr. Russell Stoneback : <https://doi.org/10.1007/s11214-017-0383-3>

Responsibility for Level 4 products falls to those scientists responsible for those products.

- * Hough Modes : Dr. Chihoko Yamashita : <https://doi.org/10.1007/s11214-017-0401-5>
- * TIEGCM : Dr. Astrid Maute : <https://doi.org/10.1007/s11214-017-0330-3>
- * SAMI3 : Dr. Joseph Huba : <https://doi.org/10.1007/s11214-017-0415-z>

Pre-production versions of all above papers are available on the ICON website. <http://icon.ssl.berkeley.edu/Publications>

Overall validation of the products is overseen by the ICON Project Scientist, Dr. Scott England.

NASA oversight for all products is provided by the Mission Scientist, Dr. Jeffrey Klenzing.

Users of these data should contact and acknowledge the Principal Investigator Dr. Immel and the party directly responsible for the data product (noted above) and acknowledge NASA funding for the collection of the data used in the research with the following statement : "ICON is supported by NASA's Explorers Program through contracts NNG12FA45C and NNG12FA42I"

These data are openly available as described in the ICON Data Management Plan available on the ICON website (<http://icon.ssl.berkeley.edu/Data>).

This document was automatically generated on 2022-05-19 08:05 using the file:

ICON_L1_IVM-A_2021-09-30_v06r000.NC

Software version: ICON_SDC > IVM L1 Generator v0.17.0

ICON Data Product 0P: IVM Ancillary Products

This document describes the data product for Ancillary Products for IVM Data Processing, which is in NetCDF4 format.

The IVM ancillary data file contains information on the ICON observatory as well as IVM specific information. This includes the pointing, position, and velocity of the ICON observatory. It also includes information on the status of the observatory such as maneuvers, being in or out of the Earth's shadow, and calibrations. Pertinent information for the IVM instrument is included such as unit vectors and magnetic footpoint parameters. These files are combined with the IVM Level 1 data to produce Level 2 data. ECEF is Earth-centered, Earth-fixed reference frame. ECI is Earth-centered inertial reference frame. We use the J2000 ECI frame. LVLH is local-vertical, local-horizontal. We have two LVLH modes: normal and reverse. LVLH Normal is when the spacecraft is looking north with latitude tangent locations between ~12 S and ~42 N. LVLH Reverse is when the spacecraft is looking south with latitude tangent locations between ~42 S and ~12 N.

History

Version 02, Created by IVM Ancillary Processor v2.0.4 on Thu, 08 Oct 2020, 2020-10-08T16:09:19.000 UTC

Dimensions

NetCDF files contain **variables** and the **dimensions** over which those variables are defined. First, the dimensions are defined, then all variables in the file are described.

The dimensions used by the variables in this file are given below, along with nominal sizes. Note that the size may vary from file to file. For example, the "Epoch" dimension, which describes the number of time samples contained in this file, will have a varying size.

Dimension Name	Nominal Size
EPOCH	21600
VECTORS	3

Variables

Variables in this file are listed below. First, "data" variables are described, followed by the "support_data" variables, and finally the "metadata" variables. The variables classified as "ignore_data" are not shown.

support_data

Variable Name	Description	Units	Dimensions
Epoch	<p>Milliseconds since 1970-01-01 00:00:00 UTC at middle of measurement integration.</p> <p>Number of milliseconds since 1970-01-01 00:00:00 UTC at the middle of the measurement integration. Taken from LOP IVM data file.</p>	milliseconds	EPOCH
ICON Ancillary IVM Time GPS	<p>Milliseconds since 1980-01-06 00:00:00 TAI (coincident with UTC) at middle of reading.</p> <p>Number of milliseconds since 1980-01-06 00:00:00 TAI at the middle of the measurement integration.</p>	milliseconds	EPOCH
ICON Ancillary IVM Time UTC	<p>ISO 8601 formatted UTC timestamp (at middle of reading).</p> <p>ISO 8601 formatted UTC timestamp (at middle of reading). E.g., 2017-05-27 00:00:00.380Z</p>	string	EPOCH
ICON Ancillary IVM SC Position ECEF	<p>ECEF Spacecraft Position</p> <p>Position of spacecraft in ECEF coordinates.</p>	km	EPOCH, VECTORS
ICON Ancillary IVM SC Velocity ECEF	<p>ECEF Spacecraft Velocity</p> <p>Velocity of spacecraft in ECEF coordinates.</p>	m/s	EPOCH, VECTORS
ICON Ancillary IVM SC Position ECI	<p>ECI Spacecraft Position</p> <p>Position of spacecraft in ECI, J2000, coordinates.</p>	km	EPOCH, VECTORS
ICON Ancillary IVM SC Velocity ECI	<p>ECI Spacecraft Velocity</p> <p>Velocity of spacecraft in ECI, J2000, coordinates.</p>	m/s	EPOCH, VECTORS
ICON Ancillary IVM Latitude	<p>WGS84 Latitude of Spacecraft Position (geodetic)</p> <p>Geodetic latitude of spacecraft in WGS84</p>	degrees North	EPOCH
ICON Ancillary IVM Longitude	<p>WGS84 Longitude of Spacecraft Position (geodetic)</p> <p>Geodetic longitude of spacecraft in WGS84</p>	degrees East	EPOCH
ICON Ancillary IVM Altitude	<p>WGS84 Altitude of Spacecraft Position (geodetic)</p> <p>Geodetic Altitude of Spacecraft in WGS84.</p>	km	EPOCH
ICON Ancillary IVM VNorth	<p>North Velocity of Spacecraft</p> <p>North component of the spacecraft velocity vector derived from WGS84.</p>	m/s	EPOCH

Variable Name	Description	Units	Dimensions
ICON Ancillary_IVM_VEAST	East Velocity of Spacecraft East component of the spacecraft velocity vector derived from WGS84.	m/s	EPOCH
ICON Ancillary_IVM_VDOWN	Down (Perpendicular to Local Earth Surface) Velocity of Spacecraft Down component of the spacecraft velocity vector derived from WGS84.	m/s	EPOCH
ICON Ancillary_IVM_MAGNETIC_LATITUDE	Magnetic Latitude of Spacecraft Position Quasi-dipole magnetic latitude of the spacecraft position. These values are obtained from passing the geodetic latitudes, longitudes, and altitudes from ICON Ancillary_IVM_LATITUDE, ICON Ancillary_IVM_LONGITUDE, and ICON Ancillary_IVM_ALTITUDE into apexpy Python module. For details on apexpy see: https://apexpy.readthedocs.org/	degrees North	EPOCH
ICON Ancillary_IVM_MAGNETIC_LONGITUDE	Magnetic Longitude of Spacecraft Position Quasi-dipole magnetic longitude of the spacecraft position. These values are obtained from passing the geodetic latitudes, longitudes, and altitudes from ICON Ancillary_IVM_LATITUDE, ICON Ancillary_IVM_LONGITUDE, and ICON Ancillary_IVM_ALTITUDE into apexpy Python module. For details on apexpy see: https://apexpy.readthedocs.org/	degrees East	EPOCH
ICON Ancillary_IVM_SZA	Solar Zenith Angle at Spacecraft Solar Zenith Angle at the spacecraft.	degrees	EPOCH
ICON Ancillary_IVM_LST	Local Solar Time at Spacecraft Local Solar Time at spacecraft.	hour	EPOCH
ICON Ancillary_IVM_SC_XHAT_ECEF	Spacecraft X Unit Vector in ECEF (Ram Direction) Spacecraft x-axis (nominal Ram direction) unit vector in ECEF.	dimensionless	EPOCH, VECTORS
ICON Ancillary_IVM_SC_YHAT_ECEF	Spacecraft Y Unit Vector in ECEF (Starboard Direction) Spacecraft y-axis (nominal Starboard direction) unit vector in ECEF.	dimensionless	EPOCH, VECTORS
ICON Ancillary_IVM_SC_ZHAT_ECEF	Spacecraft Z Unit Vector in ECEF (Nadir Direction) Spacecraft z-axis (nominal Nadir direction) unit vector in ECEF.	dimensionless	EPOCH, VECTORS
ICON Ancillary_IVM_SC_XHAT_ECI	Spacecraft X unit Vector in ECI (Ram Direction) Spacecraft x-axis (nominal Ram direction) unit vector in ECI, J2000.	dimensionless	EPOCH, VECTORS

Variable Name	Description	Units	Dimensions
ICON_ANCILLARY_IVM_SC_YHAT_ECI	Spacecraft Y Unit Vector in ECI (Starboard Direction) Spacecraft y-axis (nominal Starboard direction) unit vector in ECI, J2000.	dimensionless	EPOCH, VECTORS
ICON_ANCILLARY_IVM_SC_ZHAT_ECI	Spacecraft Z Unit Vector in ECI (Nadir Direction) Spacecraft z-axis (nominal Nadir direction) unit vector in ECI, J2000.	dimensionless	EPOCH, VECTORS
ICON_ANCILLARY_IVM_INSTRUMENT_XHAT_ECEF	Instrument X Unit Vector in ECEF (Ram Direction) IVM x-axis (nominal Ram direction) unit vector in ECEF.	dimensionless	EPOCH, VECTORS
ICON_ANCILLARY_IVM_INSTRUMENT_YHAT_ECEF	Instrument Y Unit Vector in ECEF (Starboard Direction) IVM y-axis (nominal Starboard direction) unit vector in ECEF.	dimensionless	EPOCH, VECTORS
ICON_ANCILLARY_IVM_INSTRUMENT_ZHAT_ECEF	Instrument Z Unit Vector in ECEF (Nadir Direction) IVM z-axis (nominal Nadir direction) unit vector in ECEF.	dimensionless	EPOCH, VECTORS
ICON_ANCILLARY_IVM_INSTRUMENT_XHAT_ECI	Instrument X Unit Vector in ECI (Ram Direction) IVM x-axis (nominal Ram direction) unit vector in ECI, J2000.	dimensionless	EPOCH, VECTORS
ICON_ANCILLARY_IVM_INSTRUMENT_YHAT_ECI	Instrument Y Unit Vector in ECI (Starboard Direction) IVM y-axis (nominal Starboard direction) unit vector in ECI, J2000.	dimensionless	EPOCH, VECTORS
ICON_ANCILLARY_IVM_INSTRUMENT_ZHAT_ECI	Instrument Z Unit Vector in ECI (Nadir Direction) IVM z-axis (nominal Nadir direction) unit vector in ECI, J2000.	dimensionless	EPOCH, VECTORS
ICON_ANCILLARY_IVM_COROTATION	ECI Earth Corotation Velocity Components in IVM Coordinates Component of Earth's corotation velocity vector projected into the IVM instrument axes by taking the dot product of the corotation vector with the instrument's axes and multiplying the Y and Z components by negative 1 (but not the X component by convention).	m/s	EPOCH, VECTORS
ICON_ANCILLARY_IVM_SUN_XY_PLANE_ANGLE	Angle Between Sun and IVM XY Plane Angle between the Sun and IVM instrument XY plane.	degrees	EPOCH
ICON_ANCILLARY_IVM_SUN_XZ_PLANE_ANGLE	Angle Between Sun and IVM XZ Plane Angle between the Sun and IVM instrument XZ plane.	degrees	EPOCH
ICON_ANCILLARY_IVM_MTB_STATUS	Magnetic Torquer Bar Firing Status If the magnetic torquers are active during any part of the measurement, it is recorded as active for whole measurement. Decoded from spacecraft housekeeping file: ICON_LO_Spacecraft_Housekeeping-MTB_2020-01-20_v01r000.CSV	binary	EPOCH

Variable Name	Description	Units	Dimensions
ICON Ancillary_IVM_SUN_STATUS	Spacecraft Sun/Shadow Status Code Data is from predictive ephemeris. 0 = spacecraft in Sun, 1 = spacecraft in Earth Shadow.	binary	EPOCH
ICON Ancillary_IVM_ORBIT_NUMBER	Orbit Number Integer Orbit Number.	integer	EPOCH
ICON Ancillary_IVM_ATTITUDE_STATUS	Slew or Off-Point Status Code Binary Coded Integer where 1: LVLH Normal Mode 2: LVLH Reverse Mode 4: Earth Limb Pointing 8: Inertial Pointing 16: Stellar Pointing 32: Attitude Slew 64: Conjugate Maneuver 128: Nadir Calibration 256: Lunar Calibration 512: Stellar Calibration 1024: Zero Wind Calibration 2048-32768: SPARE	binary	EPOCH
ICON Ancillary_IVM_SPACE_ENVIRONMENT_REGION_STATUS	Space Environment Region Status Standardized for several missions, not all codes are relevant for ICON where 1: Earth Shadow 2: Lunar Shadow 4: Atmospheric Absorption Zone 8: South Atlantic Anomaly 16: Northern Auroral Zone 32: Southern Auroral Zone 64: Periapsis Passage 128: Inner & Outer Radiation Belts 256: Deep Plasma Sphere 512: Foreshock Solar Wind 1024: Solar Wind Beam 2048: High Magnetic Field 4096: Average Plasma Sheet 8192: Bowshock Crossing 16384: Magnetopause Crossing 32768: Ground Based Observatories 65536: 2-Day Conjunctions 131072: 4-Day Conjunctions 262144: Time Based Conjunctions 524288: Radial Distance Region 1 1048576: Orbit Outbound 2097152: Orbit Inbound 4194304: Lunar Wake 8388608: Magnetotail 16777216: Magnetosheath 33554432: Science 67108864: Low Magnetic Latitude 134217728: Conjugate Observation	binary	EPOCH

Variable Name	Description	Units	Dimensions
ICON_ANCILLARY_IVM_A_STATUS	<p>IVM-A Status</p> <p>Binary Coded Integer where</p> <ul style="list-style-type: none"> 1: Earth Day View 2: Earth Night View 4: Calibration Target View 8: Off-target View 16: Sun Proximity View 32: Moon Proximity View 64: North Magnetic Footpoint View 128: South Magnetic Footpoint View 256: Science Data Collection View 512: Calibration Data Collection View 1024: RAM Proximity View 2048-32768: SPARE <p>Activity is what the spacecraft was commanded to do while status is the spacecraft's natural state of operations. This means that activity should always be used over status if they differ, but will almost always be the same.</p>	binary	EPOCH
ICON_ANCILLARY_IVM_B_STATUS	<p>IVM-B Status</p> <p>Binary Coded Integer where</p> <ul style="list-style-type: none"> 1: Earth Day View 2: Earth Night View 4: Calibration Target View 8: Off-target View 16: Sun Proximity View 32: Moon Proximity View 64: North Magnetic Footpoint View 128: South Magnetic Footpoint View 256: Science Data Collection View 512: Calibration Data Collection View 1024: RAM Proximity View 2048-32768: SPARE <p>Activity is what the spacecraft was commanded to do while status is the spacecraft's natural state of operations. This means that activity should always be used over status if they differ, but will almost always be the same.</p>	binary	EPOCH

Variable Name	Description	Units	Dimensions
ICON_ANCILLARY_IVM_A_ACTIVITY	<p>IVM-A Activity</p> <p>Binary Coded Integer where:</p> <ul style="list-style-type: none"> 1: Earth Day View 2: Earth Night View 4: Calibration Target View 8: Off-target View 16: Sun Proximity View 32: Moon Proximity View 64: North Magnetic Footpoint View 128: South Magnetic Footpoint View 256: Science Data Collection View 512: Calibration Data Collection View 1024: RAM Proximity View 2048-32768: SPARE <p>Activity is what the spacecraft was commanded to do while status is the spacecraft's natural state of operations. This means that activity should always be used over status if they differ, but will almost always be the same.</p>	binary	EPOCH
ICON_ANCILLARY_IVM_B_ACTIVITY	<p>IVM-A Activity</p> <p>Binary Coded Integer where:</p> <ul style="list-style-type: none"> 1: Earth Day View 2: Earth Night View 4: Calibration Target View 8: Off-target View 16: Sun Proximity View 32: Moon Proximity View 64: North Magnetic Footpoint View 128: South Magnetic Footpoint View 256: Science Data Collection View 512: Calibration Data Collection View 1024: RAM Proximity View 2048-32768: SPARE <p>Activity is what the spacecraft was commanded to do while status is the spacecraft's natural state of operations. This means that activity should always be used over status if they differ, but will almost always be the same.</p>	binary	EPOCH
ICON_ANCILLARY_IVM_INSTRUMENT_VELOCITY_ECEF	<p>Spacecraft ECEF Velocity in Instrument Coordinates</p> <p>Component of spacecraft velocity in ECEF projected into IVM instrument axes by taking the dot product of the spacecraft velocity vector and the IVM axes in the ECEF frame.</p>	m/s	EPOCH, VECTORS
ICON_ANCILLARY_IVM_INSTRUMENT_VELOCITY_ECI	<p>Spacecraft ECI Velocity in Instrument Coordinates</p> <p>Component of spacecraft velocity in ECI projected into IVM instrument axes by taking the dot product of the spacecraft velocity vector and the IVM axes in the ECI frame.</p>	m/s	EPOCH, VECTORS
ICON_ANCILLARY_IVM_SC_MLT	<p>Magnetic Local Time at Spacecraft</p> <p>Magnetic Local Time at the spacecraft.</p>	hour	EPOCH

Variable Name	Description	Units	Dimensions
ICON_ANCILLARY_IVM_SC_B_X	X Component of the Magnetic Field at the Spacecraft X-component of the magnetic field from IGRF at the spacecraft position, expressed in the ECEF frame.	nT	EPOCH
ICON_ANCILLARY_IVM_SC_B_Y	Y Component of the Magnetic Field at the Spacecraft Y-component of the magnetic field from IGRF at the spacecraft position, expressed in the ECEF frame.	nT	EPOCH
ICON_ANCILLARY_IVM_SC_B_Z	Z Component of the Magnetic Field at the Spacecraft Z-component of the magnetic field from IGRF at the spacecraft position, expressed in the ECEF frame.	nT	EPOCH
ICON_ANCILLARY_IVM_NORTH_FOOTPOINT_LAT	Latitude of North Footpoint of Geomagnetic Line at 150 km from IGRF Latitude location of the magnetic footpoint in the Northern Hemisphere at 150 km. These data were interpolated using a tricubic algorithm from IGRF and ephemeris data then linearly interplotted to IVM times.	degree s	EPOCH
ICON_ANCILLARY_IVM_NORTH_FOOTPOINT_LON	Longitude of North Footpoint of Geomagnetic Line at 150 km from IGRF Longitude location of the magnetic footpoint in the Northern Hemisphere at 150 km. These data were interpolated using a tricubic algorithm from IGRF and ephemeris data then linearly interplotted to IVM times.	degree s	EPOCH
ICON_ANCILLARY_IVM_NORTH_FOOTPOINT_ALT	Altitude of North Footpoint of Geomagnetic Line at 150 km from IGRF Altitude location of the magnetic footpoint in the Northern Hemisphere at 150 km. These data were interpolated using a tricubic algorithm from IGRF and ephemeris data then linearly interplotted to IVM times.	km	EPOCH
ICON_ANCILLARY_IVM_SOUTH_FOOTPOINT_LAT	Latitude of South Footpoint of Geomagnetic Line at 150 km from IGRF Latitude location of the magnetic footpoint in the Southern Hemisphere at 150 km. These data were interpolated using a tricubic algorithm from IGRF and ephemeris data then linearly interplotted to IVM times.	degree s	EPOCH
ICON_ANCILLARY_IVM_SOUTH_FOOTPOINT_LON	Longitude of South Footpoint of Geomagnetic Line at 150 km from IGRF Longitude location of the magnetic footpoint in the Southern Hemisphere at 150 km. These data were interpolated using a tricubic algorithm from IGRF and ephemeris data then linearly interplotted to IVM times.	degree s	EPOCH

Variable Name	Description	Units	Dimensions
ICON_ANCILLARY_IVM_SOUTH_FOOTPOINT_ALT	Altitude of South Footpoint of Geomagnetic Line at 150 km from IGRF Altitude location of the magnetic footpoint in the Northern Hemisphere at 150 km. These data were interpolated using a tricubic algorithm from IGRF and ephemeris data then linearly interplotted to IVM times.	km	EPOCH
ICON_ANCILLARY_IVM_NORTH_FOOTPOINT_ZON_ECEF_X	ECEF X-Component of Zonal Drift Direcrion at Northern Footpoint At the northern footpoint this is the x-component of the unit vector for zonal ion drifts expressed in the ECEF frame.	dimensi onless	EPOCH
ICON_ANCILLARY_IVM_NORTH_FOOTPOINT_ZON_ECEF_Y	ECEF Y-Component of Zonal Drift Direcrion at Northern Footpoint At the northern footpoint this is the y-component of the unit vector for zonal ion drifts expressed in the ECEF frame.	dimensi onless	EPOCH
ICON_ANCILLARY_IVM_NORTH_FOOTPOINT_ZON_ECEF_Z	ECEF Z-Component of Zonal Drift Direction at Northern Footpoint At the northern footpoint this is the z-component of the unit vector for zonal ion drifts expressed in the ECEF frame.	dimensi onless	EPOCH
ICON_ANCILLARY_IVM_SOUTH_FOOTPOINT_ZON_ECEF_X	ECEF X-Component of Zonal Drift Direction at Southern Footpoint At the Southern footpoint this is the x-component of the unit vector for zonal ion drifts expressed in the ECEF frame.	dimensi onless	EPOCH
ICON_ANCILLARY_IVM_SOUTH_FOOTPOINT_ZON_ECEF_Y	ECEF Y-Component of Zonal Drift Direction at Southern Footpoint At the Southern footpoint this is the y-component of the unit vector for zonal ion drifts expressed in the ECEF frame.	dimensi onless	EPOCH
ICON_ANCILLARY_IVM_SOUTH_FOOTPOINT_ZON_ECEF_Z	ECEF Z-Component of Zonal Drift Direction at Southern Footpoint At the Southern footpoint this is the z-component of the unit vector for zonal ion drifts expressed in the ECEF frame.	dimensi onless	EPOCH
ICON_ANCILLARY_IVM_NORTH_FOOTPOINT_MER_ECEF_X	ECEF X-Component of Meridional Drift Direction at Northern Footpoint At the northern footpoint this is the x-component of the unit vector for meridional ion drifts expressed in the ECEF frame.	dimensi onless	EPOCH
ICON_ANCILLARY_IVM_NORTH_FOOTPOINT_MER_ECEF_Y	ECEF Y-Component of Meridional Drift Direction at Northern Footpoint At the northern footpoint this is the y-component of the unit vector for meridional ion drifts expressed in the ECEF frame.	dimensi onless	EPOCH

Variable Name	Description	Units	Dimensions
ICON_ANCILLARY_IVM_NORTH_FOOTPOINT_MER_ECEF_Z	ECEF Z-Component of Meridional Drift Direction at Northern Footpoint At the northern footpoint this is the z-component of the unit vector for meridional ion drifts expressed in the ECEF frame.	dimensionless	EPOCH
ICON_ANCILLARY_IVM_SOUTH_FOOTPOINT_MER_ECEF_X	ECEF X-Component of Meridional Drift Direction at Southern Footpoint At the Southern footpoint this is the x-component of the unit vector for meridional ion drifts expressed in the ECEF frame.	dimensionless	EPOCH
ICON_ANCILLARY_IVM_SOUTH_FOOTPOINT_MER_ECEF_Y	ECEF Y-Component of Meridional Drift Direction at Southern Footpoint At the Southern footpoint this is the y-component of the unit vector for meridional ion drifts expressed in the ECEF frame.	dimensionless	EPOCH
ICON_ANCILLARY_IVM_SOUTH_FOOTPOINT_MER_ECEF_Z	ECEF Z-Component of Meridional Drift Direction at Southern Footpoint At the Southern footpoint this is the z-component of the unit vector for meridional ion drifts expressed in the ECEF frame.	dimensionless	EPOCH
ICON_ANCILLARY_IVM_NORTH_FOOTPOINT_FA_ECEF_X	ECEF X-Component of Field Aligned Drift Direction at Northern Footpoint At the northern footpoint this is the x-component of the unit vector for field aligned ion drifts expressed in the ECEF frame.	dimensionless	EPOCH
ICON_ANCILLARY_IVM_NORTH_FOOTPOINT_FA_ECEF_Y	ECEF Y-Component of Field Aligned Drift Direction at Northern Footpoint At the northern footpoint this is the y-component of the unit vector for field aligned ion drifts expressed in the ECEF frame.	dimensionless	EPOCH
ICON_ANCILLARY_IVM_NORTH_FOOTPOINT_FA_ECEF_Z	ECEF Z-Component of Field Aligned Drift Direction at Northern Footpoint At the northern footpoint this is the z-component of the unit vector for field aligned ion drifts expressed in the ECEF frame.	dimensionless	EPOCH
ICON_ANCILLARY_IVM_SOUTH_FOOTPOINT_FA_ECEF_X	ECEF X-Component of Field Aligned Drift Direction at Southern Footpoint At the Southern footpoint this is the x-component of the unit vector for field aligned ion drifts expressed in the ECEF frame.	dimensionless	EPOCH
ICON_ANCILLARY_IVM_SOUTH_FOOTPOINT_FA_ECEF_Y	ECEF Y-Component of Field Aligned Drift Direction at Southern Footpoint At the Southern footpoint this is the y-component of the unit vector for field aligned ion drifts expressed in the ECEF frame.	dimensionless	EPOCH
ICON_ANCILLARY_IVM_SOUTH_FOOTPOINT_FA_ECEF_Z	ECEF Z-Component of Field Aligned Drift Direction at Southern Footpoint At the Southern footpoint this is the z-component of the unit vector for field aligned ion drifts expressed in the ECEF frame.	dimensionless	EPOCH

Variable Name	Description	Units	Dimensions
ICON_ANCILLARY_IVM_NORTH_FOOTPOINT_ZON_DRIFT	Translating Scalars of Zonal Ion Drifts at Northern Footpoint Scalars for translating zonal ion drifts (meridional E fields) measured at the spacecraft down to the northern footpoint.	dimensionless	EPOCH
ICON_ANCILLARY_IVM_NORTH_FOOTPOINT_MER_DRIFT	Translating Scalars of Meridional Ion Drifts at Northern Footpoint Scalars for translating meridional ion drifts (zonal E fields) measured at the spacecraft down to the northern footpoint.	dimensionless	EPOCH
ICON_ANCILLARY_IVM_SOUTH_FOOTPOINT_ZON_DRIFT	Translating Scalars of Zonal Ion Drifts at Southern Footpoint Scalars for translating zonal ion drifts (meridional E fields) measured at the spacecraft down to the southern footpoint.	dimensionless	EPOCH
ICON_ANCILLARY_IVM_SOUTH_FOOTPOINT_MER_DRIFT	Translating Scalars of Meridional Ion Drifts at Southern Footpoint Scalars for translating meridional ion drifts (zonal E fields) measured at the spacecraft down to the southern footpoint.	dimensionless	EPOCH
ICON_ANCILLARY_IVM_EQU_ZON_DRIFT	Translating Scalars of Zonal Ion Drifts at Equator Scalars for translating zonal ion drifts (meridional E fields) measured at the spacecraft down to the magnetic equator.	dimensionless	EPOCH
ICON_ANCILLARY_IVM_EQU_MER_DRIFT	Translating Scalars of Meridional Ion Drifts at Equator Scalars for translating meridional ion drifts (zonal E fields) measured at the spacecraft down to the magnetic equator.	dimensionless	EPOCH
ICON_ANCILLARY_IVM_APEX_HEIGHT	Modified APEX Height Modified APEX height of the spacecraft position.	km	EPOCH
ICON_ANCILLARY_IVM_NORTH_FOOTPOINT_QD_LAT	Quasi-dipole Latitude of Northern Footpoint Calculated value of quasi-dipole latitude of northern footpoint from IGRF.	degrees	EPOCH
ICON_ANCILLARY_IVM_NORTH_FOOTPOINT_QD_LON	Quasi-dipole Longitude of Northern Footpoint Calculated value of quasi-dipole longitude of northern footpoint from IGRF	degrees	EPOCH
ICON_ANCILLARY_IVM_SOUTH_FOOTPOINT_QD_LAT	Quasi-dipole Latitude of Southern Footpoint Calculated value of quasi-dipole latitude of southern footpoint from IGRF	degrees	EPOCH
ICON_ANCILLARY_IVM_SOUTH_FOOTPOINT_QD_LON	Quasi-dipole Longitude of Southern Footpoint Calculated value of quasi-dipole longitude of southern footpoint from IGRF	degrees	EPOCH

Variable Name	Description	Units	Dimensions
ICON Ancillary IVM Quality Flag ICON Ancillary IVM Quality Flag	<p>Quality Flag</p> <p>Binary Coded Integer where</p> <p>1: STATE_NO_DATA 2: STATE_UNCONVERGED 4: STATE_LOW 8: STATE_MED 16: STATE_HIGH 32: AD_NO_DATA 64: AD_DIVERGING 128: AD_NOT_STARTED 256: AD_CONVERGING 512: AD_COARSE_CONVERGED 1024: AD_FINE_CONVERGED 2048-32768: SPARE</p> <p>STATE_NO_DATA: No telemetry available for this time period. States are propagated from the last valid solution.</p> <p>STATE_UNCONVERGED: The GOODS KF solution is unconverged and should not be used. States are propagated from the last valid solution.</p> <p>STATE_LOW: The GPSR solution is better than the GOODS solution (The position accuracy is worse than 150 m, 1-sigma)</p> <p>STATE_MEDIUM: The GOODS solution is better than the GPSR solution (The position accuracy is better than 150 m, 1-sigma)</p> <p>STATE_HIGH: The GOODS solution is better than the GPSR solution, and meets its performance requirements (20 m position and 0.02 m/sec velocity, 1-sigma).</p> <p>AD_NO_DATA: No telemetry available for this time period. Attitude is copied from the last valid solution.</p> <p>AD_DIVERGING: Tolerances on the diagonal elements of the covariance matrix diverging and exceeds 9.9e9 asec² for attitude sigma and 9.9e9 asec²/sec² for rate sigma or negative values</p> <p>AD_NOT_STARTED: KF has not started processing measurements</p> <p>AD_CONVERGING: KF is in state of updating measurements and filter started to converge</p> <p>AD_COARSE_CONVERGED: Tolerances on the diagonal elements of the covariance matrix converging and below 200K asec² for x, y and 1000K for z in tracker frame for attitude and 10 asec²/sec² for x, y and z for rate</p> <p>AD_FINE_CONVERGED: Tolerances on the diagonal elements of the covariance matrix converging and below 1000 asec² for x, y and z in tracker frame for attitude and 1 asec²/sec² x, y and z for rate</p> <p>Nominal value of 1040: STATE_HIGH (16) and AD_FINE_CONVERGED (1024). All values are a combination of a STATE value and an AD (attitude determination) value. It is up to the user to determine if data outside 1040 is usable. AD values NOT AD_FINE_CONVERGED should be suspect. STATE_HIGH is expected, but STATE_MED is possible during maneuvers.</p>	binary	EPOCH

Acknowledgement

This is a data product from the NASA Ionospheric Connection Explorer mission, an Explorer launched at 21:59:45 EDT on October 10, 2019. Guidelines for the use of this product are described in the ICON Rules of the Road (<https://icon.ssl.berkeley.edu/Data>)

Responsibility for the mission science falls to the Principal Investigator, Dr. Thomas Immel at UC Berkeley: Immel, T.J., England, S.L., Mende, S.B. et al. Space Sci Rev (2018) 214: 13. <https://doi.org/10.1007/s11214-017-0449-2>

Responsibility for the validation of the L1 data products falls to the instrument lead investigators/scientists.

- * EUV: Dr. Eric Korpela : <https://doi.org/10.1007/s11214-017-0384-2>
- * FUV: Dr. Harald Frey : <https://doi.org/10.1007/s11214-017-0386-0>
- * MIGHTI: Dr. Christoph Englert : <https://doi.org/10.1007/s11214-017-0358-4>, and <https://doi.org/10.1007/s11214-017-0374-4>
- * IVM: Dr. Roderick Heelis : <https://doi.org/10.1007/s11214-017-0383-3>

Responsibility for the validation of the L2 data products falls to those scientists responsible for those products.

- * Daytime O and N2 profiles: Dr. Andrew Stephan : <https://doi.org/10.1007/s11214-018-0477-6>
- * Daytime (EUV) O+ profiles: Dr. Andrew Stephan : <https://doi.org/10.1007/s11214-017-0385-1>
- * Nighttime (FUV) O+ profiles: Dr. Farzad Kamalabadi : <https://doi.org/10.1007/s11214-018-0502-9>
- * Neutral Wind profiles: Dr. Jonathan Makela : <https://doi.org/10.1007/s11214-017-0359-3>
- * Neutral Temperature profiles: Dr. Christoph Englert : <https://doi.org/10.1007/s11214-017-0434-9>
- * Ion Velocity Measurements : Dr. Russell Stoneback : <https://doi.org/10.1007/s11214-017-0383-3>

Responsibility for Level 4 products falls to those scientists responsible for those products.

- * Hough Modes : Dr. Chihoko Yamashita : <https://doi.org/10.1007/s11214-017-0401-5>
- * TIEGCM : Dr. Astrid Maute : <https://doi.org/10.1007/s11214-017-0330-3>
- * SAMI3 : Dr. Joseph Huba : <https://doi.org/10.1007/s11214-017-0415-z>

Pre-production versions of all above papers are available on the ICON website.
<http://icon.ssl.berkeley.edu/Publications>

Overall validation of the products is overseen by the ICON Project Scientist, Dr. Scott England.

NASA oversight for all products is provided by the Mission Scientist, Dr. Jeffrey Klenzing.

Users of these data should contact and acknowledge the Principal Investigator Dr. Immel and the party directly responsible for the data product (noted above) and acknowledge NASA funding for the collection of the data used in the research with the following statement : "ICON is supported by NASA's Explorers Program through contracts NNG12FA45C and NNG12FA42I"

These data are openly available as described in the ICON Data Management Plan available on the ICON website (<http://icon.ssl.berkeley.edu/Data>).

This document was automatically generated on 2020-10-08 09:18 using the file:

ICON_L0P_IVM-A_Ancillary_2020-01-20_v02r099.NC

Software version: ICON_SDC > IVM Prime Generator 2.0.4

ICON Data Product 2.7: IVM Ionospheric Parameters

This document describes the data product for IVM L2 Thermal Plasma file, which is in NetCDF4 format.

This is the version 6 release of geophysical data for the Ion Velocity Meter (IVM) on-board the Ionospheric Connections Explorer (ICON) satellite. The IVM is comprised of two instruments, the Retarding Potential Analyzer (RPA) and the Drift Meter (DM). The IVM is operating very well and with low noise, generally producing high quality outputs. Current work on the data processing is driven by the generally low ionospheric densities resulting from low solar activity. During daytime hours, particularly mid-morning and later, all parameters are generally available and high quality.

This product contains several data quality flags that should be examined to ensure the highest fidelity data. Good data for all parameters, including ion drifts, may be down-selected by selecting times where two flags, `ICON_L27_RPA_FLAG_PROCESS` and `ICON_L27_DM_FLAG_PROCESS`, are both zero or one. Parameters such as ion density and composition are generally always reliable, followed by ion temperature, then the three dimensional ion drift vector. The ion temperature may demonstrate an increased variance in the early morning hours but early analysis indicates the values are otherwise high quality. Unlike the other parameters, determination of the ion drifts requires a minimum absolute O⁺ density. At night, the absolute O⁺ densities can fall below the detection limit of the IVM. When this occurs, resolving the ion motion along the IVM look direction can be challenging. During these periods the ion velocity is set to the co-rotation velocity. Use of the full 3D vectors (`ICON_L27_Ion_Velocity_Meridional`, `ICON_L27_Ion_Velocity_Zonal`, and `ICON_L27_Ion_Velocity_Field_Aligned`) during these periods is not recommended (`ICON_L27_RPA_FLAG_PROCESS=2`). The magnetic meridional ion drift near the magnetic equator, magnetic latitudes +/- 5 degrees, is primarily given by `ICON_L27_Ion_Velocity_Z` (positive towards Earth), and may be used as an approximation even when the `RPA_FLAG_PROCESS=2`. The Drift Meter (DM) measures cross-track motions and excludes H⁺ ions. Low O⁺ densities, particularly at dawn, make measurements a challenge. A flag is set when O⁺ densities are too low for the hardware to function (`ICON_L27_DM_FLAG_PROCESS=32`). The low O⁺ densities exacerbates the impact of photoemission upon measurements within the DM. A first-order model has been developed and work is progressing on producing high-quality outputs during these periods. In the interim, ion drifts that require a significant photoemission correction have been masked (`ICON_L27_DM_FLAG_PROCESS=64`). Any spacecraft operations that may have the potential to impact the outputs are currently flagged (`ICON_L27_RPA_FLAG_PROCESS=8`, `ICON_L27_DM_FLAG_PROCESS=8`). Impacts are likely more prevalent in the DM than RPA, depending upon the operation. See spacecraft flags for more.

History

Version 001, R. A. Stoneback, 2019-08-06T00:00:00, Initial Release

Version 002, R. A. Stoneback, 2020-06-19T00:00:00, Update for public release, adds quality flags

Version 003, R. A. Stoneback, 2020-04-10T00:00:00, Adds first order photoemission correction

Version 004, R. A. Stoneback, 2020-12-03T00:00:00, Adjustments to IVM offsets

Version 005, R. A. Stoneback, 2021-03-21T00:00:00, Improvements to RPA Fit noise, Drifts in East, North, Up. Data between 0500 and 1200 should be rejected at this time due to poor S/N and contaminant signals from internally generated photocurrents that have not been removed.

The V05 data product has been corrected for long-term systematic offsets produced by uncertainties in the electrostatic environment of the spacecraft. The corrected variables are:

`ICON_L27_Ion_Velocity_X`

`ICON_L27_Ion_Velocity_Y`

`ICON_L27_Ion_Velocity_Z`

They are used to compute the plasma drifts in magnetic coordinates.

The uncorrected data may be accessed directly in the variables

`ICON_L27_Raw_Ion_Velocity_X`

ICON_L27_Raw_Ion_Velocity_Y
ICON_L27_Raw_Ion_Velocity_Z

Short term variations with periods less than 10 days have not been removed but may be accurately assessed from examination of the zonal (daily) average of the meridional drift ICON_L27_Ion_Velocity_Meridional within 1 hour of 1800 MLT. Zonal averages in excess of 5 m/s over this local time range provide a reliable estimate of the short-term offset.

Version 006, Matthew Depew 2022-03-14, The V06 data product has been improved to handle large O+ fractions and to include cross-track ion drifts derived by neglecting inputs from the RPA. Data products has been corrected for long-term systematic offsets produced by uncertainties in the electrostatic environment of the spacecraft. The corrected variables are: ICON_L27_Ion_Velocity_X, ICON_L27_Ion_Velocity_Y, ICON_L27_Ion_Velocity_Z. They are used to compute the plasma drifts in magnetic coordinates. The uncorrected data may be accessed directly in the variables ICON_L27_Raw_Ion_Velocity_X, ICON_L27_Raw_Ion_Velocity_Y, ICON_L27_Raw_Ion_Velocity_Z. Transverse ion drifts derived by neglecting RPA inputs may be accessed directly in the variables ICON_L27_Original_Velocity_Y, ICON_L27_Original_Velocity_Z. Short term variations with periods less than 10 days have not been removed but may be accurately assessed from examination of the zonal (daily) average of the meridional drift ICON_L27_Ion_Velocity_Meridional within 1 hour of 1800 MLT. Zonal averages in excess of 5 m/s over this local time range provide a reliable estimate of the short-term offset.

Dimensions

NetCDF files contain **variables** and the **dimensions** over which those variables are defined. First, the dimensions are defined, then all variables in the file are described.

The dimensions used by the variables in this file are given below, along with nominal sizes. Note that the size may vary from file to file. For example, the "Epoch" dimension, which describes the number of time samples contained in this file, will have a varying size.

Dimension Name	Nominal Size
Epoch	unlimited

Variables

Variables in this file are listed below. First, "data" variables are described, followed by the "support_data" variables, and finally the "metadata" variables. The variables classified as "ignore_data" are not shown.

data

Variable Name	Description	Units	Dimensions
Epoch	Universal Time (UTC) Time at the midpoint of the IVM measurements.	Milliseconds since 1970-01-01 00:00:00	Epoch
ICON_L27_Altitude	WGS84 Altitude of Spacecraft Position (geodetic) Geodetic Altitude of Spacecraft in WGS84.	km	Epoch
ICON_L27_Fractional_Ion_Density_H	Fraction of total plasma number density that is H+ Determined via a non-linear least squares fit of RPA currents to the Whipple equation		Epoch
ICON_L27_Fractional_Ion_Density_O	Fraction of total plasma number density that is O+ Determined via a non-linear least squares fit of RPA currents to the Whipple equation		Epoch
ICON_L27_Latitude	WGS84 Latitude of Spacecraft Position (geodetic) Geodetic latitude of spacecraft in WGS84	degrees North	Epoch
ICON_L27_Solar_Local_Time	Local Solar Time at Spacecraft Local Solar Time at spacecraft.	hour	Epoch
ICON_L27_Magnetic_Local_Time	Magnetic Local Time at Spacecraft Magnetic Local Time at the spacecraft.	hour	Epoch
ICON_L27_Longitude	WGS84 Longitude of Spacecraft Position (geodetic) Geodetic longitude of spacecraft in WGS84	degrees East	Epoch
ICON_L27_Ion_Density	Ion density determined using RPA measurements. Ion density uses measured currents and co-rotating atmosphere to determine density.	N/cc	Epoch
ICON_L27_Ion_Temperature	Ion temperature determined using a best fit of RPA measurements to Whipple equation. Temperature is obtained by assuming single temperature value for all plasma.	K	Epoch

Variable Name	Description	Units	Dimensions
ICON_L27_Ion_Velocity_Field_Aligned	<p>Field-Aligned Ion Velocity</p> <p>Ion velocity relative to co-rotation along geomagnetic field lines. Positive along the main field vector.</p> <p>Velocity obtained using ion velocities relative to co-rotation in the instrument frame along with the corresponding unit vectors expressed in the instrument frame to express the observed vector along a geomagnetic basis.</p>	m/s	Epoch
ICON_L27_Ion_Velocity_Meridional	<p>Meridional Ion Velocity</p> <p>Ion velocity along local magnetic meridional direction, perpendicular to geomagnetic field and within local magnetic meridional plane. The local meridional vector maps to vertical at the magnetic equator, positive is up.</p> <p>Velocity obtained using ion velocities relative to co-rotation in the instrument frame along with the corresponding unit vectors expressed in the instrument frame to express the observed vector along a geomagnetic basis.</p>	m/s	Epoch
ICON_L27_Ion_Velocity_X	<p>Ion velocity along IVM-x</p> <p>Cross-track velocity is relative to co-rotation and in the instrument frame. Positive-x is normal to IVM aperture plane and in the direction of satellite motion. Velocity obtained through fitting of RPA currents to the Whipple equation to get a measure of the total along track ion velocity as observed within the instrument. Signals produced by the motion of the spacecraft and the rotation of the Earth are removed to produce this result. Mean offset of 49.2 added by R. A. Heelis.</p>	m/s	Epoch
ICON_L27_Ion_Velocity_Y	<p>Ion velocity along IVM-y</p> <p>Cross-track velocity is relative to co-rotation and in the instrument frame. Positive-y points generally southward when the instrument is pointed along the ram direction. Velocity obtained through conversion of arrival angles measured by the DM into a cross track velocity using trigonometry. Signals produced by the motion of the spacecraft and the rotation of the Earth are removed to produce this result. Mean offset of -0.0 added by R. A. Heelis.</p>	m/s	Epoch
ICON_L27_Ion_Velocity_Z	<p>Ion velocity along IVM-z</p> <p>Cross-track velocity is relative to co-rotation and in the instrument frame. Positive-z is directed towards nadir (Earth). Velocity obtained through conversion of arrival angles measured by the DM into a cross track velocity using trigonometry. Signals produced by the motion of the spacecraft and the rotation of the Earth are removed to produce this result. Mean offset of -7.0 added by R. A. Heelis.</p>	m/s	Epoch

Variable Name	Description	Units	Dimensions
ICON_L27_Ion_Velocity_Zonal	<p>Zonal ion velocity</p> <p>Ion velocity relative to co-rotation along the magnetic zonal direction, normal to local magnetic meridional plane and the geomagnetic field (positive east). The local zonal vector maps to purely horizontal at the magnetic equator. Velocity obtained using ion velocities relative to co-rotation in the instrument frame along with the corresponding unit vectors expressed in the instrument frame to express the observed vector along a geomagnetic basis.</p>	m/s	Epoch
ICON_L27_Raw_Ion_Velocity_X	<p>Raw ion velocity determined using a best fit of RPA measurements to the Whipple equation.</p> <p>This is the total ion velocity along normal direction into the RPA, including s/c motion.</p>	m/s	Epoch
ICON_L27_Raw_Ion_Velocity_Y	<p>Total ion velocity measured along IVM-y.</p> <p>Total observed ion velocity along instrument cross-track direction, reported in the instrument frame. The translation of DM measured angles to ion velocities uses knowledge of the ram velocity of the plasma and the electric potential of the instrument aperture relative to the ambient plasma, both of which are provided by the RPA.</p>	m/s	Epoch
ICON_L27_Raw_Ion_Velocity_Z	<p>Total ion velocity measured along IVM-z.</p> <p>Total observed ion velocity along instrument cross-track direction, reported in the instrument frame. The translation of DM measured angles to ion velocities uses knowledge of the ram velocity of the plasma and the electric potential of the instrument aperture relative to the ambient plasma, both of which are provided by the RPA.</p>	m/s	Epoch
ICON_L27_Original_Ion_Velocity_Y	<p>Total ion velocity measured along IVM-y.</p> <p>Total observed ion velocity along instrument cross-track direction, reported in the instrument frame. The translation of DM measured angles to ion velocities with no RPA corrections.</p>	m/s	Epoch
ICON_L27_Original_Ion_Velocity_Z	<p>Total ion velocity measured along IVM-z.</p> <p>Total observed ion velocity along instrument cross-track direction, reported in the instrument frame. The translation of DM measured angles to ion velocities with no RPA corrections.</p>	m/s	Epoch
ICON_L27_Unit_Vector_Meridional_X	<p>Unit vector for the geomagnetic meridional direction.</p> <p>The meridional unit vector is perpendicular to the geomagnetic field and maps along magnetic field lines to vertical at the magnetic equator, where positive is up. The unit vector is expressed here in the IVM coordinate system, where x is along the IVM boresight, nominally along ram when in standard pointing. Calculated using the corresponding unit vector in ECEF and the orientation of the IVM also expressed in ECEF (\hat{sc}_*).</p>		Epoch

Variable Name	Description	Units	Dimensions
ICON_L27_Unit_Vector_Meridional_Y	<p>Unit vector for the geomagnetic meridional direction.</p> <p>The meridional unit vector is perpendicular to the geomagnetic field and maps along magnetic field lines to vertical at the magnetic equator, where positive is up. The unit vector is expressed here in the IVM coordinate system, where $Y = Z \times X$, nominally southward when in standard pointing, X along ram. Calculated using the corresponding unit vector in ECEF and the orientation of the IVM also expressed in ECEF (sc_hat_*).</p>		Epoch
ICON_L27_Unit_Vector_Meridional_Z	<p>Unit vector for the geomagnetic meridional direction.</p> <p>The meridional unit vector is perpendicular to the geomagnetic field and maps along magnetic field lines to vertical at the magnetic equator, where positive is up. The unit vector is expressed here in the IVM coordinate system, where Z is nadir pointing (towards Earth), when in standard pointing, X along ram. Calculated using the corresponding unit vector in ECEF and the orientation of the IVM also expressed in ECEF (sc_hat_*).</p>		Epoch
ICON_L27_IVM_Aperture_Potential	<p>Plasma potential relative to instrument aperture plane - determined using a best fit to RPA measurements.</p> <p>Incident plasma will have some potential to the IVM aperture plane. The aperture plane voltage matches that of a conductor allowed to float electrically with respect to the spacecraft. The flux of ions (driven by s/c motion) must be balanced by the flux of electrons (driven by electron temperature). The value of the aperture plane potential evolves naturally to limit the collection of electrons such the net flux is zero.</p>	V	Epoch
ICON_L27_Unit_Vector_Field_Aligned_X	<p>Unit vector for the geomagnetic field line direction.</p> <p>The field-aligned vector points along the geomagnetic field, with positive values along the field direction, and is expressed here in the IVM instrument frame. The IVM-x direction points along the instrument boresight, which is pointed into ram for standard operations. Calculated using the corresponding unit vector in ECEF and the orientation of the IVM also expressed in ECEF (sc_hat_*).</p>		Epoch
ICON_L27_Unit_Vector_Field_Aligned_Y	<p>Unit vector for the geomagnetic field line direction.</p> <p>The field-aligned vector points along the geomagnetic field, with positive values along the field direction. The unit vector is expressed here in the IVM coordinate system, where $Y = Z \times X$, nominally southward when in standard pointing, X along ram. Calculated using the corresponding unit vector in ECEF and the orientation of the IVM also expressed in ECEF (sc_hat_*).</p>		Epoch

Variable Name	Description	Units	Dimensions
ICON_L27_Unit_Vector_Field_Aligned_Z	<p>Unit vector for the geomagnetic field line direction.</p> <p>The field-aligned vector points along the geomagnetic field, with positive values along the field direction, and is expressed here in the IVM instrument frame. The IVM-Z direction points towards nadir when IVM-X is pointed into ram for standard operations. Calculated using the corresponding unit vector in ECEF and the orientation of the IVM also expressed in ECEF (sc_*hat_*).</p>		Epoch
ICON_L27_Unit_Vector_Zonal_X	<p>Unit vector for the zonal geomagnetic direction.</p> <p>The zonal vector is perpendicular to the local magnetic field and the magnetic meridional plane. The zonal vector maps to purely horizontal at the magnetic equator, with positive values pointed generally eastward. This vector is expressed here in the IVM instrument frame. The IVM-x direction points along the instrument boresight, which is pointed into ram for standard operations. Calculated using the corresponding unit vector in ECEF and the orientation of the IVM also expressed in ECEF (sc_*hat_*).</p>		Epoch
ICON_L27_Unit_Vector_Zonal_Y	<p>Unit vector for the zonal geomagnetic direction.</p> <p>The zonal vector is perpendicular to the local magnetic field and the magnetic meridional plane. The zonal vector maps to purely horizontal at the magnetic equator, with positive values pointed generally eastward. The unit vector is expressed here in the IVM coordinate system, where $Y = Z \times X$, nominally southward when in standard pointing, X along ram. Calculated using the corresponding unit vector in ECEF and the orientation of the IVM also expressed in ECEF (sc_*hat_*).</p>		Epoch
ICON_L27_Unit_Vector_Zonal_Z	<p>Unit vector for the zonal geomagnetic direction.</p> <p>The zonal vector is perpendicular to the local magnetic field and the magnetic meridional plane. The zonal vector maps to purely horizontal at the magnetic equator, with positive values pointed generally eastward. This vector is expressed here in the IVM instrument frame. The IVM-Z direction points towards nadir when IVM-X is pointed into ram for standard operations. Calculated using the corresponding unit vector in ECEF and the orientation of the IVM also expressed in ECEF (sc_*hat_*).</p>		Epoch
ICON_L27_MTB_Status	<p>Magnetic Torquer Bar Firing Status</p> <p>If the magnetic torquers are active during any part of the measurement, it is recorded as active for whole measurement. Decoded from spacecraft housekeeping file: ICON_L0_Spacecraft_Housekeeping-MTB_2022-01-01_v01r000.CSV</p>	binary	Epoch
ICON_L27_Slew_Status			Epoch

Variable Name	Description	Units	Dimensions
ICON_L27_Sun_Status	<p>Spacecraft Sun/Shadow Status Code</p> <p>Data is from predictive ephemeris. 0 = spacecraft in Sun, 1 = spacecraft in Earth Shadow.</p>	binary	Epoch
ICON_L27_Space_Environment_Region_Status	<p>Space Environment Region Status</p> <p>Standardized for several missions, not all codes are relevant for ICON where</p> <ul style="list-style-type: none"> 1: Earth Shadow 2: Lunar Shadow 4: Atmospheric Absorption Zone 8: South Atlantic Anomaly 16: Northern Auroral Zone 32: Southern Auroral Zone 64: Periapsis Passage 128: Inner & Outer Radiation Belts 256: Deep Plasma Sphere 512: Foreshock Solar Wind 1024: Solar Wind Beam 2048: High Magnetic Field 4096: Average Plasma Sheet 8192: Bowshock Crossing 16384: Magnetopause Crossing 32768: Ground Based Observatories 65536: 2-Day Conjunctions 131072: 4-Day Conjunctions 262144: Time Based Conjunctions 524288: Radial Distance Region 1 1048576: Orbit Outbound 2097152: Orbit Inbound 4194304: Lunar Wake 8388608: Magnetotail 16777216: Magnetosheath 33554432: Science 67108864: Low Magnetic Latitude 134217728: Conjugate Observation 	binary	Epoch
ICON_L27_Attitude_Status	<p>Slew or Off-Point Status Code</p> <p>Binary Coded Integer where</p> <ul style="list-style-type: none"> 1: LVLH Normal Mode 2: LVLH Reverse Mode 4: Earth Limb Pointing 8: Inertial Pointing 16: Stellar Pointing 32: Attitude Slew 64: Conjugate Maneuver 128: Nadir Calibration 256: Lunar Calibration 512: Stellar Calibration 1024: Zero Wind Calibration 2048-32768: SPARE 	binary	Epoch
ICON_L27_Orbit_Number	<p>Orbit Number</p> <p>Integer Orbit Number.</p>	integer	Epoch

Variable Name	Description	Units	Dimensions
ICON_L27_Magnetic_Latitude	<p>Magnetic Latitude of Spacecraft Position</p> <p>Quasi-dipole magnetic latitude of the spacecraft position. These values are obtained from passing the geodetic latitudes, longitudes, and altitudes from ICON Ancillary IVM Latitude, ICON Ancillary IVM Longitude, and ICON Ancillary IVM Altitude into apexpy Python module. For details on apexpy see: https://apexpy.readthedocs.org/</p>	degrees North	Epoch
ICON_L27_Magnetic_Longitude	<p>Magnetic Longitude of Spacecraft Position</p> <p>Quasi-dipole magnetic longitude of the spacecraft position. These values are obtained from passing the geodetic latitudes, longitudes, and altitudes from ICON Ancillary IVM Latitude, ICON Ancillary IVM Longitude, and ICON Ancillary IVM Altitude into apexpy Python module. For details on apexpy see: https://apexpy.readthedocs.org/</p>	degrees East	Epoch
ICON_L27_DM_Flag_Process	<p>Drift meter quality flag. This flag applies to the following variables: ICON_L27_Raw_Ion_Velocity_Y, ICON_L27_Raw_Ion_Velocity_Z, ICON_L27_Original_Ion_Velocity_Y, ICON_L27_Original_Ion_Velocity_Z, ICON_L27_Ion_Velocity_Y, ICON_L27_Ion_Velocity_Z, ICON_L27_Ion_Velocity_Meridional, ICON_L27_Ion_Velocity_Zonal, ICON_L27_Ion_Velocity_Field_Aligned, ICON_L27_Ion_Velocity_East, ICON_L27_Ion_Velocity_North, ICON_L27_Ion_Velocity_Up, ICON_L27_Footpoint_Meridional_Ion_Velocity_North, ICON_L27_Footpoint_Meridional_Ion_Velocity_South, ICON_L27_Footpoint_Zonal_Ion_Velocity_North, ICON_L27_Footpoint_Zonal_Ion_Velocity_South, ICON_L27_Footpoint_Up_Ion_Velocity_North, ICON_L27_Footpoint_Up_Ion_Velocity_South, Values represent bits of the flag, multiple of which may be set at a time. This flag is less than or equal to 1 when the data is of highest quality. Vx and magnetic component drifts should be rejected when this flag is greater than 0. 0 - Good data. 1 - Drift components utilize model for ram drift. 2 - Data possibly degraded by signal noise. 4 - Data probably degraded by signal noise. 8 - Data may have artifacts due to s/c operations. 16 - Spacecraft attitude may significantly impact performance. 32 - Not enough O+ to measure arrival angle. 64 - Data temporarily removed for photoemission. e.g. DM_Flag=9 Velocity obtained using ram drift model during torquer rod firing</p>		Epoch

Variable Name	Description	Units	Dimensions
ICON_L27_RPA_Flag_Process	<p>RPA Quality Flag</p> <p>Status flag for RPA. This flag applies to the following variables: ICON_L27_Raw_Ion_Velocity_X, ICON_L27_IVM_Aperture_Potential, ICON_L27_Ion_Velocity_X, ICON_L27_Ion_Temperature, ICON_L27_Fractional_Ion_Density_O, ICON_L27_Fractional_Ion_Density_H, ICON_L27_Ion_Velocity_Meridional, ICON_L27_Ion_Velocity_Zonal, ICON_L27_Ion_Velocity_Field_Aligned, ICON_L27_Ion_Velocity_East, ICON_L27_Ion_Velocity_North, ICON_L27_Ion_Velocity_Up, ICON_L27_Footpoint_Meridional_Ion_Velocity_North, ICON_L27_Footpoint_Meridional_Ion_Velocity_South, ICON_L27_Footpoint_Zonal_Ion_Velocity_North, ICON_L27_Footpoint_Zonal_Ion_Velocity_South, ICON_L27_Footpoint_Up_Ion_Velocity_North, ICON_L27_Footpoint_Up_Ion_Velocity_South, Values represent bits of the flag, multiple of which may be set at a time. This flag is less than 1 when the data is of highest quality. When the flag is 2, data should be used with caution as it is partially derived from a model. Data when the flag is greater than 2 should be rejected 0 - All RPA parameters are good. Ion temperatures correspond to both O+ and H+. 1 - Ram Ion Velocities are computed with aperture potential model. Other parameters unchanged. 2 - Model values for ram drift use when fitting RPA curves that have an insufficient quantity of O+. Ion temperatures correspond to H+ only. 4 - Unsuccessful fit to RPA. 8 - Geophysical outputs may be impacted by spacecraft operations. 16 - Geophysical outputs may be significantly impacted by spacecraft attitude. e.g. RPA_Flag=9 Velocity obtained using aperture potential model during torquer rod firing</p>		Epoch
ICON_L27_DM_Flag	<p>Drift meter quality flag. This flag applies to the following variables: ICON_L27_Raw_Ion_Velocity_Y, ICON_L27_Raw_Ion_Velocity_Z, ICON_L27_Original_Ion_Velocity_Y, ICON_L27_Original_Ion_Velocity_Z, ICON_L27_Ion_Velocity_Y, ICON_L27_Ion_Velocity_Z, ICON_L27_Ion_Velocity_Meridional, ICON_L27_Ion_Velocity_Zonal, ICON_L27_Ion_Velocity_Field_Aligned, ICON_L27_Ion_Velocity_East, ICON_L27_Ion_Velocity_North, ICON_L27_Ion_Velocity_Up, ICON_L27_Footpoint_Meridional_Ion_Velocity_North, ICON_L27_Footpoint_Meridional_Ion_Velocity_South, ICON_L27_Footpoint_Zonal_Ion_Velocity_North, ICON_L27_Footpoint_Zonal_Ion_Velocity_South, ICON_L27_Footpoint_Up_Ion_Velocity_North, ICON_L27_Footpoint_Up_Ion_Velocity_South, 0 - Good data. 1 - Use with caution. 2 - Corrected with Photoemission model. 3 - Should be rejected.</p>		Epoch

Variable Name	Description	Units	Dimensions
ICON_L27_RPA_Flag	<p>RPA Quality Flag</p> <p>Quality flag for RPA. This flag applies to the following variables: ICON_L27_Raw_Ion_Velocity_X, ICON_L27_IVM_Aperture_Potential, ICON_L27_Ion_Velocity_X, ICON_L27_Ion_Temperature, ICON_L27_Fractional_Ion_Density_O, ICON_L27_Fractional_Ion_Density_H, ICON_L27_Ion_Velocity_Meridional, ICON_L27_Ion_Velocity_Zonal, ICON_L27_Ion_Velocity_Field_Aligned, ICON_L27_Ion_Velocity_East, ICON_L27_Ion_Velocity_North, ICON_L27_Ion_Velocity_Up, ICON_L27_Footpoint_Meridional_Ion_Velocity_North, ICON_L27_Footpoint_Meridional_Ion_Velocity_South, ICON_L27_Footpoint_Zonal_Ion_Velocity_North, ICON_L27_Footpoint_Zonal_Ion_Velocity_South, ICON_L27_Footpoint_Up_Ion_Velocity_North, ICON_L27_Footpoint_Up_Ion_Velocity_South, 0 - Good data. 1 - Use with caution. 2 - Should be rejected.</p>		Epoch
ICON_L27.UTC_Time	<p>ISO 9601 formatted UTC timestamp (at middle of reading).</p> <p>ISO 9601 formatted UTC timestamp (at middle of reading).</p> <p>Time is generated from the time-code at byte 1015 of the IVM packet minus the time sync at byte 1019 of the IVM packet. This is the GPS time at the start of the integration period. The integration period is assumed to be 4 seconds so the center time is 2 seconds after that. The formula is (time-code * 1000ms) + 2000ms - (16 * time sync / 1000) in GPS milliseconds then converted to UTC time. See the UTD 206-024 Rev A document.</p> <p>Time may be delayed by up to 10 ms due to FSW polling delay.</p> <p>Maximum time is ~2150 UTC and minimum time is ~1970 UTC.</p>		Epoch
ICON_L27_Time_UTC_Start	<p>Milliseconds since 1970-01-01 00:00:00 UTC at start of reading.</p> <p>Milliseconds since 1970-01-01 00:00:00 UTC at start of reading.</p> <p>Time is generated from the time-code at byte 1015 of the IVM packet minus the time sync at byte 1019 of the IVM packet. This is the GPS time at the start of the integration period. The integration period is assumed to be 4 seconds so the center time is 2 seconds after that. The formula is (time-code * 1000ms) + 2000ms - (16 * time sync / 1000) in GPS milliseconds then converted to UTC time. See the UTD 206-024 Rev A document.</p> <p>Time may be delayed by up to 10 ms due to FSW polling delay.</p> <p>Maximum time is ~2150 UTC and minimum time is ~1970 UTC.</p>	milliseconds	Epoch

Variable Name	Description	Units	Dimensions
ICON_L27_Time_UTC_S top	<p>Milliseconds since 1970-01-01 00:00:00 UTC at end of reading.</p> <p>Milliseconds since 1970-01-01 00:00:00 UTC at end of reading.</p> <p>Time is generated from the time-code at byte 1015 of the IVM packet minus the time sync at byte 1019 of the IVM packet. This is the GPS time at the start of the integration period. The integration period is assumed to be 4 seconds so the center time is 2 seconds after that. The formula is (time-code * 1000ms) + 2000ms - (16 * time sync / 1000) in GPS milliseconds then converted to UTC time. See the UTD 206-024 Rev A document.</p> <p>Time may be delayed by up to 10 ms due to FSW polling delay.</p> <p>Maximum time is ~2150 UTC and minimum time is ~1970 UTC.</p>	milliseconds	Epoch
ICON_L27_Apex_Height	<p>Modified APEX Height</p> <p>Modified APEX height of the spacecraft position.</p>	km	Epoch
ICON_L27_GPS_Epoch	<p>Milliseconds since 1980-01-06 00:00:00 TAI (coincident with UTC) at middle of reading.</p> <p>Milliseconds since 1980-01-06 00:00:00 TAI (coincident with UTC) at middle of reading.</p> <p>Time is generated from the time-code at byte 1015 of the IVM packet minus the time sync at byte 1019 of the IVM packet. This is the GPS time at the start of the integration period. The integration period is assumed to be 4 seconds so the center time is 2 seconds after that. The formula is (time-code * 1000ms) + 2000ms - (16 * time sync / 1000) in GPS milliseconds then converted to UTC time. See the UTD 206-024 Rev A document.</p> <p>Time may be delayed by up to 10 ms due to FSW polling delay.</p> <p>Maximum time is ~2150 UTC and minimum time is ~1970 UTC.</p>	milliseconds	Epoch

Variable Name	Description	Units	Dimensions
ICON_L27_A_Status	<p>IVM-A Status</p> <p>Binary Coded Integer where</p> <ul style="list-style-type: none"> 1: Earth Day View 2: Earth Night View 4: Calibration Target View 8: Off-target View 16: Sun Proximity View 32: Moon Proximity View 64: North Magnetic Footpoint View 128: South Magnetic Footpoint View 256: Science Data Collection View 512: Calibration Data Collection View 1024: RAM Proximity View 2048-32768: SPARE <p>Activity is what the spacecraft was commanded to do while status is the spacecraft's natural state of operations. This means that activity should always be used over status if they differ, but will almost always be the same.</p>	binary	Epoch
ICON_L27_B_Status	<p>IVM-B Status</p> <p>Binary Coded Integer where</p> <ul style="list-style-type: none"> 1: Earth Day View 2: Earth Night View 4: Calibration Target View 8: Off-target View 16: Sun Proximity View 32: Moon Proximity View 64: North Magnetic Footpoint View 128: South Magnetic Footpoint View 256: Science Data Collection View 512: Calibration Data Collection View 1024: RAM Proximity View 2048-32768: SPARE <p>Activity is what the spacecraft was commanded to do while status is the spacecraft's natural state of operations. This means that activity should always be used over status if they differ, but will almost always be the same.</p>	binary	Epoch

Variable Name	Description	Units	Dimensions
ICON_L27_A_Activity	<p>IVM-A Activity</p> <p>Binary Coded Integer where: 1: Earth Day View 2: Earth Night View 4: Calibration Target View 8: Off-target View 16: Sun Proximity View 32: Moon Proximity View 64: North Magnetic Footpoint View 128: South Magnetic Footpoint View 256: Science Data Collection View 512: Calibration Data Collection View 1024: RAM Proximity View 2048-32768: SPARE</p> <p>Activity is what the spacecraft was commanded to do while status is the spacecraft's natural state of operations. This means that activity should always be used over status if they differ, but will almost always be the same.</p>	binary	Epoch
ICON_L27_B_Activity	<p>IVM-A Activity</p> <p>Binary Coded Integer where: 1: Earth Day View 2: Earth Night View 4: Calibration Target View 8: Off-target View 16: Sun Proximity View 32: Moon Proximity View 64: North Magnetic Footpoint View 128: South Magnetic Footpoint View 256: Science Data Collection View 512: Calibration Data Collection View 1024: RAM Proximity View 2048-32768: SPARE</p> <p>Activity is what the spacecraft was commanded to do while status is the spacecraft's natural state of operations. This means that activity should always be used over status if they differ, but will almost always be the same.</p>	binary	Epoch
ICON_L27_Footpoint_Altitude_North	<p>Altitude of North Footpoint of Geomagnetic Line at 150 km from IGRF</p> <p>Altitude location of the magnetic footpoint in the Northern Hemisphere at 150 km. These data were interpolated using a tricubic algorithm from IGRF and ephemeris data then linearly interpolated to IVM times.</p>	km	Epoch
ICON_L27_Footpoint_Field_Aligned_Vector_ECEF_X_North	<p>ECEF X-Component of Field Aligned Drift Direction at Northern Footpoint</p> <p>At the northern footpoint this is the x-component of the unit vector for field aligned ion drifts expressed in the ECEF frame.</p>	dimensionless	Epoch

Variable Name	Description	Units	Dimensions
ICON_L27_Footpoint_Field_Aligned_Vector_ECEF_Y_North	ECEF Y-Component of Field Aligned Drift Direction at Northern Footpoint At the northern footpoint this is the y-component of the unit vector for field aligned ion drifts expressed in the ECEF frame.	dimensionless	Epoch
ICON_L27_Footpoint_Field_Aligned_Vector_ECEF_Z_North	ECEF Z-Component of Field Aligned Drift Direction at Northern Footpoint At the northern footpoint this is the z-component of the unit vector for field aligned ion drifts expressed in the ECEF frame.	dimensionless	Epoch
ICON_L27_Footpoint_Latitude_North	Latitude of North Footpoint of Geomagnetic Line at 150 km from IGRF Latitude location of the magnetic footpoint in the Northern Hemisphere at 150 km. These data were interpolated using a tricubic algorithm from IGRF and ephemeris data then linearly interpolated to IVM times.	degrees	Epoch
ICON_L27_Footpoint_Longitude_North	Longitude of North Footpoint of Geomagnetic Line at 150 km from IGRF Longitude location of the magnetic footpoint in the Northern Hemisphere at 150 km. These data were interpolated using a tricubic algorithm from IGRF and ephemeris data then linearly interpolated to IVM times.	degrees	Epoch
ICON_L27_Footpoint_Meridional_Ion_Velocity_North	Northern Meridional Ion Velocity Velocity along local magnetic meridional direction, perpendicular to geomagnetic field and within local magnetic meridional plane, field-line mapped to northern footpoint. The meridional vector is purely vertical at the magnetic equator, positive up. Velocity obtained using ion velocities relative to co-rotation in the instrument frame along with the corresponding unit vectors expressed in the instrument frame. Field-line mapping and the assumption of equi-potential field lines is used to translate the locally measured ion motion to the magnetic footpoint. The mapping is used to determine the change in magnetic field line distance, which, under assumption of equipotential field lines, in turn alters the electric field at that location ($E=V/d$).	m/s	Epoch
ICON_L27_Footpoint_Magnetic_Latitude_North	Quasi-dipole Latitude of Northern Footpoint Calculated value of quasi-dipole latitude of northern footpoint from IGRF.	degrees	Epoch
ICON_L27_Footpoint_Magnetic_Longitude_North	Quasi-dipole Longitude of Northern Footpoint Calculated value of quasi-dipole longitude of northern footpoint from IGRF	degrees	Epoch
ICON_L27_Footpoint_Meridional_Vector_ECEF_X_North	ECEF X-Component of Meridional Drift Direction at Northern Footpoint At the northern footpoint this is the x-component of the unit vector for meridional ion drifts expressed in the ECEF frame.	dimensionless	Epoch

Variable Name	Description	Units	Dimensions
ICON_L27_Footpoint_Meridional_Vector_ECEF_Y_North	ECEF Y-Component of Meridional Drift Direction at Northern Footpoint At the northern footpoint this is the y-component of the unit vector for meridional ion drifts expressed in the ECEF frame.	dimensionless	Epoch
ICON_L27_Footpoint_Meridional_Vector_ECEF_Z_North	ECEF Z-Component of Meridional Drift Direction at Northern Footpoint At the northern footpoint this is the z-component of the unit vector for meridional ion drifts expressed in the ECEF frame.	dimensionless	Epoch
ICON_L27_Footpoint_Zonal_Ion_Velocity_North	Northern Zonal Ion Velocity Velocity along local magnetic zonal direction, perpendicular to geomagnetic field and the local magnetic meridional plane, field-line mapped to northern footpoint. The zonal vector is purely horizontal when mapped to the magnetic equator, positive is generally eastward. Velocity obtained using ion velocities relative to co-rotation in the instrument frame along with the corresponding unit vectors expressed in the instrument frame. Field-line mapping and the assumption of equi-potential field lines is used to translate the locally measured ion motion to the northern footpoint. The mapping is used to determine the change in magnetic field line distance, which, under assumption of equipotential field lines, in turn alters the electric field at that location ($E=V/d$).	m/s	Epoch
ICON_L27_Footpoint_Zonal_Vector_ECEF_X_North	ECEF X-Component of Zonal Drift Direction at Northern Footpoint At the northern footpoint this is the x-component of the unit vector for zonal ion drifts expressed in the ECEF frame.	dimensionless	Epoch
ICON_L27_Footpoint_Zonal_Vector_ECEF_Y_North	ECEF Y-Component of Zonal Drift Direction at Northern Footpoint At the northern footpoint this is the y-component of the unit vector for zonal ion drifts expressed in the ECEF frame.	dimensionless	Epoch
ICON_L27_Footpoint_Zonal_Vector_ECEF_Z_North	ECEF Z-Component of Zonal Drift Direction at Northern Footpoint At the northern footpoint this is the z-component of the unit vector for zonal ion drifts expressed in the ECEF frame.	dimensionless	Epoch
ICON_L27_Footpoint_Altitude_South	Altitude of South Footpoint of Geomagnetic Line at 150 km from IGRF Altitude location of the magnetic footpoint in the Northern Hemisphere at 150 km. These data were interpolated using a tricubic algorithm from IGRF and ephemeris data then linearly interpolated to IVM times.	km	Epoch
ICON_L27_Footpoint_Field_Aligned_Vector_ECEF_X_South	ECEF X-Component of Field Aligned Drift Direction at Southern Footpoint At the Southern footpoint this is the x-component of the unit vector for field aligned ion drifts expressed in the ECEF frame.	dimensionless	Epoch

Variable Name	Description	Units	Dimensions
ICON_L27_Footpoint_Field_Aligned_Vector_ECEF_Y_South	ECEF Y-Component of Field Aligned Drift Direction at Southern Footpoint At the Southern footpoint this is the y-component of the unit vector for field aligned ion drifts expressed in the ECEF frame.	dimensionless	Epoch
ICON_L27_Footpoint_Field_Aligned_Vector_ECEF_Z_South	ECEF Z-Component of Field Aligned Drift Direction at Southern Footpoint At the Southern footpoint this is the z-component of the unit vector for field aligned ion drifts expressed in the ECEF frame.	dimensionless	Epoch
ICON_L27_Footpoint_Latitude_South	Latitude of South Footpoint of Geomagnetic Line at 150 km from IGRF Latitude location of the magnetic footpoint in the Southern Hemisphere at 150 km. These data were interpolated using a tricubic algorithm from IGRF and ephemeris data then linearly interpolated to IVM times.	degrees	Epoch
ICON_L27_Footpoint_Longitude_South	Longitude of South Footpoint of Geomagnetic Line at 150 km from IGRF Longitude location of the magnetic footpoint in the Southern Hemisphere at 150 km. These data were interpolated using a tricubic algorithm from IGRF and ephemeris data then linearly interpolated to IVM times.	degrees	Epoch
ICON_L27_Footpoint_Meridional_Ion_Velocity_South	Southern Meridional Ion Velocity Velocity along local magnetic meridional direction, perpendicular to geomagnetic field and within local magnetic meridional plane, field-line mapped to southern footpoint. The meridional vector is purely vertical at the magnetic equator, positive up. Velocity obtained using ion velocities relative to co-rotation in the instrument frame along with the corresponding unit vectors expressed in the instrument frame. Field-line mapping and the assumption of equi-potential field lines is used to translate the locally measured ion motion to the magnetic footpoint. The mapping is used to determine the change in magnetic field line distance, which, under assumption of equipotential field lines, in turn alters the electric field at that location ($E=V/d$).	m/s	Epoch
ICON_L27_Footpoint_Magnetic_Latitude_South	Quasi-dipole Latitude of Southern Footpoint Calculated value of quasi-dipole latitude of southern footpoint from IGRF	degrees	Epoch
ICON_L27_Footpoint_Magnetic_Longitude_South	Quasi-dipole Longitude of Southern Footpoint Calculated value of quasi-dipole longitude of southern footpoint from IGRF	degrees	Epoch
ICON_L27_Footpoint_Meridional_Vector_ECEF_X_South	ECEF X-Component of Meridional Drift Direction at Southern Footpoint At the Southern footpoint this is the x-component of the unit vector for meridional ion drifts expressed in the ECEF frame.	dimensionless	Epoch

Variable Name	Description	Units	Dimensions
ICON_L27_Footpoint_Meridional_Vector_ECEF_Y_South	<p>ECEF Y-Component of Meridional Drift Direction at Southern Footpoint</p> <p>At the Southern footpoint this is the y-component of the unit vector for meridional ion drifts expressed in the ECEF frame.</p>	dimensionless	Epoch
ICON_L27_Footpoint_Meridional_Vector_ECEF_Z_South	<p>ECEF Z-Component of Meridional Drift Direction at Southern Footpoint</p> <p>At the Southern footpoint this is the z-component of the unit vector for meridional ion drifts expressed in the ECEF frame.</p>	dimensionless	Epoch
ICON_L27_Footpoint_Zonal_Ion_Velocity_South	<p>Southern Zonal Ion Velocity</p> <p>Velocity along local magnetic zonal direction, perpendicular to geomagnetic field and the local magnetic meridional plane, field-line mapped to southern footpoint. The zonal vector is purely horizontal when mapped to the magnetic equator, positive is generally eastward. Velocity obtained using ion velocities relative to co-rotation in the instrument frame along with the corresponding unit vectors expressed in the instrument frame. Field-line mapping and the assumption of equi-potential field lines is used to translate the locally measured ion motion to the southern footpoint. The mapping is used to determine the change in magnetic field line distance, which, under assumption of equipotential field lines, in turn alters the electric field at that location ($E=V/d$).</p>	m/s	Epoch
ICON_L27_Footpoint_Zonal_Vector_ECEF_X_South	<p>ECEF X-Component of Zonal Drift Direction at Southern Footpoint</p> <p>At the Southern footpoint this is the x-component of the unit vector for zonal ion drifts expressed in the ECEF frame.</p>	dimensionless	Epoch
ICON_L27_Footpoint_Zonal_Vector_ECEF_Y_South	<p>ECEF Y-Component of Zonal Drift Direction at Southern Footpoint</p> <p>At the Southern footpoint this is the y-component of the unit vector for zonal ion drifts expressed in the ECEF frame.</p>	dimensionless	Epoch
ICON_L27_Footpoint_Zonal_Vector_ECEF_Z_South	<p>ECEF Z-Component of Zonal Drift Direction at Southern Footpoint</p> <p>At the Southern footpoint this is the z-component of the unit vector for zonal ion drifts expressed in the ECEF frame.</p>	dimensionless	Epoch
ICON_L27_Observator_y_Magnetic_Field_X	<p>X Component of the Magnetic Field at the Spacecraft</p> <p>X-component of the magnetic field from IGRF at the spacecraft position, expressed in the ECEF frame.</p>	nT	Epoch
ICON_L27_Observator_y_Magnetic_Field_Y	<p>Y Component of the Magnetic Field at the Spacecraft</p> <p>Y-component of the magnetic field from IGRF at the spacecraft position, expressed in the ECEF frame.</p>	nT	Epoch

Variable Name	Description	Units	Dimensions
ICON_L27_Observator y_Magnetic_Field_Z	Z Component of the Magnetic Field at the Spacecraft Z-component of the magnetic field from IGRF at the spacecraft position, expressed in the ECEF frame.	nT	Epoch
ICON_L27_Equator_Io n_Velocity_Meridional	Equatorial Meridional Ion Velocity Velocity along local magnetic meridional direction, perpendicular to geomagnetic field and within local magnetic meridional plane, field-line mapped to apex/magnetic equator. The meridional vector is purely vertical at the magnetic equator, positive up. Velocity obtained using ion velocities relative to co-rotation in the instrument frame along with the corresponding unit vectors expressed in the instrument frame. Field-line mapping and the assumption of equi-potential field lines is used to translate the locally measured ion motion to the magnetic equator. The mapping is used to determine the change in magnetic field line distance, which, under assumption of equipotential field lines, in turn alters the electric field at that location ($E=V/d$).	m/s	Epoch
ICON_L27_Equator_Io n_Velocity_Zonal	Equatorial Zonal Ion Velocity Velocity along local magnetic zonal direction, perpendicular to geomagnetic field and the local magnetic meridional plane, field-line mapped to apex/magnetic equator. The zonal vector is purely horizontal when mapped to the magnetic equator, positive is generally eastward. Velocity obtained using ion velocities relative to co-rotation in the instrument frame along with the corresponding unit vectors expressed in the instrument frame. Field-line mapping and the assumption of equi-potential field lines is used to translate the locally measured ion motion to the magnetic equator. The mapping is used to determine the change in magnetic field line distance, which, under assumption of equipotential field lines, in turn alters the electric field at that location ($E=V/d$).	m/s	Epoch
ICON_L27_Observator y_Velocity_X	ECI Spacecraft Velocity Velocity of spacecraft in ECI, J2000, coordinates.	m/s	Epoch
ICON_L27_Observator y_Velocity_Y	ECI Spacecraft Velocity Velocity of spacecraft in ECI, J2000, coordinates.	m/s	Epoch
ICON_L27_Observator y_Velocity_Z	ECI Spacecraft Velocity Velocity of spacecraft in ECI, J2000, coordinates.	m/s	Epoch
ICON_L27_Observator y_Corotation_X	ECI Earth Corotation Velocity Components in IVM Coordinates Component of Earth's corotation velocity vector projected into the IVM instrument axes by taking the dot product of the corotation vector with the instrument's axes and multiplying the Y and Z components by negative 1 (but not the X component by convention).	m/s	Epoch

Variable Name	Description	Units	Dimensions
ICON_L27_Observator y_Corotation_Y	ECI Earth Corotation Velocity Components in IVM Coordinates Component of Earth's corotation velocity vector projected into the IVM instrument axes by taking the dot product of the corotation vector with the instrument's axes and multiplying the Y and Z components by negative 1 (but not the X component by convention).	m/s	Epoch
ICON_L27_Observator y_Corotation_Z	ECI Earth Corotation Velocity Components in IVM Coordinates Component of Earth's corotation velocity vector projected into the IVM instrument axes by taking the dot product of the corotation vector with the instrument's axes and multiplying the Y and Z components by negative 1 (but not the X component by convention).	m/s	Epoch
ICON_L27_Solar_Zeni th_Angle	Solar Zenith Angle at Spacecraft Solar Zenith Angle at the spacecraft.	degree s	Epoch
ICON_L27_Ion_Veloci ty_East	IVM measured ion drifts along East, North, and Up directions.	m/s	Epoch
ICON_L27_Ion_Veloci ty_North	IVM measured ion drifts along East, North, and Up directions.	m/s	Epoch
ICON_L27_Ion_Veloci ty_Up	IVM measured ion drifts along East, North, and Up directions.	m/s	Epoch
ICON_L27_Unit_Vecto r_X_East	Basis vector system along East, North, and Up directions for IVM-x axis.		Epoch
ICON_L27_Unit_Vecto r_X_North	Basis vector system along East, North, and Up directions for IVM-x axis.		Epoch
ICON_L27_Unit_Vecto r_X_Up	Basis vector system along East, North, and Up directions for IVM-x axis.		Epoch
ICON_L27_Unit_Vecto r_Y_East	Basis vector system along East, North, and Up directions for IVM-y axis.		Epoch
ICON_L27_Unit_Vecto r_Y_North	Basis vector system along East, North, and Up directions for IVM-y axis.		Epoch
ICON_L27_Unit_Vecto r_Y_Up	Basis vector system along East, North, and Up directions for IVM-y axis.		Epoch
ICON_L27_Unit_Vecto r_Z_East	Basis vector system along East, North, and Up directions for IVM-z axis.		Epoch

Variable Name	Description	Units	Dimensions
ICON_L27_Unit_Vector_Z_North	Basis vector system along East, North, and Up directions for IVM-z axis.		Epoch
ICON_L27_Unit_Vector_Z_Up	Basis vector system along East, North, and Up directions for IVM-z axis.		Epoch
ICON_L27_Footpoint_East_Ion_Velocity_South	Ion drifts at southern footpoint along East, North, and Up directions.	m/s	Epoch
ICON_L27_Footpoint_North_Ion_Velocity_South	Ion drifts at southern footpoint along East, North, and Up directions.	m/s	Epoch
ICON_L27_Footpoint_Up_Ion_Velocity_South	Ion drifts at southern footpoint along East, North, and Up directions.	m/s	Epoch
ICON_L27_Footpoint_East_Ion_Velocity_North	Ion drifts at northern footpoint along East, North, and Up directions.	m/s	Epoch
ICON_L27_Footpoint_North_Ion_Velocity_North	Ion drifts at northern footpoint along East, North, and Up directions.	m/s	Epoch
ICON_L27_Footpoint_Up_Ion_Velocity_North	Ion drifts at northern footpoint along East, North, and Up directions.	m/s	Epoch

Acknowledgement

This is a data product from the NASA Ionospheric Connection Explorer mission, an Explorer launched at 21:59:45 EDT on October 10, 2019. Guidelines for the use of this product are described in the ICON Rules of the Road (<https://icon.ssl.berkeley.edu/Data>)

Responsibility for the mission science falls to the Principal Investigator, Dr. Thomas Immel at UC Berkeley: Immel, T.J., England, S.L., Mende, S.B. et al. Space Sci Rev (2018) 214: 13. <https://doi.org/10.1007/s11214-017-0449-2>

Responsibility for the validation of the L1 data products falls to the instrument lead investigators/scientists.

- * EUV: Dr. Eric Korpela : <https://doi.org/10.1007/s11214-017-0384-2>
- * FUV: Dr. Harald Frey : <https://doi.org/10.1007/s11214-017-0386-0>
- * MIGHTI: Dr. Christoph Englert : <https://doi.org/10.1007/s11214-017-0358-4>, and <https://doi.org/10.1007/s11214-017-0374-4>
- * IVM: Dr. Roderick Heelis : <https://doi.org/10.1007/s11214-017-0383-3>

Responsibility for the validation of the L2 data products falls to those scientists responsible for those products.

- * Daytime O and N2 profiles: Dr. Andrew Stephan : <https://doi.org/10.1007/s11214-018-0477-6>
- * Daytime (EUV) O+ profiles: Dr. Andrew Stephan : <https://doi.org/10.1007/s11214-017-0385-1>
- * Nighttime (FUV) O+ profiles: Dr. Farzad Kamalabadi : <https://doi.org/10.1007/s11214-018-0502-9>
- * Neutral Wind profiles: Dr. Jonathan Makela : <https://doi.org/10.1007/s11214-017-0359-3>
- * Neutral Temperature profiles: Dr. Christoph Englert : <https://doi.org/10.1007/s11214-017-0434-9>
- * Ion Velocity Measurements : Dr. Russell Stoneback : <https://doi.org/10.1007/s11214-017-0383-3>

Responsibility for Level 4 products falls to those scientists responsible for those products.

- * Hough Modes : Dr. Chihoko Yamashita : <https://doi.org/10.1007/s11214-017-0401-5>
- * TIEGCM : Dr. Astrid Maute : <https://doi.org/10.1007/s11214-017-0330-3>
- * SAMI3 : Dr. Joseph Huba : <https://doi.org/10.1007/s11214-017-0415-z>

Pre-production versions of all above papers are available on the ICON website.
<http://icon.ssl.berkeley.edu/Publications>

Overall validation of the products is overseen by the ICON Project Scientist, Dr. Scott England.

NASA oversight for all products is provided by the Mission Scientist, Dr. Jeffrey Klenzing.

Users of these data should contact and acknowledge the Principal Investigator Dr. Immel and the party directly responsible for the data product (noted above) and acknowledge NASA funding for the collection of the data used in the research with the following statement : "ICON is supported by NASA's Explorers Program through contracts NNG12FA45C and NNG12FA42I"

These data are openly available as described in the ICON Data Management Plan available on the ICON website (<http://icon.ssl.berkeley.edu/Data>).

This document was automatically generated on 2022-04-21 11:16 using the file:

ICON_L2-7_IVM-A_2022-01-01_v06r003.NC

Software version: ICON_SDC > IVM L2 Generator v0.17.1

4.1.3 FUV Data Products Functional Description

This subsection details the science data products produced by a particular mission instrument or ground system element (e.g., SOC).

Following this brief overview, details of the data products are provided for L1, L2 and Ancillary products. L0 are instrument level (raw CCD counts, voltages, currents, temperatures, instrument codes etc.) and not interpretable for anyone without intimate knowledge of the instrumentation.

The mission-specific data levels should be defined, and the steps needed to process each level of data shall be described.

The introduction to Section 4 describes the overall data levels for ICON. Table 4.1.3.1 lists the FUV products by level. The FUV Ancillary file provides the geometry relevant to the observations, using knowledge of the spacecraft position and pointing derived from the spacecraft telemetry. The L1 Profiles provide the brightness of the Far Ultraviolet airglow observed by the two instrument wavelength channels, in the form of 6 columns (approximately horizontal) and 256 rows (approximately vertical) for each channel. The Ancillary files provide the corresponding geometry information that accompanies the geometry for both the Shortwave and Longwave Profiles. The L1 Time Delay Integration Images utilize a priori knowledge of the spacecraft position, pointing and motion to motion-compensate the images taken approximately perpendicular to the line of sight. More information is provided in Section 3. The Time Delay Integration Images are currently not used by any higher-level data products. Two Level 2 products are produced for FUV, both utilizing the Ancillary and Profile data. During the daytime the data from both wavelengths are used to determine Column O/N₂ and during nighttime the data from the shortwave profiles are used to determine ionospheric O⁺.

Level	Source (Instrument/Model)	Data Product
0	FUV	L0 FUV Science Data
0	FUV	L0 FUV Engineering Data
Anc.	Ground	FUV Ancillary Data
1	FUV	L1 FUV Shortwave Profiles
1	FUV	L1 FUV Longwave Profiles
1	FUV	L1 FUV Time Delay Integration Sub-limb Images
1	FUV	L1 FUV Time Delay Integration Limb Images
2	FUV	L2 Column O/N ₂
2	FUV	L2 Nighttime O ⁺

Table 4.1.3.1 – List of FUV data products by level.

At a high level, the flow of the FUV data products is shown in Figure 4.1.3.1.

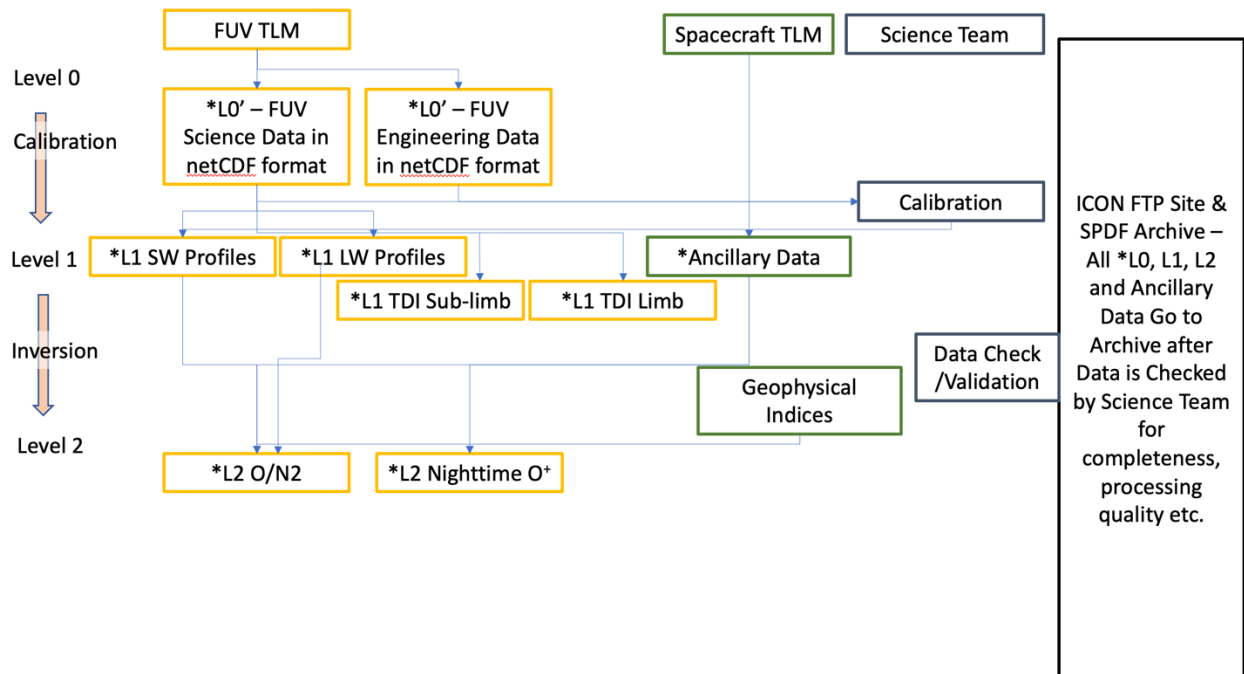


Figure 4.1.3.1 – Schematic of the FUV Data Products and their Flow.

The overall concept for producing the L2 thermospheric composition and ion density is as follows: The FUV instrument measures the brightness of the 135.6 emission from O and a portion of the LBH band structure from N₂ on the limb and sub-limb. From these, the ratio of O to N₂ in the thermosphere can be determined during the day and the density of O⁺ in the ionosphere can be determined during the night (Level 2 products). The L1 product includes the calibrated brightness of the 135.6 and LBH emissions. The view direction of the FUV instrument is nominally 90° to the spacecraft track during day, and moves during nighttime to image along the local magnetic meridian. During the day, the 135.6 and LBH images are given in 6 horizontal and 256 vertical bins, spanning from below the limb to around 500 km altitude. During the night, a 135.6 image is given in 6 horizontal and 256 vertical bins, spanning from below the limb to around 500 km altitude. During the night, a 2 dimensional 135.6 image is given that spans the 24 degree vertical and 18 degree horizontal field of view. During the night, no LBH data is collected. Images are taken every 12s (approximately 100 km along the orbit track) during normal operations. The overall process of producing FUV L1 is shown in Figure 4.1.3.2.

FUV L0 to L1 Calibrated FUV Limb Brightness - Algorithm

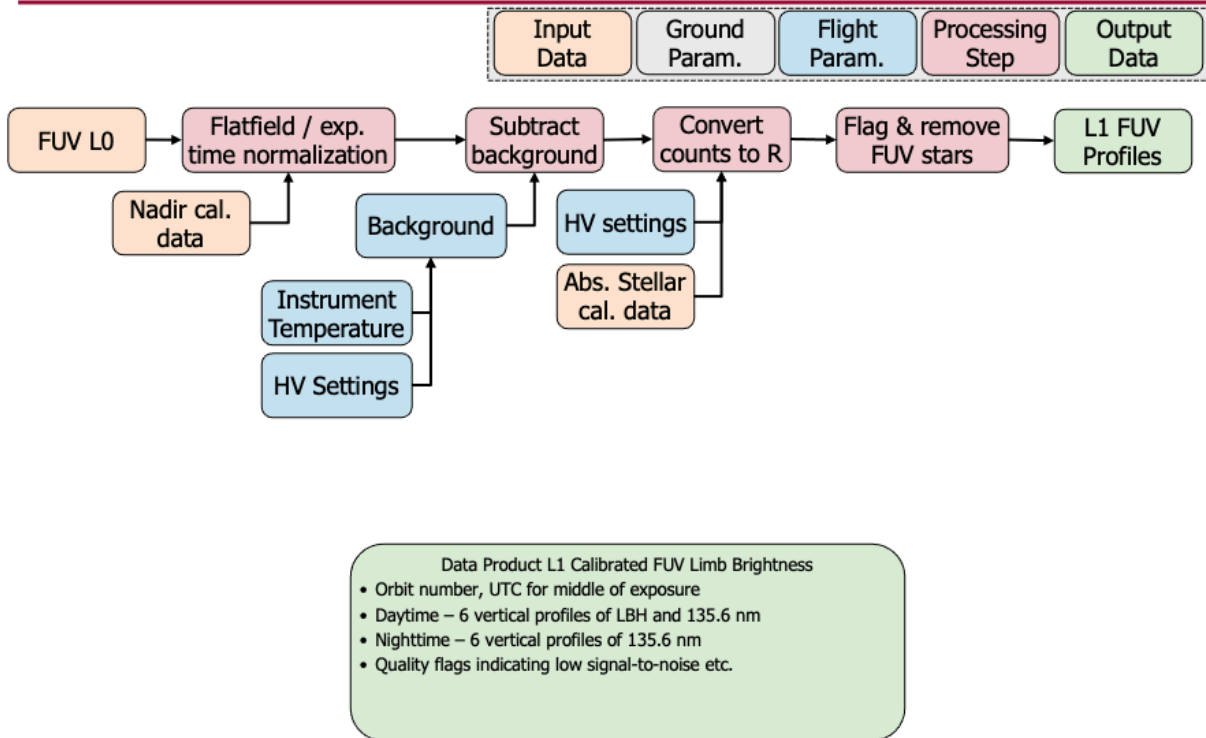


Figure 4.1.3.2 – Overall process for producing FUV L1 Data Product.

L2 thermospheric composition (column O/N₂) is then produced from the FUV L1 (both SW and LW profiles) and Ancillary data product. The FUV instrument measures the brightness of the 135.6 emission from O and a portion of the LBH band structure from N₂ on the limb and sub-limb. The L1 product includes the calibrated ratio of O to N₂ in the thermosphere during the day. The view direction of the FUV instrument is nominally 90° to the spacecraft track during day. During the day, the 135.6 and LBH images are given in 6 horizontal and 256 vertical bins, spanning from below the limb to around 500 km altitude. Using a portion of the image that is below the limb (on the disk), these are converted to total column O/N₂. The remote locations (tangent latitude, longitude etc.) associated with these remotely observed points are reported. Images are taken every 12s (approximately 100 km along the orbit track) during normal operations. The overall process of producing FUV L2 Column O/N₂ Product is shown in Figure 4.1.3.3.

FUV L1 to L2 Disk Column O/N₂ Algorithm

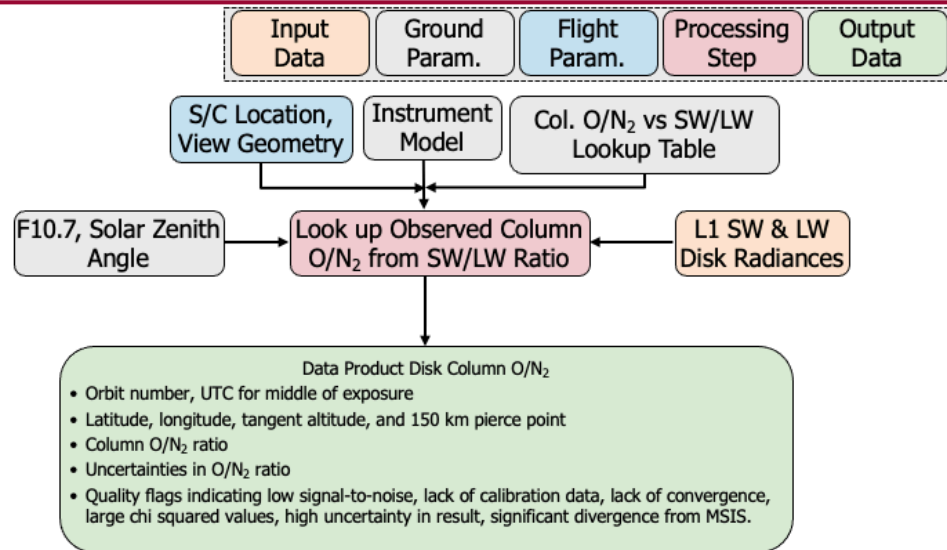


Figure 4.1.3.3 – Overall process for producing FUV L2 Column O/N₂ Data Product.

L2 ionospheric density (O⁺) is produced from the FUV L1 SW profiles and Ancillary data product. The FUV instrument measures the brightness of the 135.6 emission from O⁺ at on the limb and sub-limb. The L1 product includes the calibrated O⁺ density in the ionosphere during the night. The view direction of the FUV instrument moves to image as close to the local magnetic meridian as possible. During the night, a 135.6 image is given in 6 horizontal and 256 vertical bins, spanning from below the limb to around 500 km altitude. These are converted into 6x256 profiles of O⁺ density on the limb / sub-limb. The remote locations (tangent latitude, longitude etc.) associated with these remotely observed points are reported. Images are taken every 12s (approximately 100 km along the orbit track) during normal operations. The overall process of producing FUV L2 nighttime O⁺ Product is shown in Figure 4.1.3.4.

FUV L1 to L2 Nighttime O⁺ - Algorithm

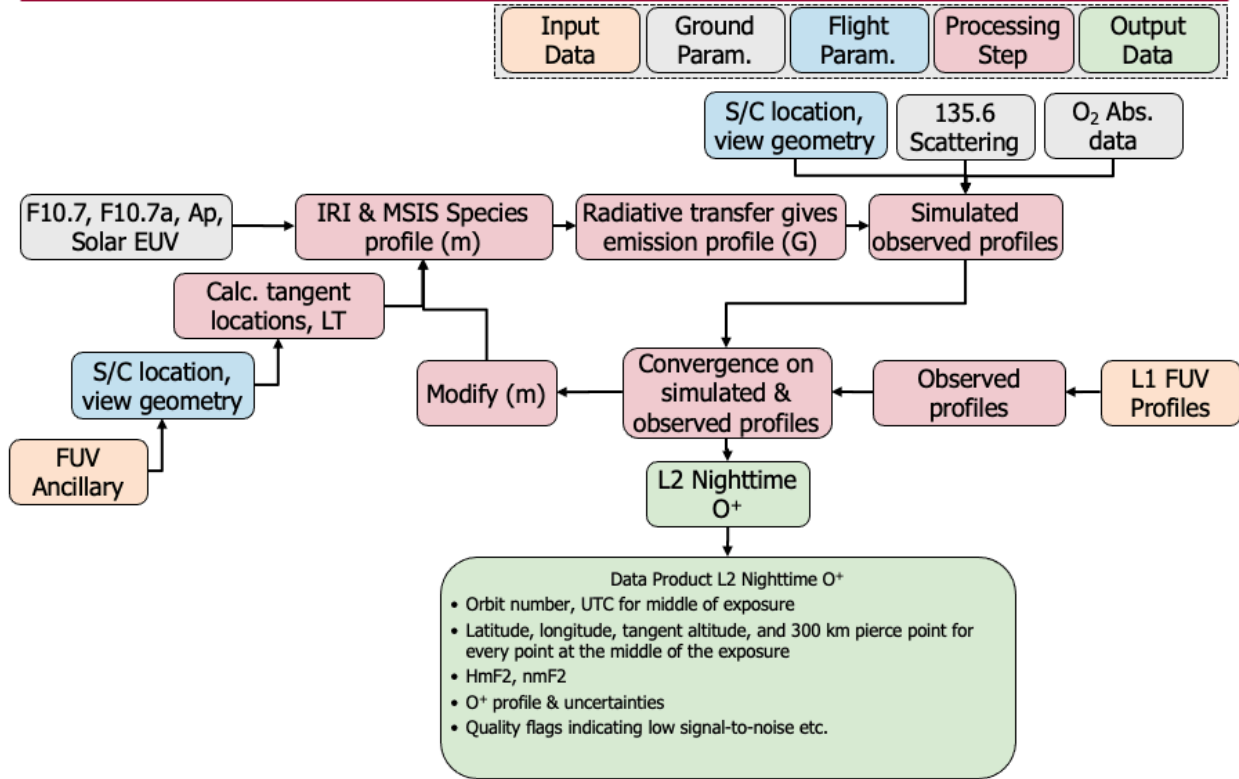


Figure 4.1.3.4 – Overall process for producing FUV L2 Nighttime O⁺ Data Product.

For more details on the data processing, the reader is directed to the ICON Calibration and Measurement Algorithms Document (CMAD).

A reference to the general data level definitions located in the Heliophysics Science Data Management Policy should be included.

The Heliophysics Science Data Management Policy, HPD-SDMP version 2.0, effective February 14, 2022 does not describe data levels. The ICON data levels closely follow those in the PDMP Template.

Any associated metadata products to be generated and maintained shall also be described.

Following this brief overview, full details of the metadata for each product are provided.

Details should also include the cadence (e.g., hourly, daily, etc.) for processing of data products.

The lowest level FUV science data (L0) has one file per 12s for each of the SW and LW profiles during the day, and the SW profiles, the sub-limb and limb TDI images at night. These are

processed as they arrive on the ground, until an entire day of data has arrived at the Science Data Center (SDC). The SDC processes the L0 into L1 and L2, and produces the Ancillary Data Products. All L1, Ancillary and L2 files have 1 file corresponding to 1 day of data. At Level 1, there is 1 file for the SW profiles, 1 for the LW profiles, 1 for the sub-limb TDI images and 1 for the limb TDI images each day. There is 1 Ancillary file per day, and 1 file for the L2 O/N₂ product and a final file for the L2 O⁺ product. The cadence for production of all products beyond L0 is daily once all inputs are available. As one example, the ancillary products use the definitive ephemeris, which is generated by the Mission Operations Center approximately 1 week after real-time. The Level 1 radiances also rely upon stellar, background, and nadir calibrations that are performed monthly, and so the Level 1 files can take a month for all inputs to be ready.

The following section contains detailed descriptions of each of the FUV Data Products, the data and metadata contained within.

ICON FUV Science Level 1 Data

This document describes the data product for ICON FUV Level 1 FUV-A Altitude Profile File, which is in NetCDF4 format.

The ICON Far UltraViolet (FUV) imager contributes to the ICON science objectives by providing remote sensing measurements of the daytime and nighttime atmosphere/ ionosphere. During sunlit atmospheric conditions, ICON FUV images the limb altitude profile in the shortwave (SW) band at 135.6 nm and the longwave (LW) band at 157 nm perpendicular to the satellite motion to retrieve the atmospheric O/N₂ ratio. In conditions of atmospheric darkness, ICON FUV measures the 135.6 nm recombination emission of O⁺ ions used to compute the nighttime ionospheric altitude distribution.

The ICON Far Ultra-Violet (FUV) imager is a Czerny–Turner design Spectrographic Imager with two exit slits and corresponding back imager cameras that produce two independent images in separate wavelength bands on two detectors. For this science product, the 18x24 degree FOV is divided and co-added to produce 6 high sensitivity profiles with each nominally 12 second integration. These inform daytime and nighttime retrievals of the ionospheric composition and density (See Stephan et al and Kamalabadi et al, noted in the acknowledgements section of this file). Pointing and geolocation information are available in the FUV ancillary data also available at <https://icon.ssl.berkeley.edu>

More details about the mission, data products, responsibility, and data use can be found at the end of this document.

Each FUV Level-1 file contains global attributes explaining the major properties of the file and variables. This is an example from one file.

0 ACKNOWLEDGEMENT This is a data product from the NASA Ionospheric Connection Explorer mission, an Explorer launched at 21:59:45 EDT on October 10, 2019, from Cape Canaveral AFB in the USA. Guidelines for the use of this product are described in the ICON Rules of the Road (<http://icon.ssl.berkeley.edu/Data>).

1 ADID_REF NASA Contract > NNG12F45C

2 CALIBRATION_FILE See calibration files in general attribute fields FLATFIELD_CORRECTION, BACKGROUND_CORRECTION, RAYLEIGH_CONVERSION

3 CONVENTIONS SPDF ISTEP/IACF Modified for NetCDF (v0.8)

4 DATA_LEVEL L1

5 DATA_TYPE APIDxE3 > ICON Application ID 0xE3: FUV Science Level 0.5 Data > FUV Science Level 1 Data

6 DATA_REVISION 0

7 DATA_VERSION 2.00000

8 DATA_VERSION_MAJOR 2

9 DATE_END 2020-07-05T00:00:00 UTC

10 DATE_START 2020-07-04T00:00:00 UTC

11 DATE_STOP 2020-07-05T00:00:00 UTC

12 DESCRIPTION ICON FUV Level 1 FUV-A Altitude Profile File

13 DESCRIPTOR FUV-A > ICON FUV-A L1 Science Altitude Profile File

14 DISCIPLINE Space Physics > Ionospheric Science

15 FILE ICON_L1_FUV_SWP_20200704_v02r000.NC

16 FILE_DATE Tue Aug 11 17:08:39 2020

17 GENERATED_BY ICON SDC > ICON FUV L1 Processor v1, Tori Fae (tfae@paradigm.ssl.berkeley.edu) and Harald Frey (hfrey@ssl.berkeley.edu)

18 GENERATION_DATE 20200812

19 HISTORY Version 2, Created by ICON FUV L1 processing with `icn_fuv_create_swp_structure.pro` Fri Sep 18 12:06:56 2020

MODIFICATION HISTORY:

Written by: Harald Frey, Date: December 08, 2016

2019-12-11 major updates for calibration conversion

2020-01-22 made stripes consistent with LW, P6 looking forward, background, error

2020-03-20 new backgrounds, flatfields, quality parameter etc.

2020-04-06 allow negative values, bkg variable in Rayleighs etc.
2020-05-28 new background, uncertainty, stars removed
2020-08-17 no negative values sublimb, new attributes, turrets, new calibration conversion 2300 V, mark insufficient HV
2020-09-14 correctly deal with forced turret for sun protection
20 HTTP_LINK <http://icon.ssl.berkeley.edu>
21 INSTRUMENT FUV-A
22 INSTRUMENT_TYPE Imagers (Space)
23 LINK_TEXT All ICON information and data can be found at the ICON web page icon.ssl.berkeley.edu
24 LINK_TITLE ICON Website
25 LOGICAL_FILE_ID ICON_L1_FUV_SWP_20200704_v02r000
26 LOGICAL_SOURCE ICON_L0P_FUV-A_Science-TDI0_2020-07-04
27 LOGICAL_SOURCE_DESCRIPTION ICON FUV-A Level 1 Science Altitude Profile File
28 MISSION_GROUP Ionospheric Investigations
29 MODS See history
30 PARENTS Names of all L0 Files
31 PI_AFFILIATION UC Berkeley > SSL
32 PI_NAME T. J. Immel
33 PROJECT NASA > ICON
34 RULES_OF_USE Public Data for Scientific Use
35 SOFTWARE_VERSION ICON SDC > ICON FUV L1 Processor v1.0
36 SOURCE_NAME ICON > Ionospheric Connection Explorer
37 SPACECRAFT_ID NASA > ICON - 493
38 TEXT ICON explores the boundary between Earth and space - the ionosphere - to understand the physical connection between our world and the immediate space environment around us. Visit '<http://icon.ssl.berkeley.edu>' for more details.
39 TIME_RESOLUTION 12000 milliseconds
40 TITLE ICON FUV Level 1 FUV-A Altitude Profile File
41 EPOCH0 1970-01-01/00:00:00
42 FILE_NAMING_CONVENTION source_datatype_descriptor
43 PROCESS_LEVEL L1
44 SAMPLE_TIME 12
45 SAMPLE_UNIT Seconds
46 SATELLITE_ID ICON
47 TEXT_SUPPLEMENT Explanation of global attributes
48 FLATFIELD_CORRECTION Values of flatfield correction for each stripe
49 BACKGROUND_CORRECTION saa_files_2020-035
50 RAYLEIGH_CONVERSION Values for Rayleigh conversion

Use of this product for analysis depends on the combined use of the ancillary FUV data product which contains geopositioning data and instrument pointing details.

History

Version 5 Created by ICON FUV L1 processing with `icn_fuv_create_swp_structure.pro` Wed Apr 20 10:30:04 2022

MODIFICATION HISTORY:

Written by: Harald Frey, Date: December 08, 2016

2019-12-11 major updates for calibration conversion

2020-01-22 made stripes consistent with LW, P6 looking forward, background, error

2020-03-20 new backgrounds, flatfields, quality parameter etc.

2020-04-06 allow negative values, bkg variable in Rayleighs etc.

2020-05-28 new background, uncertainty, stars removed

2020-08-17 no negative values sublimb, new attributes, turrets, new calibration conversion 2300 V, mark insufficient HV

2020-09-14 correctly deal with forced turret for sun protection
2020-10-22 MCP sensitivity loss corrected
2021-06-08 major update on background and flatfield
2022-02-20 major update on background, calibration, day cleanup
2022-04-06 new uncertainty calculator uncertainty_calculator_v3r1.py

Dimensions

NetCDF files contain **variables** and the **dimensions** over which those variables are defined. First, the dimensions are defined, then all variables in the file are described.

The dimensions used by the variables in this file are given below, along with nominal sizes. Note that the size may vary from file to file. For example, the "Epoch" dimension, which describes the number of time samples contained in this file, will have a varying size.

Dimension Name	Nominal Size
Epoch	6938
Rows	256
Columns	1
Stripes	6

Variables

Variables in this file are listed below. First, "data" variables are described, followed by the "support_data" variables, and finally the "metadata" variables. The variables classified as "ignore_data" are not shown.

data

Variable Name	Description	Units	Dimensions
ICON_L1_FUVA_SWP_Raw_M9	FUVA SW channel raw CCD counts profile for -9 to -6 degrees FOV Vertical raw CCD counts profile for -9 to -6 degrees FOV	counts	Epoch, Rows
ICON_L1_FUVA_SWP_Raw_M6	FUVA SW channel raw CCD counts profile for -6 to -3 degrees FOV Vertical raw CCD counts profile for -6 to -3 degrees FOV	counts	Epoch, Rows
ICON_L1_FUVA_SWP_Raw_M3	FUVA SW channel raw CCD counts profile for -3 to 0 degrees FOV Vertical raw CCD counts profile for -3 to 0 degrees FOV	counts	Epoch, Rows
ICON_L1_FUVA_SWP_Raw_P0	FUVA SW channel raw CCD counts profile for 0 to +3 degrees FOV Vertical raw CCD counts profile for 0 to +3 degrees FOV	counts	Epoch, Rows
ICON_L1_FUVA_SWP_Raw_P3	FUVA SW channel raw CCD counts profile for +3 to +6 degrees FOV Vertical raw CCD counts profile for +3 to +6 degrees FOV	counts	Epoch, Rows
ICON_L1_FUVA_SWP_Raw_P6	FUVA SW channel raw CCD counts profile for +6 to +9 degrees FOV Vertical raw CCD counts profile for +6 to +9 degrees FOV	counts	Epoch, Rows
ICON_L1_FUVA_SWP_PROFILE_M9	FUVA SW channel altitude column brightness for -9 to -6 degrees FOV Vertical profile for -9 to -6 degrees FOV	Rayleigh	Epoch, Rows
ICON_L1_FUVA_SWP_PROFILE_M6	FUVA SW channel altitude column brightness for -6 to -3 degrees FOV Vertical profile for -6 to -3 degrees FOV	Rayleigh	Epoch, Rows
ICON_L1_FUVA_SWP_PROFILE_M3	FUVA SW channel altitude column brightness for -3 to 0 degrees FOV Vertical profile for -3 to 0 degrees FOV	Rayleigh	Epoch, Rows
ICON_L1_FUVA_SWP_PROFILE_P0	FUVA SW channel altitude column brightness for 0 to +3 degrees FOV Vertical profile for 0 to +3 degrees FOV	Rayleigh	Epoch, Rows

Variable Name	Description	Units	Dimensions
ICON_L1_FUVA_SWP_PR OF_P3	FUVA SW channel altitude column brightness for +3 to +6 degrees FOV Vertical profile for +3 to +6 degrees FOV	Rayleigh	Epoch, Rows
ICON_L1_FUVA_SWP_PR OF_P6	FUVA SW channel altitude column brightness for +6 to +9 degrees FOV Vertical profile for +6 to +9 degrees FOV	Rayleigh	Epoch, Rows
ICON_L1_FUVA_SWP_PR OF_M9_Error	FUVA SW channel altitude column brightness for -9 to -6 degrees FOV error Vertical profile for -9 to -6 degrees FOV error using uncertainty_calculator_v2r0. Statistical 1-sigma error values associated with the brightness profiles. After estimating the instrument gain and the background signal statistics from the 24 hours of brightness profiles, 1-sigma errors are calculated for each altitude profile as a function of these quantities and the measured signal level.	Rayleigh	Epoch, Rows
ICON_L1_FUVA_SWP_PR OF_M6_Error	FUVA SW channel altitude column brightness for -6 to -3 degrees FOV error Vertical profile for -6 to -3 degrees FOV error using uncertainty_calculator_v2r0. Statistical 1-sigma error values associated with the brightness profiles. After estimating the instrument gain and the background signal statistics from the 24 hours of brightness profiles, 1-sigma errors are calculated for each altitude profile as a function of these quantities and the measured signal level.	Rayleigh	Epoch, Rows
ICON_L1_FUVA_SWP_PR OF_M3_Error	FUVA SW channel altitude column brightness for -3 to 0 degrees FOV error Vertical profile for -3 to 0 degrees FOV error using uncertainty_calculator_v2r0. Statistical 1-sigma error values associated with the brightness profiles. After estimating the instrument gain and the background signal statistics from the 24 hours of brightness profiles, 1-sigma errors are calculated for each altitude profile as a function of these quantities and the measured signal level.	Rayleigh	Epoch, Rows
ICON_L1_FUVA_SWP_PR OF_P0_Error	FUVA SW channel altitude column brightness for 0 to +3 degrees FOV error Vertical profile for 0 to +3 degrees FOV error using uncertainty_calculator_v2r0. Statistical 1-sigma error values associated with the brightness profiles. After estimating the instrument gain and the background signal statistics from the 24 hours of brightness profiles, 1-sigma errors are calculated for each altitude profile as a function of these quantities and the measured signal level.	Rayleigh	Epoch, Rows

Variable Name	Description	Units	Dimensions
ICON_L1_FUVA_SWP_PR OF_P3_Error	FUVA SW channel altitude column brightness for +3 to +6 degrees FOV error Vertical profile for +3 to +6 degrees FOV error using uncertainty_calculator_v2r0. Statistical 1-sigma error values associated with the brightness profiles. After estimating the instrument gain and the background signal statistics from the 24 hours of brightness profiles, 1-sigma errors are calculated for each altitude profile as a function of these quantities and the measured signal level.	Rayleigh	Epoch, Rows
ICON_L1_FUVA_SWP_PR OF_P6_Error	FUVA SW channel altitude column brightness for +6 to +9 degrees FOV error Vertical profile for +6 to +9 degrees FOV error using uncertainty_calculator_v2r0. Statistical 1-sigma error values associated with the brightness profiles. After estimating the instrument gain and the background signal statistics from the 24 hours of brightness profiles, 1-sigma errors are calculated for each altitude profile as a function of these quantities and the measured signal level.	Rayleigh	Epoch, Rows
ICON_L1_FUVA_SWP_PR OF_M9_BKG	FUVA SW channel altitude column brightness for -9 to -6 degrees FOV background Vertical profile for -9 to -6 degrees FOV bkg	Rayleigh	Epoch, Rows
ICON_L1_FUVA_SWP_PR OF_M6_BKG	FUVA SW channel altitude column brightness for -6 to -3 degrees FOV background Vertical profile for -6 to -3 degrees FOV bkg	Rayleigh	Epoch, Rows
ICON_L1_FUVA_SWP_PR OF_M3_BKG	FUVA SW channel altitude column brightness for -3 to 0 degrees FOV background Vertical profile for -3 to 0 degrees FOV bkg	Rayleigh	Epoch, Rows
ICON_L1_FUVA_SWP_PR OF_P0_BKG	FUVA SW channel altitude column brightness for 0 to +3 degrees FOV background Vertical profile for 0 to +3 degrees FOV bkg	Rayleigh	Epoch, Rows
ICON_L1_FUVA_SWP_PR OF_P3_BKG	FUVA SW channel altitude column brightness for +3 to +6 degrees FOV background Vertical profile for +3 to +6 degrees FOV bkg	Rayleigh	Epoch, Rows
ICON_L1_FUVA_SWP_PR OF_P6_BKG	FUVA SW channel altitude column brightness for +6 to +9 degrees FOV background Vertical profile for +6 to +9 degrees FOV bkg	Rayleigh	Epoch, Rows
ICON_L1_FUVA_SWP_PR OF_M9_CLEAN	FUVA SW channel altitude column brightness for -9 to -6 degrees FOV without stars Vertical profile for -9 to -6 degrees FOV without stars using artifact_removal_v2r2	Rayleigh	Epoch, Rows

Variable Name	Description	Units	Dimensions
ICON_L1_FUVA_SWP_P OF_M6_CLEAN	FUVA SW channel altitude column brightness for -6 to -3 degrees FOV without stars Vertical profile for -6 to -3 degrees FOV without stars using artifact_removal_v2r2	Rayleigh	Epoch, Rows
ICON_L1_FUVA_SWP_P OF_M3_CLEAN	FUVA SW channel altitude column brightness for -3 to 0 degrees FOV without stars Vertical profile for -3 to 0 degrees FOV without stars using artifact_removal_v2r2	Rayleigh	Epoch, Rows
ICON_L1_FUVA_SWP_P OF_P0_CLEAN	FUVA SW channel altitude column brightness for 0 to +3 degrees FOV without stars Vertical profile for 0 to +3 degrees FOV without stars using artifact_removal_v2r2	Rayleigh	Epoch, Rows
ICON_L1_FUVA_SWP_P OF_P3_CLEAN	FUVA SW channel altitude column brightness for +3 to +6 degrees FOV without stars Vertical profile for +3 to +6 degrees FOV without stars using artifact_removal_v2r2	Rayleigh	Epoch, Rows
ICON_L1_FUVA_SWP_P OF_P6_CLEAN	FUVA SW channel altitude column brightness for +6 to +9 degrees FOV without stars Vertical profile for +6 to +9 degrees FOV without stars using artifact_removal_v2r2	Rayleigh	Epoch, Rows

support_data

Variable Name	Description	Units	Dimensions
Epoch	Epoch Center time of the exposure, milliseconds after 1970-01-01/00:00:00 UT	milliseconds	Epoch
ICON_L1_FUVA_SWP_Start_Times	Start time Start time of the exposure, UT		Epoch
ICON_L1_FUVA_SWP_Stop_Times	Stop time Stop time of the exposure, UT		Epoch
ICON_L1_FUVA_SWP_Center_Times	Center time Center time of the exposure, UT		Epoch
ICON_L1_FUVA_SWP_Integration_Time	Time Integration time for integration in seconds	seconds	Epoch

Variable Name	Description	Units	Dimensions
ICON_L1_FUVA_SWP_Chain_ID	Number Chain ID for integration in seconds	number	Epoch
ICON_L1_FUVA_SWP_Quality_Flag	Quality indicator (also quickly shows times when images are available) QUALITY_FLAG is an indicator of data quality = 0 = No errors or quality conditions, LVLH 1 = No errors or quality conditions, R-LVLH 2 = Lunar calibration 3 = Insufficient high voltage 4 = Nadir calibration 5 = Zero wind calibration 6 = Bad pointing 7 = S/C attitude slew 8 = Conjugate observation 9 = Stellar calibration 10 = Unreliable background subtracted 17 = unspecified error condition	number	Epoch
ICON_L1_FUV_Mode	Data collection mode Data collection mode of FUV instrument 1 = Dayside science 2 = Nightside science 3 = Calibration 4 = Nadir 5 = Conjugate 6 = Stars 7 = Ram 8 = Off Target 9 = Engineering 13 = Unknown	number	Epoch
ICON_L1_FUVA_SWP_HV_PHOS	HV of SW channel phosphor HV of phosphor screen	Volt	Epoch
ICON_L1_FUVA_SWP_HV_MCP	HV of SW channel MCP HV of MCP	Volt	Epoch
ICON_L1_FUV_Turret	FUV turret angle FUV turret angle in degrees with respect to nominal center position	degree	Epoch
ICON_L1_FUVA_CCD_TEMP	FUVA CCD temperature FUVA CCD temperature	degree C	Epoch
ICON_L1_FUVA_Board_TEMP	FUVA board temperature FUVA digital board temperature	degree C	Epoch
ICON_L1_FUVA_HV_TEMP	FUVA HVPS temperature FUVA HVPS temperature	degree C	Epoch

Variable Name	Description	Units	Dimensions
ICON_L1_FUV_IMG_TEMP	FUV imager enclosure temperature FUV imager enclosure temperature	degree C	Epoch
ICON_L1_FUV_OPT_TEMP	FUV optics bench temperature FUV optics bench temperature	degree C	Epoch
ICON_L1_FUV_Turret_TEMP	FUV turret temperature FUV turret temperature	degree C	Epoch
ICON_L1_FUV_Scan_TEMP	FUV scan mirror temperature FUV scan mirror temperature	degree C	Epoch
ICON_L1_FUVA_SWP_GAIN_DAY	Average value of CCD output electrons per primary photo-electron in the image tube during day. It is calculated using the statistics of 24 hours of day profiles. Gain of each stripe is calculated independently. Gain for profiles	CCD electrons / photo-electron	Stripes
ICON_L1_FUVA_SWP_GAIN_NIGHT	Average value of CCD output electrons per primary photo-electron in the image tube during night. It is calculated using the statistics of 24 hours of night profiles. Gain of each stripe is calculated independently. Gain for profiles	CCD electrons / photo-electron	Stripes

metadata

Variable Name	Description	Units	Dimensions
Rows	Row Number Vertical row numbers for profiles	number	Rows
ICON_L1_FUVA_Azimuth	Azimuth of FUVA channel with respect to spacecraft coordinates FUVA channel pointing azimuth	degree	Epoch
ICON_L1_FUVA_Elevation	Elevation of FUVA channel with respect to spacecraft coordinates FUVA channel pointing elevation	degree	Epoch
ICON_L1_FUVA_Roll	Roll of FUVA channel with respect to spacecraft coordinates FUVA channel pointing roll	degree	Epoch

Acknowledgement

This is a data product from the NASA Ionospheric Connection Explorer mission, an Explorer launched at 21:59:45 EDT on October 10, 2019, from Cape Canaveral AFB in the USA. Guidelines for the use of this product are described in the ICON Rules of the Road (<http://icon.ssl.berkeley.edu/Data>).

Responsibility for the mission science falls to the Principal Investigator, Dr. Thomas Immel at UC Berkeley: Immel, T.J., England, S.L., Mende, S.B. et al. Space Sci Rev (2018) 214: 13. <https://doi.org/10.1007/s11214-017-0449-2>

Responsibility for the validation of the L1 data products falls to the instrument lead investigators/scientists.

* EUV: Dr. Eric Korpela : <https://doi.org/10.1007/s11214-017-0384-2>

* FUV: Dr. Harald Frey : <https://doi.org/10.1007/s11214-017-0386-0>

* MIGHTI: Dr. Christoph Englert : <https://doi.org/10.1007/s11214-017-0358-4>, and <https://doi.org/10.1007/s11214-017-0374-4>

* IVM: Dr. Roderick Heelis : <https://doi.org/10.1007/s11214-017-0383-3>

Responsibility for the validation of the L2 data products falls to those scientists responsible for those products.

* Daytime O and N2 profiles: Dr. Andrew Stephan : <https://doi.org/10.1007/s11214-018-0477-6>

* Daytime (EUV) O+ profiles: Dr. Andrew Stephan : <https://doi.org/10.1007/s11214-017-0385-1>

* Nighttime (FUV) O+ profiles: Dr. Farzad Kamalabadi : <https://doi.org/10.1007/s11214-018-0502-9>

* Neutral Wind profiles: Dr. Jonathan Makela : <https://doi.org/10.1007/s11214-017-0359-3>

* Neutral Temperature profiles: Dr. Christoph Englert : <https://doi.org/10.1007/s11214-017-0434-9>

* Ion Velocity Measurements : Dr. Russell Stoneback : <https://doi.org/10.1007/s11214-017-0383-3>

Responsibility for Level 4 products falls to those scientists responsible for those products.

* Hough Modes : Dr. Chihoko Yamashita : <https://doi.org/10.1007/s11214-017-0401-5>

* TIEGCM : Dr. Astrid Maute : <https://doi.org/10.1007/s11214-017-0330-3>

* SAMI3 : Dr. Joseph Huba : <https://doi.org/10.1007/s11214-017-0415-z>

Pre-production versions of all above papers are available on the ICON website.

<http://icon.ssl.berkeley.edu/Publications>

Overall validation of the products is overseen by the ICON Project Scientist, Dr. Scott England.

NASA oversight for all products is provided by the Mission Scientist, Dr. Jeffrey Klenzing.

Users of these data should contact and acknowledge the Principal Investigator Dr. Immel and the party directly responsible for the data product (noted above) and acknowledge NASA funding for the collection of the data used in the research with the following statement : "ICON is supported by NASA's Explorers Program through contracts NNG12FA45C and NNG12FA42I".

These data are openly available as described in the ICON Data Management Plan available on the ICON website (<http://icon.ssl.berkeley.edu/Data>).

This document was automatically generated on 2022-04-25 09:11 using the file:

ICON_L1_FUV_SWP_2022-03-31_v05r001.NC

Software version: ICON SDC > ICON FUV L1 Processor version 2022-04-06 > UIUC FUV L1 Post-Processor v1.2

ICON FUV Science Level 1 Data

This document describes the data product for ICON FUV Level 1 FUV-B Altitude Profile File, which is in NetCDF4 format.

The ICON Far UltraViolet (FUV) imager contributes to the ICON science objectives by providing remote sensing measurements of the daytime and nighttime atmosphere/ ionosphere. During sunlit atmospheric conditions, ICON FUV images the limb altitude profile in the shortwave (SW) band at 135.6 nm and the longwave (LW) band at 157 nm perpendicular to the satellite motion to retrieve the atmospheric O/N₂ ratio. In conditions of atmospheric darkness, ICON FUV measures the 135.6 nm recombination emission of O⁺ ions used to compute the nighttime ionospheric altitude distribution.

The ICON Far Ultra-Violet (FUV) imager is a Czerny–Turner design Spectrographic Imager with two exit slits and corresponding back imager cameras that produce two independent images in separate wavelength bands on two detectors. For this science product, the 18x24 degree FOV is divided and co-added to produce 6 high sensitivity profiles with each nominally 12 second integration. These inform daytime and nighttime retrievals of the ionospheric composition and density (See Stephan et al and Kamalabadi et al, noted in the acknowledgements section of this file). Pointing and geolocation information are available in the FUV ancillary data also available at <https://icon.ssl.berkeley.edu>

More details about the mission, data products, responsibility, and data use can be found at the end of this document.

Each FUVB Level-1 file contains global attributes explaining the major properties of the file and variables. This is an example from one file.

0 ACKNOWLEDGEMENT This is a data product from the NASA Ionospheric Connection Explorer mission, an Explorer launched at 21:59:45 EDT on October 10, 2019, from Cape Canaveral AFB in the USA. Guidelines for the use of this product are described in the ICON Rules of the Road (<http://icon.ssl.berkeley.edu/Data>).

1 ADID_REF NASA Contract > NNG12F45C

2 CALIBRATION_FILE See calibration files in general attribute fields FLATFIELD_CORRECTION, BACKGROUND_CORRECTION, RAYLEIGH_CONVERSION

3 CONVENTIONS SPDF ISTEP/IACF Modified for NetCDF (v0.8)

4 DATA_LEVEL L1

5 DATA_TYPE APIDxE3 > ICON Application ID 0xE3: FUV Science Level 0.5 Data > FUV Science Level 1 Data

6 DATA_REVISION 0

7 DATA_VERSION 2.00000

8 DATA_VERSION_MAJOR 2

9 DATE_END 2020-02-04T23:59:53 UTC

10 DATE_START 2020-02-04T00:00:00 UTC

11 DATE_STOP 2020-02-04T23:59:53 UTC

12 DESCRIPTION ICON FUV Level 1 FUV-B Altitude Profile File

13 DESCRIPTOR FUV-B > ICON FUV-B L1 Science Altitude Profile File

14 DISCIPLINE Space Physics > Ionospheric Science

15 FILE ICON_L1_FUV_LWP_20200204_v02r000.NC

16 FILE_DATE Fri Aug 14 08:31:44 2020

17 GENERATED_BY ICON SDC > ICON FUV L1 Processor v1, Tori Fae (tfae@paradigm.ssl.berkeley.edu) and Harald Frey (hfrey@ssl.berkeley.edu)

18 GENERATION_DATE 20200814

19 HISTORY Version 2 Created by ICON FUV L1 processing with `icn_fuv_create_lwp_structure.pro` Fri Sep 18 12:06:56 2020

MODIFICATION HISTORY:

Written by: Harald Frey, Date: January 27, 2017

2019-12-11 major updates for calibration conversion

2020-01-22 made stripes consistent with LW, P6 looking forward, background, error

2020-03-20 new backgrounds, flatfields, quality parameter etc.

2020-04-06 allow negative values, bkg variable in Rayleighs etc.
2020-05-28 new background, uncertainty, stars removed
2020-08-17 no negative values sublimb, new attributes, turrets, mark insufficient HV
2020-09-14 correctly deal with forced turret for sun protection
20 HTTP_LINK <http://icon.ssl.berkeley.edu>
21 INSTRUMENT FUV-B
22 INSTRUMENT_TYPE Imagers (Space)
23 LINK_TEXT All ICON information and data can be found at the ICON web page icon.ssl.berkeley.edu
24 LINK_TITLE ICON Website
25 LOGICAL_FILE_ID ICON_L1_FUV_LWP_20200204_v02r000
26 LOGICAL_SOURCE ICON_L0P_FUV-B_Science-TD11_2020-02-04
27 LOGICAL_SOURCE_DESCRIPTION ICON FUV-B Level 1 Science Altitude Profile File
28 MISSION_GROUP Ionospheric Investigations
29 MODS See history
30 PARENTS Names of all L0 Files
31 PI_AFFILIATION UC Berkeley > SSL
32 PI_NAME T. J. Immel
33 PROJECT NASA > ICON
34 RULES_OF_USE Public Data for Scientific Use
35 SOFTWARE_VERSION ICON SDC > ICON FUV L1 Processor v1.0
36 SOURCE_NAME ICON > Ionospheric Connection Explorer
37 SPACECRAFT_ID NASA > ICON - 493
38 TEXT ICON explores the boundary between Earth and space - the ionosphere - to understand the physical connection between our world and the immediate space environment around us. Visit '<http://icon.ssl.berkeley.edu>' for more details.
39 TIME_RESOLUTION 12000 milliseconds
40 TITLE ICON FUV Level 1 FUV-B Altitude Profile File
41 EPOCH0 1970-01-01/00:00:00
42 FILE_NAMING_CONVENTION source_datatype_descriptor
43 PROCESS_LEVEL L1
44 SAMPLE_TIME 12
45 SAMPLE_UNIT Seconds
46 SATELLITE_ID ICON
47 TEXT_SUPPLEMENT Explanation of global attributes
48 FLATFIELD_CORRECTION Values of flatfield correction for each stripe
49 BACKGROUND_CORRECTION saa_files_2020-035
50 RAYLEIGH_CONVERSION Values for Rayleigh conversion

Use of this product for analysis depends on the combined use of the ancillary FUV data product which contains geopositioning data and instrument pointing details.

History

Version 5 Created by ICON FUV L1 processing with `icn_fuv_create_lwp_structure.pro` Wed Apr 20 10:21:52 2022

MODIFICATION HISTORY:

Written by: Harald Frey, Date: January 27, 2017

2019-12-11 major updates for calibration conversion

2020-01-22 made stripes consistent with LW, P6 looking forward, background, error

2020-03-20 new backgrounds, flatfields, quality parameter etc.

2020-04-06 allow negative values, bkg variable in Rayleighs etc.

2020-05-28 new background, uncertainty, stars removed

2020-08-17 no negative values sublimb, new attributes, turrets, mark insufficient HV

2020-09-14 correctly deal with forced turret for sun protection

2020-10-22 MCP sensitivity loss corrected

2021-06-08 major update on background and flatfield
2022-02-20 major update on background, calibration, day cleanup
2022-04-06 new uncertainty calculator uncertainty_calculator_v3r1.py

Dimensions

NetCDF files contain **variables** and the **dimensions** over which those variables are defined. First, the dimensions are defined, then all variables in the file are described.

The dimensions used by the variables in this file are given below, along with nominal sizes. Note that the size may vary from file to file. For example, the "Epoch" dimension, which describes the number of time samples contained in this file, will have a varying size.

Dimension Name	Nominal Size
Epoch	4558
Rows	256
Columns	1
Stripes	6

Variables

Variables in this file are listed below. First, "data" variables are described, followed by the "support_data" variables, and finally the "metadata" variables. The variables classified as "ignore_data" are not shown.

data

Variable Name	Description	Units	Dimensions
ICON_L1_FUVB_LWP_Raw_M9	FUVB LW channel raw CCD counts profile for -9 to -6 degrees FOV Vertical raw CCD counts profile for -9 to -6 degrees FOV	counts	Epoch, Rows
ICON_L1_FUVB_LWP_Raw_M6	FUVB LW channel raw CCD counts profile for -6 to -3 degrees FOV Vertical raw CCD counts profile for -6 to -3 degrees FOV	counts	Epoch, Rows
ICON_L1_FUVB_LWP_Raw_M3	FUVB LW channel raw CCD counts profile for -3 to 0 degrees FOV Vertical raw CCD counts profile for -3 to 0 degrees FOV	counts	Epoch, Rows
ICON_L1_FUVB_LWP_Raw_P0	FUVB LW channel raw CCD counts profile for 0 to +3 degrees FOV Vertical raw CCD counts profile for 0 to +3 degrees FOV	counts	Epoch, Rows
ICON_L1_FUVB_LWP_Raw_P3	FUVB LW channel raw CCD counts profile for +3 to +6 degrees FOV Vertical raw CCD counts profile for +3 to +6 degrees FOV	counts	Epoch, Rows
ICON_L1_FUVB_LWP_Raw_P6	FUVB LW channel raw CCD counts profile for +6 to +9 degrees FOV Vertical raw CCD counts profile for +6 to +9 degrees FOV	counts	Epoch, Rows
ICON_L1_FUVB_LWP_PROFILE_M9	FUVB LW channel altitude column brightness for -9 to -6 degrees FOV Vertical profile for -9 to -6 degrees FOV	Rayleigh	Epoch, Rows
ICON_L1_FUVB_LWP_PROFILE_M6	FUVB LW channel altitude column brightness for -6 to -3 degrees FOV Vertical profile for -6 to -3 degrees FOV	Rayleigh	Epoch, Rows
ICON_L1_FUVB_LWP_PROFILE_M3	FUVB LW channel altitude column brightness for -3 to 0 degrees FOV Vertical profile for -3 to 0 degrees FOV	Rayleigh	Epoch, Rows
ICON_L1_FUVB_LWP_PROFILE_P0	FUVB LW channel altitude column brightness for 0 to +3 degrees FOV Vertical profile for 0 to +3 degrees FOV	Rayleigh	Epoch, Rows

Variable Name	Description	Units	Dimensions
ICON_L1_FUVB_LWP_PR OF_P3	FUVB LW channel altitude column brightness for +3 to +6 degrees FOV Vertical profile for +3 to +6 degrees FOV	Rayleigh	Epoch, Rows
ICON_L1_FUVB_LWP_PR OF_P6	FUVB LW channel altitude column brightness for +6 to +9 degrees FOV Vertical profile for +6 to +9 degrees FOV	Rayleigh	Epoch, Rows
ICON_L1_FUVB_LWP_PR OF_M9_Error	FUVB LW channel altitude column brightness for -9 to -6 degrees FOV error Vertical profile for -9 to -6 degrees FOV error using uncertainty_calculator_v2r0. Statistical 1-sigma error values associated with the brightness profiles. After estimating the instrument gain and the background signal statistics from the 24 hours of brightness profiles, 1-sigma errors are calculated for each altitude profile as a function of these quantities and the measured signal level.	Rayleigh	Epoch, Rows
ICON_L1_FUVB_LWP_PR OF_M6_Error	FUVB LW channel altitude column brightness for -6 to -3 degrees FOV error Vertical profile for -6 to -3 degrees FOV error using uncertainty_calculator_v2r0. Statistical 1-sigma error values associated with the brightness profiles. After estimating the instrument gain and the background signal statistics from the 24 hours of brightness profiles, 1-sigma errors are calculated for each altitude profile as a function of these quantities and the measured signal level.	Rayleigh	Epoch, Rows
ICON_L1_FUVB_LWP_PR OF_M3_Error	FUVB LW channel altitude column brightness for -3 to 0 degrees FOV error Vertical profile for -3 to 0 degrees FOV error using uncertainty_calculator_v2r0. Statistical 1-sigma error values associated with the brightness profiles. After estimating the instrument gain and the background signal statistics from the 24 hours of brightness profiles, 1-sigma errors are calculated for each altitude profile as a function of these quantities and the measured signal level.	Rayleigh	Epoch, Rows
ICON_L1_FUVB_LWP_PR OF_P0_Error	FUVB LW channel altitude column brightness for 0 to +3 degrees FOV error Vertical profile for 0 to +3 degrees FOV error using uncertainty_calculator_v2r0. Statistical 1-sigma error values associated with the brightness profiles. After estimating the instrument gain and the background signal statistics from the 24 hours of brightness profiles, 1-sigma errors are calculated for each altitude profile as a function of these quantities and the measured signal level.	Rayleigh	Epoch, Rows

Variable Name	Description	Units	Dimensions
ICON_L1_FUVB_LWP_PR OF_P3_Error	FUVB LW channel altitude column brightness for +3 to +6 degrees FOV error Vertical profile for +3 to +6 degrees FOV error using uncertainty_calculator_v2r0. Statistical 1-sigma error values associated with the brightness profiles. After estimating the instrument gain and the background signal statistics from the 24 hours of brightness profiles, 1-sigma errors are calculated for each altitude profile as a function of these quantities and the measured signal level.	Rayleigh	Epoch, Rows
ICON_L1_FUVB_LWP_PR OF_P6_Error	FUVB LW channel altitude column brightness for +6 to +9 degrees FOV error Vertical profile for +6 to +9 degrees FOV error using uncertainty_calculator_v2r0. Statistical 1-sigma error values associated with the brightness profiles. After estimating the instrument gain and the background signal statistics from the 24 hours of brightness profiles, 1-sigma errors are calculated for each altitude profile as a function of these quantities and the measured signal level.	Rayleigh	Epoch, Rows
ICON_L1_FUVB_LWP_PR OF_M9_BKG	FUVB LW channel altitude column brightness for -9 to -6 degrees FOV background Vertical profile for -9 to -6 degrees FOV bkg	Rayleigh	Epoch, Rows
ICON_L1_FUVB_LWP_PR OF_M6_BKG	FUVB LW channel altitude column brightness for -6 to -3 degrees FOV background Vertical profile for -6 to -3 degrees FOV bkg	Rayleigh	Epoch, Rows
ICON_L1_FUVB_LWP_PR OF_M3_BKG	FUVB LW channel altitude column brightness for -3 to 0 degrees FOV background Vertical profile for -3 to 0 degrees FOV bkg	Rayleigh	Epoch, Rows
ICON_L1_FUVB_LWP_PR OF_P0_BKG	FUVB LW channel altitude column brightness for 0 to +3 degrees FOV background Vertical profile for 0 to +3 degrees FOV bkg	Rayleigh	Epoch, Rows
ICON_L1_FUVB_LWP_PR OF_P3_BKG	FUVB LW channel altitude column brightness for +3 to +6 degrees FOV background Vertical profile for +3 to +6 degrees FOV bkg	Rayleigh	Epoch, Rows
ICON_L1_FUVB_LWP_PR OF_P6_BKG	FUVB LW channel altitude column brightness for +6 to +9 degrees FOV background Vertical profile for +6 to +9 degrees FOV bkg	Rayleigh	Epoch, Rows
ICON_L1_FUVB_LWP_PR OF_M9_CLEAN	FUVB LW channel altitude column brightness for -9 to -6 degrees FOV without stars Vertical profile for -9 to -6 degrees FOV without stars using artifact_removal_v2r2	Rayleigh	Epoch, Rows

Variable Name	Description	Units	Dimensions
ICON_L1_FUVB_LWP_PR OF_M6_CLEAN	FUVB LW channel altitude column brightness for -6 to -3 degrees FOV without stars Vertical profile for -6 to -3 degrees FOV without stars using artifact_removal_v2r2	Rayleigh	Epoch, Rows
ICON_L1_FUVB_LWP_PR OF_M3_CLEAN	FUVB LW channel altitude column brightness for -3 to 0 degrees FOV without stars Vertical profile for -3 to 0 degrees FOV without stars using artifact_removal_v2r2	Rayleigh	Epoch, Rows
ICON_L1_FUVB_LWP_PR OF_P0_CLEAN	FUVB LW channel altitude column brightness for 0 to +3 degrees FOV without stars Vertical profile for 0 to +3 degrees FOV without stars using artifact_removal_v2r2	Rayleigh	Epoch, Rows
ICON_L1_FUVB_LWP_PR OF_P3_CLEAN	FUVB LW channel altitude column brightness for +3 to +6 degrees FOV without stars Vertical profile for +3 to +6 degrees FOV without stars using artifact_removal_v2r2	Rayleigh	Epoch, Rows
ICON_L1_FUVB_LWP_PR OF_P6_CLEAN	FUVB LW channel altitude column brightness for +6 to +9 degrees FOV without stars Vertical profile for +6 to +9 degrees FOV without stars using artifact_removal_v2r2	Rayleigh	Epoch, Rows

support_data

Variable Name	Description	Units	Dimensions
Epoch	Epoch Center time of the exposure, milliseconds after 1970-01-01/00:00:00 UT	milliseconds	Epoch
ICON_L1_FUVB_LWP_Start_Times	Start time Start time of the exposure, UT		Epoch
ICON_L1_FUVB_LWP_Stop_Times	Stop time Stop time of the exposure, UT		Epoch
ICON_L1_FUVB_LWP_Center_Times	Center time Center time of the exposure, UT		Epoch
ICON_L1_FUVB_LWP_Integration_Time	Time Integration time for integration in seconds	seconds	Epoch

Variable Name	Description	Units	Dimensions
ICON_L1_FUVB_LWP_Chain_ID	Number Chain ID for integration in seconds	number	Epoch
ICON_L1_FUVB_LWP_Quality_Flag	Quality indicator (also quickly shows times when images are available) QUALITY_FLAG is an indicator of data quality = 0 = No errors or quality conditions, LVLH 1 = No errors or quality conditions, R-LVLH 2 = Lunar calibration 3 = Insufficient high voltage 4 = Nadir calibration 5 = Zero wind calibration 6 = Bad pointing 7 = S/C attitude slew 8 = Conjugate observation 9 = Stellar calibration 10 = Unreliable background subtracted 17 = unspecified error condition	number	Epoch
ICON_L1_FUV_Mode	Data collection mode Data collection mode of FUV instrument 1 = Dayside science 2 = Nightside science 3 = Calibration 4 = Nadir 5 = Conjugate 6 = Stars 7 = Ram 8 = Off Target 9 = Engineering 13 = Unknown	number	Epoch
ICON_L1_FUVB_LWP_HV_PHOS	HV of LW channel phosphor HV of phosphor screen	Volt	Epoch
ICON_L1_FUVB_LWP_HV_MCP	HV of LW channel MCP HV of MCP	Volt	Epoch
ICON_L1_FUV_Turret	FUV turret angle FUV turret angle in degrees with respect to nominal center position	degree	Epoch
ICON_L1_FUVB_CCD_TEMP	FUVB CCD temperature FUVB CCD temperature	degree C	Epoch
ICON_L1_FUVB_Board_TEMP	FUVB board temperature FUVB digital board temperature	degree C	Epoch
ICON_L1_FUVB_HV_TEMP	FUVB HVPS temperature FUVB HVPS temperature	degree C	Epoch

Variable Name	Description	Units	Dimensions
ICON_L1_FUV_IMG_TEMP	FUV imager enclosure temperature FUV imager enclosure temperature	degree C	Epoch
ICON_L1_FUV_OPT_TEMP	FUV optics bench temperature FUV optics bench temperature	degree C	Epoch
ICON_L1_FUV_Turret_TEMP	FUV turret temperature FUV turret temperature	degree C	Epoch
ICON_L1_FUV_Scan_TEMP	FUV scan mirror temperature FUV scan mirror temperature	degree C	Epoch
ICON_L1_FUVB_LWP_GAIN_DAY	Average value of CCD output electrons per primary photo-electron in the image tube during day. It is calculated using the statistics of 24 hours of day profiles. Gain of each stripe is calculated independently. Gain for profiles	CCD electrons / photo-electron	Stripes

metadata

Variable Name	Description	Units	Dimensions
Rows	Row Number Vertical row numbers for profiles	number	Rows
ICON_L1_FUVB_Azimuth	Azimuth of FUVB channel with respect to spacecraft coordinates FUVB channel pointing azimuth	degree	Epoch
ICON_L1_FUVB_Elevation	Elevation of FUVB channel with respect to spacecraft coordinates FUVB channel pointing elevation	degree	Epoch
ICON_L1_FUVB_Roll	Roll of FUVB channel with respect to spacecraft coordinates FUVB channel pointing roll	degree	Epoch

Acknowledgement

This is a data product from the NASA Ionospheric Connection Explorer mission, an Explorer launched at 21:59:45 EDT on October 10, 2019, from Cape Canaveral AFB in the USA. Guidelines for the use of this product are described in the ICON Rules of the Road (<http://icon.ssl.berkeley.edu/Data>).

Responsibility for the mission science falls to the Principal Investigator, Dr. Thomas Immel at UC Berkeley: Immel, T.J., England, S.L., Mende, S.B. et al. Space Sci Rev (2018) 214: 13. <https://doi.org/10.1007/s11214-017-0449-2>

Responsibility for the validation of the L1 data products falls to the instrument lead investigators/scientists.

- * EUV: Dr. Eric Korpela : <https://doi.org/10.1007/s11214-017-0384-2>
- * FUV: Dr. Harald Frey : <https://doi.org/10.1007/s11214-017-0386-0>
- * MIGHTI: Dr. Christoph Englert : <https://doi.org/10.1007/s11214-017-0358-4>, and <https://doi.org/10.1007/s11214-017-0374-4>
- * IVM: Dr. Roderick Heelis : <https://doi.org/10.1007/s11214-017-0383-3>

Responsibility for the validation of the L2 data products falls to those scientists responsible for those products.

- * Daytime O and N2 profiles: Dr. Andrew Stephan : <https://doi.org/10.1007/s11214-018-0477-6>
- * Daytime (EUV) O+ profiles: Dr. Andrew Stephan : <https://doi.org/10.1007/s11214-017-0385-1>
- * Nighttime (FUV) O+ profiles: Dr. Farzad Kamalabadi : <https://doi.org/10.1007/s11214-018-0502-9>
- * Neutral Wind profiles: Dr. Jonathan Makela : <https://doi.org/10.1007/s11214-017-0359-3>
- * Neutral Temperature profiles: Dr. Christoph Englert : <https://doi.org/10.1007/s11214-017-0434-9>
- * Ion Velocity Measurements : Dr. Russell Stoneback : <https://doi.org/10.1007/s11214-017-0383-3>

Responsibility for Level 4 products falls to those scientists responsible for those products.

- * Hough Modes : Dr. Chihoko Yamashita : <https://doi.org/10.1007/s11214-017-0401-5>
- * TIEGCM : Dr. Astrid Maute : <https://doi.org/10.1007/s11214-017-0330-3>
- * SAMI3 : Dr. Joseph Huba : <https://doi.org/10.1007/s11214-017-0415-z>

Pre-production versions of all above papers are available on the ICON website.
<http://icon.ssl.berkeley.edu/Publications>

Overall validation of the products is overseen by the ICON Project Scientist, Dr. Scott England.

NASA oversight for all products is provided by the Mission Scientist, Dr. Jeffrey Klenzing.

Users of these data should contact and acknowledge the Principal Investigator Dr. Immel and the party directly responsible for the data product (noted above) and acknowledge NASA funding for the collection of the data used in the research with the following statement : "ICON is supported by NASA's Explorers Program through contracts NNG12FA45C and NNG12FA42I".

These data are openly available as described in the ICON Data Management Plan available on the ICON website (<http://icon.ssl.berkeley.edu/Data>).

This document was automatically generated on 2022-04-25 09:11 using the file:

ICON_L1_FUV_LWP_2022-03-31_v05r001.NC

Software version: ICON SDC > ICON FUV L1 Processor version 2022-04-06 > UIUC FUV L1 Post-Processor v1.2

ICON FUV Science Level 1 Data

This document describes the data product for ICON FUV Level 1 FUV-A Limb Image File, which is in NetCDF4 format.

The ICON Far UltraViolet (FUV) imager contributes to the ICON science objectives by providing remote sensing measurements of the daytime and nighttime atmosphere/ ionosphere. During sunlit atmospheric conditions, ICON FUV images the limb altitude profile in the shortwave (SW) band at 135.6 nm and the longwave (LW) band at 157 nm perpendicular to the satellite motion to retrieve the atmospheric O/N₂ ratio. In conditions of atmospheric darkness, ICON FUV measures the 135.6 nm recombination emission of O⁺ ions used to compute the nighttime ionospheric altitude distribution.

The ICON Far Ultra-Violet (FUV) imager is a Czerny–Turner design Spectrographic Imager with two exit slits and corresponding back imager cameras that produce two independent images in separate wavelength bands on two detectors. For this science product, the 18x24 degree FOV is divided and co-added to produce 6 high sensitivity profiles with each nominally 12 second integration. These inform daytime and nighttime retrievals of the ionospheric composition and density (See Stephan et al and Kamalabadi et al, noted in the acknowledgements section of this file). Pointing and geolocation information are available in the FUV ancillary data also available at <https://icon.ssl.berkeley.edu>

This particular product used the Time Delay Integration technique to map the limb emissions to an orbit-related latitude-longitude grid as described in

* TDI: C. Wilkins: <https://doi.org/10.1007/s11214-017-0410-4>

More details about the mission, data products, responsibility, and data use can be found at the end of this document.

Each FUV Level-1 file contains global attributes explaining the major properties of the file and variables. This is an example from one file.

0 ACKNOWLEDGEMENT This is a data product from the NASA Ionospheric Connection Explorer mission, an Explorer launched at 21:59:45 EDT on October 10, 2019, from Cape Canaveral AFB in the USA. Guidelines for the use of this product are described in the ICON Rules of the Road (<http://icon.ssl.berkeley.edu/Data>).

1 ADID_REF NASA Contract > NNG12F45C

2 CALIBRATION_FILE See calibration files in general attribute fields FLATFIELD_CORRECTION, BACKGROUND_CORRECTION, RAYLEIGH_CONVERSION

3 CONVENTIONS SPDF ISTEP/IACF Modified for NetCDF (v0.8)

4 DATA_LEVEL L1

5 DATA_TYPE APIDxE3 > ICON Application ID 0xE3: FUV Science Level 0.5 Data > FUV Science Level 1 Data

6 DATA_REVISION 0

7 DATA_VERSION 2.00000

8 DATA_VERSION_MAJOR 2

9 DATE_END 2020-07-01T22:48:08 UTC

10 DATE_START 2020-07-01T00:00:05 UTC

11 DATE_STOP 2020-07-01T22:48:08 UTC

12 DESCRIPTION ICON FUV Level 1 FUV-A Limb Image File

13 DESCRIPTOR FUV-A > ICON FUV-A L1 Science Limb Image File

14 DISCIPLINE Space Physics > Ionospheric Science

15 FILE ICON_L1_FUV_SLI_20200701_v02r000.NC

16 FILE_DATE Sun Aug 9 05:35:38 2020

17 GENERATED_BY ICON SDC > ICON FUV L1 Processor v1, Tori Fae (tfae@paradigm.ssl.berkeley.edu) and Harald Frey (hfrey@ssl.berkeley.edu)

18 GENERATION_DATE 20200809

19 HISTORY Version 2, Created by ICON FUV L1 processing with `icn_fuv_create_swi_structure.pro` Fri Sep 18 12:06:56 2020

MODIFICATION HISTORY:

Written by: Harald Frey, Date: January 19, 2017, Version v01
2019-12-01 some updates
2020-01-25 many updates for background etc.
2020-03-20 new backgrounds, flatfields, quality parameter etc.
2020-04-06 allow negative values, bkg variable in Rayleighs etc.
2020-06-12 new background, distortion correction
2020-08-17 new attributes
20 HTTP_LINK <http://icon.ssl.berkeley.edu>
21 INSTRUMENT FUV-A
22 INSTRUMENT_TYPE Imagers (Space)
23 LINK_TEXT All ICON information and data can be found at the ICON web page icon.ssl.berkeley.edu
24 LINK_TITLE ICON Website
25 LOGICAL_FILE_ID ICON_L1_FUV_SLI_20200701_v02r000
26 LOGICAL_SOURCE ICON_L0P_FUV-A_Science-TDI0_2020-07-01
27 LOGICAL_SOURCE_DESCRIPTION ICON FUV-A Level 1 Science Limb Image File
28 MISSION_GROUP Ionospheric Investigations
29 MODS See history
30 PARENTS Names of the Level-0 files for this product
31 PI_AFFILIATION UC Berkeley > SSL
32 PI_NAME T. J. Immel
33 PROJECT NASA > ICON
34 RULES_OF_USE Public Data for Scientific Use
35 SOFTWARE_VERSION ICON SDC > ICON FUV L1 Processor v1.0
36 SOURCE_NAME ICON > Ionospheric Connection Explorer
37 SPACECRAFT_ID NASA > ICON - 493
38 TEXT ICON explores the boundary between Earth and space - the ionosphere - to understand the physical connection between our world and the immediate space environment around us. Visit '<http://icon.ssl.berkeley.edu>' for more details.
39 TIME_RESOLUTION 12000 milliseconds
40 TITLE ICON FUV Level 1 FUV-A Limb Image File
41 EPOCH0 1970-01-01/00:00:00
42 FILE_NAMING_CONVENTION source_datatype_descriptor
43 PROCESS_LEVEL L1
44 SAMPLE_TIME 12
45 SAMPLE_UNIT Seconds
46 SATELLITE_ID ICON
47 TEXT_SUPPLEMENT Explanation of global attributes
48 FLATFIELD_CORRECTION File names for flatfield correction
49 BACKGROUND_CORRECTION saa_files_2020-183
50 RAYLEIGH_CONVERSION Values for Rayleigh conversion

Use of this product for analysis depends on the combined use of the ancillary FUV data product which contains geopositioning data and instrument pointing details.

History

Version 5 Created by ICON FUV L1 processing with `icn_fuv_create_swi_structure.pro` Wed Apr 20 10:31:49 2022

MODIFICATION HISTORY:

Written by: Harald Frey, Date: January 19, 2017, Version v01
2019-12-01 some updates
2020-01-25 many updates for background etc.
2020-03-20 new backgrounds, flatfields, quality parameter etc.
2020-04-06 allow negative values, bkg variable in Rayleighs etc.
2020-06-12 new background, distortion correction

2020-08-17 new attributes
2020-10-22 MCP sensitivity loss corrected
2021-06-08 major update on background and flatfield
2022-02-20 major update on background, calibration, day cleanup

Dimensions

NetCDF files contain **variables** and the **dimensions** over which those variables are defined. First, the dimensions are defined, then all variables in the file are described.

The dimensions used by the variables in this file are given below, along with nominal sizes. Note that the size may vary from file to file. For example, the "Epoch" dimension, which describes the number of time samples contained in this file, will have a varying size.

Dimension Name	Nominal Size
Epoch	2379
Rows	256
Columns	256

Variables

Variables in this file are listed below. First, "data" variables are described, followed by the "support_data" variables, and finally the "metadata" variables. The variables classified as "ignore_data" are not shown.

data

Variable Name	Description	Units	Dimensions
ICON_L1_FUVA_Limb_Raw	FUVA SW channel raw CCD count limb image Raw limb image	counts	Epoch, Rows, Columns
ICON_L1_FUVA_Limb_IMG	FUVA SW channel calibrated limb image Calibrated limb image	Rayleigh	Epoch, Rows, Columns
ICON_L1_FUVA_Limb_Error	FUVA SW channel calibrated limb image error Calibrated limb image error. Statistical 1-sigma error values associated with the mapped image.	Rayleigh	Epoch, Rows, Columns
ICON_L1_FUVA_LIMB_BKG	FUVA SW channel calibrated limb image background Calibrated limb image bkg	Rayleigh	Epoch, Rows

support_data

Variable Name	Description	Units	Dimensions
Epoch	Epoch Center time of the exposure, milliseconds after 1970-01-01/00:00:00 UT	milliseconds	Epoch
ICON_L1_FUVA_SWI_Start_Times	Start time Start time of the exposure, UT		Epoch
ICON_L1_FUVA_SWI_Stop_Times	Stop time Stop time of the exposure, UT		Epoch
ICON_L1_FUVA_SWI_Center_Times	Center time Center time of the exposure, UT		Epoch
ICON_L1_FUVA_SWI_Integration_Time	Time Integration time for integration in seconds	seconds	Epoch
ICON_L1_FUVA_SWI_Chain_ID	Number Chain ID for integration in seconds	number	Epoch

Variable Name	Description	Units	Dimensions
ICON_L1_FUVA_SWI_Quality_Flag	<p>Quality indicator (also quickly shows times when images are available)</p> <p>QUALITY_FLAG is an indicator of data quality =</p> <p>0 = No errors or quality conditions, LVLH 1 = No errors or quality conditions, R-LVLH 2 = Lunar calibration 3 = Insufficient high voltage 4 = Nadir calibration 5 = Zero wind calibration 6 = Bad pointing 7 = S/C attitude slew 8 = Conjugate observation 9 = Stellar calibration 10 = Unreliable background subtracted 17 = unspecified error condition</p>	number	Epoch
ICON_L1_FUV_Mode	<p>Data collection mode</p> <p>Data collection mode of FUV instrument</p> <p>1 = Dayside science 2 = Nightside science 3 = Calibration 4 = Nadir 5 = Conjugate 6 = Stars 7 = Ram 8 = Off Target 9 = Engineering 13 = Unknown</p>	number	Epoch
ICON_L1_FUVA_SWI_HV_PHOS	<p>HV of SW channel phosphor</p> <p>HV of phosphor screen</p>	Volt	Epoch
ICON_L1_FUVA_SWI_HV_MCP	<p>HV of SW channel MCP</p> <p>HV of MCP</p>	Volt	Epoch
ICON_L1_FUV_Turret	<p>FUV turret angle</p> <p>FUV turret angle in degrees with respect to nominal center position</p>	degree	Epoch
ICON_L1_FUVA_CCD_TEMP	<p>FUVA CCD temperature</p> <p>FUVA CCD temperature</p>	degree C	Epoch
ICON_L1_FUVA_Board_TEMP	<p>FUVA board temperature</p> <p>FUVA digital board temperature</p>	degree C	Epoch
ICON_L1_FUVA_HV_TEMP	<p>FUVA HVPS temperature</p> <p>FUVA HVPS temperature</p>	degree C	Epoch
ICON_L1_FUV_IMG_TEMP	<p>FUV imager enclosure temperature</p> <p>FUV imager enclosure temperature</p>	degree C	Epoch

Variable Name	Description	Units	Dimensions
ICON_L1_FUV_OPT_TEMP	FUV optics bench temperature FUV optics temperature	degree C	Epoch
ICON_L1_FUV_Turret_TEMP	FUV turret temperature FUV turret temperature	degree C	Epoch
ICON_L1_FUV_Scan_TEMP	FUV scan mirror temperature FUV scan mirror temperature	degree C	Epoch

metadata

Variable Name	Description	Units	Dimensions
Rows	Row Number Vertical row numbers for images	number	Rows
Columns	Column Number Horizontal column numbers for images	number	Columns
ICON_L1_FUVA_Azimuth	Azimuth of FUVA channel with respect to spacecraft coordinates FUVA channel pointing azimuth	degree	Epoch
ICON_L1_FUVA_Elevation	Elevation of FUVA channel with respect to spacecraft coordinates FUVA channel pointing elevation	degree	Epoch
ICON_L1_FUVA_Roll	Roll of FUVA channel with respect to spacecraft coordinates FUVA channel pointing roll	degree	Epoch

Acknowledgement

This is a data product from the NASA Ionospheric Connection Explorer mission, an Explorer launched at 21:59:45 EDT on October 10, 2019, from Cape Canaveral AFB in the USA. Guidelines for the use of this product are described in the ICON Rules of the Road (<http://icon.ssl.berkeley.edu/Data>).

Responsibility for the mission science falls to the Principal Investigator, Dr. Thomas Immel at UC Berkeley: Immel, T.J., England, S.L., Mende, S.B. et al. Space Sci Rev (2018) 214: 13. <https://doi.org/10.1007/s11214-017-0449-2>

Responsibility for the validation of the L1 data products falls to the instrument lead investigators/scientists.

* EUV: Dr. Eric Korpela : <https://doi.org/10.1007/s11214-017-0384-2>

* FUV: Dr. Harald Frey : <https://doi.org/10.1007/s11214-017-0386-0>

* MIGHTI: Dr. Christoph Englert : <https://doi.org/10.1007/s11214-017-0358-4>, and <https://doi.org/10.1007/s11214-017-0374-4>

* IVM: Dr. Roderick Heelis : <https://doi.org/10.1007/s11214-017-0383-3>

Responsibility for the validation of the L2 data products falls to those scientists responsible for those products.

* Daytime O and N2 profiles: Dr. Andrew Stephan : <https://doi.org/10.1007/s11214-018-0477-6>

* Daytime (EUV) O+ profiles: Dr. Andrew Stephan : <https://doi.org/10.1007/s11214-017-0385-1>

* Nighttime (FUV) O+ profiles: Dr. Farzad Kamalabadi : <https://doi.org/10.1007/s11214-018-0502-9>

* Neutral Wind profiles: Dr. Jonathan Makela : <https://doi.org/10.1007/s11214-017-0359-3>

* Neutral Temperature profiles: Dr. Christoph Englert : <https://doi.org/10.1007/s11214-017-0434-9>

* Ion Velocity Measurements : Dr. Russell Stoneback : <https://doi.org/10.1007/s11214-017-0383-3>

Responsibility for Level 4 products falls to those scientists responsible for those products.

* Hough Modes : Dr. Chihoko Yamashita : <https://doi.org/10.1007/s11214-017-0401-5>

* TIEGCM : Dr. Astrid Maute : <https://doi.org/10.1007/s11214-017-0330-3>

* SAMI3 : Dr. Joseph Huba : <https://doi.org/10.1007/s11214-017-0415-z>

Pre-production versions of all above papers are available on the ICON website.

<http://icon.ssl.berkeley.edu/Publications>

Overall validation of the products is overseen by the ICON Project Scientist, Dr. Scott England.

NASA oversight for all products is provided by the Mission Scientist, Dr. Jeffrey Klenzing.

Users of these data should contact and acknowledge the Principal Investigator Dr. Immel and the party directly responsible for the data product (noted above) and acknowledge NASA funding for the collection of the data used in the research with the following statement : "ICON is supported by NASA's Explorers Program through contracts NNG12FA45C and NNG12FA42I".

These data are openly available as described in the ICON Data Management Plan available on the ICON website (<http://icon.ssl.berkeley.edu/Data>).

This document was automatically generated on 2022-04-25 09:11 using the file:

ICON_L1_FUV_SLI_2022-03-31_v05r001.NC

Software version: ICON SDC > ICON FUV L1 Processor version 2022-04-06

ICON FUV Science Level 1 Data

This document describes the data product for ICON FUV Level 1 FUV-A Sublimb Image File, which is in NetCDF4 format.

The ICON Far UltraViolet (FUV) imager contributes to the ICON science objectives by providing remote sensing measurements of the daytime and nighttime atmosphere/ ionosphere. During sunlit atmospheric conditions, ICON FUV images the limb altitude profile in the shortwave (SW) band at 135.6 nm and the longwave (LW) band at 157 nm perpendicular to the satellite motion to retrieve the atmospheric O/N₂ ratio. In conditions of atmospheric darkness, ICON FUV measures the 135.6 nm recombination emission of O⁺ ions used to compute the nighttime ionospheric altitude distribution.

The ICON Far Ultra-Violet (FUV) imager is a Czerny–Turner design Spectrographic Imager with two exit slits and corresponding back imager cameras that produce two independent images in separate wavelength bands on two detectors. For this science product, the 18x24 degree FOV is divided and co-added to produce 6 high sensitivity profiles with each nominally 12 second integration. These inform daytime and nighttime retrievals of the ionospheric composition and density (See Stephan et al and Kamalabadi et al, noted in the acknowledgements section of this file). Pointing and geolocation information are available in the FUV ancillary data also available at <https://icon.ssl.berkeley.edu>

This particular product used the Time Delay Integration technique to map the sublimb emissions to an orbit-related latitude-longitude grid as described in

* TDI: C. Wilkins: <https://doi.org/10.1007/s11214-017-0410-4>

More details about the mission, data products, responsibility, and data use can be found at the end of this document.

Each FUV Level-1 file contains global attributes explaining the major properties of the file and variables. This is an example from one file.

0 ACKNOWLEDGEMENT This is a data product from the NASA Ionospheric Connection Explorer mission, an Explorer launched at 21:59:45 EDT on October 10, 2019, from Cape Canaveral AFB in the USA. Guidelines for the use of this product are described in the ICON Rules of the Road (<http://icon.ssl.berkeley.edu/Data>).

1 ADID_REF NASA Contract > NNG12F45C

2 CALIBRATION_FILE See calibration files in general attribute fields FLATFIELD_CORRECTION, BACKGROUND_CORRECTION, RAYLEIGH_CONVERSION

3 CONVENTIONS SPDF ISTEP/IACF Modified for NetCDF (v0.8)

4 DATA_LEVEL L1

5 DATA_TYPE APIDxE3 > ICON Application ID 0xE3: FUV Science Level 0.5 Data > FUV Science Level 1 Data

6 DATA_REVISION 0

7 DATA_VERSION 2.00000

8 DATA_VERSION_MAJOR 2

9 DATE_END 2020-07-01T22:48:08 UTC

10 DATE_START 2020-07-01T00:00:05 UTC

11 DATE_STOP 2020-07-01T22:48:08 UTC

12 DESCRIPTION ICON FUV Level 1 FUV-A Sublimb Image File

13 DESCRIPTOR FUV-A > ICON FUV-A L1 Science Sublimb Image File

14 DISCIPLINE Space Physics > Ionospheric Science

15 FILE ICON_L1_FUV_SSI_20200701_v02r000.NC

16 FILE_DATE Sun Aug 9 05:35:38 2020

17 GENERATED_BY ICON SDC > ICON FUV L1 Processor v1, Tori Fae (tfae@paradigm.ssl.berkeley.edu) and Harald Frey (hfrey@ssl.berkeley.edu)

18 GENERATION_DATE 20200809

19 HISTORY Version 2, Created by ICON FUV L1 processing with `icn_fuv_create_swi_structure.pro` Fri Sep 18 12:06:56 2020

MODIFICATION HISTORY:

Written by: Harald Frey, Date: January 19, 2017, Version v01

2019-12-01 some updates

2020-01-25 many updates for background etc.

2020-03-20 new backgrounds, flatfields, quality parameter etc.

2020-04-06 allow negative values, bkg variable in Rayleighs etc.

2020-06-12 new background, distortion correction

2020-08-17 new attributes

Generated: 20200818

20 HTTP_LINK <http://icon.ssl.berkeley.edu>

21 INSTRUMENT FUV-A

22 INSTRUMENT_TYPE Imagers (Space)

23 LINK_TEXT All ICON information and data can be found at the ICON web page icon.ssl.berkeley.edu

24 LINK_TITLE ICON Website

25 LOGICAL_FILE_ID ICON_L1_FUV_SSI_20200701_v02r000

26 LOGICAL_SOURCE ICON_L0P_FUV-A_Science-TDI0_2020-07-01

27 LOGICAL_SOURCE_DESCRIPTION ICON FUV-A Level 1 Science Sublimb Image File

28 MISSION_GROUP Ionospheric Investigations

29 MODS See history

30 PARENTS Names of the Level-0 files for this product

31 PI_AFFILIATION UC Berkeley > SSL

32 PI_NAME T. J. Immel

33 PROJECT NASA > ICON

34 RULES_OF_USE Public Data for Scientific Use

35 SOFTWARE_VERSION ICON SDC > ICON FUV L1 Processor v1.0

36 SOURCE_NAME ICON > Ionospheric Connection Explorer

37 SPACECRAFT_ID NASA > ICON - 493

38 TEXT ICON explores the boundary between Earth and space - the ionosphere - to understand the physical connection between our world and the immediate space environment around us. Visit '<http://icon.ssl.berkeley.edu>' for more details.

39 TIME_RESOLUTION 12000 milliseconds

40 TITLE ICON FUV Level 1 FUV-A Limb Image File

41 EPOCH0 1970-01-01/00:00:00

42 FILE_NAMING_CONVENTION source_datatype_descriptor

43 PROCESS_LEVEL L1

44 SAMPLE_TIME 12

45 SAMPLE_UNIT Seconds

46 SATELLITE_ID ICON

47 TEXT_SUPPLEMENT Explanation of global attributes

48 FLATFIELD_CORRECTION File names for flatfield correction

49 BACKGROUND_CORRECTION saa_files_2020-183

50 RAYLEIGH_CONVERSION Values for Rayleigh conversion

Use of this product for analysis depends on the combined use of the ancillary FUV data product which contains geopositioning data and instrument pointing details.

History

Version 5 Created by ICON FUV L1 processing with `icn_fuv_create_swi_structure.pro` Wed Apr 20 10:31:49 2022

MODIFICATION HISTORY:

Written by: Harald Frey, Date: January 19, 2017, Version v01

2019-12-01 some updates

2020-01-25 many updates for background etc.

2020-03-20 new backgrounds, flatfields, quality parameter etc.

2020-04-06 allow negative values, bkg variable in Rayleighs etc.

2020-06-12 new background, distortion correction
2020-08-17 new attributes
2020-10-22 MCP sensitivity loss corrected
2021-06-08 major update on background and flatfield
2022-02-20 major update on background, calibration, day cleanup

Dimensions

NetCDF files contain **variables** and the **dimensions** over which those variables are defined. First, the dimensions are defined, then all variables in the file are described.

The dimensions used by the variables in this file are given below, along with nominal sizes. Note that the size may vary from file to file. For example, the "Epoch" dimension, which describes the number of time samples contained in this file, will have a varying size.

Dimension Name	Nominal Size
Epoch	2379
Rows	256
Columns	256

Variables

Variables in this file are listed below. First, "data" variables are described, followed by the "support_data" variables, and finally the "metadata" variables. The variables classified as "ignore_data" are not shown.

data

Variable Name	Description	Units	Dimensions
ICON_L1_FUVA_Sublimb_Raw	FUVA SW channel raw CCD count sublimb image Raw sublimb image	counts	Epoch, Rows, Columns
ICON_L1_FUVA_Sublimb_IMG	FUVA SW channel calibrated sublimb image Calibrated sublimb image	Rayleigh	Epoch, Rows, Columns
ICON_L1_FUVA_Sublimb_Error	FUVA SW channel calibrated sublimb image error Calibrated sublimb image error. Statistical 1-sigma error values associated with the mapped image.	Rayleigh	Epoch, Rows, Columns
ICON_L1_FUVA_SUBLIMB_BKG	FUVA SW channel calibrated sublimb image background Calibrated sublimb image bkg	Rayleigh	Epoch, Rows

support_data

Variable Name	Description	Units	Dimensions
Epoch	Epoch Center time of the exposure, milliseconds after 1970-01-01/00:00:00 UT	milliseconds	Epoch
ICON_L1_FUVA_SWI_Start_Times	Start time Start time of the exposure, UT		Epoch
ICON_L1_FUVA_SWI_Stop_Times	Stop time Stop time of the exposure, UT		Epoch
ICON_L1_FUVA_SWI_Center_Times	Center time Center time of the exposure, UT		Epoch
ICON_L1_FUVA_SWI_Integration_Time	Time Integration time for integration in seconds	seconds	Epoch
ICON_L1_FUVA_SWI_Chain_ID	Number Chain ID for integration in seconds	number	Epoch

Variable Name	Description	Units	Dimensions
ICON_L1_FUVA_SWI_Quality_Flag	<p>Quality indicator (also quickly shows times when images are available)</p> <p>QUALITY_FLAG is an indicator of data quality =</p> <p>0 = No errors or quality conditions, LVLH 1 = No errors or quality conditions, R-LVLH 2 = Lunar calibration 3 = Insufficient high voltage 4 = Nadir calibration 5 = Zero wind calibration 6 = Bad pointing 7 = S/C attitude slew 8 = Conjugate observation 9 = Stellar calibration 10 = Unreliable background subtracted 17 = unspecified error condition</p>	number	Epoch
ICON_L1_FUV_Mode	<p>Data collection mode</p> <p>Data collection mode of FUV instrument</p> <p>1 = Dayside science 2 = Nightside science 3 = Calibration 4 = Nadir 5 = Conjugate 6 = Stars 7 = Ram 8 = Off Target 9 = Engineering 13 = Unknown</p>	number	Epoch
ICON_L1_FUVA_SWI_HV_PHOS	<p>HV of SW channel phosphor</p> <p>HV of phosphor screen</p>	Volt	Epoch
ICON_L1_FUVA_SWI_HV_MCP	<p>HV of SW channel MCP</p> <p>HV of MCP</p>	Volt	Epoch
ICON_L1_FUV_Turret	<p>FUV turret angle</p> <p>FUV turret angle in degrees with respect to nominal center position</p>	degree	Epoch
ICON_L1_FUVA_CCD_TEMP	<p>FUVA CCD temperature</p> <p>FUVA CCD temperature</p>	degree C	Epoch
ICON_L1_FUVA_Board_TEMP	<p>FUVA board temperature</p> <p>FUVA digital board temperature</p>	degree C	Epoch
ICON_L1_FUVA_HV_TEMP	<p>FUVA HVPS temperature</p> <p>FUVA HVPS temperature</p>	degree C	Epoch
ICON_L1_FUV_IMG_TEMP	<p>FUV imager enclosure temperature</p> <p>FUV imager enclosure temperature</p>	degree C	Epoch

Variable Name	Description	Units	Dimensions
ICON_L1_FUV_OPT_TEMP	FUV optics bench temperature FUV optics temperature	degree C	Epoch
ICON_L1_FUV_Turret_TEMP	FUV turret temperature FUV turret temperature	degree C	Epoch
ICON_L1_FUV_Scan_TEMP	FUV scan mirror temperature FUV scan mirror temperature	degree C	Epoch

metadata

Variable Name	Description	Units	Dimensions
Rows	Row Number Vertical row numbers for images	number	Rows
Columns	Column Number Horizontal column numbers for images	number	Columns
ICON_L1_FUVA_Azimuth	Azimuth of FUVA channel with respect to spacecraft coordinates FUVA channel pointing azimuth	degree	Epoch
ICON_L1_FUVA_Elevation	Elevation of FUVA channel with respect to spacecraft coordinates FUVA channel pointing elevation	degree	Epoch
ICON_L1_FUVA_Roll	Roll of FUVA channel with respect to spacecraft coordinates FUVA channel pointing roll	degree	Epoch

Acknowledgement

This is a data product from the NASA Ionospheric Connection Explorer mission, an Explorer launched at 21:59:45 EDT on October 10, 2019, from Cape Canaveral AFB in the USA. Guidelines for the use of this product are described in the ICON Rules of the Road (<http://icon.ssl.berkeley.edu/Data>).

Responsibility for the mission science falls to the Principal Investigator, Dr. Thomas Immel at UC Berkeley: Immel, T.J., England, S.L., Mende, S.B. et al. *Space Sci Rev* (2018) 214: 13. <https://doi.org/10.1007/s11214-017-0449-2>

Responsibility for the validation of the L1 data products falls to the instrument lead investigators/scientists.

- * EUV: Dr. Eric Korpela : <https://doi.org/10.1007/s11214-017-0384-2>
- * FUV: Dr. Harald Frey : <https://doi.org/10.1007/s11214-017-0386-0>
- * MIGHTI: Dr. Christoph Englert : <https://doi.org/10.1007/s11214-017-0358-4>, and <https://doi.org/10.1007/s11214-017-0374-4>
- * IVM: Dr. Roderick Heelis : <https://doi.org/10.1007/s11214-017-0383-3>

Responsibility for the validation of the L2 data products falls to those scientists responsible for those products.

- * Daytime O and N2 profiles: Dr. Andrew Stephan : <https://doi.org/10.1007/s11214-018-0477-6>
- * Daytime (EUV) O+ profiles: Dr. Andrew Stephan : <https://doi.org/10.1007/s11214-017-0385-1>
- * Nighttime (FUV) O+ profiles: Dr. Farzad Kamalabadi : <https://doi.org/10.1007/s11214-018-0502-9>
- * Neutral Wind profiles: Dr. Jonathan Makela : <https://doi.org/10.1007/s11214-017-0359-3>
- * Neutral Temperature profiles: Dr. Christoph Englert : <https://doi.org/10.1007/s11214-017-0434-9>
- * Ion Velocity Measurements : Dr. Russell Stoneback : <https://doi.org/10.1007/s11214-017-0383-3>

Responsibility for Level 4 products falls to those scientists responsible for those products.

- * Hough Modes : Dr. Chihoko Yamashita : <https://doi.org/10.1007/s11214-017-0401-5>
- * TIEGCM : Dr. Astrid Maute : <https://doi.org/10.1007/s11214-017-0330-3>
- * SAMI3 : Dr. Joseph Huba : <https://doi.org/10.1007/s11214-017-0415-z>

Pre-production versions of all above papers are available on the ICON website.
<http://icon.ssl.berkeley.edu/Publications>

Overall validation of the products is overseen by the ICON Project Scientist, Dr. Scott England.

NASA oversight for all products is provided by the Mission Scientist, Dr. Jeffrey Klenzing.

Users of these data should contact and acknowledge the Principal Investigator Dr. Immel and the party directly responsible for the data product (noted above) and acknowledge NASA funding for the collection of the data used in the research with the following statement : "ICON is supported by NASA's Explorers Program through contracts NNG12FA45C and NNG12FA42I".

These data are openly available as described in the ICON Data Management Plan available on the ICON website (<http://icon.ssl.berkeley.edu/Data>).

This document was automatically generated on 2022-04-25 09:11 using the file:

ICON_L1_FUV_SSI_2022-03-31_v05r001.NC

Software version: ICON SDC > ICON FUV L1 Processor version 2022-04-06

ICON Data Product 0P: FUV Ancillary Products

This document describes the data product for Ancillary Products for FUV Data Processing, which is in NetCDF4 format.

The FUV ancillary data file contains information on the ICON observatory as well as FUV specific information. This includes the pointing, position, and velocity of the ICON observatory. It also includes information on the status of the observatory such as maneuvers, being in or out of the Earth's shadow, and calibrations. Pertinent information for the FUV instrument is included such as locations and details at the FUV tangent points. These files are combined with the FUV Level 1 data to produce Level 2 data. Variables labeled FUVA are for the short wave data only. Variables labeled FUVB are for the long wave data only. Variables label FUV are for both. ECEF is Earth-centered, Earth-fixed reference frame. ECI is Earth-centered inertial reference frame. We use the J2000 ECI frame. LVLH is local-vertical, local-horizontal. We have two LVLH modes: normal and reverse. LVLH Normal is when the spacecraft is looking north with latitude tangent locations between ~12 S and ~42 N. LVLH Reverse is when the spacecraft is looking south with latitude tangent locations between ~42 S and ~12 N.

History

Version 03, Created by FUV Ancillary Processor v3.0.2 on Thu, 08 Oct 2020, 2020-10-08T18:28:41.000 UTC

Dimensions

NetCDF files contain **variables** and the **dimensions** over which those variables are defined. First, the dimensions are defined, then all variables in the file are described.

The dimensions used by the variables in this file are given below, along with nominal sizes. Note that the size may vary from file to file. For example, the "Epoch" dimension, which describes the number of time samples contained in this file, will have a varying size.

Dimension Name	Nominal Size
EPOCH	7013
HORIZONTAL	6
VERTICAL	256
VECTORS	3

Variables

Variables in this file are listed below. First, "data" variables are described, followed by the "support_data" variables, and finally the "metadata" variables. The variables classified as "ignore_data" are not shown.

support_data

Variable Name	Description	Units	Dimensions
EPOCH	<p>Milliseconds since 1970-01-01 00:00:00 UTC at middle of measurement integration.</p> <p>Number of milliseconds since 1970-01-01 00:00:00 UTC at the middle of the measurement integration.</p>	milliseconds	EPOCH
ICON Ancillary FUV Time UTC	<p>Date and Time in UTC format</p> <p>ISO 8601 formatted UTC timestamp (at middle of reading). E.g., 2017-05-27 00:00:00.380Z</p>	UTC	EPOCH
ICON Ancillary FUV SC Position ECEF	<p>Spacecraft Position in ECEF Coordinates</p> <p>Position of spacecraft in ECEF coordinates.</p>	km	EPOCH, VECTORS
ICON Ancillary FUV Latitude	<p>WGS84 Latitude of Spacecraft Position (Geodetic)</p> <p>Geodetic Latitude of Spacecraft in WGS84</p>	degrees North	EPOCH
ICON Ancillary FUV Longitude	<p>WGS84 Longitude of Spacecraft Position (Geodetic)</p> <p>Geodetic Longitude of Spacecraft in WGS84</p>	degrees East	EPOCH
ICON Ancillary FUV Altitude	<p>WGS84 Altitude of Spacecraft Position (Geodetic)</p> <p>Geodetic Altitude of Spacecraft in WGS84</p>	km	EPOCH
ICON Ancillary FUV SC SZA	<p>Spacecraft Solar Zenith Angle</p> <p>Solar Zenith Angle at the spacecraft</p>	degrees	EPOCH
ICON Ancillary FUV SUN STATUS	<p>Spacecraft Sun/Shadow Status Code</p> <p>Binary flag indicating if the spacecraft is in the sun or shadow, where 1 = shadow, 0 = sun</p>	binary	EPOCH
ICON Ancillary FUV ORBIT NUMBER	<p>Orbit Number</p> <p>Integer Orbit Number</p>	integer	EPOCH

Variable Name	Description	Units	Dimensions
ICON Ancillary_FUV_SLEW_STATUS	<p>Slew or off-point Status Code</p> <p>Binary Coded Integer where</p> <ul style="list-style-type: none"> 1: LVLH Normal Mode 2: LVLH Reverse Mode 4: Earth Limb Pointing 8: Inertial Pointing 16: Stellar Pointing 32: Attitude Slew 64: Conjugate Maneuver 128: Nadir Calibration 256: Lunar Calibration 512: Stellar Calibration 1024: Zero Wind Calibration 2048-32768: SPARE 	binary	EPOCH
ICON Ancillary_FUVA_TANGENTPOINTS_LATLONG	<p>Tangent Locations of FUVA (SW) in WGS84 (Latitude, Longitude, Altitude)</p> <p>Location of tangent points in WGS84 for all 6 stripes and 256 vertical pixels for the shortwave channel. Locations are in Latitude, Longitude, Altitude.</p>	mixed	EPOCH, VERTICAL, HORIZONTAL, VECTORS
ICON Ancillary_FUVA_TANGENTPOINTS_SZA	<p>Tangent Points of FUVA (SW) Solar Zenith Angle</p> <p>Solar zenith angle at tangent points for all 6 stripes and 256 vertical pixels for the shortwave channel.</p>	degrees	EPOCH, VERTICAL, HORIZONTAL
ICON Ancillary_FUVA_FOV_UNITVECTORS_ECEF	<p>FOV Unit Vectors of FUVA (SW) in ECEF</p> <p>Unit look vectors in ECEF for all 6 stripes across the image and 256 vertical pixels for the shortwave channel.</p>	dimensionless	EPOCH, VERTICAL, HORIZONTAL, VECTORS
ICON Ancillary_FUVA_HORIZONTAL_BORESIGHT_SUN_ANGLE	<p>Horizontal Boresight of FUVA (SW) to Sun Angle</p> <p>Angle between the Sun and the horizontal plane at the center of the current instrument field of view for FUVA (Short Wave).</p>	degrees	EPOCH
ICON Ancillary_FUVA_VERTICAL_BORESIGHT_SUN_ANGLE	<p>Vertical Boresight of FUVA (SW) to Sun Angle</p> <p>Angle between the Sun and the vertical plane at the center of the current instrument field of view for FUVA (Short Wave).</p>	degrees	EPOCH
ICON Ancillary_FUVA_TOTAL_BORESIGHT_SUN_ANGLE	<p>Total Boresight of FUVA (SW) to Sun Angle</p> <p>Magnitude of the angle between the Sun and the boresight of the current instrument field of view for FUVA (Short Wave).</p>	degrees	EPOCH
ICON Ancillary_FUVA_FOV_AZIMUTH_ANGLE	<p>FUVA (SW) FOV Celestial Azimuth</p> <p>Celestial azimuth with respect to geographic north for all 6 stripes across the image and 256 vertical pixels for the shortwave channel.</p>	degrees	EPOCH, VERTICAL, HORIZONTAL
ICON Ancillary_FUVA_FOV_ZENITH_ANGLE	<p>FUVA (SW) FOV Celestial Zenith</p> <p>Celestial zenith with respect to geographic north for all 6 stripes across the image and 256 vertical pixels for the shortwave channel.</p>	degrees	EPOCH, VERTICAL, HORIZONTAL

Variable Name	Description	Units	Dimensions
ICON Ancillary FUV Space Environment Region Status	<p>Space Environment Region Status</p> <p>Standardized for several missions, not all codes are relevant for ICON. Binary Coded Integer where</p> <ul style="list-style-type: none"> 1: Earth Shadow 2: Lunar Shadow 4: Atmospheric Absorption Zone 8: South Atlantic Anomaly 16: Northern Auroral Zone 32: Southern Auroral Zone 64: Periapsis Passage 128: Inner & Outer Radiation Belts 256: Deep Plasma Sphere 512: Foreshock Solar Wind 1024: Solar Wind Beam 2048: High Magnetic Field 4096: Average Plasma Sheet 8192: Bowshock Crossing 16384: Magnetopause Crossing 32768: Ground Based Observatories 65536: 2-Day Conjunctions 131072: 4-Day Conjunctions 262144: Time Based Conjunctions 524288: Radial Distance Region 1 1048576: Orbit Outbound 2097152: Orbit Inbound 4194304: Lunar Wake 8388608: Magnetotail 16777216: Magnetosheath 33554432: Science 67108864: Low Magnetic Latitude 134217728: Conjugate Observation 	binary	EPOCH
ICON Ancillary FUV Status	<p>FUV Status</p> <p>Binary Coded Integer where</p> <ul style="list-style-type: none"> 1: Earth Day View 2: Earth Night View 4: Calibration Target View 8: Off-target View 16: Sun Proximity View 32: Moon Proximity View 64: North Magnetic Footpoint View 128: South Magnetic Footpoint View 256: Science Data Collection View 512: Calibration Data Collection View 1024: RAM Proximity View 2048-32768: SPARE <p>Activity is what the spacecraft was commanded to do while status is the spacecraft's natural state of operations. This means that activity should always be used over status if they differ, but will almost always be the same.</p>	binary	EPOCH

Variable Name	Description	Units	Dimensions
ICON_ANCILLARY_FUV_ACTIVITY	<p>FUV Activity</p> <p>Binary Coded Integer of where</p> <p>1: Earth Day View 2: Earth Night View 4: Calibration Target View 8: Off-target View 16: Sun Proximity View 32: Moon Proximity View 64: North Magnetic Footpoint View 128: South Magnetic Footpoint View 256: Science Data Collection View 512: Calibration Data Collection View 1024: RAM Proximity View 2048-32768: SPARE</p> <p>Activity is what the spacecraft was commanded to do while status is the spacecraft's natural state of operations. This means that activity should always be used over status if they differ, but will almost always be the same.</p>	bianry	EPOCH
ICON_ANCILLARY_FUV_LOOK_AZIMUTH	<p>Look Azimuth</p> <p>Direction of nominal instrument pointing relative to spacecraft axes, in the yaw direction.</p>	degrees	EPOCH
ICON_ANCILLARY_FUV_LOOK_ROLL	<p>Look Roll</p> <p>Direction of nominal instrument pointing relative to spacecraft axes, in the roll direction.</p>	degrees	EPOCH
ICON_ANCILLARY_FUVA_PIERCEPOINTS_LATLONGALT_150	<p>FUVA (SW) Pierce Point Locations at 150 km in WGS84 (Latitude, Longitude, Altitude)</p> <p>Location of pierce points of a 150 km altitude surface in WGS84 for all 6 stripes across the image and 256 vertical pixels for the shortwave channel. Location is in Latitude, Longitude, Altitude.</p>	mixed	EPOCH, VERTICAL, HORIZONTAL, VECTORS
ICON_ANCILLARY_FUVA_PIERCEPOINTS_LATLONGALT_300	<p>FUVA (SW) Pierce Point Locations at 300 km in WGS84 (Latitude, Longitude, Altitude)</p> <p>Location of pierce points at 300 km altitude surface in WGS84 for all 6 stripes across the image and 256 vertical pixels for the shortwave channel. Location is in Latitude, Longitude, and Altitude.</p>	mixed	EPOCH, VERTICAL, HORIZONTAL, VECTORS
ICON_ANCILLARY_FUVA_PIERCEPOINTS_SZA_150	<p>FUVA (SW) Solar Zenith Angle of Pierce Points at 150 km</p> <p>Solar zenith angle of pierce points of a 150 km altitude surface for all 6 stripes across the image and 256 vertical pixels for the shortwave channel.</p>	degrees	EPOCH, VERTICAL, HORIZONTAL

Variable Name	Description	Units	Dimensions
ICON Ancillary_FUVA_PIERCEPOINTS_SZA_300	FUVA (SW) Solar Zenith Angle of Pierce Points at 300 km Solar zenith angle of pierce points of a 300 km altitude surface for all 6 stripes across the image and 256 vertical pixels for the shortwave channel.	degrees	EPOCH, VERTICAL, HORIZONTAL
ICON Ancillary_FUV_SUBSOLAR_LATITUDE	Subsolar Latitude Geodetic latitude of subsolar point, in WGS84.	degrees	EPOCH
ICON Ancillary_FUV_SUBSOLAR_LONGITUDE	Subsolar Longitude Geodetic longitude of subsolar point, in WGS84.	degrees	EPOCH
ICON Ancillary_FUV_TURRET_ANGLE	Turret Angle Position of the FUV turret with respect to nominal center position.	degrees	EPOCH
ICON Ancillary_FUVA_TANGENTPOINTS_LST	Tangent Points Local Solar Time of FUVA (SW) Local Solar Time at tangent points for all 6 stripes across the image and 256 vertical pixels for the shortwave channel.	hours, decimal	EPOCH, VERTICAL, HORIZONTAL
ICON Ancillary_FUVA_PIERCEPOINTS_LST_150	Local Solar Time at Pierce Points of FUVA (SW) at 150 km Local Solar Time at pierce points of a 150 km altitude surface for all 6 stripes across the image and 256 vertical pixels for the shortwave channel.	hours, decimal	EPOCH, VERTICAL, HORIZONTAL
ICON Ancillary_FUVA_PIERCEPOINTS_LST_300	Local Solar Time at Pierce Points of FUVA (SW) at 300 km Local Solar Time at pierce points of a 300 km altitude surface for all 6 stripes across the image and 256 vertical pixels for the shortwave channel.	hours, decimal	EPOCH, VERTICAL, HORIZONTAL
ICON Ancillary_FUVB_TANGENTPOINTS_LATLONGALT	Tangent Locations of FUVB (LW) in WGS84 (Latitude, Longitude, Altitude) Location of tangent points of in WGS84 for all 6 stripes across the image and 256 vertical pixels for the longwave channel. Locations are in Latitude, Longitude, Altitude.	mixed	EPOCH, VERTICAL, HORIZONTAL, VECTORS
ICON Ancillary_FUVB_TANGENTPOINTS_SZA	Tangent Points of FUVB (LW) Solar Zenith Angle Solar zenith angle at tangent points for all 6 stripes across the image and 256 vertical pixels for the longwave channel.	degrees	EPOCH, VERTICAL, HORIZONTAL
ICON Ancillary_FUVB_FOV_UNITVECTORS_ECEF	FOV Unit Vectors of FUVB (LW) in ECEF Unit vectors in ECEF for all 6 stripes across the image and 256 vertical pixels for the longwave channel.	dimensionless	EPOCH, VERTICAL, HORIZONTAL, VECTORS
ICON Ancillary_FUVB_HORIZONTAL_BORESIGHT_SUN_ANGLE	Horizontal Boresight of FUVB (LW) to Sun Angle Angle between the Sun and the horizontal plane at the center of the current instrument field of view for FUVB (Long Wave).	degrees	EPOCH

Variable Name	Description	Units	Dimensions
ICON Ancillary_FUVB_VERTICAL_BORESIGHT_SUN_ANGLE	Vertical Boresight of FUVB (LW) to Sun Angle Angle between the Sun and the vertical plane at the center of the current instrument field of view for FUVB (Long Wave).	degrees	EPOCH
ICON Ancillary_FUVB_TOTAL_BORESIGHT_SUN_ANGLE	Total Boresight of FUVB (LW) to Sun Angle Magnitude of the angle between the Sun and the boresight of the current instrument field of view for FUVB (Long Wave).	degrees	EPOCH
ICON Ancillary_FUVB_FOV_AZIMUTH_ANGLE	FUVB (LW) FOV Celestial Azimuth Celestial azimuth with respect to geographic north for all 6 stripes across the image and 256 vertical pixels for the longwave channel.	degrees	EPOCH, VERTICAL, HORIZONTAL
ICON Ancillary_FUVB_FOV_ZENITH_ANGLE	FUVB (LW) FOV Celestial Zenith Celestial zenith with respect to geographic north for all 6 stripes across the image and 256 vertical pixels for the longwave channel.	degrees	EPOCH, VERTICAL, HORIZONTAL
ICON Ancillary_FUVB_PIERCEPOINTS_LATLONGALT_150	FUVB (LW) Pierce Point Locations at 150 km in WGS84 (Latitude, Longitude, Altitude) Location of pierce points of a 150 km altitude surface in WGS84 for all 6 stripes across the image and 256 vertical pixels for the longwave channel. Location is in Latitude, Longitude, Altitude.	mixed	EPOCH, VERTICAL, HORIZONTAL, VECTORS
ICON Ancillary_FUVB_PIERCEPOINTS_LATLONGALT_300	FUVB (LW) Pierce Point Locations at 300 km in WGS84 (Latitude, Longitude, Altitude) Location of pierce points of a 300 km altitude surface in WGS84 for all 6 stripes across the image and 256 vertical pixels for the longwave channel. Location is in Latitude, Longitude, Altitude.	mixed	EPOCH, VERTICAL, HORIZONTAL, VECTORS
ICON Ancillary_FUVB_PIERCEPOINTS_SZA_150	FUVB (LW) Solar Zenith Angle of Pierce Points at 150 km Solar zenith angle of pierce points of a 150 km altitude surface for all 6 stripes across the image and 256 vertical pixels for the longwave channel.	degrees	EPOCH, VERTICAL, HORIZONTAL
ICON Ancillary_FUVB_PIERCEPOINTS_SZA_300	FUVB (LW) Solar Zenith Angle of Pierce Points at 300 km Solar zenith angle of pierce points of a 300 km altitude surface for all 6 stripes across the image and 256 vertical pixels for the longwave channel.	degrees	EPOCH, VERTICAL, HORIZONTAL
ICON Ancillary_FUVB_TANGENTPOINTS_LST	Tangent Points Local Solar Time of FUVB (LW) Local Solar Time at tangent points for all 6 stripes across the image and 256 vertical pixels for the longwave channel.	hours, decimal	EPOCH, VERTICAL, HORIZONTAL

Variable Name	Description	Units	Dimensions
ICON Ancillary FUVB Piercepoints LST_150	<p>Local Solar Time at Pierce Points of FUVB (LW) at 150 km</p> <p>Local Solar Time at pierce points of a 150 km altitude surface for all 6 stripes across the image and 256 vertical pixels for the longwave channel.</p>	hours, decimal	EPOCH, VERTICAL, HORIZONTAL
ICON Ancillary FUVB Piercepoints LST_300	<p>Local Solar Time at Pierce Points of FUVB (LW) at 300 km</p> <p>Local Solar Time at pierce points of a 300 km altitude surface for all 6 stripes across the image and 256 vertical pixels for the longwave channel.</p>	hours, decimal	EPOCH, VERTICAL, HORIZONTAL

Variable Name	Description	Units	Dimensions
ICON Ancillary FUV Quality Flag ICON Ancillary FUV Quality Flag	<p>Quality Flag</p> <p>Binary Coded Integer where</p> <ul style="list-style-type: none"> 1: STATE_NO_DATA 2: STATE_UNCONVERGED 4: STATE_LOW 8: STATE_MED 16: STATE_HIGH 32: AD_NO_DATA 64: AD_DIVERGING 128: AD_NOT_STARTED 256: AD_CONVERGING 512: AD_COARSE_CONVERGED 1024: AD_FINE_CONVERGED 2048-32768: SPARE <p>STATE_NO_DATA: No telemetry available for this time period. States are propagated from the last valid solution.</p> <p>STATE_UNCONVERGED: The GOODS KF solution is unconverged and should not be used. States are propagated from the last valid solution.</p> <p>STATE_LOW: The GPSR solution is better than the GOODS solution (The position accuracy is worse than 150 m, 1-sigma)</p> <p>STATE_MEDIUM: The GOODS solution is better than the GPSR solution (The position accuracy is better than 150 m, 1-sigma)</p> <p>STATE_HIGH: The GOODS solution is better than the GPSR solution, and meets its performance requirements (20 m position and 0.02 m/sec velocity, 1-sigma).</p> <p>AD_NO_DATA: No telemetry available for this time period. Attitude is copied from the last valid solution.</p> <p>AD_DIVERGING: Tolerances on the diagonal elements of the covariance matrix diverging and exceeds 9.9e9 asec² for attitude sigma and 9.9e9 asec²/sec² for rate sigma or negative values</p> <p>AD_NOT_STARTED: KF has not started processing measurements</p> <p>AD_CONVERGING: KF is in state of updating measurements and filter started to converge</p> <p>AD_COARSE_CONVERGED: Tolerances on the diagonal elements of the covariance matrix converging and below 200K asec² for x, y and 1000K for z in tracker frame for attitude and 10 asec²/sec² for x, y and z for rate</p> <p>AD_FINE_CONVERGED: Tolerances on the diagonal elements of the covariance matrix converging and below 1000 asec² for x, y and z in tracker frame for attitude and 1 asec²/sec² x, y and z for rate</p> <p>Nominal value of 1040: STATE_HIGH (16) and AD_FINE_CONVERGED (1024). All values are a combination of a STATE value and an AD (attitude determination) value. It is up to the user to determine if data outside 1040 is usable. AD values NOT AD_FINE_CONVERGED should be suspect. STATE_HIGH is expected, but STATE_MED is possible during maneuvers.</p>	binary	EPOCH

metadata

Variable Name	Description	Units	Dimensions
ICON Ancillary FUV Turret Flag	Turret Angle Flag Binary flag indicating when the turret angle information is unavailable. 0 is when angle is known, 1 is when the angle is not reported and has been set to zero.	binary	EPOCH

Acknowledgement

This is a data product from the NASA Ionospheric Connection Explorer mission, an Explorer launched on 21:59:45 EDT on October 10, 2019. Guidelines for the use of this product are described in the ICON Rules of the Road (<https://icon.ssl.berkeley.edu/Data>)

Responsibility for the mission science falls to the Principal Investigator, Dr. Thomas Immel at UC Berkeley: Immel, T.J., England, S.L., Mende, S.B. et al. Space Sci Rev (2018) 214: 13. <https://doi.org/10.1007/s11214-017-0449-2>

Responsibility for the validation of the L1 data products falls to the instrument lead investigators/scientists.

* EUV: Dr. Eric Korpela : <https://doi.org/10.1007/s11214-017-0384-2>

* FUV: Dr. Harald Frey : <https://doi.org/10.1007/s11214-017-0386-0>

* MIGHTI: Dr. Christoph Englert : <https://doi.org/10.1007/s11214-017-0358-4>, and <https://doi.org/10.1007/s11214-017-0374-4>

* IVM: Dr. Roderick Heelis : <https://doi.org/10.1007/s11214-017-0383-3>

Responsibility for the validation of the L2 data products falls to those scientists responsible for those products.

* Daytime O and N2 profiles: Dr. Andrew Stephan : <https://doi.org/10.1007/s11214-018-0477-6>

* Daytime (EUV) O+ profiles: Dr. Andrew Stephan : <https://doi.org/10.1007/s11214-017-0385-1>

* Nighttime (FUV) O+ profiles: Dr. Farzad Kamalabadi : <https://doi.org/10.1007/s11214-018-0502-9>

* Neutral Wind profiles: Dr. Jonathan Makela : <https://doi.org/10.1007/s11214-017-0359-3>

* Neutral Temperature profiles: Dr. Christoph Englert : <https://doi.org/10.1007/s11214-017-0434-9>

* Ion Velocity Measurements : Dr. Russell Stoneback : <https://doi.org/10.1007/s11214-017-0383-3>

Responsibility for Level 4 products falls to those scientists responsible for those products.

* Hough Modes : Dr. Chihoko Yamashita : <https://doi.org/10.1007/s11214-017-0401-5>

* TIEGCM : Dr. Astrid Maute : <https://doi.org/10.1007/s11214-017-0330-3>

* SAMI3 : Dr. Joseph Huba : <https://doi.org/10.1007/s11214-017-0415-z>

Pre-production versions of all above papers are available on the ICON website.

Overall validation of the products is overseen by the ICON Project Scientist, Dr. Scott England.

NASA oversight for all products is provided by the Mission Scientist, Dr. Jeffrey Klenzing.

Users of these data should contact and acknowledge the Principal Investigator Dr. Immel and the party directly responsible for the data product (noted above) and acknowledge NASA funding for the collection of the data used in the research with the following statement : "ICON is supported by NASA's Explorers Program through contracts NNG12FA45C and NNG12FA42I"

These data are openly available as described in the ICON Data Management Plan available on the ICON website (<http://icon.ssl.berkeley.edu/Data>).

This document was automatically generated on 2020-10-08 11:37 using the file:

ICON_L0P_FUV_Ancillary_2020-06-17_v03r099.NC

Software version: ICON SDC > FUV Prime Generator v3.0.2

ICON Data Product 2.4: FUV Daytime

This document describes the data product for ICON FUV Daytime, which is in NetCDF4 format.

This describes the data product for ICON FUV Daytime O/N2 (DP 2.4), which is in NetCDF4 format.

The ratio of oxygen to nitrogen in the thermosphere is obtained from the two channels of ICON FUV instrument data in,

through an inversion process described in <https://doi.org/10.1007/s11214-018-0477-6>.

NOTE: In this, the initial release of the data, only the disk parameters are included.

These files are named ICON_L2-4_FUV_Day_YYYY-MM-DD_vXXrZZZ.NC, where YYYY-MM-DD is the year month day and vXX shows the version number

and ZZZ shows the revision number of this file. Each individual file nominally contains 1 day (24 hours) of data.

The L2 FUV Daytime

files are produced from the L1 FUV files.

In addition, many other parameters and geophysical data products are included in the file.

All variables within the file are described in their Var_notes attribute. The data are identified in one of 3 var_types: data – which

contains the primary data product; support data – which contains parameters used in the retrieval such as geometry etc. that may also

be useful in any analysis of this data; and ignore_data – which are recorded for debugging purposes and should not be used for publication

without detailed discussion with the ICON team.

The dimensions of the data also indicate its type. For example, anything with epoch as a dimension means there is 1 value corresponding

to each instrument exposure. Anything with dimension Input_data corresponds to the input data, passed from Level 1. Anything with a

dimension of model refers to the forward model parameters used as part of the inversion. Anything with dimension altitude corresponds

to the altitude grid used for the inverted parameters.

History

Version 003, Frist public release, disk data only. S. L. England

Version 004, Updated to account for changes made to Level 1 files in version 05 (changes to background, radiances at Level 1). S. L. England, R. R. Meier

Dimensions

NetCDF files contain **variables** and the **dimensions** over which those variables are defined. First, the dimensions are defined, then all variables in the file are described.

The dimensions used by the variables in this file are given below, along with nominal sizes. Note that the size may vary from file to file. For example, the "Epoch" dimension, which describes the number of time samples contained in this file, will have a varying size.

Dimension Name	Nominal Size
Epoch	6970
Model Initial Values	13
Input Data	104
Altitude	22

Dimension Name	Nominal Size
Disk Retrieval Flag	3
Covariance Matrix 1st Dimension	13
Covariance Matrix 2nd Dimension	13

Variables

Variables in this file are listed below. First, "data" variables are described, followed by the "support_data" variables, and finally the "metadata" variables. The variables classified as "ignore_data" are not shown.

data

Variable Name	Description	Units	Dimensions
ICON_L24_Disk_ON2	Retrieved disk column O/N2 Retrieved column O/N2 ratio on the disk	Dimensionless	Epoch
ICON_L24_Disk_Sigma_ON2	Retrieved disk column O/N2 uncertainty Uncertainty in retrieved column O/N2 ratio on the disk, based on spread in reported uncertainty in input data	Dimensionless	Epoch

support_data

Variable Name	Description	Units	Dimensions
Epoch	Milliseconds since 1970-01-01 00:00:00 UTC Time corresponding to the center of each observation, in milliseconds since Jan 1 1970.	milliseconds	Epoch
ICON_L24.UTC_Time	Date and Time in UTC format UTC time corresponding to the retrieved parameters, in string format, as a function of time, in the format: 2017-05-27/00:00:01.435	string	Epoch
ICON_L24_F107	F10.7 used in retrieval Unscaled value of F10.7 used as an input to the inversion process, as a function of time. These data are from ftp://ftp.seismo.nrcan.gc.ca/spaceweather/solar_flux/fluxtable.txt . These are the solar radio flux values tabulated from the Space Weather Canada which is a part of Natural Resources Canada.	sfu	Epoch
ICON_L24_Ap	Ap used in retrieval Value of Ap used in the forward model, as a function of time. These data are from http://www-app3.gfz-potsdam.de/kp_index/ . These are the tabulated Kp values from GFZ German Research Centre for Geosciences at the Helmholtz Centre Potsdam.	index	Epoch
ICON_L24_Disk_Magnetic_Latitude	Magnetic Latitude on Disk Quasi-Dipole Magnetic Latitude at 150 km at Disk Retrieval location, in degrees	degrees	Epoch
ICON_L24_Disk_Magnetic_Longitude	Magnetic Longitude on Disk Quasi-Dipole Magnetic Longitude at 150 km at Disk Retrieval location, in degrees	degrees	Epoch

Variable Name	Description	Units	Dimensions
ICON_L24_Observatory_Latitude	Observatory Latitude Geodetic latitude (WGS84) of the spacecraft at the time corresponding to the middle of each FUV image, in degrees	degrees	Epoch
ICON_L24_Observatory_Longitude	Observatory Longitude Geodetic longitude (WGS84) of the spacecraft at the time corresponding to the middle of each FUV image, in degrees	degrees	Epoch
ICON_L24_Observatory_Altitude	Observatory Altitude Geodetic altitude (WGS84) of the spacecraft at the time corresponding to the middle of each FUV image, in kilometers	km	Epoch
ICON_L24_1356_Emission	Disk short wave emission Short wave disk column emission rate	Rayleighs	Epoch
ICON_L24_LBH_Emission	Disk long wave emission Long wave disk column emission rate	Rayleighs	Epoch
ICON_L24_Disk_Latitude	Retrieved disk latitude Geodetic latitude (WGS84) corresponding to disk retrieval	Degrees	Epoch
ICON_L24_Disk_Longitude	Retrieved disk longitude Geodetic longitude (WGS84) corresponding to disk retrieval	Degrees	Epoch
ICON_L24_Disk_SZA	Retrieved disk SZA Solar zenith angle corresponding to disk retrieval	Degrees	Epoch
ICON_L24_Local_Solar_Time_Disk	Local time on the disk Local solar time of the retrieval on the disk, in hours	hours	Epoch
ICON_L24_Disk_LOS_Zen_Angle	Retrieved disk LOS zenith angle Line of sight zenith angle corresponding to disk retrieval	Degrees	Epoch
ICON_L24_Instrument_Mode_Flag	Data collection mode Data collection mode of FUV instrument 1 = Dayside science 2 = Nightside science 3 = Calibration 4 = Nadir 5 = Conjugate 6 = Stars 7 = Ram 8 = Off Target 9 = Engineering 13 = Unknown	N/A	Epoch

Variable Name	Description	Units	Dimensions
ICON_L24_Level_1_Quality_Flag	<p>Quality indicator (also quickly shows times when images are available)</p> <p>QUALITY_FLAG is an indicator of data quality =</p> <ul style="list-style-type: none"> 0 = No errors or quality conditions, LVLH 1 = No errors or quality conditions, R-LVLH 2 = Lunar calibration 3 = Insufficient high voltage 4 = Nadir calibration 5 = Zero wind calibration 6 = Bad pointing 7 = S/C attitude slew 8 = Conjugate observation 9 = Stellar calibration 10 = Unreliable background subtracted 17 = unspecified error condition 	N/A	Epoch
ICON_L24_Disk_Retrieval_Flags	<p>Disk Retrieval Flags</p> <p>Disk retrieval quality flag, where 0 = nominal retrieval, 1 = Disk short/long wave ratio out of model range, 2 = Disk O/N2 value out of expected range, 3 = Disk P/N2 uncertainty out of expected range.</p>	integer	Epoch
ICON_L24_Limb_Retrieval_Flags	<p>Limb Retrieval Flags</p> <p>Limb retrieval quality flag, where 0 = no limb inversion, 1 = retrieval nominal, 2 = number of iterations in retrieval algorithm reaches 10 without convergence, 3 = one or more inversion model parameters hits a priori upper or lower limit, 4 = altitude of peak intensity too close to boundary, 5 = standard deviation of one or more variables exceeds expected limit, 6 = Chi-squared value is outside of expected range - either too large or too small, 7 = one or more uncertainties is outside of expected range.</p>	integer	Epoch
ICON_L24_Whole_Day_Retrieval_Flag	<p>Whole Day Retrieval Flags</p> <p>Single flag set for whole day, where 0 = nominal data set, 1 = whole day skipped because no solar zenith angles were within range.</p>	Integer	

Acknowledgement

This is a data product from the NASA Ionospheric Connection Explorer mission, an Explorer launched in 2019.

Guidelines for the use of this product are described in the ICON Rules of the Road (<https://http://icon.ssl.berkeley.edu/Data>).

Responsibility for the mission science falls to the Principal Investigator, Dr. Thomas Immel at UC Berkeley:
Immel, T.J., England, S.L., Mende, S.B. et al. Space Sci Rev (2018) 214: 13. <https://doi.org/10.1007/s11214-017-0449-2>

Responsibility for the validation of the L1 data products falls to the instrument lead investigators/scientists.

- * EUV: Dr. Eric Korpela : <https://doi.org/10.1007/s11214-017-0384-2>
- * FUV: Dr. Harald Frey : <https://doi.org/10.1007/s11214-017-0386-0>
- * MIGHTI: Dr. Christoph Englert : <https://doi.org/10.1007/s11214-017-0358-4>, and <https://doi.org/10.1007/s11214-017-0374-4>
- * IVM: Dr. Roderick Heelis : <https://doi.org/10.1007/s11214-017-0383-3>

Responsibility for the validation of the L2 data products falls to those scientists responsible for those products.

- * Daytime O and N2 profiles: Dr. Andrew Stephan : <https://doi.org/10.1007/s11214-018-0477-6>
- * Daytime (EUV) O+ profiles: Dr. Andrew Stephan : <https://doi.org/10.1007/s11214-017-0385-1>
- * Nighttime (FUV) O+ profiles: Dr. Farzad Kamalabadi : <https://doi.org/10.1007/s11214-018-0502-9>
- * Neutral Wind profiles: Dr. Jonathan Makela : <https://doi.org/10.1007/s11214-017-0359-3>
- * Neutral Temperature profiles: Dr. Christoph Englert : <https://doi.org/10.1007/s11214-017-0434-9>
- * Ion Velocity Measurements : Dr. Russell Stoneback : <https://doi.org/10.1007/s11214-017-0383-3>

Responsibility for Level 4 products falls to those scientists responsible for those products.

- * Hough Modes : Dr. Chihoko Yamashita : <https://doi.org/10.1007/s11214-017-0401-5>
- * TIEGCM : Dr. Astrid Maute : <https://doi.org/10.1007/s11214-017-0330-3>
- * SAMI3 : Dr. Joseph Huba : <https://doi.org/10.1007/s11214-017-0415-z>

Pre-production versions of all above papers are available on the ICON website.

Overall validation of the products is overseen by the ICON Project Scientist, Dr. Scott England.

NASA oversight for all products is provided by the Mission Scientist, Dr. Jeffrey Klenzing.

Users of these data should contact and acknowledge the Principal Investigator Dr. Immel and the party directly responsible for the data product (noted above) and acknowledge NASA funding for the collection of the data used in the research with the following statement : "ICON is supported by NASA's Explorers Program through contracts NNG12FA45C and NNG12FA42I".

These data are openly available as described in the ICON Data Management Plan available on the ICON website (<http://icon.ssl.berkeley.edu/Data>).

This document was automatically generated on 2022-10-19 12:22 using the file:

ICON_L2-4_FUV_Day_2022-01-01_v04r003.NC

Software version: ICON_SDC > FUV v04r003

ICON Data Product 2.5: FUV Nighttime O+ profile

This document describes the data product for ICON FUV Nighttime O+ profiles (DP 2.5), which is in NetCDF4 format.

This data product contains (nominally) 24 hours of data, including O+ density profiles of the nighttime ionosphere as well as ancillary data such as satellite locations and measurement times. In this data product, all the time variables and time dependent variables (with dimension Epoch) contain only the nighttime measurements. We neither use any daytime measurements nor output them in this data product. The O+ density profiles are estimated from the measured brightness profiles of 135.6 nm emissions by solving a regularized linear inverse problem. Due to multiple scattering (yields non-linearity) and low brightness (yields low SNR), we do not use the brightness measurements having tangent altitudes below 150 km, consequently we do not estimate the O+ density profile at tangent altitudes below 150 km (i.e. on the disk). The Altitude dimension is the maximum number of tangent points that are above 150 km for the entire 24-hour period. The Stripe dimension represents the dimension from left to right along the horizon for any one given image. Nominally 6 stripes are used, and each stripe samples a 3-degree wide field of view. O+ density profiles are estimated separately for each stripe. ICON_L25_Quality variable indicates the quality of the retrieved data and it needs to be checked when using the data.

History

FUV L2.5 Processor v4.00: Flag the data affected by conjugate photoelectrons and adjust the qualities accordingly. Add a new variable `ICON_L25_Sunlit_Conjugate_Raypath_Percentage` to indicate how much the data is affected by photoelectrons . Fix the Date_Start-Date_End bug., U. Kamaci, 5 Feb 2021

Dimensions

NetCDF files contain **variables** and the **dimensions** over which those variables are defined. First, the dimensions are defined, then all variables in the file are described.

The dimensions used by the variables in this file are given below, along with nominal sizes. Note that the size may vary from file to file. For example, the "Epoch" dimension, which describes the number of time samples contained in this file, will have a varying size.

Dimension Name	Nominal Size
Epoch	unlimited
Altitude	108
Stripe	6

Variables

Variables in this file are listed below. First, "data" variables are described, followed by the "support_data" variables, and finally the "metadata" variables. The variables classified as "ignore_data" are not shown.

data

Variable Name	Description	Units	Dimensions
ICON_L25_VER	<p>VER of 135.6-nm emission as a function of altitude</p> <p>The volume emission rates (VER) are estimated from the brightness profiles of the 135.6 nm emissions by solving a regularized linear (multiple scattering is negligible) inverse problem. In the inverse problem, atmosphere is divided into spherical shells with boundaries determined by the tangent altitudes, and VER is assumed to be uniform inside those shells. Solving the inverse problem, VER value for each shell is estimated. The details of the inversion are given in Kamalabadi et al. [2018, doi: 10.1007/s11214-018-0502-9].</p>	ph/cm ³ /s	Epoch, Altitude, Stripe
ICON_L25_VER_Error	<p>Error in VER of 135.6-nm emission as a function of altitude</p> <p>The statistical 1-sigma errors computed for the estimated VER values. Errors are obtained by propagating the uncertainties in the given brightness profiles (provided in the L1 input file) through the VER estimation process. Some other error sources are not included in this variable (such as the bias introduced by the regularization, or the errors due to the assumption that the VER is uniform between two adjacent tangent altitudes).</p>	ph/cm ³ /s	Epoch, Altitude, Stripe
ICON_L25_O_Plus_Density	<p>O+ density as a function of altitude</p> <p>The O+ profiles are obtained from the estimated volume emission rate (VER) profiles assuming the emission arises from radiative recombination and mutual neutralization. The NRLMSISE00 model is used to characterize the oxygen density needed to model the mutual neutralization contribution.</p>	1/cm ³	Epoch, Altitude, Stripe
ICON_L25_O_Plus_Density_Error	<p>Error in O+ density as a function of altitude</p> <p>The statistical 1-sigma errors computed for the estimated O+ density profiles. Errors are obtained by propagating the uncertainties in the estimated VER profiles through the O+ density profile calculations. Some other error sources are not included in this variable (such as the bias introduced by the regularization, or the errors due to the assumption that the VER is uniform between two adjacent tangent altitudes).</p>	1/cm ³	Epoch, Altitude, Stripe
ICON_L25_HMF2	<p>Altitudes of the peak O+ densities</p> <p>The altitudes of the peak O+ densities that are obtained by performing cubic spline interpolation on each profile.</p>	km	Epoch, Stripe

Variable Name	Description	Units	Dimensions
ICON_L25_Latitude	<p>Latitudes of the peak O+ densities in WGS84</p> <p>The geodetic latitudes of the peak O+ densities that are obtained by performing nearest neighbor interpolation on each profile.</p>	degrees North	Epoch, Stripe
ICON_L25_Longitude	<p>Longitudes of the peak O+ densities in WGS84</p> <p>The geodetic longitudes of the peak O+ densities that are obtained by performing nearest neighbor interpolation on each profile.</p>	degrees East	Epoch, Stripe
ICON_L25_Magnetic_Latitude	<p>Magnetic latitudes of the peak O+ densities</p> <p>The magnetic latitudes of the peak O+ densities that are obtained by performing nearest neighbor interpolation on each profile.</p>	degrees North	Epoch, Stripe
ICON_L25_Magnetic_Longitude	<p>Magnetic longitudes of the peak O+ densities</p> <p>The magnetic longitudes of the peak O+ densities that are obtained by performing nearest neighbor interpolation on each profile.</p>	degrees East	Epoch, Stripe
ICON_L25_HMF2_Error	<p>Error in estimated altitudes of the peak O+ densities</p> <p>The propagated statistical errors from the O+ density profiles through the hmF2 estimation. Errors are propagated through the cubic spline interpolation using a Monte Carlo method. The details can be found in Kamalabadi et al. [2018, doi: 10.1007/s11214-018-0502-9].</p>	km	Epoch, Stripe
ICON_L25_NMF2	<p>Estimated peak O+ densities</p> <p>The peak O+ densities that are obtained by performing cubic spline interpolation on each profile.</p>	1/cm ³	Epoch, Stripe
ICON_L25_NMF2_Error	<p>Error in estimated peak O+ densities</p> <p>The propagated statistical 1-sigma errors from the O+ density profiles through the NmF2 estimation. Errors are propagated through the cubic spline interpolation using a Monte Carlo method. The details can be found in Kamalabadi et al. [2018, doi: 10.1007/s11214-018-0502-9].</p>	1/cm ³	Epoch, Stripe
ICON_L25_Local_Solar_Time	<p>Local solar times at the retrieved peak O+ density locations</p> <p>Local solar times (0-24 hours decimal) at the locations of the retrieved peak O+ densities.</p>	hours	Epoch, Stripe

Variable Name	Description	Units	Dimensions
ICON_L25_Quality	<p>A quantification of the inversion quality, from 0 (Bad) to 1 (Good)</p> <p>While the intent is that the variable ICON_L25_O_Plus_Density_Error accurately characterizes the statistical error in the O+ density data, it is possible that systematic errors are present, or that the statistical error estimation is not accurate. If it is suspected that this is the case, the quality will be less than 1.0, which is determined based on the brightness values and other considerations. If the data are definitely unusable, the quality will be 0.0. Users should exercise caution when the quality is less than 1.0. The reason for low quality can be learned from the ICON_L25_Quality_Flags variable.</p>		Epoch, Stripe
ICON_L25_Quality_Flags	<p>Provides description about the observed inversion quality</p> <p>This variable is intended to provide a description to the user why `ICON_L25_Quality` is less than 1, if that is the case. This is a binary coded integer whose binary representation indicates the quality conditions which were present during or before the inversion. Here are the quality conditions represented by each digit:</p> <ul style="list-style-type: none"> 1: Error occurred during inversion. Makes the quality 0, no retrieval available. 2: No reliable quality L1 data available. Makes the quality 0, no retrieval produced. 4: Very low input signal level (very low brightness). Makes the quality 0, retrieval available. 8: Low input signal level (low brightness). Makes the quality 0.5, retrieval available. 16: Unexpected hmF2 value. Makes the quality 0.5, retrieval available. 32: Nmf2 retrieval affected by conjugate photoelectron contribution in the measurements that is not modeled in the inversion. If the variable `ICON_L25_Sunlit_Conjugate_Raypath_Percentage` is more than 10%, this flag is activated. Makes the quality 0.5, retrieval available. 		Epoch, Stripe

support_data

Variable Name	Description	Units	Dimensions
Epoch	<p>Milliseconds since 1970-01-01 00:00:00 UTC at middle of measurement integration</p> <p>The center times of the exposures, measured as milliseconds after 1970-01-01/00:00:00 UT. There might be time jumps that are larger than the nominal measurement integration time between two consecutive elements of this array, which is because we neither include daytime measurements nor their times. There also could be larger time jumps due to calibration maneuvers or turret movements.</p>	ms	Epoch
ICON_L25_UTC_Time	<p>Center time of 12-second profile integration</p> <p>The center times of the exposures. Different than Epoch, array elements are not in milliseconds, but they are strings of the date in UT, with the format YYYY-MM-DD HH:MM:SS.FFFZ</p>		Epoch
ICON_L25_Start_Times	<p>Start time of 12-second profile integration</p> <p>The start times of the exposures, in UT, with the format YYYY-MM-DD/HH:MM:SS.</p>		Epoch
ICON_L25_Stop_Times	<p>Stop time of 12-second profile integration</p> <p>The stop times of the exposures, in UT, with the format YYYY-MM-DD/HH:MM:SS.</p>		Epoch
ICON_L25_Observatory_Position_Latitude	<p>Spacecraft WGS84 latitude</p> <p>The geodetic latitudes of the spacecraft, evaluated using the WGS84 ellipsoid.</p>	degrees North	Epoch
ICON_L25_Observatory_Position_Longitude	<p>Spacecraft WGS84 longitude</p> <p>The geodetic longitudes of the spacecraft, evaluated using the WGS84 ellipsoid.</p>	degrees East	Epoch
ICON_L25_Observatory_Position_Altitude	<p>Spacecraft WGS84 altitude</p> <p>The geodetic altitudes of the spacecraft, evaluated using the WGS84 ellipsoid.</p>	km	Epoch
ICON_L25_Orbit_Number	<p>ICON Orbit Number</p> <p>Integer orbit numbers for each measurement.</p>		Epoch
ICON_L25_O_Plus_Profile_Latitude	<p>O+ latitude in WGS84</p> <p>The latitudes of each point in the O+ profile, evaluated using the WGS84 ellipsoid. It should be noted that while a single latitude value (the tangent latitude) is given for each point, the observation is inherently a horizontal average over many hundreds of kilometers.</p>	degrees North	Epoch, Altitude, Stripe

Variable Name	Description	Units	Dimensions
ICON_L25_O_Plus_Profile_Longitude	<p>O+ longitude in WGS84</p> <p>The longitudes of each point in the O+ profile, evaluated using the WGS84 ellipsoid. It should be noted that while a single longitude value (the tangent longitude) is given for each point, the observation is inherently a horizontal average over many hundreds of kilometers.</p>	degrees East	Epoch, Altitude, Stripe
ICON_L25_O_Plus_Profile_Altitude	<p>O+ altitude in WGS84</p> <p>The altitudes of each point in the O+ profile, evaluated using the WGS84 ellipsoid. These altitudes are one half sample above the tangent altitudes of each pixel's line of sight (consistent with the assumption implicit in the inversion that the emission rate is constant within the layer between tangent altitudes).</p>	km	Epoch, Altitude, Stripe
ICON_L25_Celestial_Azimuth_Angle_Profile	<p>FOV Celestial Azimuth</p> <p>Celestial azimuth angles associated with the brightness measurements. Each pixel of the instrument has its own azimuth angle associated with its line of sight.</p>	degrees	Epoch, Altitude, Stripe
ICON_L25_Celestial_Zenith_Angle_Profile	<p>FOV Celestial Zenith</p> <p>Celestial zenith angles associated with the brightness measurements. Each pixel of the instrument has its own zenith angle associated with its line of sight.</p>	degrees	Epoch, Altitude, Stripe
ICON_L25_Solar_Zenith_Angle	<p>Solar zenith angles of NmF2 points</p> <p>Solar zenith angles of the retrieved NmF2 points.</p>	degrees	Epoch, Stripe
ICON_L25_Sunlit_Conjugate_Raypath_Percentage	<p>Percentage of sunlit conjugate raypath</p> <p>For each retrieval, this variable returns what percent of the magnetically conjugate points of the raypath passing through the NmF2 point are sunlit. Higher value indicates potentially higher contribution in the 135.6 nm emissions from conjugate photoelectrons.</p>		Epoch, Stripe

metadata

Variable Name	Description	Units	Dimensions
ICON_L25_Inversion_Method	<p>Used inversion method to get VER from brightness</p> <p>This string specifies the inversion method used in the estimation of the VER profiles from the brightness profiles. It has the form Tikhonov_k where k (0,1, or 2) specifies the order used in the Tikhonov regularization. Since the brightness profiles are noisy, we incorporate our prior knowledge on the characteristics of the VER profiles into the inverse problem for regularization. The order k is determined by what kind of prior knowledge we want to incorporate. The estimation of VER profile can be considered as choosing one among infinitely many: order 0 (zero) penalizes VER profiles with high l2 norm, but does not incorporate any structural information about the profile ; order 1 (one) penalizes VER profiles whose first derivatives have high l2 norm (meaning that it penalizes high VER variations through altitudes) ; order 2 (two) penalizes VER profiles whose second derivatives have high l2 norm (meaning that it penalizes VER profiles with high VER curvatures through altitudes).</p>		

Acknowledgement

This is a data product from the NASA Ionospheric Connection Explorer mission, an Explorer launched at 21:59:45 EDT on October 10, 2019, from Cape Canaveral AFB in the USA. Guidelines for the use of this product are described in the ICON Rules of the Road (<http://icon.ssl.berkeley.edu/Data>).

Responsibility for the mission science falls to the Principal Investigator, Dr. Thomas Immel at UC Berkeley: Immel, T.J., England, S.L., Mende, S.B. et al. Space Sci Rev (2018) 214: 13. <https://doi.org/10.1007/s11214-017-0449-2>

Responsibility for the validation of the L1 data products falls to the instrument lead investigators/scientists.

* EUV: Dr. Eric Korpela : <https://doi.org/10.1007/s11214-017-0384-2>

* FUV: Dr. Harald Frey : <https://doi.org/10.1007/s11214-017-0386-0>

* MIGHTI: Dr. Christoph Englert : <https://doi.org/10.1007/s11214-017-0358-4>, and <https://doi.org/10.1007/s11214-017-0374-4>

* IVM: Dr. Roderick Heelis : <https://doi.org/10.1007/s11214-017-0383-3>

Responsibility for the validation of the L2 data products falls to those scientists responsible for those products.

* Daytime O and N2 profiles: Dr. Andrew Stephan : <https://doi.org/10.1007/s11214-018-0477-6>

* Daytime (EUV) O+ profiles: Dr. Andrew Stephan : <https://doi.org/10.1007/s11214-017-0385-1>

* Nighttime (FUV) O+ profiles: Dr. Farzad Kamalabadi : <https://doi.org/10.1007/s11214-018-0502-9>

* Neutral Wind profiles: Dr. Jonathan Makela : <https://doi.org/10.1007/s11214-017-0359-3>

* Neutral Temperature profiles: Dr. Christoph Englert : <https://doi.org/10.1007/s11214-017-0434-9>

* Ion Velocity Measurements : Dr. Russell Stoneback : <https://doi.org/10.1007/s11214-017-0383-3>

Responsibility for Level 4 products falls to those scientists responsible for those products.

* Hough Modes : Dr. Chihoko Yamashita : <https://doi.org/10.1007/s11214-017-0401-5>

* TIEGCM : Dr. Astrid Maute : <https://doi.org/10.1007/s11214-017-0330-3>

* SAMI3 : Dr. Joseph Huba : <https://doi.org/10.1007/s11214-017-0415-z>

Pre-production versions of all above papers are available on the ICON website.

<http://icon.ssl.berkeley.edu/Publications>

Overall validation of the products is overseen by the ICON Project Scientist, Dr. Scott England.

NASA oversight for all products is provided by the Mission Scientist, Dr. Jeffrey Klenzing.

Users of these data should contact and acknowledge the Principal Investigator Dr. Immel and the party directly responsible for the data product (noted above) and acknowledge NASA funding for the collection of the data used in the research with the following statement : "ICON is supported by NASA's Explorers Program through contracts NNG12FA45C and NNG12FA42I".

These data are openly available as described in the ICON Data Management Plan available on the ICON website (<http://icon.ssl.berkeley.edu/Data>).

This document was automatically generated on 2021-02-17 13:41 using the file:

ICON_L2-5_FUV_Night_2020-03-20_v04r000.NC

Software version: ICON_SDC > ICON_UIUC_FUV_L2.5_Processor v4.000

4.1.4 EUV Data Products Functional Description

This subsection details the science data products produced by a particular mission instrument or ground system element (e.g., SOC).

Following this brief overview, details of the data products are provided for L1, L2 and Ancillary products. L0 are instrument level (voltages, currents, instrument codes etc.) and not interpretable for anyone without intimate knowledge of the instrumentation.

The mission-specific data levels should be defined, and the steps needed to process each level of data shall be described.

The introduction to Section 4 describes the overall data levels for ICON. Table 4.1.4.1 lists the EUV products by level. The EUV Ancillary file provides the geometry relevant to the observations, using knowledge of the spacecraft position and pointing derived from the spacecraft telemetry. The L1 calibrated spectra provide the brightness of the extreme Ultraviolet airglow observed by the instrument, in the form of 2D images with 169 columns (approximately horizontal) and 108 rows (imaging direction - approximately vertical). In addition, the brightness of 12 airglow wavelength ranges is provided for the 108 pixels in the imaging direction. The Ancillary files provide the corresponding geometry information for each time point in the L1 file. The Level 2 product is produced for EUV utilizing the Ancillary and Level 1 calibrated spectra. During the daytime the data are used to determine ionospheric O⁺.

Level	Source (Instrument/Model)	Data Product
0	EUV	L0 EUV Science Data
0	EUV	L0 EUV Engineering Data
Anc.	Ground	EUV Ancillary Data
1	EUV	L1 EUV Calibrated Spectra
2	EUV	L2 Daytime O ⁺

Table 4.1.4.1 – List of EUV data products by level.

At a high level, the flow of the EUV data products is shown in Figure 4.1.4.1.

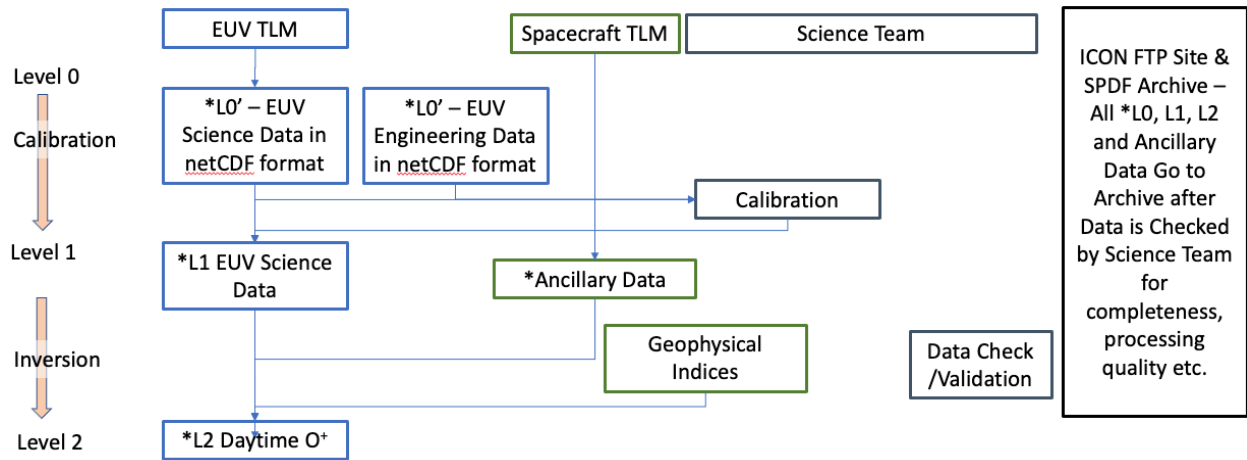


Figure 4.1.4.1 – Schematic of the EUV Data Products and their Flow.

The overall concept for producing the Level 2 daytime O⁺ is as follows: The EUV instrument measures the brightness of the extreme ultraviolet on the limb, including the most prominent emissions from He at 58.4 nm, O⁺ at 61.7 nm and O⁺ at 83.4 nm. From the latter two, the altitude profile of O⁺ can be determined during the daytime (Level 2 product). The Level 1 product includes the calibrated brightness of the 61.7 and 83.4 nm emissions during the daytime (the EUV instrument does not collect ionospheric O⁺ data during the night). The view direction of the EUV instrument is ~90° to the spacecraft track and spans tangent altitudes from the base of the ionosphere to ~500 km. Images are taken up to every 12s (approximately 100 km along the orbit track) during normal operations. For more details on instrument operations, see Section 3. The tangent points associated with the image, and other geometry are provided in the Ancillary file, and combined with the Level 1 data at Level 2. The overall process of producing EUV Level 1 is shown in Figure 4.1.4.2.

EUV L0 to L1 Calibrated EUV Limb Brightness - Algorithm

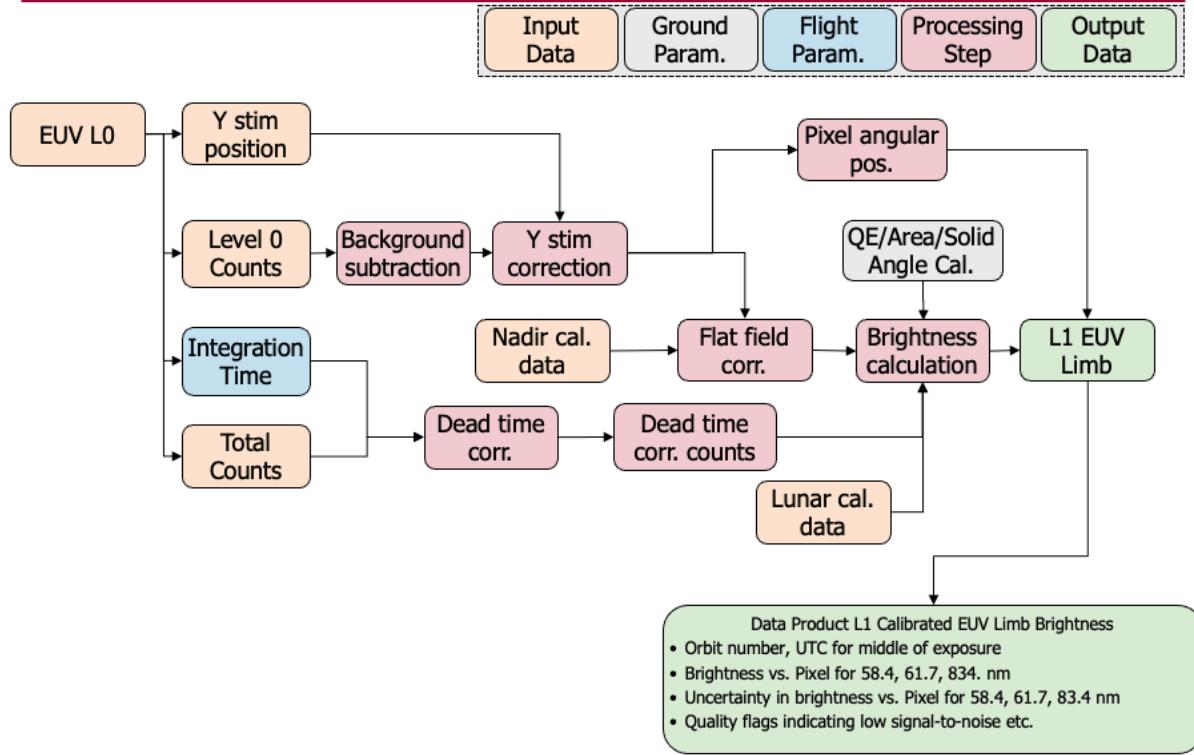


Figure 4.1.4.2 – Overall process for producing EUV Level 1 Data Product.

Level 2 Daytime O⁺ is then determined from the EUV Level 1 and Ancillary data products. At Level 2, the inversion of the 61.7 and 83.4 nm emissions into O⁺ makes use of the fact that the 61.7 nm emission is optically thin, whereas the 83.4 nm emission is resonantly scattered by ionospheric O⁺. The density of O⁺ as a function of tangent altitude, latitude, longitude etc. reported. These values are reported for each dayside image, corresponding to 1 every ~100 km along the orbit track during normal operations. More information on the EUV data collection, and its changes over the lifetime of ICON are reported in Section 3. The overall process of producing EUV Level 2 Daytime O⁺ Product is shown in Figure 4.1.4.3.

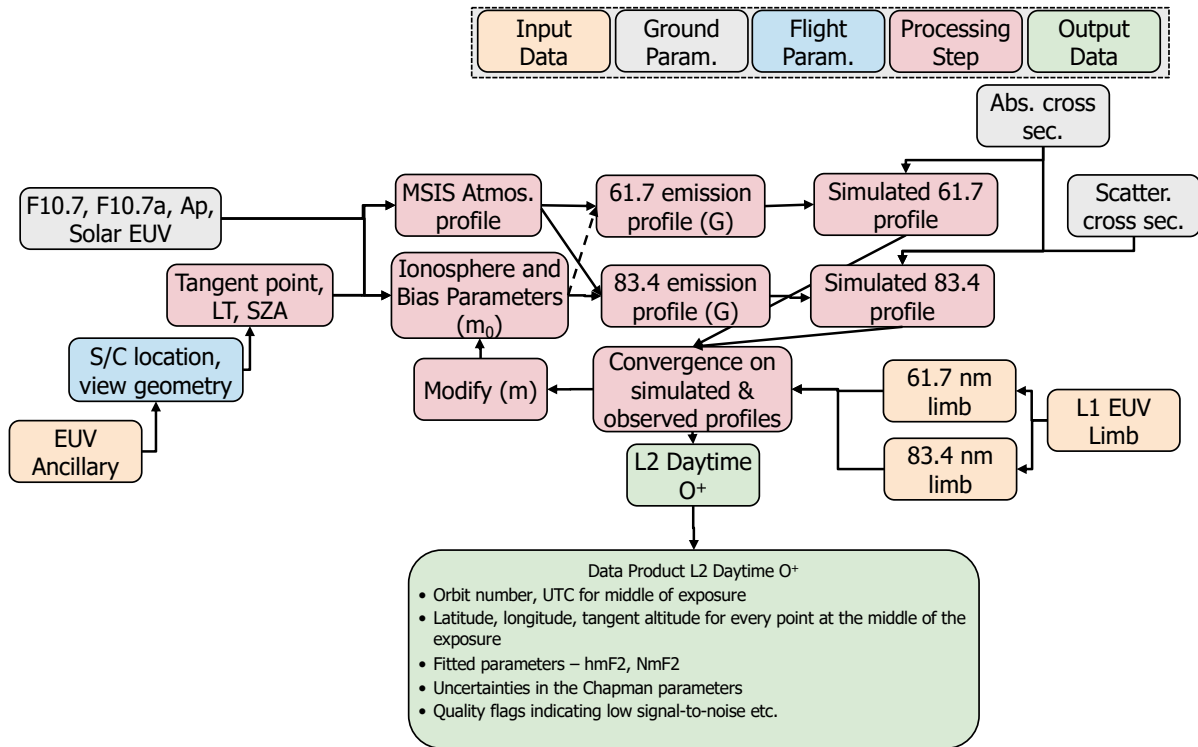


Figure 4.1.4.3 – Overall process for producing EUV Level 2 Daytime O⁺ Data Product.

For more details on the data processing, the reader is directed to the ICON Calibration and Measurement Algorithms Document (CMAD).

A reference to the general data level definitions located in the Heliophysics Science Data Management Policy should be included.

The Heliophysics Science Data Management Policy, HPD-SDMP version 2.0, effective February 14, 2022 does not describe data levels. The ICON data levels closely follow those in the PDMP Template.

Any associated metadata products to be generated and maintained shall also be described.

Following this brief overview, full details of the metadata for each product are provided.

Details should also include the cadence (e.g., hourly, daily, etc.) for processing of data products.

The lowest level EUV science data (L0) has one file per 12s exposure. These are processed as they arrive on the ground, until an entire day of data has arrived at the Science Data Center (SDC). The SDC processes the L0 into L1 and L2, and produces the Ancillary Data Products. The Level 1 files correspond to 1 file per science image at Level 0. The Ancillary and Level 2 product have 1 file per day of data. The cadence for production of all products beyond Level 0 is daily, and begins once all inputs are available. As one example, the ancillary products use the

definitive ephemeris, which is generated by the Mission Operations Center approximately 1 week after real-time. The Level 1 radiances also rely upon lunar and nadir calibrations that are performed monthly, so the Level 1 files can take up to a month for all inputs to be ready.

The following section contains detailed descriptions of each of the EUV Data Products, the data and metadata contained within.

ICON Data Product 1: Calibrated EUV Brightness Profiles

This document describes the data product for ICON EUV Level 1 Calibrated Flux and Error altitude profiles Software Version = 3.2.0, which is in NetCDF4 format.

ICON is a NASA low-Earth-orbit (~586 km) satellite dedicated to the study of the Earth's ionosphere. Its four instruments are designed to measure the temperature, velocity, and ion density of the atmosphere along vertical profiles from 100 to 600 km. The typical observation cadence is one exposure every 12 s. Orbital precession ensures rapid coverage of all available ranges of latitude, longitude, and local time-of-day.

This document describes the ICON Extreme Ultraviolet Imaging Spectrograph (EUV) Level 1 (L1) science products which are the emission line radiances required for the altitude-profile ion density inversion modeling (Level 2 products, Stephan et al. 2017, DOI: 10.1007/s11214-017-0385-1). Inputs are the raw Level 0 products which are 2D Altitude Profile Region (APR) images in units of counts (with the horizontal axis representing wavelength, and the vertical axis tangent altitude). Outputs are intensities as a function of altitude bin in units of flux (Rayleighs) along with the corresponding random and systematic errors for twelve emission lines. The profiles are 108 elements long [0:107] with the active EUV Field-of-View spanning 99 elements [5:103]. In addition to the essential flux and error variables, several other L1 vector and scalar variables are provided that are used in the flux calculations. For each emission line profile the vector variables are: the raw number of counts, the number of background counts, and the ratio of the source-count area to background-count area. The scalar variable is the detector dead-time that is applied to the L0 exposure time variable.

The following L1 variables are provided for convenience: a vector of the 12 emission line center wavelengths, a vector containing the integrated counts (i.e. a spectrum) of the entire detector, a scalar which is an estimate of the total number of Solar Stray Light counts, and an image (same dimensions as the input Counts image) in flux units (Rayleighs per pixel). This image is flat-fielded, but not background subtracted. It may prove useful to future investigators who wish to do more sophisticated modeling of background, stray light, blended features etc...

All the L0 variables are passed along to the L1 products unchanged (except for the Counts Image which is replaced with the Flux Image). To create the Level 2 products from the Level 1 products, additional information is required concerning the satellite's position and orientation as a function of time. This information is provided for every L1 file in Ancillary NetCDFs (one file per day). Note that the Ancillary data is not used in creating EUV Level 1 products. Written by Martin M. Sirk and Eric Korpela. See Sirk et al 2017 (doi:10.1007/s11214-017-0384-2) for more information about EUV, and Immel et al 2017 for the ICON mission (doi:10.1007/s11214-017-0449-2)

History

Notes for Version 2.0.21 2020 April 3

0) In the beginning there were Photons, and they were good. Then the slaughter began ...

1) Added 5 emission lines (i.e. 5 new Region Masks)

2) Updated Stim Fiducial Average positions

3) Background is fit with a 2nd order polynomial to reduce Poisson noise.

For exposures with very low background (< 25 counts in Background region)

the background is set to a constant (mean of the counts/pixel)

4) Get_flux does better small and large scale flat-fielding before

extracting lines. Errors for pixels with small or negative counts are now correct. Errors for out-of-FOV pixels are set to 99999.9

Fractional Poisson error in the Flat Field is now added in Quadrature (with factor of 2 applied to denominator) to the Random fractional flux error

5) Solid angles are now correct for flight image scale. Look Angles of FOV are now centered on pixel 51.5, not 54. A text file containing pixel #, look angle, solid angle, and mean tangent altitude is now part of the calibration files for user convenience.

6) If significant SAA counts are detected in the region where there are no emission features (pixels [48:104,64:107]), then perform SAA subtraction by scaling a pure SAA calibration image by the appropriate amount.

7) QEs for all lines are based on the QE model curve scaled to the SSL measurements (at 584, 616, and 834). Since the two emission lines at the extreme edges of the spectral range are known to be blended and vignetted as well as contaminated by detector edge effects (and SAA counts), the systematic error was arbitrarily increased by a factor of 1.5.

Notes for Version 2.1.0 2020 Aug 19

1) Fixed conceptual error in Deadtime Correction. Now only uses the observed number of Stimulsor events to determine detector deadtime.

2) Calculates the loss in gain for He 584 and O 834 based on slope of gain loss curves determined from Lunar Calibrations.

3) Interpolated Flat Field is determined as a function of EPOCH from a single program that loads all the flatfields into a data cube.

4) Added a new variable to the L1 product that is an estimate of Solar Stray Light (caused by pointing too close to the Sun). L2 products can use this variable and set a threshold of around 450 counts. Solar light changes significantly as a function of viewing geometry, so this threshold is likely

to change with the seasons.

5) Center of EUV FOV is now at Pixel 51.91 +/- 0.14. This is the number used for the EUV L1 Ancillary products.

Notes for Version 2.1.1 2020 Sep 17

1) Trivial edits to History Attribute, and Software Version number strings

Version_3-0-0_notes.txt M.M.Sirk April 30 2021

1) Adjusted slopes in GAIN_LOSS_CORRECTION.PRO to better correct O 834 and He 584 fluxes

2) Modified ISPY.PRO to skip very first file of each day in case it happens to have the HV ramping up

3) Shifted the vector of solid angles in DOMEGA.PRO by 1/2 pixel to center the value on the middle of pixel, not the edge

4) The L1 COUNTS (line counts vector) variable returned by GET_FLUX.PRO is now the raw counts, not background subtracted counts

Version_3-2-0_notes.txt M.M.Sirk Sept 21 2021

1) Re-Adjusted slopes in GAIN_LOSS_CORRECTION.PRO to better correct O 834 and He 584 fluxes. Now, the first year is fit with a second order polynomial and then a straight line for most of 2021.

2) Modified ISPY.PRO to check for valid time intervals. If Bad, skip the file and say so in the error log.

3) Modified the way background counts are estimated to account for regions of high gain loss where the background counts are lower.

4) Fixed a conceptual error in the way the Flat Fields are determined. Now the average gain loss across each line profile is determined for each altitude bin. The flats are normalized to the Average number of counts in the line, not the Median.

Dimensions

NetCDF files contain **variables** and the **dimensions** over which those variables are defined. First, the dimensions are defined, then all variables in the file are described.

The dimensions used by the variables in this file are given below, along with nominal sizes. Note that the size may vary from file to file. For example, the "Epoch" dimension, which describes the number of time samples contained in this file, will have a varying size.

Dimension Name	Nominal Size
Epoch	1
Vertical	108
Horizontal	169
ICON_L0_EUV_SR_SumCnt	16
ICON_L0_EUV_PulseHH	64
ICON_L1_EUV_Lines	12

Variables

Variables in this file are listed below. First, "data" variables are described, followed by the "support_data" variables, and finally the "metadata" variables. The variables classified as "ignore_data" are not shown.

data

Variable Name	Description	Units	Dimensions
Epoch	<p>Exposure epoch, midpoint of exposure. Number of msec since Jan 1, 1970.</p> <p>Exposure epoch, midpoint of exposure. Number of msec since Jan 1, 1970. This variable contains the time corresponding to the wind profile reported in this file. It is evaluated at the midpoint of the exposure time. It is in UTC and has units of milliseconds since Jan 1, 1970. A human-readable version of the time can be found in the global attributes Date_Start and Date_Stop.</p>	milliseconds	Epoch
ICON_L1_EUV_Deadc	<p>Deadtime Correction</p> <p>Exposure time correction factor due to detector deadtime. Calculate deadtime correction based on the exposure time, and the known Stimulsor rate, and the observed Stimulsor counts. Calculate the ratio of observed (NStim) to expected stim counts (this is the electronics deadtime). If routine fails, Set DEADCOR=1.0 and set stim warning flag.</p>		Epoch
ICON_L1_EUV_BackRatio	<p>Ratio of background to total counts</p> <p>Ratio of background region counts to total image counts. This ratio can be used to quickly identify observations with high background such as SAA. If greater than 0.25 then a warning flag is set. This flag is often set at night since the lines fluxes are low, and, thus, the background relatively high. The ratio is for convenience and non-essential.</p>		Epoch
ICON_L1_EUV_Lines	<p>Wavelengths of Science Lines</p> <p>Wavelengths of Science Lines. Counts are extracted from the counts image using the REGIONS_MASK variable, and fluxes and their errors are calculated for these wavelengths</p>	nanometers	Epoch, ICON_L1_EUV_Lines
ICON_L1_EUV_Spectrum	<p>Integrated Spectrum in Raw Counts</p> <p>Integrated Spectrum of entire APR in Raw Counts. Useful for assessing general spectrum quality, background level etc. Provided as a non-essential convenience</p>	Counts	Epoch, Horizontal

Variable Name	Description	Units	Dimensions
ICON_L1_EUV_Flux	<p>Line Fluxes in Rayleighs</p> <p>Flux in Rayleighs for the extracted lines.</p> <p>This is the primary L1 product. For every science line the flux is determined for each altitude bin. Converting from raw image counts to Rayleighs is as follows</p> <p>Corrected_Counts = Region_Mask * (APR_Image - Background) / Flatfield</p> <p>Flux = Corrected_Counts / (ExposureTime * DeadCor * QE * GeoArea * Omega)</p> <p>GeoArea is the area of the slit in cm², and Omega is the solid angle (in radians) subtended by each altitude bin.</p> <p>The same math is applied to the random and systematic errors in the flux.</p>	Rayleighs	Epoch, Vertical, ICON_L1_EUV_Lines

Variable Name	Description	Units	Dimensions
ICON_L1_EUV_RandomError	<p>Poisson errors in Rayleighs</p> <p>Random Error in Flux in Rayleighs for the extracted lines Random errors are determined based on the *observed* number of counts in the source region and the background region prior to any of the corrections outlined above using this scheme:</p> <p>S = source counts</p> <p>B = background counts</p> <p>SA = source area</p> <p>BA = background area</p> <p>$R = SA/SB$</p> <p>$Net = S - R*B$</p> <p>$\sigma_S = \sqrt{S}$</p> <p>$\sigma_B = \sqrt{B}*R$</p> <p>$\sigma_{Net}^2 = \sigma_S^2 + \sigma_B^2$</p> <p>$\sigma_{Net} = \sqrt{S + (B * R^2)}$</p> <p>$Flux_error = flux * \sigma_{net}/Net$</p> <p>Additionally, the fractional error in the Flat Field is added in Quadrature to the Random Error.</p>	Rayleighs	Epoch, Vertical, ICON_L1_EUV_Lines

Variable Name	Description	Units	Dimensions
ICON_L1_EUV_SystematicErr	<p>Systematic errors in Rayleighs</p> <p>Systematic Error in Flux in Rayleighs for the extracted lines The systematic error was determined during ground calibration at three wavelengths (834, 584, and 616 Ang) and represents a multiplicative uncertainty in the instrument throughput, not a lack of knowledge in the Zero Point. The absolute QE of ICON EUV was measured with a calibrated NIST photodiode, and was cross-checked by a MCP detector that was calibrated against a second NIST photodiode. The two methods agreed to within 11% (the two photodiodes were measured at SSL side by side and agree to within 5%). The uncertainty in the absolute photometric sensitivity quoted by NIST for the diodes is 7%. Thus, combining in quadrature</p> $\text{Sys Error} = \text{Sqrt}(0.11^2 + 0.07^2) = 13\%$ <p>For other wavelengths we used interpolated values of the grating and detector efficiency curves. For these wavelengths we add another 5% in quadrature to get 14%. For the two lines at the extreme edges of the detector, He 537 and O 878, we add another 7% since the first line is vignetted, and the second often shows scattered Lyman Alpha.</p>	Rayleighs	Epoch, Vertical, ICON_L1_EUV_Lines
ICON_L1_EUV_Backgrounds	<p>Backgrounds in Rayleighs</p> <p>Backgrounds in Rayleighs for each extracted line</p>	Rayleighs	Epoch, Vertical, ICON_L1_EUV_Lines
ICON_L1_EUV_Counts	<p>Raw Counts</p> <p>Raw counts for each extracted line per altitude pixel</p>	counts	Epoch, Vertical, ICON_L1_EUV_Lines
ICON_L1_EUV_Background_Counts	<p>Raw Background Counts</p> <p>Raw Background Counts for each line per altitude bin</p>	counts	Epoch, Vertical, ICON_L1_EUV_Lines

support_data

Variable Name	Description	Units	Dimensions
ICON_L0_EUV_TimeGPS	Calculated number of GPS milliseconds since 1980 January 06 00:00:00 UTC to center of image integration.	milliseconds	Epoch
ICON_L0_EUV_TimeUTC_Start	UTC milliseconds since 1970 January 01 00:00:00 to beginning of image integration.	milliseconds	Epoch
ICON_L0_EUV_TimeUTC_Stop	UTC milliseconds since 1970 January 01 00:00:00 to end of image integration.	milliseconds	Epoch
ICON_L0_EUV_TimeIntegration	Time to integrate EUV buffer (transmitted as N where time is $10 \times (N+1)$ ms).	milliseconds	Epoch
ICON_L0_EUV_SecondsGPS	Reported GPS seconds.	seconds	Epoch
ICON_L0_EUV_50_NanosecondOffsetGPS	Reported flight clock GPS offset in 50ns increments (always less than 2 seconds worth).	count	Epoch
ICON_L0_EUV_CountPulseFEC	Number of FEC pulses during integration. Number of Fast Event Counter pulses during integration	count	Epoch
ICON_L0_EUV_APR_BinsX	X (column) dimension of the APR image (X maximum - X minimum + 1).	count	Epoch
ICON_L0_EUV_APR_BinsY	Y (row) dimension of the APR image (Y maximum - Y minimum + 1).	count	Epoch
ICON_L0_EUV_APR_ErrorFlag	Indicates processing error in APR (some photons in region were ignored) when set.	flag	Epoch
ICON_L0_EUV_APR_MaximumX	APR maximum X value in region of interest.		Epoch
ICON_L0_EUV_APR_MaximumY	APR maximum Y value in region of interest.		Epoch
ICON_L0_EUV_APR_MinimumX	APR minimum X value in region of interest.		Epoch
ICON_L0_EUV_APR_MinimumY	APR minimum Y value in region of interest.		Epoch
ICON_L0_EUV_APR_PhotonCount	Altitude profile region photons collected during integration.	count	Epoch
ICON_L0_EUV_APR_ShiftRightX	Number of bits each APR X value has been right shifted.	bits	Epoch
ICON_L0_EUV_APR_ShiftRightY	Number of bits each APR Y value has been right shifted.	bits	Epoch
ICON_L0_EUV_CompressionErrorFlag	Data transmitted via delta-compression mode contained errors during compression if set.	flag	Epoch

Variable Name	Description	Units	Dimensions
ICON_L0_EUV_CompressionFlag	Data transmitted via delta-compression mode.	flag	Epoch
ICON_L0_EUV_DiagnosticPhotonCount	Total number of photons received on EUV interface by DCB FPGA before ROI filtering during integration.	count	Epoch
ICON_L0_EUV_HV_ActiveFlag	HV power supply activity flag (0=OFF, 1=ON).	flag	Epoch
ICON_L0_EUV_HV_DAC_Day	DAC HV count / level programmed for EUV day mode.	count	Epoch
ICON_L0_EUV_HV_DAC_Night	DAC HV count / level programmed for EUV night mode.	count	Epoch
ICON_L0_EUV_HV_DAC_Safe	DAC HV count / level programmed for EUV safe mode.	count	Epoch
ICON_L0_EUV_ModeSelect	Currently selected EUV mode (0=SAFE, 1=?, 2=DAY, 3=NIGHT).	flag	Epoch
ICON_L0_EUV_Q_Maximum	Maximum charge/pulse height (q) (higher q photons not histogrammed).		Epoch
ICON_L0_EUV_Q_Minimum	Minimum charge/pulse height (q) (lower q photons not histogrammed).		Epoch
ICON_L0_EUV_SR_ErrorFlag	Indicates processing error in SR (some photons in region were ignored) when set.	flag	Epoch
ICON_L0_EUV_SR_PhotonCount	Stimulation region (1 and 2) photons collected during integration.	count	Epoch
ICON_L0_EUV_SR1_MinimumX	SR 1 minimum X value (always of size 128 x 128 prior to binning).		Epoch
ICON_L0_EUV_SR1_MinimumY	SR 1 minimum Y value (always of size 128 x 128 prior to binning).		Epoch
ICON_L0_EUV_SR2_MinimumX	SR 2 minimum X value (always of size 128 x 128 prior to binning).		Epoch
ICON_L0_EUV_SR2_MinimumY	SR 2 minimum Y value (always of size 128 x 128 prior to binning).		Epoch
ICON_L0_EUV_PulseHeightHistogram	Pulse height / charge histogram bin for Q.		Epoch, ICON_L0_EUV_PulseHH
ICON_L0_EUV_SR1_SumColumn	Sum of stimulation region 1 binned column photon counts.	count	Epoch, ICON_L0_EUV_SR_SumCnt
ICON_L0_EUV_SR1_SumRow	Sum of stimulation region 1 binned row photon counts.	count	Epoch, ICON_L0_EUV_SR_SumCnt

Variable Name	Description	Units	Dimensions
ICON_L0_EUV_SR2_Sum Column	Sum of stimulation region 2 binned column photon counts.	count	Epoch, ICON_L0_EUV_SR_SumCnt
ICON_L0_EUV_SR2_Sum Row	Sum of stimulation region 2 binned row photon counts.	count	Epoch, ICON_L0_EUV_SR_SumCnt
ICON_L1_EUV_Max_Stim_Shift	<p>Maximum observed shift of Stim Pulsors</p> <p>Maximum observed shift of Stimulsors. StimPulsors are current pulses injected directly into the micro-channel plate (MCP) anode and are processed by detector electronics. They are used to track positional drifts of photon events and changes in plate-scale of the MCP. If this number exceeds 0.65 pixels then the Flatfield and Regions Mask will be warped to match the APR Image. If this number ever exceeds 2 pixels there is probably something wrong, e.g. not enough stim counts to determine a good centroid, or bad SAA contamination.</p>	Pixels	Epoch
ICON_L1_EUV_Error_bit_field	<p>Warning Bit-field</p> <p>Non-fatal Warning bit field Warnings:1 = Invalid Deadtime correction, 2 = Stimulsor counts saturated, 4 = High Background warning, 8 = Stim shift (in pixels) GT Stim_Shift_Limit</p>		Epoch
ICON_L1_EUV_Version	<p>Pipeline Version Number</p> <p>ICON EUV L0 to L1 Pipeline Software Version Number</p>		Epoch
ICON_L1_EUV_Solar_Counts	<p>Total Raw Solar Counts</p> <p>Total Raw Solar Counts. Stray Solar counts are not subtracted from the raw data, thus, line fluxes will be contaminated if this number is larger than ~ 450 counts).</p>	counts	Epoch
ICON_L1_EUV_Source_to_Back_ratio	<p>Area Ratio of line region to background region</p> <p>Area Ratio of each line region to background region This ratio is used in the random error calculation</p>		Epoch, Vertical, ICON_L1_EUV_Lines
ICON_L1_EUV_Flux_Image	<p>Flux Image in Rayleighs per pixel</p> <p>Flux Image in units of Rayleighs per Pixel. This image is NOT background subtracted. This image IS Flat Fielded. This image is not needed for creating L2 products but may be useful to future users who may wish to do additional analysis.</p>	Rayleighs	Epoch, Vertical, Horizontal

metadata

Variable Name	Description	Units	Dimensions
ICON_L0_EUV_TimeUTC	UTC ISO 8601 timestamp at middle of image integration.		Epoch
ICON_L1_EUV_Feng_Shui_Index	<p>Feng Shui Index</p> <p>Feng Shui Index Feng Shui is important. ICONs Pa Kua # is 3 and flies East, and EUV looks North which corresponds to Growth and Health, Both Good!</p>		Epoch

Acknowledgement

This is a data product from the NASA Ionospheric Connection Explorer mission, an Explorer launched at 21:59:45 EDT on October 10, 2019, from Cape Canaveral AFB in the USA. Guidelines for the use of this product are described in the ICON Rules of the Road (<http://icon.ssl.berkeley.edu/Data>).

Responsibility for the mission science falls to the Principal Investigator, Dr. Thomas Immel at UC Berkeley: Immel, T.J., England, S.L., Mende, S.B. et al. Space Sci Rev (2018) 214: 13. <https://doi.org/10.1007/s11214-017-0449-2>

Responsibility for the validation of the L1 data products falls to the instrument lead investigators/scientists.

* EUV: Dr. Eric Korpela : <https://doi.org/10.1007/s11214-017-0384-2>

* FUV: Dr. Harald Frey : <https://doi.org/10.1007/s11214-017-0386-0>

* MIGHTI: Dr. Christoph Englert : <https://doi.org/10.1007/s11214-017-0358-4>, and <https://doi.org/10.1007/s11214-017-0374-4>

* IVM: Dr. Roderick Heelis : <https://doi.org/10.1007/s11214-017-0383-3>

Responsibility for the validation of the L2 data products falls to those scientists responsible for those products.

* Daytime O and N2 profiles: Dr. Andrew Stephan : <https://doi.org/10.1007/s11214-018-0477-6>

* Daytime (EUV) O+ profiles: Dr. Andrew Stephan : <https://doi.org/10.1007/s11214-017-0385-1>

* Nighttime (FUV) O+ profiles: Dr. Farzad Kamalabadi : <https://doi.org/10.1007/s11214-018-0502-9>

* Neutral Wind profiles: Dr. Jonathan Makela : <https://doi.org/10.1007/s11214-017-0359-3>

* Neutral Temperature profiles: Dr. Christoph Englert : <https://doi.org/10.1007/s11214-017-0434-9>

* Ion Velocity Measurements : Dr. Russell Stoneback : <https://doi.org/10.1007/s11214-017-0383-3>

Responsibility for Level 4 products falls to those scientists responsible for those products.

* Hough Modes : Dr. Chihoko Yamashita : <https://doi.org/10.1007/s11214-017-0401-5>

* TIEGCM : Dr. Astrid Maute : <https://doi.org/10.1007/s11214-017-0330-3>

* SAMI3 : Dr. Joseph Huba : <https://doi.org/10.1007/s11214-017-0415-z>

Pre-production versions of all above papers are available on the ICON website.

<http://icon.ssl.berkeley.edu/Publications>

Overall validation of the products is overseen by the ICON Project Scientist, Dr. Scott England.

NASA oversight for all products is provided by the Mission Scientist, Dr. Jeffrey Klenzing.

Users of these data should contact and acknowledge the Principal Investigator Dr. Immel and the party directly responsible for the data product (noted above) and acknowledge NASA funding for the collection of the data used in the research with the following statement : "ICON is supported by NASA's Explorers Program through contracts NNG12FA45C and NNG12FA42I".

These data are openly available as described in the ICON Data Management Plan available on the ICON website (<http://icon.ssl.berkeley.edu/Data>).

This document was automatically generated on 2021-11-05 11:39 using the file:

ICON_L1_EUV_Flux_2021-01-02_235946_v03r001.nc

Software version: 3.2.0

4.1.5 Hough Mode Extensions (HME) Functional Description

This subsection details the science data products produced by a particular mission instrument or ground system element (e.g., SOC).

Following this brief overview, details of the Level 4 HME data products are provided.

The mission-specific data levels should be defined, and the steps needed to process each level of data shall be described.

The introduction to Section 4 describes the overall data levels for ICON. Table 4.1.5.1 lists the HME products at Level 4.

Level	Source (Instrument/Model)	Data Product
4	HME – derived from MIGHTI L2	Hough Mode Extensions
4	HME – derived from MIGHTI L2	TIEGCM Lower Boundary File

Table 4.1.5.1 – List of HME data products at Level 4.

At a high level, the flow of the HME data products is shown in Figure 4.1.5.1. The start-point for the HMEs is the MIGHTI winds and temperature data from Level 2.

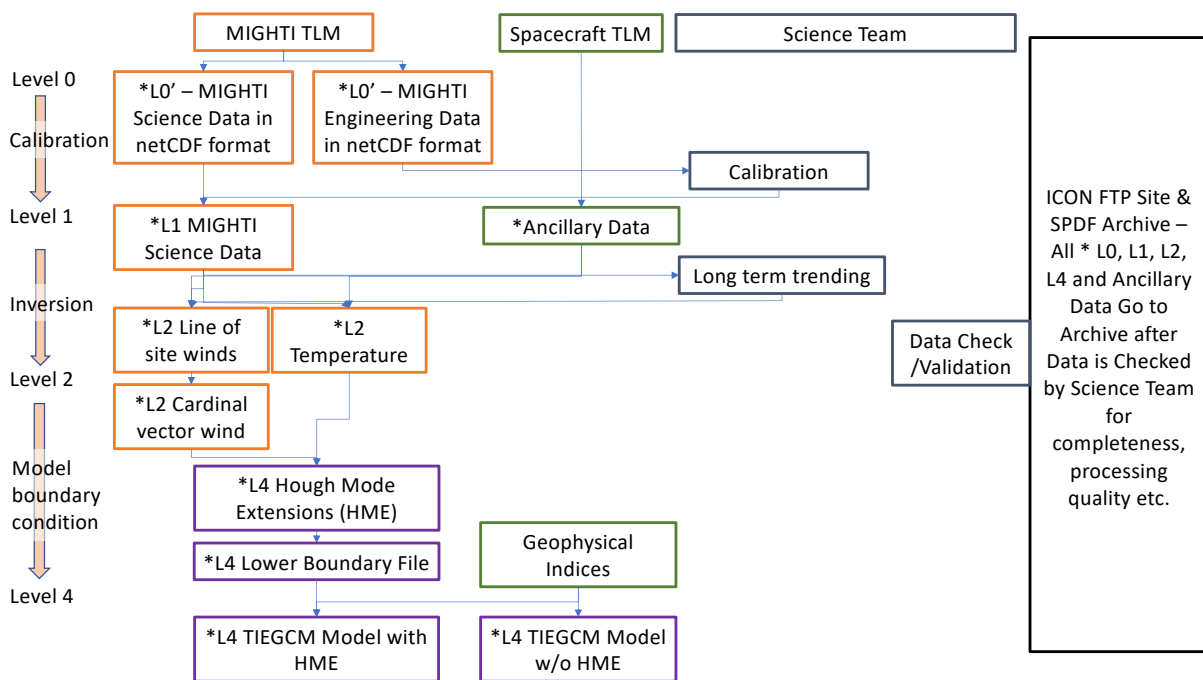


Figure 4.1.5.1 – Schematic of the HME Data Products and their Flow.

The overall concept for producing the L4 HME products are as follows: MIGHTI provides wind and temperature data over both day and night in the lower thermosphere (approx. 94 – 105 km). Over an observational cycle (approx. 42 days), these wind and temperature data fill up every combination of latitude, longitude and local time that MIGHTI sees. These are used to derive global fits to empirical functions – the Hough Mode Extensions. These fit simultaneously to the wind and temperature data in this region, and provide an estimate of the global structure of the upward propagating tides throughout the upper atmosphere. Two products are created – the first is the HME fits that come out of the process described above. The second is a lower boundary file that can be used with the TIEGCM model to allow the tides determined from this HME fit to drive the model at its ~97 km lower boundary. Further details on the HME fits for ICON can be found in Forbes et al., (2017; <https://doi.org/10.1007/s11214-017-0401-5>) and Cullens et al., (2020; <https://doi.org/10.1186/s40645-020-00330-6>).

A reference to the general data level definitions located in the Heliophysics Science Data Management Policy should be included.

The Heliophysics Science Data Management Policy, HPD-SDMP version 2.0, effective February 14, 2022 does not describe data levels. The ICON data levels closely follow those in the PDMP Template.

Any associated metadata products to be generated and maintained shall also be described. Details should also include the cadence (e.g., hourly, daily, etc.) for processing of data products.

Following this brief overview, full details of the metadata for each product are provided.

Level 4 HMEs are generated using 42 days of Level 2 temperature and wind data. Further, the outputs are smoothed with a 10 day mean, meaning these require 52 days of data to begin processing. At present the HME products are produced in batches of approximately 3-6 months of data at a time.

The following section contains detailed descriptions of the Hough Mode Extensions product, and the data and metadata contained within. The TIEGCM lower boundary file contains the parameters required for TIEGCM to run, and is only usable with that model.

ICON Data Product 4.1: HME Amplitudes and Phases

This data product contains HME tidal amplitudes and phases of zonal wind, meridional wind, temperature from 0-400 km in the latitude range of 10°S-40°N. Tidal structures obtained from ICON-MIGHTI observations are fitted to Hough Mode Extension (HME). ICON-MIGHTI winds and temperature from 94 km to 102 km in the latitude range of 10°S-40°N are used to fit to the HME. To cover all local time for tidal analysis, ICON-MIGHTI data are accumulated with a 35-day window. HME has been widely used and tested before, and detailed HME methodologies are summarized in *Forbes et al.* [1994] and *Oberheide et al.* [2011]. HME for ICON is summarized in *Forbes et al.* [2017], and a sensitivity analysis of HME fitting to the local-time and altitude coverage and variables can be found in *Cullens et al.* [2020]. HME is only consider vertical propagation from below and do not include in-situ generations and non-linear interactions. For obtaining realistic tidal structures including in-situ generated tides, propagation, and nonlinear interaction, TIE-GCM simulations forced by ICON-HME, ICON data product 4.3, is recommended to use.

Dimensions

NetCDF files contain variables and the dimensions over which those variables are defined. First, the dimensions are defined, then all variables in the file are described.

The dimensions used by the variables in this file are given below, along with nominal sizes.

Dimension Name	Nominal Size
Latitude	36
Altitude	150
Date	35

Variables

Variables in this file are listed below.

Variable Name	Description	Unit	Dimension
DAMP_XX_T	Diurnal tidal temperature amplitudes. XX represents different tidal components. The notation Ws or Es are used to indicate a westward or eastward-propagating diurnal tide, respectively, with zonal wavenumber s. For example, E3 will be a eastward propagating diurnal tides with zonal wavenumber 3.	K	Latitude, Altitude
SDAMP_XX_T	Semi-diurnal tidal temperature amplitudes. XX represents different tidal components. The notation Ws or Es are used to indicate a westward or eastward-propagating diurnal tide, respectively, with zonal wavenumber s. For example, w3 will be a westward propagating semi-diurnal tides with zonal wavenumber 3.	K	Latitude, Altitude
DAMP_XX_U	Diurnal tidal zonal wind amplitudes. XX represents different tidal components. The notation Ws or Es are used to indicate a westward or eastward-propagating diurnal tide, respectively, with zonal wavenumber s.	m/s	Latitude, Altitude

	For example, E3 will be a eastward propagating diurnal tides with zonal wavenumber 3.		
SDAMP_XX_U	Semi-diurnal tidal zonal wind amplitudes. XX represents different tidal components. The notation Ws or Es are used to indicate a westward or eastward-propagating diurnal tide, respectively, with zonal wavenumber s. For example, w3 will be a westward propagating semi-diurnal tides with zonal wavenumber 3.	m/s	Latitude, Altitude
DAMP_XX_V	Diurnal tidal meridional wind amplitudes. XX represents different tidal components. The notation Ws or Es are used to indicate a westward or eastward-propagating diurnal tide, respectively, with zonal wavenumber s. For example, E3 will be a eastward propagating diurnal tides with zonal wavenumber 3.	m/s	Latitude, Altitude
SDAMP_XX_V	Semi-diurnal tidal meridional wind amplitudes. XX represents different tidal components. The notation Ws or Es are used to indicate a westward or eastward-propagating diurnal tide, respectively, with zonal wavenumber s. For example, w3 will be a westward propagating semi-diurnal tides with zonal wavenumber 3.	m/s	Latitude, Altitude
DPHASE_XX_T	Diurnal tidal temperature phases. XX represents different tidal components. The notation Ws or Es are used to indicate a westward or eastward-propagating diurnal tide, respectively, with zonal wavenumber s. the phase is defined as the time when the maximum is observed at 0 longitude.	hour	Latitude, Altitude
SDPHASE_XX_T	Semi-diurnal tidal temperature phases. XX represents different tidal components. The notation Ws or Es are used to indicate a westward or eastward-propagating diurnal tide, respectively, with zonal wavenumber s.	hour	Latitude, Altitude
DPHASE_XX_U	Diurnal tidal zonal wind phases. XX represents different tidal components. The notation Ws or Es are used to indicate a westward or eastward-propagating diurnal tide, respectively, with zonal wavenumber s.	hour	Latitude, Altitude
SDPHASE_XX_U	Semi-diurnal tidal zonal wind phases. XX represents different tidal components. The notation Ws or Es are used to indicate a westward or eastward-propagating diurnal tide, respectively, with zonal wavenumber s.	hour	Latitude, Altitude

DPHASE_XX_V	Diurnal tidal meridional wind phases. XX represents different tidal components. The notation Ws or Es are used to indicate a westward or eastward-propagating diurnal tide, respectively, with zonal wavenumber s.	hour	Latitude, Altitude
SDPHASE_XX_V	Semi-diurnal tidal meridional wind phases. XX represents different tidal components. The notation Ws or Es are used to indicate a westward or eastward-propagating diurnal tide, respectively, with zonal wavenumber s.	hour	Latitude, Altitude
MissingData	MIGHTI tides are calculated using 35 days of observations. Missing Data indicate which days are used to estimated MIGHTI tidal structures for HME fit. A 35 day windows is +/- 17 days from the date indicated in this file. 0: data is not missing 1: data is missing.	None	Date

Acknowledgement

This is a data product from the NASA Ionospheric Connection Explorer mission, an Explorer launched at 21:59:45 EDT on October 10, 2019, from Cape Canaveral AFB in the USA. Guidelines for the use of this product are described in the ICON Rules of the Road (<http://icon.ssl.berkeley.edu/Data>).

Responsibility for the mission science falls to the Principal Investigator, Dr. Thomas Immel at UC Berkeley: Immel, T.J., England, S.L., Mende, S.B. et al. Space Sci Rev (2018) 214: 13.
<https://doi.org/10.1007/s11214-017-0449-2>

Responsibility for the validation of the L1 data products falls to the instrument lead investigators/scientists.

- * EUV: Dr. Eric Korpela : <https://doi.org/10.1007/s11214-017-0384-2>
- * FUV: Dr. Harald Frey : <https://doi.org/10.1007/s11214-017-0386-0>
- * MIGHTI: Dr. Christoph Englert : <https://doi.org/10.1007/s11214-017-0358-4>, and <https://doi.org/10.1007/s11214-017-0374-4>
- * IVM: Dr. Roderick Heelis : <https://doi.org/10.1007/s11214-017-0383-3>

Responsibility for the validation of the L2 data products falls to those scientists responsible for those products.

- * Daytime O and N2 profiles: Dr. Andrew Stephan : <https://doi.org/10.1007/s11214-018-0477-6>
- * Daytime (EUV) O+ profiles: Dr. Andrew Stephan : <https://doi.org/10.1007/s11214-017-0385-1>
- * Nighttime (FUV) O+ profiles: Dr. Farzad Kamalabadi : <https://doi.org/10.1007/s11214-018-0502-9>
- * Neutral Wind profiles: Dr. Jonathan Makela : <https://doi.org/10.1007/s11214-017-0359-3>
- * Neutral Temperature profiles: Dr. Christoph Englert : <https://doi.org/10.1007/s11214-017-0434-9>
- * Ion Velocity Measurements : Dr. Russell Stoneback : <https://doi.org/10.1007/s11214-017-0383-3>

Responsibility for Level 4 products falls to those scientists responsible for those products.

- * Hough Modes : Dr. Chihoko Cullens : <https://doi.org/10.1007/s11214-017-0401-5>
- * TIEGCM : Dr. Astrid Maute : <https://doi.org/10.1007/s11214-017-0330-3>
- * SAMI3 : Dr. Joseph Huba : <https://doi.org/10.1007/s11214-017-0415-z>

Pre-production versions of all above papers are available on the ICON website.
<http://icon.ssl.berkeley.edu/Publications>

Overall validation of the products is overseen by the ICON Project Scientist, Dr. Scott England.

NASA oversight for all products is provided by the Mission Scientist, Dr. Jeffrey Klenzing.

Users of these data should contact and acknowledge the Principal Investigator Dr. Immel and the party directly responsible for the data product (noted above) and acknowledge NASA funding for the collection of the data used in the research with the following statement : "ICON is supported by NASA's Explorers Program through contracts NNG12FA45C and NNG12FA42I".

These data are openly available as described in the ICON Data Management Plan available on the ICON website (<http://icon.ssl.berkeley.edu/Data>).

ICON Data Product 4.1: HME The Lower Boundary for TIE-GCM

This data product contains the lower boundary of TIE-GCM including zonal wind, meridional wind, temperature, and geopotential height. Tidal structures obtained from ICON-MIGHTI observations are fitted to Hough Mode Extension (HME). Global tidal perturbation field are reconstructed using ICON-HME at 97 km. ICON-MIGHTI winds and temperature from 94 km to 102 km in the latitude range of 10°S-40°N are used to fit to the HME. To cover all local time for tidal analysis, ICON-MIGHTI data are accumulated with a 35-day window. HME has been widely used and tested before, and detailed HME methodologies are summarized in *Forbes et al.* [1994] and *Oberheide et al.* [2011]. HME for ICON and application to TIE-GCM simulation is summarized in *Forbes et al.* [2017] and *Maute* [2017], respectively, and sensitivity of HME fitting to the data coverage can be found in *Cullens et al.* [2020].

Dimensions

NetCDF files contain variables and the dimensions over which those variables are defined. First, the dimensions are defined, then all variables in the file are described. The dimensions used by the variables in this file are given below, along with nominal sizes.

Dimension Name	Nominal Size
lat	74
lon	144
time	24
mtimedim	3

Variables

Variables in this file are listed below.

Variable Name	Description	Unit	Dimension
UN	Reconstructed zonal wind tidal structure at 97 km. Reconstructed field contains superpositions of diurnal tides (DW2 to DE3) and semi-diurnal tides (SW4 to SE3).	m/s	lon, lat, time
VN	Reconstructed meridional wind tidal structure at 97 km. Reconstructed field contains superpositions of diurnal tides (DW2 to DE3) and semi-diurnal tides (SW4 to SE3).	m/s	lon, lat, time
TN	Reconstructed temperature tidal structure at 97 km. Reconstructed field contains superpositions of diurnal tides (DW2 to DE3) and semi-diurnal tides (SW4 to SE3).	K	lon, lat, time
Z	Reconstructed geopotential height tidal structure at 97 km. Reconstructed field contains superpositions of diurnal tides (DW2 to DE3) and semi-diurnal tides (SW4 to SE3).	m	lon, lat, time
lat	Latitude	degree	lat
lon	Longitude	degree	lon
time	Hours since 0 UT		time
UT	Universal Time		time
year	Year		time
day	Day of year		time
mtime	[Day, hour, min]		time, mtimedim

Acknowledgement

This is a data product from the NASA Ionospheric Connection Explorer mission, an Explorer launched at 21:59:45 EDT on October 10, 2019, from Cape Canaveral AFB in the USA. Guidelines for the use of this product are described in the ICON Rules of the Road (<http://icon.ssl.berkeley.edu/Data>).

Responsibility for the mission science falls to the Principal Investigator, Dr. Thomas Immel at UC Berkeley: Immel, T.J., England, S.L., Mende, S.B. et al. Space Sci Rev (2018) 214: 13.
<https://doi.org/10.1007/s11214-017-0449-2>

Responsibility for the validation of the L1 data products falls to the instrument lead investigators/scientists.

- * EUV: Dr. Eric Korpela : <https://doi.org/10.1007/s11214-017-0384-2>
- * FUV: Dr. Harald Frey : <https://doi.org/10.1007/s11214-017-0386-0>
- * MIGHTI: Dr. Christoph Englert : <https://doi.org/10.1007/s11214-017-0358-4>, and <https://doi.org/10.1007/s11214-017-0374-4>
- * IVM: Dr. Roderick Heelis : <https://doi.org/10.1007/s11214-017-0383-3>

Responsibility for the validation of the L2 data products falls to those scientists responsible for those products.

- * Daytime O and N2 profiles: Dr. Andrew Stephan : <https://doi.org/10.1007/s11214-018-0477-6>
- * Daytime (EUV) O+ profiles: Dr. Andrew Stephan : <https://doi.org/10.1007/s11214-017-0385-1>
- * Nighttime (FUV) O+ profiles: Dr. Farzad Kamalabadi : <https://doi.org/10.1007/s11214-018-0502-9>
- * Neutral Wind profiles: Dr. Jonathan Makela : <https://doi.org/10.1007/s11214-017-0359-3>
- * Neutral Temperature profiles: Dr. Christoph Englert : <https://doi.org/10.1007/s11214-017-0434-9>
- * Ion Velocity Measurements : Dr. Russell Stoneback : <https://doi.org/10.1007/s11214-017-0383-3>

Responsibility for Level 4 products falls to those scientists responsible for those products.

- * Hough Modes : Dr. Chihoko Cullens : <https://doi.org/10.1007/s11214-017-0401-5>
- * TIEGCM : Dr. Astrid Maute : <https://doi.org/10.1007/s11214-017-0330-3>
- * SAMI3 : Dr. Joseph Huba : <https://doi.org/10.1007/s11214-017-0415-z>

Pre-production versions of all above papers are available on the ICON website.
<http://icon.ssl.berkeley.edu/Publications>

Overall validation of the products is overseen by the ICON Project Scientist, Dr. Scott England.

NASA oversight for all products is provided by the Mission Scientist, Dr. Jeffrey Klenzing.

Users of these data should contact and acknowledge the Principal Investigator Dr. Immel and the party directly responsible for the data product (noted above) and acknowledge NASA funding for the collection of the data used in the research with the following statement : "ICON is supported by NASA's Explorers Program through contracts NNG12FA45C and NNG12FA42I".

These data are openly available as described in the ICON Data Management Plan available on the ICON website (<http://icon.ssl.berkeley.edu/Data>).

4.1.6 Thermosphere Ionosphere Electrodynamics Model (TIEGCM) Functional Description

This subsection details the science data products produced by a particular mission instrument or ground system element (e.g., SOC).

Following this brief overview, details of the Level 4 TIEGCM data products are provided.

The mission-specific data levels should be defined, and the steps needed to process each level of data shall be described.

The introduction to Section 4 describes the overall data levels for ICON. Table 4.1.6.1 lists the TIEGCM products at Level 4.

Level	Source (Instrument/Model)	Data Product
4	TIEGCM – driven by HME	TIEGCM driven by ICON tides (HMEs)
4	TIEGCM	TIEGCM control run – not driven by ICON tides

Table 4.1.6.1 – List of TIEGCM data products at Level 4.

At a high level, the flow of the TIEGCM data products is shown in Figure 4.1.6.1. The start-point for the TIEGCM is a number of data sources including the ICON HME lower boundary file, along with standard geophysical indices that are not listed in this figure.

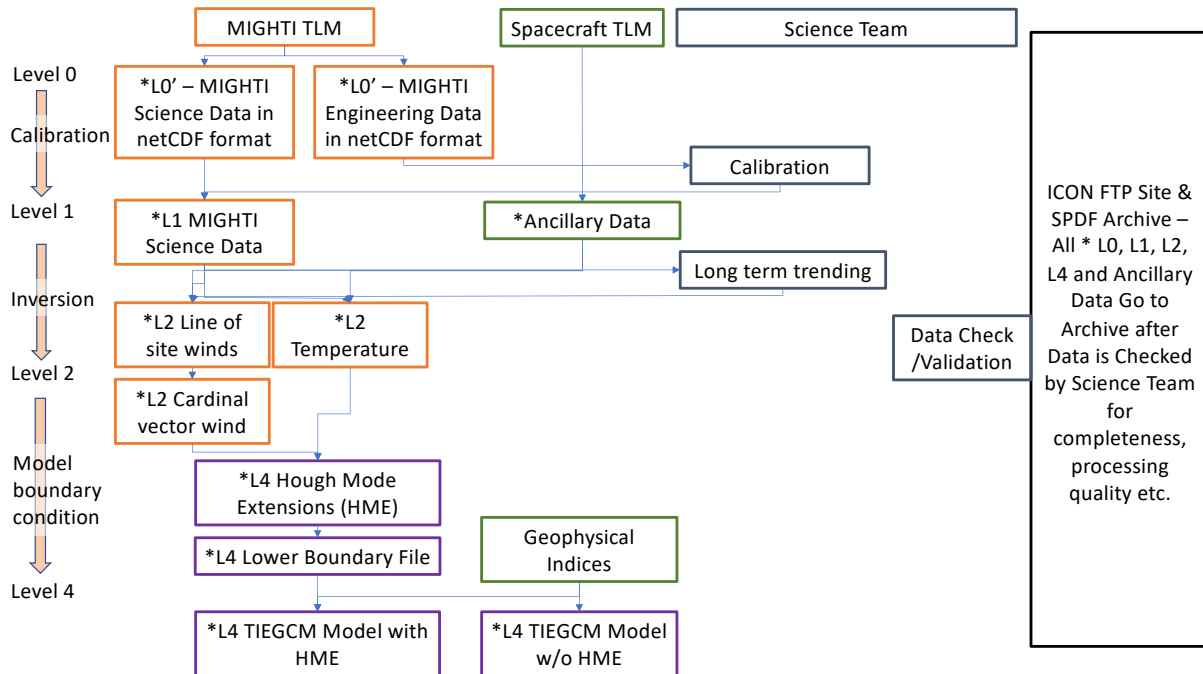


Figure 4.1.6.1 – Schematic of the TIEGCM Data Products and their Flow.

The overall concept for producing the L4 TIEGCM products are as follows: Observations from MIGHTI are used to derive upward propagating tides (HME product). These can be used to drive the lower boundary of the TIEGCM model, which then simulates the thermosphere and ionosphere in a self-consistent manner. To aid with identification of the tidal impact, a control run, using the same geophysical indices but without the ICON HME is also produced. The format of both outputs and nature of the runs is the same, only the lower boundary is changed. Further details on the ICON TIEGCM can be found in Maute et al., (2017; DOI: 10.1007/s11214-017-0330-3).

A reference to the general data level definitions located in the Heliophysics Science Data Management Policy should be included.

The Heliophysics Science Data Management Policy, HPD-SDMP version 2.0, effective February 14, 2022 does not describe data levels. The ICON data levels closely follow those in the PDMP Template.

Any associated metadata products to be generated and maintained shall also be described. Details should also include the cadence (e.g., hourly, daily, etc.) for processing of data products.

Following this brief overview, full details of the metadata for each product are provided.

Level 4 TIEGCM are generated using the HME lower boundary file (along with a control run that does not use this). At present the TIEGCM products are produced in batches of approximately 3-6 months of data at a time.

The following section contains detailed descriptions of the TIEGCM product.

ICON Data Product 4.3: TIEGCM

This document describes the TIEGCM output files.

Note that there are two types of TIEGCM output files

1. tidal HME forcing at its lower boundary
(naming convention `ICON_L4-3_TIEGCM_YYYY-MM-DD_vXXrZZZ.NC`)
2. without tidal forcing
(naming convention `ICON_L4-3_TIEGCM-NOHME_YYYY-MM-DD_vXXrZZZ.NC`).

For the TIEGCM output with tidal forcing at its lower boundary:

The TIEGCM is forced by the HME-TIEGCM data product L4.1 at the TIEGCM lower boundary. The HME-TIEGCM product defines the tidal perturbations in the zonal wind, meridional wind, temperature, and geopotential height based on ICON-MIGHTI observations. We refer to the documentation of data product L4.1 for details of the HME-TIEGCM product.

For the TIEGCM output with and without tidal forcing at its lower boundary:

The TIEGCM is based on TIEGCM2.0 release with descriptions of the model by *Qian et al. [2014]* and *Richmond and Maute (2013)*. The TIEGCM-ICON and the differences to TIEGCM2.0 are described in *Maute [2017]* Section 2.2, and briefly summarized:

1. the soft X-Ray fluxes in the 8-40A wavelength range were increased by a factor of 4.4 following *Fang et al. (2008)* to better match E-region plasma density from IRI model (this is a source code change in TIEGCM-ICON from TIEGCM2.0).
2. at the TIEGCM lower boundary the background atmosphere (zonal and diurnal mean) is defined by HWM07 and MSISE00 as published by *Jones Jr. et al (2014)* (name list* read variable `BGRDDATA=hwm07_97km_msise00_plev_zonalmean_fields_v3.nc`). This is used for TIEGCM output with and without HME tidal forcing at the lower boundary.
3. The HME-TIEGCM files with hourly gridded perturbations can be used at the TIEGCM lower boundary. For TIEGCM with HME tidal forcing at its lower boundary the name list* read variable `HME_NCFILES` are set to L4.1 file names. For TIEGCM without HME tidal forcing at its lower boundary the name list* read variable `HME_NCFILES` is not used.

In the case of TIEGCM with HME tidal forcing the lower boundary includes the added values of the background (item 2 above) and the tidal forcing (item 3 above), while for the TIEGCM without HME the lower boundary includes only the background (item 2 above).

*Name list read variable refer to variables/parameters defined at run time in an input script.

Run time parameters

The simulations use a timestep size of 30 secs (`STEP=30`). Helium is included as a major species (`CALC_HELIUM=1`) following *Sutton et al. (2015)*. This needs to be considered in the mean mass calculation and existing processors should be checked for including Helium. Gravity and plasma pressure gradient driven ionospheric current (`CURRENT_PG=1`) are included in the ionospheric electrodynamic equation but the influence on the ExB drift is mainly limited to the dawn and dusk sector (*Maute & Richmond, 2017*). The Joule heating is increased by 50% which

is the default in the TIEGCM (JOULEFAC=1.5) to account for the effect of small-scale electric field variability not captured by the TIEGCM. The *Weimer (2005)* ion convection patterns are employed driven by 5-min Interplanetary Magnetic Field (IMF) By and Bz magnitudes and solar wind velocity and density. The solar radio flux is used with a daily (F107d) value and a 81-day averaged solar flux (F107a). The 81day average value of a day is averaged over 7 days after the day and 73 days before the day. If the name list variable GPI_NCFILE uses “ICON_Ancillary_GPI” a 7-73 day averaging in F107a is used otherwise the averaging is centered on the day. The resolution of the simulation is 2.5°x2.5° in geographic latitude and longitude with a ¼ scale height resolution in altitude. The geomagnetic grid is regular in longitude (4.5°) and irregular in magnetic latitude varying between 0.34° to 3.07° from the magnetic equator to the magnetic pole at 90km altitude.

We refer to the TIEGCM2.0 user guide

(<https://www.hao.ucar.edu/modeling/tgcm/tiegcm2.0/userguide/html/>) and draft model description (https://www.hao.ucar.edu/modeling/tgcm/doc/description/model_description.pdf) for details.

Dimensions

NetCDF files contain coordinates (variable name is the same as the dimension), and variables with dimensions over which those variables are defined. The dimensions are given below, along with nominal sizes.

Dimension name	size	description
time	unlimited	Number of time steps on file (for L4.3 this is 24)
lon	144	Geographic longitudes
lat	72	Geographic latitudes
lev	57	Midpoint pressure coordinate
ilev	57	Interface pressure coordinate
m lon	81	Magnetic longitude
m lat	97	Magnetic latitude
mlev	63	Pressure coordinate (like ilev but downward and one level upward extended)
mtimedim	3	Model time dimension for (day,ut,min)
latlon	2	Dimension for NH and SH magnetic pole
dtidedim	2	Dimension of diurnal Hough mode (1,1) (Amplitude, Phase) NOT used for TIEGCM-ICON L4.3
sdtidedim	10	Dimension of five semidiurnal Hough mode (Amplitude, Phase) NOT used for TIEGCM-ICON L4.3
datelen	24	For written date
filelen	1024	Max. length for filename output

Variables

In the following we describe the variables we consider as important or not described in the user guide. We do not include the coordinate variables which are described by their dimensions in the table above. For a list of variables we refer to the user guide please see <https://www.hao.ucar.edu/modeling/tgcm/teigcm2.0/userguide/html/output.html#netcdf-history-output-files> and <https://www.hao.ucar.edu/modeling/tgcm/teigcm2.0/userguide/html/diags.html#table-of-available-diagnostics>.

Variable Name	Description	unit	dimension
time	Minutes since initial start date & time, start date & time are given as variable attributes (for easy access of time use variable mtime)	Minutes since initial start date & time	unlimited
mtime	Model time (integer)	(day of year, ut, minute)	(time,mtimedim)
year	Calendar year	year	time
ut	Universal time (from mtime)	hour	time
day	Day of year	day	time
timestep	Timestep size	sec	time
Calendar_advance	calendar advance flag (1 if advancing calendar time as for L4.3 product)		time
f107d	Daily F10.7 radio flux	1.e-22 W/m ² /Hz	time
f107a	81-day average F10.7 solar radio flux (note for L4.3 average might not be centered see variable gpi_ncfile)	1.e-22 W/m ² /Hz	time
hpower	Hemispheric power (parametrized)	GW	time
ctpoten	Cross polar cap potential drop (for L4.3 from Weimer model)	kV	time
Kp	Kp index (for L4.3 not used)		time
byimf	IMF By component from imf_ncfile	nT	time
bzimf	IMF Bz component from imf_ncfile	nT	time
swvel	Solar wind velocity from imf_ncfile	km/s	time
swden	Solar wind density from imf_ncfile	1/cm ³	time
gpi_ncfile	Path & name of gpi file contains (Kp,F107d,F107a, ap, ap3) (For L4.3 F10.7 values are used, see comment under run time parameter)		time
imf_ncfile	Path & name of imf file contains (Bx,By,Bz,Swvel,Swden) (used for L4.3)		time
hme_ncfile	HME file name and path used for lower boundary perturbation (used for L4.3 with HME at LB; not used for L4.3 without HME at LB)		time

bgrddata_ncfile	background lbc data file (for L4.3 based on HWM07 & MSISE00)		time
e1	Peak energy flux in noon sector of aurora	ergs/cm ² /s	time
e2	Peak energy flux in midnight sector of aurora	ergs/cm ² /s	time
h1	Gaussian half-width of the noon auroral oval	degrees	time
h2	Gaussian half-width of the midnight auroral oval	degrees	time
alfac	Characteristic Maxwellian energy of polar cusp electrons	keV	time
ec	Column energy input of polar cusp electron	ergs/cm ² /s	time
alfad	characteristic Maxwellian energy of drizzle electrons	keV	time
ed	Column energy input of drizzle electrons	ergs/cm ² /s	time
crit1	Magnetic colatitude for electrodynamics (poleward of crit1 the high latitude potential is prescribed)	degree	time
crit2	Magnetic colatitude for electrodynamics (equatorward of crit2 pure wind dynamo & gravity and plasma pressure gradient current forcing is applied)	degree	time
mag	geog. lat & lon coordinates of S,N magnetic poles (note that the magnetic main field is set up once per simulation)		Latlon,latlon
p0	Reference pressure (to convert to hPa)	millibars	
p0_model	Reference pressure (as used by the model) (to convert to hPa see global attribute for formula)	microbars	
grav	gravitational acceleration (constant with altitude see global attribute for formula)	cm/s ²	
TN	Neutral temperature	K	time,lev,lat,lon
UN	Zonal neutral wind	cm/s	time,lev,lat,lon
VN	Meridional neutral wind	cm/s	time,lev,lat,lon
WN	Upward neutral wind (note that the vertical dimension is using ilev)	cm/s	time,ilev,lat,lon
O2	Molecular oxygen	Mass mixing ration (mmr)	time,lev,lat,lon

O1	Atomic oxygen	mmr	time,lev,lat,lon
N2	Molecular nitrogen	mmr	time,lev,lat,lon
NO	Nitric oxide	mmr	time,lev,lat,lon
N4S	N(⁴ S)	mmr	time,lev,lat,lon
HE	Helium	mmr	time,lev,lat,lon
NE	Electron density (note that the vertical dimension is ilev)	1/cm ³	time,ilev,lat,lon
TE	Electron temperature	K	time,lev,lat,lon
TI	Ion temperature	K	time,lev,lat,lon
O2P	O ²⁺ ion	1/cm ³	time,lev,lat,lon
OP	O ⁺ ion	1/cm ³	time,lev,lat,lon
POTEN	Electric potential (on geographic grid)	V	time,ilev,lat,lon
UI_ExB	Zonal ExB velocity (geog.eastward)	cm/s	time, ilev, lat, lon
VI_ExB	Meridional (geog. northward) ExB velocity	cm/s	time, ilev, lat, lon
WI_ExB	Vertical (geog. Upward) ExB velocity	cm/s	time, ilev, lat, lon
Z	Geopotential height (used in the code with constant gravity)	cm	time, ilev, lat, lon
ZG	Geometric height (just postprocessing with variable gravity)	cm	time, ilev, lat, lon
PHIM2D	Electric potential at 90 km on magnetic grid	V	time,mlat,mlon
ED12D	E _{d1} see <i>Richmond (1995)</i> at 90km (magnetic eastward direction)	V/m	time,mlat,mlon
ED22D	E _{d2} see <i>Richmond (1995)</i> at 90km (down-/equatorward direction)	V/m	time,mlat,mlon
SIGMA_PED	Pedersen Conductivity	S/m	time, lev, lat, lon
SIGMA_HAL	Hall Conductivity	S/m	time, lev, lat, lon
EEX	Geog. eastward electric field on geog. grid	V/cm	time, lev, lat, lon
EEY	Geog. northward electric field on geog. grid	V/cm	time, lev, lat, lon
EEZ	Geog. upward electric field on geog. grid	V/cm	time, lev, lat, lon
QJOULE	Joule heating	erg/g/s	time, lev, lat, lon
QJOULE_INTEG	Height integrated Joule heating	erg/cm ² /s	time, lev, lat, lon
QAURORA	Aurora ionization rate	1/(cm ³ s)	time, lev, lat, lon
PHIMW	Prescribed high latitude potential (for L4.3 Weimer potential)	V	time,mlat,mlon
JE1PG_DYN	Magnetic eastward gravity and plasma pressure gradient driven current density (used in	A/m ²	time, lev, lat, lon

	electrodynamo if CALC_JPG=1, used in L4.3)		
JE2PG_DYN	Magnetic down-/equatorward gravity and plasma pressure gradient driven current density (used in electro-dynamo if CALC_JPG=1, used in L4.3)	A/m ²	time, lev, lat, lon
ZMAG	Geopotential height (constant gravity) on magnetic grid	cm	time, imlev, mlat, mlon
TLBC	Lower boundary of TN (background and perturbation)	K	time, lat, lon
ULBC	Lower boundary of UN (background and perturbation)	cm/s	time, lat, lon
VLBC	Lower boundary of VN (background and perturbation)	cm/s	time, lat, lon

Global Attributes

In the following we mention a few global attributes which might be helpful for a user

Potential_model	Describes which prescribed high latitude potential model was used (Weimer for L4.3 TIEGCM-ICON)
lev_to_hPa_method1	Formula to convert from pressure level lev to hPa
lev_to_hPa_method2	Alternative formula to convert from pressure level lev to hPa
contents	Content time range yyddd day hour min to yyddd day hour min by delta_mins
Version	Version number of the L4.3 product
Description	Describes ICON product
lowerBoundary_type	For TIEGCM with HME at LB: HME with version number for L4.3 For TIEGCM without HME “noHME” specified

References

- Fang T., A. Richmond, J. Liu, A. Maute, C. Lin, C. Chen, B. Harper, Model simulation of the equatorial electrojet in the Peruvian and Philippine sectors. *J. Atmos. Sol.-Terr. Phys.* **70**(17), 2203–2211 (2008). doi:[10.1016/j.jastp.2008.04.021](https://doi.org/10.1016/j.jastp.2008.04.021)
- Jones Jr., M, J.M. Forbes, M.E. Hagan, A. Maute, Impacts of vertically propagating tides on the mean state of the ionosphere-thermosphere system. *J. Geophys. Res. Space Phys.* **119**(3), 2197–2213 (2014). doi:[10.1002/2013JA019744](https://doi.org/10.1002/2013JA019744)
- Qian L., et al., The NCAR TIE-GCM: a community model of the coupled thermosphere/ionosphere system, in *Modeling the Ionosphere-Thermosphere System*. Geophys. Monogr. Ser, vol. 201 (2014), pp. 73–83

- Richmond A., A. Maute, Ionospheric electrodynamic modeling, in *Modeling the Ionosphere-Thermosphere*, ed. by R.S.J.D. Huba, G. Khazanov. AGU Geophysical Monograph Series, vol. 201 (Wiley, Chichester, 2013), p. 417. doi:[10.1002/9781118704](https://doi.org/10.1002/9781118704)
- Sutton, E.K., J.P. Thayer, W. Wang, S.C. Solomon, X. Liu, B.T. Foster, A self-consistent model of helium in the thermosphere. *J. Geophys. Res. Space Phys.* **120**(8), 6884–6900 (2015). doi:[10.1002/2015JA021223](https://doi.org/10.1002/2015JA021223)
- Weimer, D.R., Improved ionospheric electrodynamic models and application to calculating joule heating rates. *J. Geophys. Res.* (2005). doi:[10.1029/2004JA010884](https://doi.org/10.1029/2004JA010884)
- Maute, A., & Richmond, A. D., Examining the magnetic signal due to gravity and plasma pressure gradient current with the TIE-GCM. *Journal of Geophysical Research: Space Physics*, 122, 12,486–12,504 (2017). <https://doi.org/10.1002/2017JA024841>

Acknowledgement

This is a data product from the NASA Ionospheric Connection Explorer mission, an Explorer launched at 21:59:45 EDT on October 10, 2019, from Cape Canaveral AFB in the USA. Guidelines for the use of this product are described in the ICON Rules of the Road (<http://icon.ssl.berkeley.edu/Data>).

Responsibility for the mission science falls to the Principal Investigator, Dr. Thomas Immel at UC Berkeley: Immel, T.J., England, S.L., Mende, S.B. et al. *Space Sci Rev* (2018) 214: 13. <https://doi.org/10.1007/s11214-017-0449-2>

Responsibility for the validation of the L1 data products falls to the instrument lead investigators/scientists.

- * EUV: Dr. Eric Korpela: <https://doi.org/10.1007/s11214-017-0384-2>
- * FUV: Dr. Harald Frey: <https://doi.org/10.1007/s11214-017-0386-0>
- * MIGHTI: Dr. Christoph Englert: <https://doi.org/10.1007/s11214-017-0358-4>, and <https://doi.org/10.1007/s11214-017-0374-4>
- * IVM: Dr. Roderick Heelis: <https://doi.org/10.1007/s11214-017-0383-3>

Responsibility for the validation of the L2 data products falls to those scientists responsible for those products.

- * Daytime O and N2 profiles: Dr. Andrew Stephan: <https://doi.org/10.1007/s11214-018-0477-6>
- * Daytime (EUV) O+ profiles: Dr. Andrew Stephan: <https://doi.org/10.1007/s11214-017-0385-1>
- * Nighttime (FUV) O+ profiles: Dr. Farzad Kamalabadi: <https://doi.org/10.1007/s11214-018-0502-9>
- * Neutral Wind profiles: Dr. Jonathan Makela: <https://doi.org/10.1007/s11214-017-0359-3>
- * Neutral Temperature profiles: Dr. Christoph Englert: <https://doi.org/10.1007/s11214-017-0434-9>
- * Ion Velocity Measurements: Dr. Russell Stoneback: <https://doi.org/10.1007/s11214-017-0383-3>

Responsibility for Level 4 products falls to those scientists responsible for those products.

- * Hough Modes: Dr. Chihoko Cullens: <https://doi.org/10.1007/s11214-017-0401-5>

- * TIEGCM: Dr. Astrid Maute: <https://doi.org/10.1007/s11214-017-0330-3>
- * SAMI3: Dr. Joseph Huba: <https://doi.org/10.1007/s11214-017-0415-z>

Pre-production versions of all above papers are available on the ICON website.
<http://icon.ssl.berkeley.edu/Publications>

Overall validation of the products is overseen by the ICON Project Scientist, Dr. Scott England.

NASA oversight for all products is provided by the Mission Scientist, Dr. Jeffrey Klenzing.

Users of these data should contact and acknowledge the Principal Investigator Dr. Immel and the party directly responsible for the data product (noted above) and acknowledge NASA funding for the collection of the data used in the research with the following statement : "ICON is supported by NASA's Explorers Program through contracts NNG12FA45C and NNG12FA42I".

These data are openly available as described in the ICON Data Management Plan available on the ICON website (<http://icon.ssl.berkeley.edu/Data>).

4.1.7 ICON Science Data Distribution

This subsection summarizes the data products and key parameters (possibly in tabular format, see example below).

The definitive ephemeris is normally between 14 and 21 days out from the actual day. For convenience we used N+21 here (though it may be as early as N+14). The rest of the data follows.

Ancillary data is produced once the definitive ephemeris comes in and then the L1 data is produced the day after. L2 is produced the day after that. Some products have intermediary steps (for example there is an intermediate step for IVM between L1 and L2 that takes a day to process).

Once data is processed to level 2, it requires approval (done by the Tohban). After approval it takes about 2 days to compress and archive. Once archived it takes about another day to be pushed to the public and to SPDF.

It should be noted that during a reprocess – these numbers are pushed out as the SDC is pegged reproducing old data. Only L0 data is processed until a reprocess is complete. Such reprocessing does cause lags of weeks until the data is published to the public.

Several phases require manual tuning by the science team which result in calibration files being dropped to the SDC. Following these calibration files the process can continue. These are usually done every 30 days or every 45 days. Such calibrations are required for:

- EUV L1
- FUV L1
- IVM DP 2.7
- MIGHTI L1
- MIGHTI DP 2.1

Level	Component	Time Resolution	Time Span	Processing Cadence	Daily Volume (MB)	Public Release of Day N Data	Date Modified
Anc	MIGHTI	30s day, 60s night	1 day	Once/day	28.0	N+21	
Anc	IVM	1s	1 day	Once/day	56.7	N+21	
Anc	FUV	15s	1 day	Once/day	1397	N+21	
Anc	EUV	12s	1 day	Once/day	159.5	N+21	

Level	Component	Time Resolution	Time Span	Processing Cadence	Daily Volume (MB)	Public Release of Day N Data	Date Modified
L1	MIGHTI	30s day, 60s night	30s day, 60s night	Once/day	20500	N+30	
L1	IVM	1s	1 day	Once/day	2100	N+22	
L1	FUV	12s	1 day	Once/day	1300	N+45	
L1	EUV	12s	12 s	Once/day	3091	N+45	
L2	MIGHTI	30s day, 60s night	1 day	Once/day	209	N+50	
L2	IVM	1s	1 day	Once/day	252	N+100	
L2	FUV	12s	1 day	Once/day	205	N+60	
L2	EUV	12s	1 day	Once/day	15.9	N+70	
L4	HME	1 day	1 day	Once/90 days	15.9	< N+180	
L4	TIEGCM		1 day	Once/90 days	4903	< N+180	

Table 4.1.7.1 Summary of the ICON data products

The science data (including housekeeping, ancillary data and calibration data) runs at about 43.5 GB per day with an excess of about double due to reprocessing (so an extra 86.5 GB per day). This excess can be removed over time. The overall distribute of data by instrument is shown in the chart below.

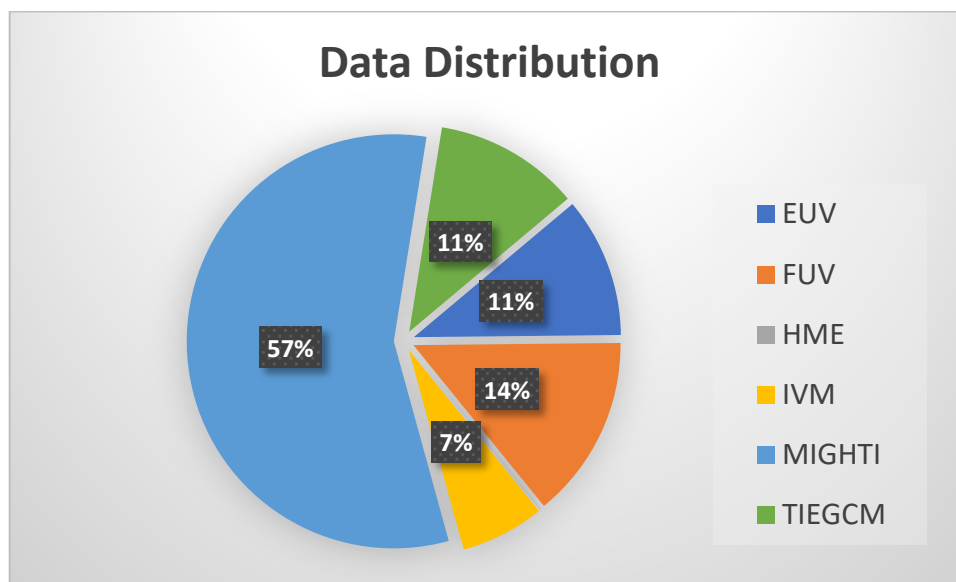


Figure 4.1.7.1 Summary of ICON data by volume.

This subsection also provides details on data storage, including storage medium and available space/volume, file format(s), backup and archival strategy, and data catalogues

Current storage is backed up by tape once per 3 months. The L0 data is backed up in three different archives in order to protect it. The science code and pipeline code is backed up in a GIT repository off site as well as per the normal back strategy (once per 3 months). Further – all L0 and all approved L1, L2 and L4 data is sent to the SPDF for archival.

All data to the public and SPDF is zipped with CRC enabled.

Storage is on remote disc which is currently sized to 100 TB but can be expanded.

Data production and pipeline status is maintained through a local MariaDB which is backed up with the normal backup scheme.

Finally, the public archive is a complete copy of the data as well.

Cleaning up of old/obsolete data products is currently a manual process.

5. Ground System

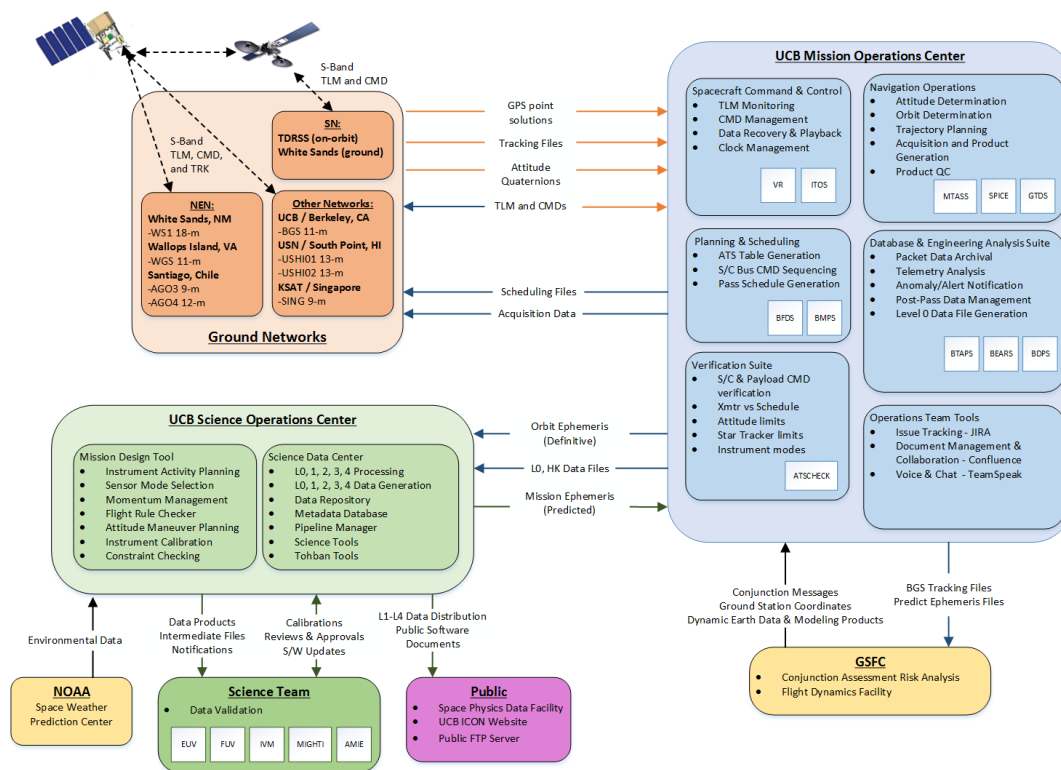
This section provides details on each element on the ground that project data is routed through.

ICON's data are routed through the Near Earth Network, including the Berkeley Ground Station, and Space Network to the Mission Operations Center and Science Data Center.

5.1 Ground System Architecture

This section lists the elements (e.g., DSN, MOC, SOC) that make up the mission's ground system.

Figure 5.1.1 shows the elements of the ICON mission ground system, and how each relates to one another for the purposes of data flow.



v. Nov 17 2015

Figure 5.1.1 – Elements of the ICON mission ground system.

5.2 Ground Segment name and function

This section provides additional details for the ground system element, such as its primary function and responsibilities. Develop a separate section for each element.

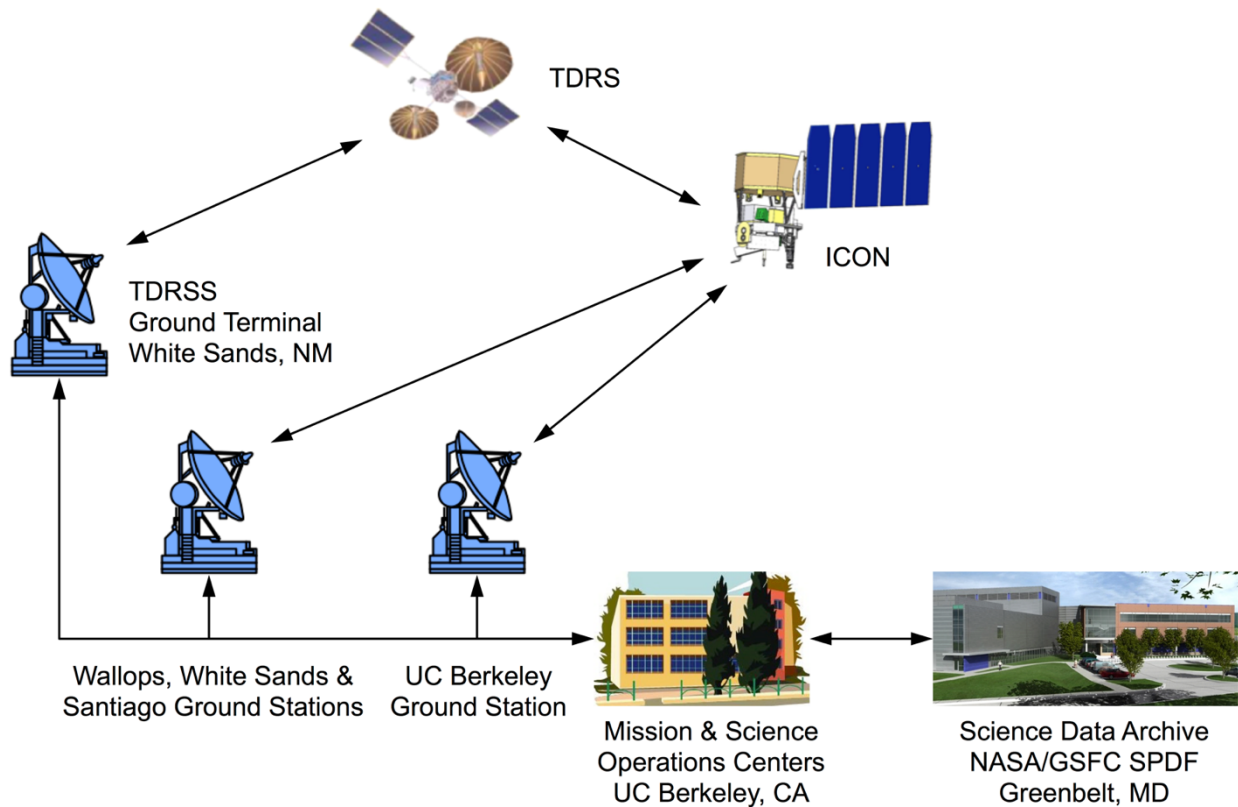


Figure 5.2.1 –ICON Ground Segments

5.2.1 NEN - Near Earth Network

Primary functions & responsibilities - The NEN provides real-time telemetry and command as well as science and engineering data downlink capabilities. ICON typically uses 60 passes per week to downlink science data. The Near Earth Network is used primarily to return science data, stored state of health as well as commanding and limit monitoring on an s-band link. The primary near earth network stations used by ICON and Wallops Island Virginia (WG11), Santiago, Chile (AGO3) and Berkeley, California (BGS). We have used other stations for contingency operations and during launch and early orbit operations. These include KSAT Singapore (SING), SSC South Africa, SSC Hawaii (USH2), and White sands New Mexico (WS1).

Requirements for ICON NEN Nominal Operations

- 2800 seconds total service per day total
- 3 contacts per day at the Berkeley Ground Station (BGS)
- 4 contacts per day at the NEN Ground Stations (WG11, AGO3 , WS1)
- 1 contact per month at each of WS1, USH2, and SING for proficiency/contingency.

5.2.2 SN - Space Network

Primary functions & responsibilities - Space Network (TDRSS) is also used by ICON for special contingency and special operations. 1 pass a month.

5.2.3 MOC - Mission Operations Center

Primary functions & responsibilities - Spacecraft and Instrument command and control, table uploads, ephemeris generation and science planning.

5.2.5 SOC - Science Operations Center

Primary functions & responsibilities - Science operations planning. Delivery of science operations plan to MOC. Instrument configuration change requests.

5.2.5 SDC - Science Data Center

Primary functions & responsibilities - Science data processing and publication. Delivery of data to SPDF.

6. Data Flow

This section provides details on the transfer of data between [flight and ground] mission elements.

6.1 Overview of End-to-End Data Flow

6.1.1 Data Flow To Spacecraft

This subsection describes the transfer (e.g., Guest Observer Office-to-Science Office, Science Office-to-POC, POC-to-MOC, MOC-to-Network) of information as it evolves from a desired observation to a spacecraft command, including the development of intermediate products (e.g., objects of interest, candidate target lists, pixel masks, target tables, instrument and spacecraft commands).

The MOC uploads an ATS (Absolute time command sequence weekly. The commanding for the ATS comes from a variety of sources. The mission ephemeris comes from the MDT (Mission Design Tool) using inputs from the onboard GPS to determine the orbit. These ephemerides are translated to spacecraft commands using the Berkeley Mission Planning Software (BMPS) in the MOC. Changes to instrument commanding normally come from the science team or Tohban using the JIRA task management software.

The spacecraft's GOODS system (GPS On-board Orbit Determination Software) needs weekly dynamic data updates (atmospheric drag coefficients, polar motion, UTC offsets, etc.) from the web:

Website	Description
http://maia.usno.navy.mil/ser7/ser7.dat	IERS Bulletin A file containing polar motion and UTC information. Required as input by tool.
http://maia.usno.navy.mil/ser7/series14.txt	Time service announcement containing the GPS-UTC time offset. Used for quality assurance.
http://services.swpc.noaa.gov/text/sgarf.txt	NOAA report of solar and geophysical activity. Required as input by tool.

Table 6.1.1.1 Locations for dynamic data updates used by ICON.

6.1.2 Data Flow From Spacecraft

This subsection describes the transfer (e.g., Network-to-FDF, Network-to-POC, POC-to-SOC, etc.) of return data and the development of products along each step (e.g., raw telemetry, Level 0 data, light curves, calibrated images, etc.) as well as transfer timeframe and expected processing time.

Flow of data from the spacecraft to the various system element as well as the transfer method is shown in Table 6.1.2.1.

Flow	Data Product	Timeline	Transfer Method
NEN to MOC	S-band data Primary Science Science Replays Stored SOH Instrument HK Spacecraft HK	Realtime, postpass files 1 day of downlink	TCP/IP over Restricted IONet and SFTP / SAFS
SN to MOC	S-band data Realtime TLM	Realtime	TCP/IP over Restricted IONet
MOC to SDC	Primary Science Science Replays Stored SOH Instrument HK Spacecraft HK Ancillary data	1 day of downlink	SFTP/Git
SDC to SPDF	Primary Science Science Replays Stored SOH Instrument HK Spacecraft HK Ancillary data	1 day of downlink	SFTP
SDC to Public/SPDF	L1 – L4 Science Products	1 day of downlink, 60 days delayed	FTP/SFTP

Table 6.1.2.1 – Data transfer from the spacecraft to science data center.

Data flow for each product within the SDC and to the SPDF archive is shown in Sections 4.1 through 4.6.

6.2 Data Handling and Timeline

This section summarizes the flow of data from the spacecraft as well as the transfer method (e.g., TCP/IP over Restricted IONet, FTP, etc.) along with the timeline for delivery to/from each element (see sample below).

Data from ICON are packetized and downlinked via a Thales Alenia Space - España S-Band transponder that includes 2 quadrifilar antennas and a hybrid assembly. The transponder supports two data transmission modes, 16 kbps BPSK (low-rate) and 4 Mbps OQPSK (high-rate).

The low-rate mode only provides real-time State of Health data and is used only for TDRSS passes or anomaly recovery. The majority of ICON passes are high-rate using ground stations. ICON currently uses the Berkeley Ground Station in Berkeley California, the Near Earth Network (NEN) stations in Wallops Island Virginia and White Sands New Mexico, the Swedish Space Corporation (SSC) antennas in Santiago Chile, and South-point, Hawaii. Finally Kongsberg Satellite Services AS (KSAT) Singapore. Except for data collected at the Berkeley Ground Station ICON data are pushed to SAFS via SFTP within 1 day of downlink on the NASCOM IONet to transfer data from the ground stations to the MOC. BGS uses a local area network to transfer data to the MOC. Although ICON has the ability to use any of the stations mentioned above it primarily uses BGS, Santiago, Wallops and TDRSS.

Flow	Data Product	Timeline	Transfer Method
NEN to MOC	S-band data Primary Science Science Replays Stored SOH Instrument HK Spacecraft HK	Realtime, postpass files within 1 day of downink	TCP/IP over NASCOM IONet and SFTP / SAFS
SN to MOC	S-band data Realtime TLM	Realtime	TCP/IP over NASCOM IONet
SSC to MOC	S-band data Primary Science Science Replays Stored SOH Instrument HK Spacecraft HK	Realtime, postpass files within 1 day of downink	TCP/IP over NASCOM IONet and SFTP / SAFS
KSAT to MOC	S-band data Primary Science Science Replays Stored SOH Instrument HK Spacecraft HK	Realtime, postpass files within 1 day of downink	TCP/IP over NASCOM IONet and SFTP / SAFS
BGS to MOC	S-band data Primary Science Science Replays Stored SOH Instrument HK Spacecraft HK	Realtime	Local Area Network

Flow	Data Product	Timeline	Transfer Method
MOC to SDC	Primary Science Science Replays Stored SOH Instrument HK Spacecraft HK Ancillary data	Within 1 day of downlink	SFTP

Table 6.2.1 – Timeline for data flow from the spacecraft to the SDC

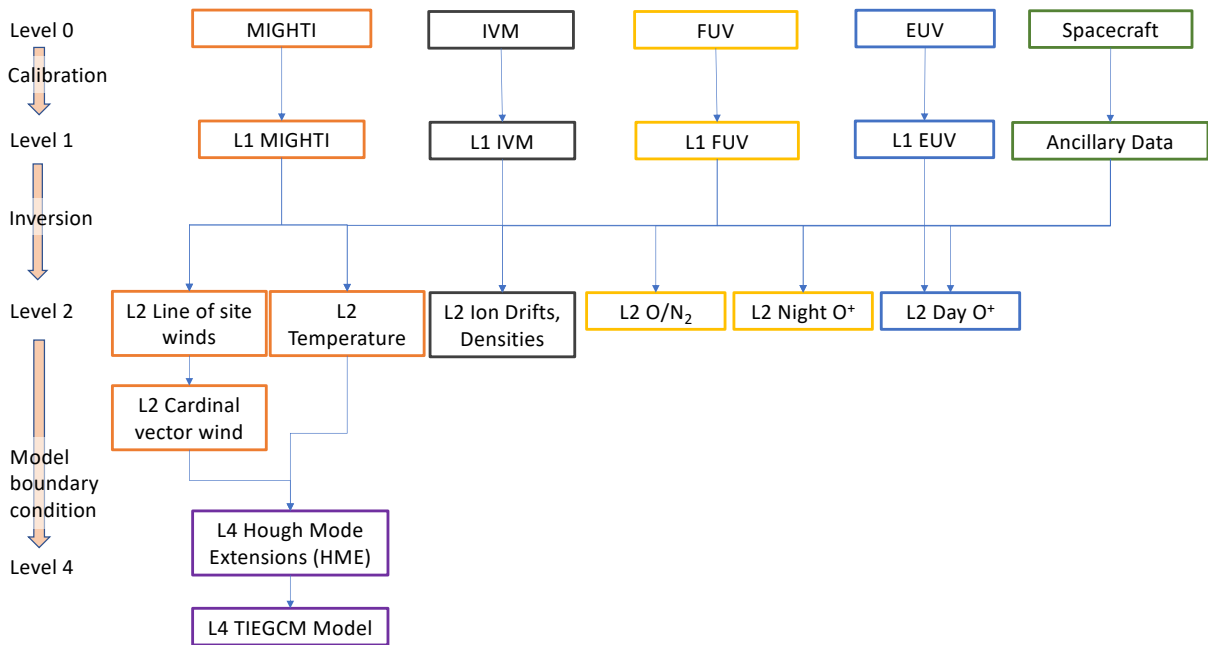


Figure 6.2.2 – High-level overview of ICON data products by Level.

Level	Component	Processing Cadence	Public Release of Day N Data
Anc	MIGHTI	Once/day	N+21
Anc	IVM	Once/day	N+21
Anc	FUV	Once/day	N+21
Anc	EUV	Once/day	N+21
L1	MIGHTI	Once/day	N+30
L1	IVM	Once/day	N+22
L1	FUV	Once/day	N+45
L1	EUV	Once/day	N+45
L2	MIGHTI	Once/day	N+50
L2	IVM	Once/day	N+100

Level	Component	Processing Cadence	Public Release of Day N Data
L2	FUV	Once/day	N+60
L2	EUV	Once/day	N+70
L4	HME	Once/90 days	< N+180
L4	TIEGCM	Once/90 days	< N+180

Table 6.2.2 – Timeline for handling the higher level data products at the SDC

The general process:

- a) L0: Pull into SDC
- b) LOP: Process from L0.
- c) Ancillary: Process from LOP and definitive ephemeris.
- d) L1: Process from LOP, ancillary and drop in calibrations.
- e) L2: Process from L1 and drop in calibrations.
- f) L4: Process monthly from 55 days sliding window of L2 inputs.

The timing is listed below:

- Level 0: Level 0 data is processed to NetCDF format the day after it is received which normally happens within 24 hours of collection. This data is called “level 0 prime”.
- Ancillary: The ancillary data product takes the level 0 data and adds the definitive ephemeris, which is between 14 and 21 days latent. Thus normally a week of ancillary for each product is produced at a time varying between N+15 and N+21 days.
- Level 1: products for level 1 typically require a customized calibration file for each instrument. These files are produced every 30 to 45 days. This adds latency to those products.
- Level 2: Some level 2 products also have a calibration file requirement which adds a latency of up to 45 days. IVM level 2 calibration files are typically every 3 months.
- Level 4:
 - HME requires a 55 day sliding window so is typically latent by 50 days.
 - TIEGCM ingests the HME files so is typically run a month after HME and thus latent about 90 days.

If available, a more detailed breakdown of the release schedule for calibrated data by campaign (e.g., Launch + xx, by orbit, by perihelion passage, etc.) may be provided.

This is not applicable for ICON.

7. Archiving and Data Access

This section describes the process for archiving data and how those archives may be accessed.

Processing software is versioned and revisioned in the SDC data servers and in a separate, remote GIT repository. Further the servers are backed up every 3 months to tape in a remote location.

L0 data is archived in the MOC (which has a separate backup system) and in the SDC. The data is retrieved from the MOC and then stored in the SDC both RAW and zipped. This archive is backed up to tape once per three months.

All other data is reproducible using the L0 inputs and the software which has been archived.

Approved L1, L2 and L4 data are zipped up and stored in two locations (the science repository and the public data archive). Further these files are backed up every 3 months and stored on tape.

Finally, all approved data and L0 data are sent to the SPDF in ZIP archives. CRC values are checked upon collection by SPDF.

The tape backup strategy used on our data servers is to do a full backup at the beginning of the year and a differential backup every three months. These backups are stored offsite.

An estimate of instrument data storage requirements over the nominal life of the mission should be provided. Revised estimates for extended mission phases shall be provided at the Senior Review.

Following are the data numbers for the current Prime Mission and the numbers extrapolated for the extended mission. Note that the “Total With Duplication” indicates numbers with and without compression and including reprocessing (multiple versions/revisions).

Total projected required data capacity for the full extended mission is **114 TB** (19 TB if only compressed data is preserved). Total projected data usage (required and excess) is **303 TB**.

Prime Mission (Dec 2019 – Nov 2021)					
Instrument	Annual (Uncompressed)	Total (Uncompressed)	Annual (Compressed)	Total (Compressed)	Total w/ Duplication
EUUV					
Level 0 (+Prime)	0.60 TB	1.1 TB	0.13 TB	0.27 TB	1.5 TB
Level 1	1.1 TB	2.2 TB	0.12 TB	0.24 TB	9.0 TB
Level 2	0.006 TB	0.01 TB	0.18 TB	0.37 TB	0.50 TB
Ancillary	0.06 TB	0.10 TB	0.002 TB	0.004 TB	0.50 TB
Intermediate	0 TB	0 TB	0 TB	0 TB	0 TB
FUV					
Level 0 (+Prime)	1.2 TB	2.4 TB	0.11 TB	0.23 TB	2.6 TB
Level 1	0.50 TB	1.0 TB	0.08 TB	0.15 TB	2.8 TB
Level 2	0.07 TB	0.15 TB	0.02 TB	0.05 TB	0.50 TB
Ancillary	0.50 TB	1.0 TB	0.25 TB	0.50 TB	2.8 TB
Intermediate	0 TB	0 TB	0 TB	0 TB	0 TB
IVM					
Level 0 (+Prime)	0.06 TB	0.11 TB	0.01 TB	0.02 TB	0.07 TB
Level 1	0.76 TB	1.5 TB	0.11 TB	0.22 TB	5.5 TB
Level 2	0.07 TB	0.18 TB	0.02 TB	0.03 TB	0.65 TB
Ancillary	0.02 TB	0.04 TB	0.005 TB	0.01 TB	0.10 TB
Intermediate	0.11 TB	0.23 TB	0.02 TB	0.05 TB	1.0 TB
MIGHTI					
Level 0 (+Prime)	1.4 TB	2.9 TB	0.35 TB	0.71 TB	4.0 TB
Level 1	7.5 TB	14.9 TB	1.1 TB	2.2 TB	57 TB
Level 2	0.08 TB	0.15 TB	0.02 TB	0.03 TB	0.45 TB
Ancillary	0.01 TB	0.02 TB	0.003 TB	0.005 TB	0.20 TB
Intermediate	0.03 TB	0.05 TB	0.005 TB	0.01 TB	0.20 TB
Level 4 Data Product					
HME	0.006 TB	0.01 TB	0.002 TB	0.004 TB	0.02 TB
TIEGCM	1.8 TB	3.6 TB	0.57 TB	1.1 TB	7.5 TB

Extended Mission (Dec 2021 – Nov 2022)					
Instrument	Annual (Uncompressed)	Total (Uncompressed)	Annual (Compressed)	Total (Compressed)	Total w/ Duplication
EUUV					
Level 0 (+Prime)	0.60 TB	1.7 TB	0.13 TB	0.40 TB	1.9 TB
Level 1	1.1 TB	3.3 TB	0.12 TB	0.36 TB	14 TB
Level 2	0.006 TB	0.02 TB	0.18 TB	0.55 TB	0.70 TB
Ancillary	0.06 TB	0.17 TB	0.002 TB	0.005 TB	0.70 TB
Intermediate	0 TB	0 TB	0 TB	0 TB	0 TB
FUV					
Level 0 (+Prime)	1.2 TB	3.6 TB	0.11 TB	0.34 TB	4.1 TB
Level 1	0.50 TB	1.5 TB	0.08 TB	0.23 TB	4.0 TB
Level 2	0.07 TB	0.22 TB	0.02 TB	0.07 TB	0.73 TB
Ancillary	0.50 TB	1.5 TB	0.25 TB	0.76 TB	4.2 TB
Intermediate	0 TB	0 TB	0 TB	0 TB	0 TB
IVM					
Level 0 (+Prime)	0.06 TB	0.17 TB	0.01 TB	0.04 TB	0.23 TB
Level 1	0.76 TB	2.3 TB	0.11 TB	0.33 TB	7.8 TB
Level 2	0.07 TB	0.26 TB	0.02 TB	0.04 TB	0.95 TB
Ancillary	0.02 TB	0.06 TB	0.005 TB	0.01 TB	0.19 TB
Intermediate	0.11 TB	0.34 TB	0.02 TB	0.07 TB	1.7 TB
MIGHTI					
Level 0 (+Prime)	1.4 TB	4.3 TB	0.35 TB	1.1 TB	5.9 TB
Level 1	7.5 TB	22 TB	1.1 TB	3.2 TB	79 TB
Level 2	0.08 TB	0.23 TB	0.02 TB	0.05 TB	0.68 TB
Ancillary	0.01 TB	0.03 TB	0.003 TB	0.007 TB	0.25 TB
Intermediate	0.03 TB	0.08 TB	0.005 TB	0.02 TB	0.28 TB
Level 4 Data Product					
HME	0.006 TB	0.02 TB	0.002 TB	0.006 TB	0.04 TB
TIEGCM	1.8 TB	5.4 TB	0.57 TB	1.7 TB	10.8 TB

Extended Mission (Dec 2022 – Nov 2025)					
Instrument	Annual (Uncompressed)	Total (Uncompressed)	Annual (Compressed)	Total (Compressed)	Total w/ Duplication
EUUV					
Level 0 (+Prime)	0.60 TB	3.4 TB	0.13 TB	0.81 TB	3.7 TB
Level 1	1.1 TB	6.6 TB	0.12 TB	0.72 TB	27 TB
Level 2	0.006 TB	0.03 TB	0.18 TB	1.1 TB	1.7 TB
Ancillary	0.06 TB	0.35 TB	0.002 TB	0.01 TB	1.3 TB
Intermediate	0 TB	0 TB	0 TB	0 TB	0 TB
FUV					
Level 0 (+Prime)	1.2 TB	7.2 TB	0.11 TB	0.69 TB	8.0 TB
Level 1	0.50 TB	2.9 TB	0.08 TB	0.46 TB	7.9 TB
Level 2	0.07 TB	0.45 TB	0.02 TB	0.14 TB	1.2 TB
Ancillary	0.50 TB	3.0 TB	0.25 TB	1.5 TB	11.1 TB
Intermediate	0 TB	0 TB	0 TB	0 TB	0 TB
IVM					
Level 0 (+Prime)	0.06 TB	0.33 TB	0.01 TB	0.07 TB	0.41 TB
Level 1	0.76 TB	4.5 TB	0.11 TB	0.66 TB	15 TB
Level 2	0.07 TB	0.55 TB	0.02 TB	0.09 TB	1.9 TB
Ancillary	0.02 TB	0.12 TB	0.005 TB	0.03 TB	0.33 TB
Intermediate	0.11 TB	0.68 TB	0.02 TB	0.14 TB	2.2 TB
MIGHTI					
Level 0 (+Prime)	1.4 TB	8.7 TB	0.35 TB	2.1 TB	10.9 TB
Level 1	7.5 TB	45 TB	1.1 TB	6.5 TB	52 TB
Level 2	0.08 TB	0.46 TB	0.02 TB	0.09 TB	1.3 TB
Ancillary	0.01 TB	0.06 TB	0.003 TB	0.01 TB	0.40 TB
Intermediate	0.03 TB	0.15 TB	0.005 TB	0.03 TB	0.45 TB
Level 4 Data Product					
HME	0.006 TB	0.03 TB	0.002 TB	0.01 TB	0.08 TB
TIEGCM	1.8 TB	10.8 TB	0.57 TB	3.4 TB	21 TB

Table 7.1 – Data storage requirements by data type

The charts below show the data distribution per instrument and per data product.

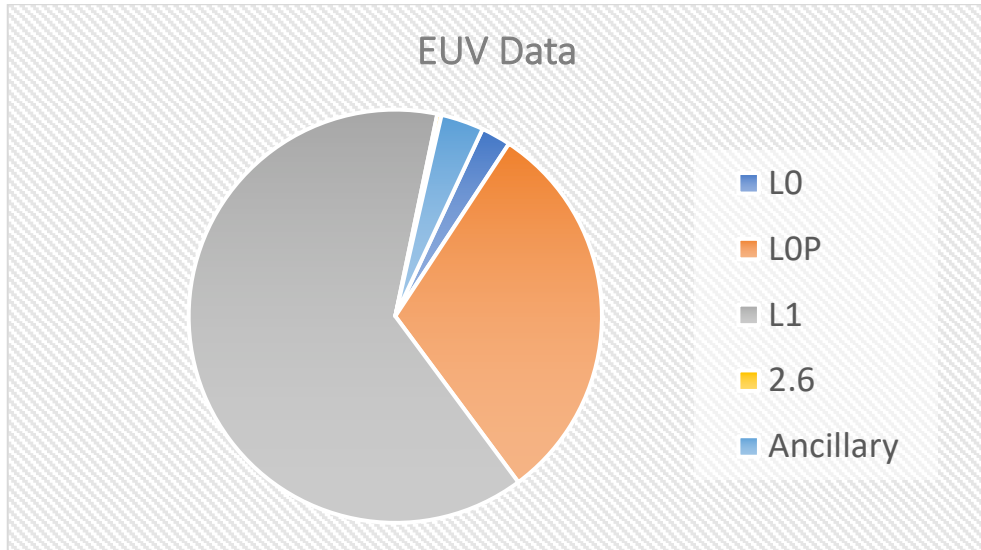


Figure 7.1 – Data volume breakdown for EUUV

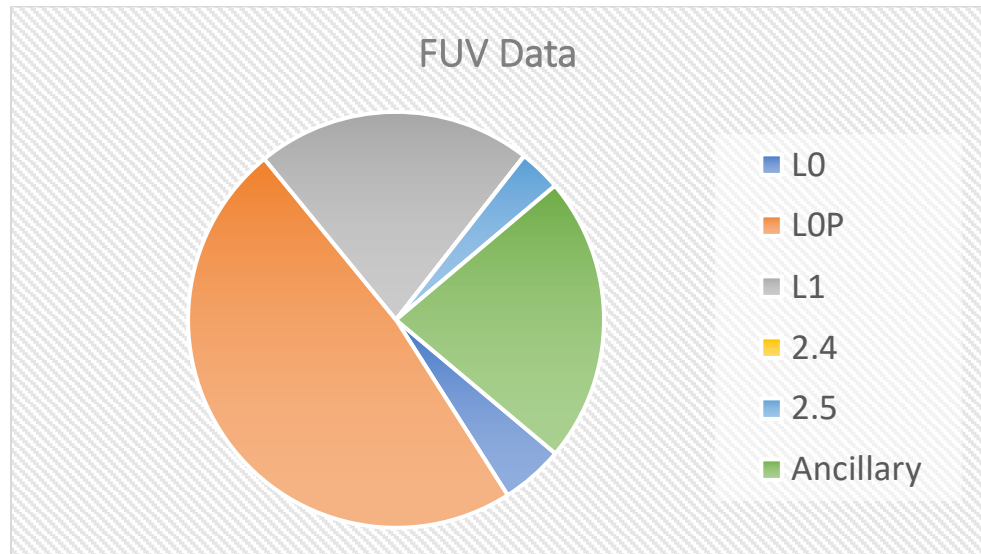


Figure 7.2 – Data volume breakdown for FUV

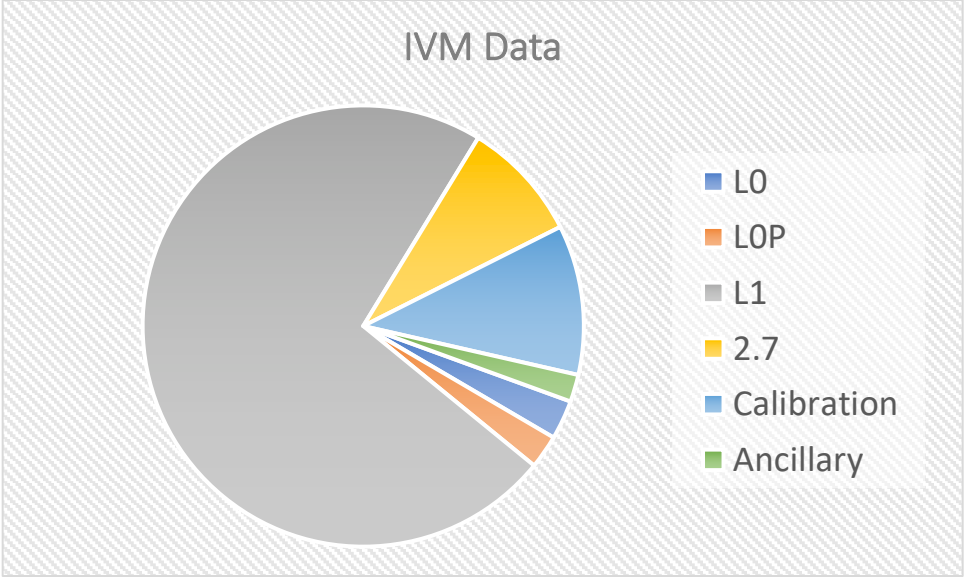


Figure 7.3 – Data volume breakdown for IVM

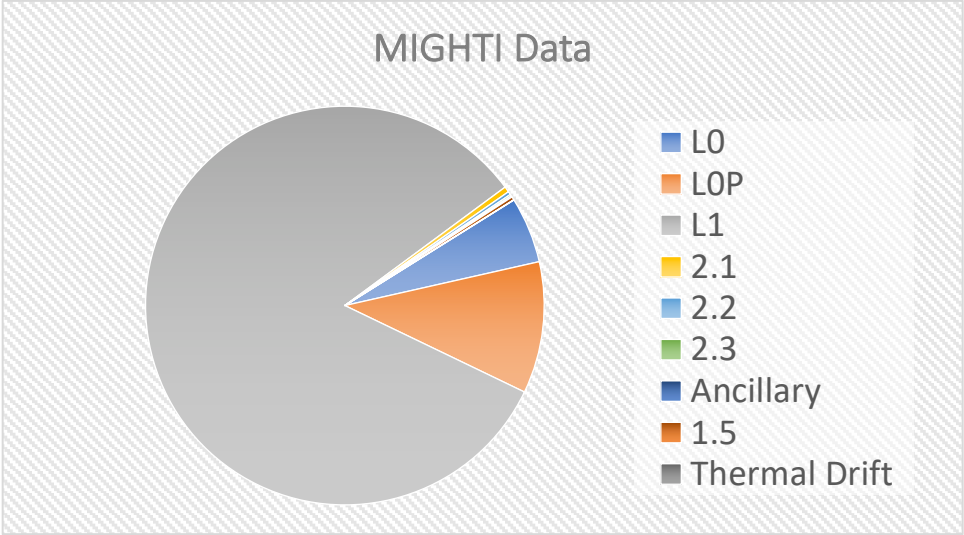


Figure 7.4 – Data volume breakdown for MIGHTI

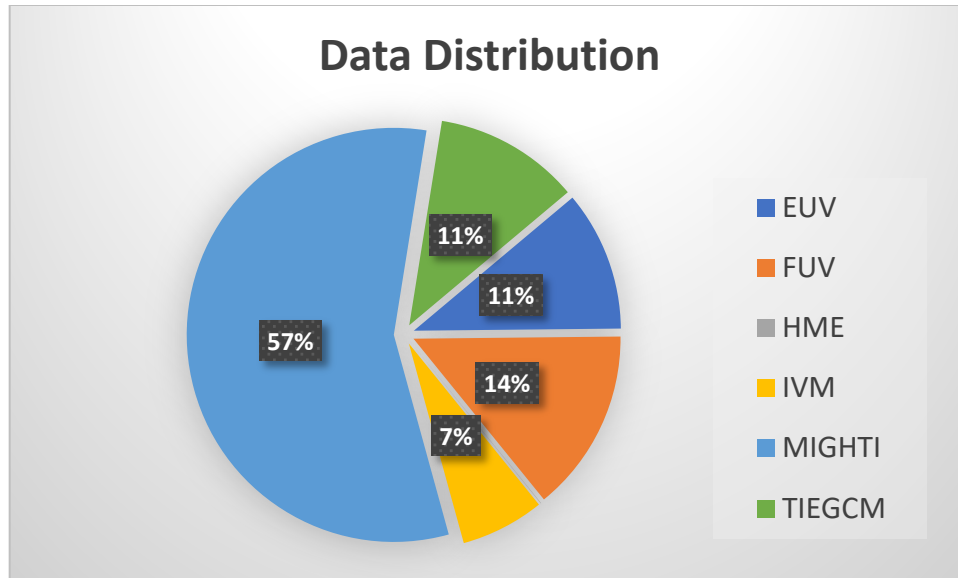


Figure 7.5 – Data volume breakdown for by all data sources

7.1 Current Archive Locations

This section describes each of the locations/repositories for science data products, any mirroring locations, and archival roles and responsibilities.

During the life of the mission, the science data products are available at the ICON Science Data Center Site - <ftp://icon-science.ssl.berkeley.edu/pub/>. These products are also available at NASA's SPDF. SPDF is responsible for archiving all of ICON's data products, and maintain them beyond the life of the mission.

There are two SSL repositories. One is the public site above. One is a private site where we host unpublished data, intermediate data and data to be compressed for publication. Both sites are local at SSL. Any data on the internal site is kept in RAW (uncompressed) format and ZIP format if it has been approved. All L0, LOP, L4 and ancillary products are automatically approved. L1 and L2 data products require science team approval before they are compressed and/or published.

The local SSL repository is backed up once every three months (differential backup) and a full backup is done at the beginning of each year. The backups are stored on tape at a remote location.

All approved (and automatically approved) data is sent to the SPDF site as soon as it is compressed to ZIP format (which allows SPDF to perform an internal CRC).

Essentially all approved data is stored 5 times:

1. Uncompressed (internal usage)
2. Compressed (internal usage)
3. SPDF (compressed)
4. Public (compressed)
5. Backup (offsite tape)

The implementation of any archive-specific naming conventions and file verification processes shall be explained (see https://spdf.gsfc.nasa.gov/guidelines/archive_newdata_req.html for requirements).

None noted for ICON.

Any requirements or restrictions for accessing the archives (e.g., accounts) are identified.

Neither the ICON Science Data Center Site nor SPDF requires any account for access. The only files that are not immediately available are the Level 0 data, which are not useable to anyone without intimate knowledge of the instrumentation and spacecraft (uncalibrated voltages, mode indicators etc.). These files are archived at SPDF.

The SPDF archive presents users with the latest version of each ICON datafile. Earlier versions are preserved at the ICON science data center, should a user need to access older / obsolete versions.

7.2 Data Access and Processing Tools

This section identifies any software available to help users search the archive catalog, access data, and further process the data. Minimum system requirements needed to install (if needed) and use the software shall be provided. This section identifies the capabilities of the software (e.g., browsing, generating light curves, performing analyses, etc.), the language it was developed in, and the file types it can be used with.

The guiding principle for these efforts is to embrace open data FAIR principles [1]. From the science data originator perspective, we only focus on findability, accessibility, and interoperability.

Findability

The ICON science dataset that has been reviewed by the ICON science team is publicly available on the FTP site hosted by the PI's institution [2] and also NASA's Space Physics Data Facility, SPDF [3]. ICON data can also be found by searching the contents of the SPASE records (see also Section 7.3). These can be searched through the Heliophysics Data Portal (HDP; <https://heliophysicsdata.gsfc.nasa.gov/>) and the upcoming SMD-wide Science Discovery Engine, along with other SPASE-based web services.

To further improve discovery of the ICON dataset in the search engines, we plan to mark up the ICON data using JSON-LD and schema.org [4] syntax. In the one-page markup, we will provide supporting information of the dataset such as the names, descriptions, and data formats.

Accessibility

One of the major hurdles for accessing the data in a large data distributing system is to download the right file for the target variables. We have developed an interactive data quick-view webpage [5], which allows users to browse the data variables within all of the level 2 data products, before downloading the data. Making the level 2 data products available on the quick-view webpage is our first priority, because those data products are the retrieved ionospheric and neutral atmospheric quantities that most of the data users can use directly in their research, such as neutral wind and ion density.

Interoperability

The ICON science data is distributed in netCDF format [6]. The programming interface is available for a large variety of the programming languages, including C, C++, Java, Fortran, Python, IDL, MATLAB, R, Ruby, and Perl. This feature allows the ICON science data to be easily retrieved, processed, re-used, and re-packaged by other systems. To demonstrate the basic steps for data downloading, reading, processing and plotting, we created a python-based ICON data tutorial webpage on Google Colab [7] that can be run on any browser without installing or setting up any programming environment beforehand. In addition, the ICON science data includes detailed variable descriptions within the variable note in the netCDF files to provide a clear history of heritaged information from the lower level data.

Demonstration of the ICON Level 2 Data Quick-View on ICON website

System requirements: Google Colab works with most major browsers, and is most thoroughly tested with the latest versions of Chrome, Firefox and Safari [8]. This quick-view is best performed with Chrome.

- Language: Python 3

The featured functions of the quick-view page are highlighted below.

1. Select a day, data product and variable. The default setting brings up the entire day of data.
2. Interactive bar provides functions to zoom in/out and download the plot.
3. Hover label shows more information about the data point when moving the mouse cursor over the plot.
4. Download button to download the netCDF file.

Ionospheric Connection Explorer Level 2 Data Quickview v0.2

10/10/2020 [Select a day](#) 1.

You have selected: October 10, 2020

l2-2_mighti_vector-wind-green [Select a data product](#)

Download: 20201010 l2-2_mighti_vector-wind-green

Meridional Wind (m/s) [Select a variable](#) 2. **Interactive bar**

You have selected Meridional Wind (m/s)

Meridional Wind (m/s)

Altitude (km)

UTC Time

Oct 10, 2020 Oct 11, 2020

Oct 10, 2020, 11:06:45
y: 156.7496
z: -53.68886
lon,lat: 9.28, 9.63

3. Moving the mouse cursor over the plot for more information about the data point.

4. Downloading the present file by one click.

[Download data](#)

Contact: yjwu at ssl.berkeley.edu

Demonstration of the ICON data tutorial on Google Colab

- System requirements: Google Colab works with most major browsers, and is most thoroughly tested with the latest versions of Chrome, Firefox and Safari [8].
- Language: Python 3
- Download ICON data from the ftp site

```
2. Download ICON data from the FTP site
```

```
1  '''Insert a target day'''
2  target_datetime=datetime(2020,4,20) # (year, month, day)
3  target_YYYY='%4i' % target_datetime.year
4  target_mm='%02i' % target_datetime.month
5  target_dd='%02i' % target_datetime.day
6  target_doy='%03i' % ((target_datetime-datetime(np.int(target_YYYY),1,1)).days+1)
7  target_date_str='%s-%s-%s' % (target_YYYY,target_mm,target_dd)
8
9  if not glob.glob('ICON*s*' % target_date_str):
10
11     ftp=FTP('icon-science.ssl.berkeley.edu')
12
13     ftp.login()
14     download_ICON_ftp(ftp, target_YYYY, target_doy, ICON_product='L2-2', ICON_instrument='MIGHTI')
15     download_ICON_ftp(ftp, target_YYYY, target_doy, ICON_product='L2-3', ICON_instrument='MIGHTI',MTAB='A')
16     download_ICON_ftp(ftp, target_YYYY, target_doy, ICON_product='L2-4', ICON_instrument='FUV')
17     download_ICON_ftp(ftp, target_YYYY, target_doy, ICON_product='L2-5', ICON_instrument='FUV')
18     download_ICON_ftp(ftp, target_YYYY, target_doy, ICON_product='L2-6', ICON_instrument='EUV')
19     download_ICON_ftp(ftp, target_YYYY, target_doy, ICON_product='L2-7', ICON_instrument='IVM-A')
20     #
21     ftp.quit()
```

- Read ICON netCDF files

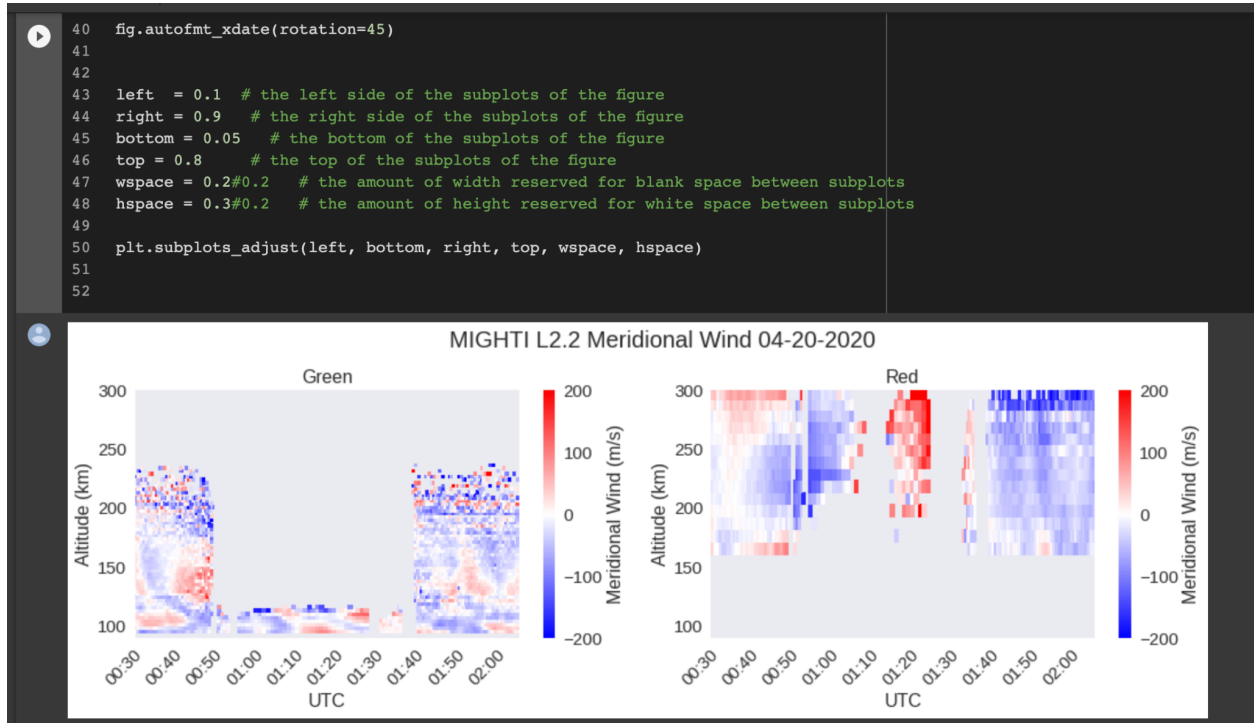
3. Read ICON netCDF files

```

1  '''MIGHTI L2.2 Vector Wind'''
2  MT_color= 'Green'
3  fn_L22=glob.glob('/content/%s/ICON_L2-2_*%s*.NC' % (target_doy,MT_color))[0]
4
5  dm_g=xr.open_dataset(fn_L22)
6  dm_g=dm_g.rename({'Epoch': 'time_ms',
7                  'ICON_L22_Orbit_Number': 'orb_num',
8                  'ICON_L22_Longitude': 'tang_lon',
9                  'ICON_L22_Latitude': 'tang_lat',
10                 'ICON_L22_Altitude': 'tang_alt',
11                 'ICON_L22_Meridional_Wind': 'umer',
12                 'ICON_L22_Zonal_Wind': 'uzon',
13                 'ICON_L22_Local_Solar_Time': 'tang_slr',
14                 'ICON_L22_Wind_Quality': 'wind_quality'})
15
16  dm_g['time']=pd.to_datetime(np.array([datetime(1970,1,1) + timedelta(seconds = 1e-3*s) for s in dm_g['time_ms'].values]))
17  # Only allow the good data: dm_g.wind_quality >= 0.5
18  good_data=(dm_g.wind_quality == 0.5)|(dm_g.wind_quality == 1)
19  dm_g[['umer', 'uzon']]=dm_g[['umer', 'uzon']].where(good_data)
20
21
22  print('Orbit numbers: %04i to %04i' % (np.nanmin(dm_g.orb_num),np.nanmax(dm_g.orb_num)))

```

- Plot ICON data



- 1] The open data principles <https://www.nature.com/articles/sdata201618>
- 2] FTP site on UC Berkeley <ftp://icon-science.ssl.berkeley.edu/pub/>
- 3] ICON data on SPDF <https://spdf.gsfc.nasa.gov/pub/data/icon/>
- 4] Schema.org <https://schema.org/>
- 5] Level 2 data quick view

<https://icon.ssl.berkeley.edu/Data/Data-Quickview>

[6] netCDF data <https://www.unidata.ucar.edu/software/netcdf/>

[7] ICON data Tutorial https://colab.research.google.com/github/YJWu-SSL/ICON_Data_Demo/blob/main/ICON_data_demo_Colab_v04.ipynb

[8] Google Colab FAQ <https://research.google.com/colaboratory/faq.html>

7.3 Documentation and Metadata

This section describes how the project will make documentation of data products and format available.

All ICON products contain documentation describing them, their history, metadata etc. inside the netCDF files themselves. These are replicated in easy-to-read formats in pdfs that are on both the ICON Science Data Center site and SPDF. They are reproduced in full in Sections 4.1 through 4.6 of this document.

Listings of any software documentation or user guides shall indicate when they were last updated as well as the version of the software they are applicable to.

The documentation in Sections 4.1 – 4.6 are all available on both the ICON Science Data Center site, and SPDF archive. These documents state when they were updated and the software version to which they are applicable as part of their global attributes. These data users guides are updated any time a revision to the data version is made.

Documentation of the Python software described above is contained in this document. No further documentation or support is provided by the ICON team, beyond what exists on the GitHub repository.

This section also identifies any metadata schemes to be employed (e.g., SPASE).

The ICON team has worked with the Space Physics Archive Search and Extract (SPASE) Metadata Working Team (SMWT) to create SPASE records for all data. The SPASE descriptions can be found at <https://heliophysicsdata.gsfc.nasa.gov/websearch/dispatcher>.

7.4 Final Archive / Mission Archive Plan

This section describes the tasks needed to adapt products/data sets in order to maintain their long-term utility with minimal (or no) support from the mission or instrument team.

The ICON data conforms to SPDF's guidelines, and the ICON team has worked with SPDF to ensure the data are compatible with CDAWEB's software. SPDF then ensures their long-term utility.

The details of this section will be updated at each Senior Review in preparation for extended mission phases and to leverage advances in Information Technology.

This will be revisited at each subsequent Senior Review.

7.4.1 Data Products

This subsection describes the classes of data products to be contained within the Final Archive including, but not limited to catalog data, calibrated data, and ancillary products.

All products listed in Table 4.1, including all Level 0 instrument data, Ancillary Data, Calibrated Level 1, Inverted Level 2 and Model Level 4 Products are available in the Final Archive at SPDF.

A summary list or table of final products and their formats shall be included.

This is in Section 4. Specifically, the table of all products is Table 7.4.1, and the formats are described in Sections 4.1 through 4.6. All files are in netCDF format.

Data Level	MIGHTI	IVM	FUV	EUV
L0	Time -ordered raw data, with communication artifacts removed. UTC time included.	Time -ordered raw data, with communication artifacts removed. UTC time included.	Time -ordered raw data, with communication artifacts removed. UTC time included.	Time -ordered raw data, with communication artifacts removed. UTC time included.
L1	Calibrated interferograms of 557.7 and 630.0 nm observations vs time and view angle. Calibrated O2 A-band and out-of-band brightness vs time and view angle. Daily netCDF files. 1 file for MIGHTI A, one for MIGHTI B.	Calibrated incoming ion current and arrival angle vs time. Daily netCDF files. 1 file for IVM A, one for IVM B as applicable.	Calibrated shortwave and longwave Far UV images (6 horizontal bins, 256 vertical bins) vs time. Time-delay-integrated motion-compensated images of the limb and sublimb in the shortwave channel. Daily netCDF files.	Calibrated extreme UV spectra vs time and view angle. Daily netCDF files.

Ancillary	Remote viewing geometry, instrument & spacecraft geometry at time of each observation. 1 file for MIGHTI A, one for MIGHTI B.	Instrument & spacecraft geometry at time of each observation. Spacecraft magneto torquer status at time of each observation. 1 file for IVM A, one for IVM B as applicable.	Remote viewing geometry, instrument & spacecraft geometry at time of each observation. Geophysical indices at time of each observation. One file for shortwave, one for longwave.	Remote viewing geometry, instrument & spacecraft geometry at time of each observation. Geophysical indices at time of each observation.
L2	Inverted line of site winds vs tangent altitude and time. Inverted vector (cardinal) horizontal winds vs altitude and time. Neutral temperatures vs altitude and time. All quantities georeferenced. Daily netCDF files. 1 file for MIGHTI A and B for the line of site and temperature, combined file for cardinal winds.	In situ ion density, composition, temperature and velocity in instrument, spacecraft and geomagnetic coordinates vs time. Daily netCDF files.	Inverted column O/N ₂ ratio vs time (daytime). O ⁺ density vs altitude (nighttime). All quantities georeferenced. Daily netCDF files.	Inverted O ⁺ density (daytime) vs altitude and time. All quantities georeferenced. Daily netCDF files.
L4	Hough Mode Extension fits to the MIGHTI L2 temperatures and winds vs altitude and time. Hough	N/A	N/A	N/A

	Mode Extension lower boundary files for the TIEGCM model. TIEGCM model output using the Hough Mode Extension lower boundary and a control run that does not use this lower boundary. Each as daily netCDF file			
--	--	--	--	--

Table 7.4.1 – List of ICON data products by level.

This subsection also includes details on each instrument team’s archiving plan.

All ICON products are done at the mission level – there is no separate plan by instrument.

7.4.2 Analysis Tools

The analysis tools developed for the ICON mission were described in Section 7.2.

7.4.3 Documentation

This subsection describes the process of reviewing existing mission documentation and downselecting to a core set that has been scrubbed to remove obsolete and/or conflicting material.

The most important portion of this documentation for anyone beyond the ICON team are the descriptions of the data products in Section 4, and the algorithms in the CMAD. Regarding the data products, these descriptions are generated automatically from the netCDF files themselves and are updated each time the data version is incremented. These are then uploaded to the ICON website and SPDF. The remainder of this document is updated with each senior review.

7.4.4 Final Archive Access and Distribution

This subsection describes how data, tools, and documentation are to be served and maintained for the long term.

SPDF maintains the archive copy of all data and documentation described above. They ensure it is available from their website and will maintain these for the long term. The tools outlined in Section 7.2 are on GitHub and will be maintained as long as that site remains available. No longer-term archiving of these tools is planned. The software for the ICON data processing pipeline is archived using Git and will be maintained for at least the duration of the mission.

Appendix A. Acronyms

EUV – Extreme Ultraviolet

FUV – Far Ultraviolet

HME – Hough Mode Extensions

IVM – Ion Velocity Meter

LVLH – Local Vertical Local Horizontal

MIGHTI - Michelson Interferometer for Global High-resolution Thermospheric Imaging

NetCDF – Network Common Data Format

PDMP – Project Data Management Plan

PLRA – Program Level Requirements Appendix

TIEGCM - Thermosphere Ionosphere Electrodynamics Model

TLM – Instrument or spacecraft telemetry